



The
University
Of
Sheffield.

Thesis Title:

c-Rel drives atherosclerosis at sites of disturbed flow

By:

Blanca Tardajos Ayllón

A thesis submitted in partial fulfilment of the requirements for the degree of
Doctor of Philosophy

The University of Sheffield
Faculty of Medicine, Dentistry & Health
Department of Infection, Immunity and Cardiovascular Disease

Submission Date

January 2020

Acknowledgements

I am very grateful to my supervisor Prof. Paul Evans for all his support, guidance and invaluable advice over the last three years. Also, to my co-supervisor, Prof. Fiona Oakley, for her help and for providing us with the *c-Rel* knockout mice. Thanks to all members of the IICD department and the technical staff, particularly to Dr. Mark Ariaans and Carl Wright. I would also like to thank everyone in the office (the ones who left and the ones who are still there) for making these years much more enjoyable and for being great company. Thanks for feeding me with all the cakes you have brought over the past years and for letting me through the O-floor doors every time I forgot my card and was locked out! Special thanks to Celine, Hannah, Jovana and Daniela, for having been amazing colleagues and friends. Thank you for all your help and for the good times in and outside the lab.

I am also very grateful to the MRC DiMeN Doctoral Training Partnership for funding my PhD, I feel very lucky to have been a part of this scheme. It has been a pleasure to share the last three years with all DiMeN students, thank you for being an incredible group of people. Special thanks to Dr. Emily Goodall, for her commitment, support and hard work. You have been a fantastic manager.

I'd also like to thank my friends, old and new, for the laughs, the trips and all the good times. And importantly, big thanks to my family- my siblings, my aunts and in particular, my parents. Thanks for your unending love, for your constant support, for the countless visits to Sheffield and for always being there for me no matter what. I am extremely lucky to have such wonderful parents and I cannot thank you enough for all you have done for us. Finally, I would also like to thank William for always being by my side. Thank you for all of the little (and big) things you do every day, you are great.

Abstract

Atherosclerosis is prone to developing at bends and branches of arteries exposed to disturbed flow and low shear stress. These mechanical conditions alter endothelial cell (EC) function, by promoting inflammation, proliferation, and other processes. Shear stress regulates various transcriptional programs, such as those controlled by the NF- κ B family. Despite the fact that some NF- κ B subunits have been revealed to respond to shear stress, the effect of this force on c-Rel and its role in atherosclerosis have not been described.

En face staining revealed that c-Rel was enhanced at the inner curvature (low shear stress) compared to the outer curvature (high shear) of the normal murine aorta. Total deletion of *c-Rel* resulted in decreased expression of the inflammatory molecules Vcam-1 and E-Selectin and reduced proliferation at low shear regions of the mouse aorta. Moreover, total *c-Rel* and EC-specific *c-Rel* deletion led to a reduction in atherosclerotic lesions in mice treated with AAV-PCSK9, indicating that total c-Rel and endothelial c-Rel induce atherogenesis. Consistent with this, c-REL protein was enriched in human umbilical vein EC (HUVEC) and human coronary artery EC (HCAEC) exposed to low shear using *in vitro* flow systems. Similarly, silencing of *c-REL* in HUVEC under low shear stress led to reduced expression of inflammatory molecules and proliferation. Microarray studies in HUVEC and subsequent validation experiments using HUVEC and *en face* staining of mouse aortas showed that c-Rel controls the expression of genes implicated in inflammation, such as TXNIP and p38, and proliferation, including RANK, NIK, p100/p52 and p21.

These data demonstrate that c-Rel is enriched under low shear and that it promotes atherosclerosis by inducing EC inflammation and proliferation. *In vitro* and *in vivo* studies show that c-Rel activates a number of genes implicated in inflammation and proliferation, providing a potential mechanism for c-Rel proinflammatory and pro-proliferative activity.

Table of contents

Chapter 1. Introduction	14
1.1 Atherosclerosis	15
1.1.2 Atherosclerosis is a focal disease	19
1.2 Shear stress	20
1.3 Therapeutic targeting of endothelium	23
1.4 Endothelial responses to shear stress	24
1.5 MAPK signalling pathway	27
1.6 Nuclear factor-kappa B (NF-κB).....	28
1.6.1 Canonical pathway	31
1.6.2 Non-canonical pathway	31
1.6.3 Crosstalk in NF-κB signalling pathways.....	33
1.6.4 Negative regulation of NF-κB.....	33
1.6.5 NF-κB and atherosclerosis	36
1.7 c-Rel	38
1.7.1 Overview of c-Rel biology	38
1.7.2 c-Rel function in B cells and T cells	39
1.7.4 c-Rel and autoimmune diseases	40
1.7.5 c-Rel and cancer	40
1.7.6 c-Rel and fibrosis	41
1.7.7 c-Rel and the nervous system.....	41
1.7.8 c-Rel and atherosclerosis.....	42
1.8 Project rationale and hypothesis.....	44
1.9 Project aims	44
Chapter 2. Methods	45
2.1 Mouse licensing	46
2.2 <i>En face</i> staining of murine vascular endothelium	46
2.2.1 Mouse sacrifice	46
2.2.2 Aortic dissection.....	46
2.2.3 <i>En face</i> staining of murine vascular endothelium	48
2.3 Mouse breeding	48
2.3.1 Genotyping.....	48
2.3.2 Cdh5-Cre-ER ^T transgenic model	49
2.3.3 Breeding of Cdh5-c-Rel ^{KO} (c-Rel-EC ^{KO}) mice	50
2.4 Induction of hypercholesterolemia in C57BL/6J mice.....	52
2.5 Analysis of plasma lipids	52
2.6 Oil red O staining and lesion analysis	53

2.7 Partial ligation of the left carotid artery (LCA) in <i>ApoE</i> knockout mice	53
2.8 Endothelial cell isolation from porcine aortas.....	56
2.8.1 RNA extraction from porcine endothelial cells.....	58
2.9 Primary endothelial cells.....	58
2.9.1 Isolation of Human Umbilical Vein Endothelial Cells (HUVEC)	58
2.9.2 Human endothelial cell culture and maintenance.....	59
2.10 Flow systems.....	59
2.10.1 Orbital shaker system.....	59
2.10.2 Parallel plate system (Ibidi® system).....	61
2.11 Immunofluorescence staining of HUVEC	61
2.12 Western Blotting	62
2.12.1 Protein isolation.....	62
2.12.2 Gel preparation and electrophoresis.....	62
2.12.3 Membrane transfer	63
2.12.4 Antibody staining	63
2.13 RNA extraction from cultured ECs.....	64
2.14 cDNA synthesis.....	64
2.15 Primer design	64
2.16 Quantitative RT-PCR (qRT-PCR)	65
2.17 HUVEC siRNA electroporation using Neon transfection system.....	66
2.18 RNA microarray in HUVEC	67
2.18 Statistical analysis	67
Chapter 3. <i>c-Rel</i> protein levels are enriched at low shear stress regions	68
3.1 Introduction.....	69
3.2 Hypothesis and aims.....	70
3.3 <i>c-Rel</i> protein levels are enriched at low shear stress regions of the murine aorta.....	71
3.4 Shear stress does not regulate <i>c-REL</i> mRNA expression in porcine aortas	75
3.5 <i>c-Rel</i> mRNA expression is reduced by partial ligation of murine carotid arteries.....	77
3.6 <i>c-REL</i> protein levels are enriched in HUVEC and HCAEC exposed to low shear stress using the orbital shaker	79
3.7 <i>c-REL</i> protein levels are enriched in HUVEC exposed to low shear stress using the Ibidi® system.....	83
3.8 <i>c-REL</i> mRNA expression does not reflect <i>c-REL</i> protein expression using the orbital shaker system.....	85
3.9 <i>c-REL</i> mRNA expression does not reflect <i>c-REL</i> protein expression using the Ibidi® system.....	87
3.10 Conclusions	89
3.11 Discussion	90

3.11.1 c-Rel expression analysis using in vivo models	90
3.11.2 c-Rel expression analysis using in vitro flow systems	92
3.11.3 Regulation of c-Rel protein levels.....	94
3.11.4 A hypothesis for shear stress-induction of c-Rel.....	95
Chapter 4. c-Rel controls proliferation and inflammation in cells exposed to low shear stress <i>in vitro</i>	97
4.1 Introduction	98
4.2 Hypothesis and aims.....	99
4.4 c-Rel promotes proliferation in HUVEC exposed to low shear stress	105
4.5 c-Rel does not have a major role in EC apoptosis.....	108
4.6 Characterisation of genes downstream of c-Rel using a RNA microarray: c-Rel positively regulates TXNIP, p38 and RANK.....	110
4.7 c-Rel positively regulates the non-canonical NF- κ B subunits NIK, p52 and p100 to promote proliferation.....	116
4.8 c-Rel negatively regulates p21 to promote proliferation.....	118
4.9 Conclusions	120
4.10 Discussion	121
4.10.1 Low shear stress increased EC proliferation, apoptosis and E-SELECTIN expression, but it did not regulate VCAM-1 protein levels.....	123
4.10.2 c-Rel controls endothelial proliferation before the onset of S-phase	124
4.10.3 c-REL silencing has modest effects in endothelium exposed to high shear stress.	126
4.10.4 c-Rel does not have a major role in EC apoptosis.....	126
4.10.5 RNA microarray in HUVEC: Characterisation of genes downstream of c-Rel	126
4.10.6 Potential mechanism for the regulation of inflammation by c-Rel	127
4.10.7 Potential mechanism for the regulation of proliferation by c-Rel	130
4.10.7.1 RANK	130
4.10.7.2 c-Rel-RANK-p52-p21 signalling	133
4.10.7.3 Other c-Rel proliferative mechanisms.....	136
Chapter 5. c-Rel promotes atherosclerosis and controls EC dysfunction at atheroprone sites <i>in vivo</i>	137
5.1 Introduction	138
5.2 Hypothesis and aims.....	139
5.3 c-Rel promotes EC inflammation at low shear stress regions in the mouse aortic arch..	140
5.4 c-Rel promotes EC proliferation at low shear stress regions in the mouse aortic arch ...	142
5.5 c-Rel induces the expression of the MAPK cascade components Txnip and p38 to promote EC inflammation in the mouse aortic arch.....	144
5.6 c-Rel induces the expression of the non-canonical NF- κ B pathway components RANK and NIK to promote EC proliferation in the mouse aortic arch	146
5.7 c-Rel promotes the development of atherosclerosis.....	148

5.8 Endothelial c-Rel promotes the development of atherosclerosis	151
5.9 Conclusions	153
5.10 Discussion	154
5.10.1 c-Rel promotes EC proliferation and inflammation in vivo	154
5.10.2 Does increased EC proliferation lead to atherosclerosis?	155
5.10.3 c-Rel promotes the development of atherosclerosis: possible mechanisms include altered lipid metabolism	156
5.10.4 Endothelial c-Rel promotes the development of atherosclerosis.....	160
Chapter 6. General discussion	161
6.1 c-Rel drives atherosclerosis at sites of disturbed blood flow by activating inflammatory and proliferative transcriptional programmes in endothelium	162
6.2 Translating results to human atherosclerosis.....	165
6.2.1 Emerging therapeutic strategies to inhibit c-Rel induction of atherosclerosis	165
6.2.2 Assessment of c-Rel in human atherosclerosis	167
6.3 Future work	167
6.3.1 Functional analysis of c-Rel in vitro using the Ibidi® system	167
6.3.2 Expression and functional analysis of c-Rel in vivo using a flow-altering constrictive cuff	168
6.3.3 Role of c-Rel in senescence	168
6.3.4 Validation of c-Rel function in vitro and in vivo	168
6.3.5 Does c-Rel regulate its target genes directly?	169
6.3.6 Effect of c-Rel signalling on other NF-κB family members	169
6.3.7 Mechanosensitive signalling pathways upstream of c-Rel.....	169
6.3.8 Assessment of c-Rel function and lipid levels using c-Rel-EC ^{KO}	170
6.3.9 Effect of c-Rel inhibitor in atherosclerosis.....	170
6.3.10 Contribution of non-vascular c-Rel to atherosclerosis	171
6.3.11 Assessment of c-Rel expression at low shear stress regions of AAV-PCSK9-treated mice and human coronary tissue sections	171
Chapter 7. Appendix	172
Appendix 1. Antibodies used	173
Appendix 2. RNA microarray in HUVEC: Genes downregulated by c-REL silencing	174
Chapter 8. References	203

List of figures

Chapter 1 Introduction

Figure 1.1. Early atherosclerosis and lesion progression.....	18
Figure 1.2. Focal distribution of atherosclerosis.....	22
Figure 1.3. Flow-mediated endothelial mechanotransduction.....	26
Figure 1.4. Members of the NF- κ B family.....	30
Figure 1.5. Canonical and non-canonical NF- κ B signalling pathways.....	35
Figure 1.6. The role of c-Rel in the immune system and disease.....	43

Chapter 2 Materials and methods

Figure 2.1. Aortic opening/dissection for <i>en face</i> staining of the murine endothelium.....	47
Figure 2.2. Generation of <i>Cdh5-c-Rel</i> ^{KO} (<i>c-Rel-EC</i> ^{KO}) mice.....	51
Figure 2.3. Partial ligation of the left carotid artery (LCA) in <i>ApoE</i> knockout mice.....	55
Figure 2.4. EC isolation from porcine aortas.....	57
Figure 2.5. Orbital shaker system.....	60

Chapter 3 c-Rel protein levels are enriched at low shear stress regions

Figure 3.1. c-Rel protein levels are enriched at low shear stress regions of the murine aorta.....	72
Figure 3.2. Validation of <i>c-Rel</i> deletion in mouse.....	73
Figure 3.3. Negative control for <i>en face</i> staining of the mouse aorta.....	74
Figure 3.4. Shear stress does not regulate <i>c-REL</i> mRNA expression in porcine aortas.....	76
Figure 3.5. <i>c-REL</i> mRNA expression is reduced by partial ligation of carotid arteries in <i>ApoE</i> knockout mice.....	78
Figure 3.6. HUVEC sensing of flow patterns.....	80
Figure 3.7. c-REL protein levels are enriched in HUVEC and HCAEC exposed to disturbed flow using the orbital shaker system.....	82
Figure 3.8. c-REL protein levels are enriched in HUVEC exposed to low shear stress using the Ibidi® parallel plate system.....	84
Figure 3.9. <i>c-REL</i> mRNA expression does not reflect c-REL protein expression using the orbital shaker system.....	86

Figure 3.10. <i>c-REL</i> mRNA expression does not reflect c-REL protein expression using the Ibidi® system.....	88
Figure 3.11. A hypothesis for shear stress-induction of c-Rel.....	96
Chapter 4 <u>c-Rel controls proliferation and inflammation in cells exposed to low shear stress <i>in vitro</i></u>	
Figure 4.1. Validation of <i>c-REL</i> silencing expression in HUVEC exposed to flow using the orbital shaker.....	101
Figure 4.2. c-Rel promotes the expression of <i>VCAM-1</i> , <i>ICAM-1</i> and <i>E-SELECTIN</i> in HUVEC exposed to low shear stress.....	102
Figure 4.3. c-Rel promotes VCAM-1 and E-SELECTIN protein levels in HUVEC exposed to low shear stress.....	104
Figure 4.4. c-Rel promotes EC proliferation by PCNA staining in HUVEC exposed to low shear stress.....	106
Figure 4.5. c-Rel promotes EC proliferation by Ki67 staining in HUVEC exposed to low shear stress.....	107
Figure 4.6. c-Rel does not have a major role in EC apoptosis.....	109
Figure 4.7. RNA microarray in HUVEC under low shear stress.....	112
Figure 4.8. Validation of microarray data by qRT-PCR.....	114
Figure 4.9. Validation of TXNIP, p38 and RANK as c-Rel target genes by Western blotting.....	115
Figure 4.10. c-Rel promotes EC proliferation by inducing the non-canonical NF-κB subunits NIK, p52 and p100.....	117
Figure 4.11. c-Rel promotes EC proliferation via inhibition of p21.....	119
Figure 4.12. c-Rel promotes EC inflammation and proliferation in regions exposed to low shear stress.....	122
Figure 4.13. The expression of PCNA and Ki67 proliferation markers peaks at different stages of the cell cycle.....	125
Figure 4.14. Potential mechanism for the regulation of inflammation by c-Rel.....	129
Figure 4.15. Potential mechanism for the regulation of proliferation by c-Rel.....	132
Figure 4.16. Pleiotropic nature of p53 and p21 in endothelial cells exposed to flow.....	135
Chapter 5 <u>c-Rel promotes atherosclerosis and controls EC dysfunction at atheroprone sites <i>in vivo</i></u>	
Figure 5.1. c-Rel promotes EC inflammation at low shear stress regions of the murine aorta.....	141

Figure 5.2. c-Rel promotes EC proliferation at low shear stress regions of the murine aorta.....	143
Figure 5.3. c-Rel promotes expression of the MAPK components Txnip and p38 at low shear stress regions of the murine aorta.....	145
Figure 5.4. c-Rel promotes expression of the non-canonical NF- κ B components Rank and Nik at low shear stress regions of the murine aorta.....	147
Figure 5.5. c-Rel promotes the development of atherosclerotic lesions at low shear stress regions of the mouse aorta	149
Figure 5.6. c-Rel increases plasma triglycerides and cholesterol levels in mouse.....	150
Figure 5.7. Endothelial c-Rel promotes the development of atherosclerotic lesions at low shear stress regions of the mouse aorta.....	152
Chapter 6 <u>General discussion</u>	
Figure 6.1. c-Rel drives atherosclerosis at sites of disturbed blood flow by activating inflammatory and proliferative transcriptional programmes in endothelium.....	164

List of tables

Chapter 2 Materials and methods

Table 2.1. PCR genotyping information.....49

Table 2.2. Western diet composition.....52

Table 2.3. PCR primer sequences.....65

Table 2.4. siRNA oligonucleotide information.....66

Chapter 4 c-Rel controls proliferation and inflammation in cells exposed to low shear stress *in vitro*

Table 4.1. Functional annotation of differentially expressed genes.....111

Chapter 5 c-Rel promotes atherosclerosis and controls EC dysfunction at atheroprone sites *in vivo*

Table 5.1. KEGG pathway annotation of differentially expressed gene.....158

Chapter 6 General discussion

Table 6.1. Summary of c-Rel-specific inhibitors.....166

List of abbreviations

AAV- Adeno-associated virus
AP-1- Activator protein 1
APS- Ammonium persulphate solution
ASK1- Apoptosis signal-regulating kinase 1
ATF2- Activated transcription factor 2
B2M- Beta-2-Microglobulin
BSA- Bovine serum albumin
CAD- Coronary artery disease
CCL- Cationic lipoparticles
CDK- Cyclin-dependent kinase inhibitor
cIAP- Cellular inhibitors of apoptosis
DMEM- Dulbecco's modified eagle medium
EA- External artery
EC- Endothelial cell
ECL- Chemoluminescence blotting substrate
EndoMT- Endothelial to mesenchymal transition
eNOS- Endothelial nitric oxide synthase
ERK- Extracellular receptor kinase
E-Selectin- Endothelial selectin
FAK- Focal adhesion kinase
GC- Germinal centres
GDD45- Growth arrest and DNA damage inducible gene 45
HAEC- Human aortic endothelial cell
HCAEC- Human coronary artery endothelial cell
HDL- High-density lipoprotein
HPRT- Hypoxanthine-guanine phosphoribosyltransferase
HRP- Horseradish peroxidase
HSS- High shear stress
HUVEC- Human umbilical vein endothelial cell
IA- Internal artery
ICAM-1- intercellular adhesion molecule 1
IFN- γ - Interferon γ
I κ B- Inhibitor of κ B
IKK- I κ B kinase complex
IL-1 β - interleukin 1 β

IL-1R- IL-1 receptor
IMS- Industrial methylated spirit
iNOS- Inducible NOS
IRAK- IL-1R-associated kinase
JNK- c-Jun N-terminal kinase
KLF2- Kruppel-like family 2
KO- Knockout
LCA- Left carotid artery
LDL- Low density lipoproteins
LPS- Lipopolysaccharide
LSS- Low shear stress
MAPK- Mitogen-activated protein kinase
MAPKK3- MAPK kinase 3
MCP-1- Monocyte chemoattractant protein 1
Mef2A- Myocyte enhancer factor 2A
miR- MicroRNA
MKP- MAPK phosphatase
MMP- Matrix metalloproteinase
MnSOD- Manganese superoxide dismutase
MyD88- Myeloid differentiation primary response protein-88
NF- κ B- Nuclear factor kappa-B
NFS- Nephrogenic systemic fibrosis
NIK- NF- κ B inducing kinase
NLS- Nuclear localisation sequence
NO- Nitric oxide
Nrf2- Nuclear factor erythroid 2-related factor
OA- Occipital artery
ox-LDL- Oxidised LDL
PBS- Phosphate buffered saline
PCNA- Proliferating cell nuclear antigen
PCR- Polymerase chain reaction
PCSK9- Proprotein convertase subtilisin/kexin type 9
PECAM-1- Platelet endothelial cell adhesion molecule
Peli-1- Pellino-1
PFA- Paraformaldehyde
PI3K- Phosphoinositide 3-kinase
PKC- Protein kinase C

P-Selectin- Platelet selectin
qRT-PCR- Quantitative reverse transcriptase PCR
RANK-Receptor activator of NF- κ B
RCA- Right carotid artery
RHD- Rel homology domain
RID- Rel inhibitory domain
RIP- Receptor interacting protein
ROS- Reactive oxygen species
RP105- Radioprotective 105
SCR- Scrambled
SDS- Sodium dodecyl sulfate
SiRNA- Small interfering RNA
SMA- Smooth muscle actin
SMC- Smooth muscle cell
STA- Superior thyroid artery
TAB- TAK1-binding protein
TAD- Transactivation domain
TAE- Tris-acetate-EDTA
TAK- Transforming growth factor beta-activated kinase
TEMED- Tetramethylethylenediamine
TGF- β - Transforming growth factor β
TLR- Toll-like receptor
TNF- Tumour necrosis factor
TNFR- TNF receptor
TOLLIP- Toll interacting protein
TRADD- TNFR-associated death domain protein
TRAF- TNF receptor-associated factor
Tregs- Regulatory T cells
TRX- Thioredoxin
TXNIP- Thioredoxin interacting protein
VCAM-1- Vascular cell adhesion molecule 1
VE-Cadherin- Vascular endothelial cadherin
VEGFR- Vascular endothelial growth factor receptor
VSMC- Vascular smooth muscle cell
WT- Wildtype
XPB1- X-box binding protein 1

Chapter 1. Introduction

1.1 Atherosclerosis

Cardiovascular disease is a leading cause of death worldwide, causing 170000 deaths each year in the UK, an estimated 28% of all deaths (British Heart Foundation, 2019). Atherosclerosis, a chronic inflammatory disease, is the main underlying cause of cardiovascular disease. It is characterised by the development of plaques inside the arteries, and it can lead to angina, heart attack or stroke (Warboys et al., 2011). Although atherosclerosis is often associated with a modern diet and a sedentary lifestyle, it is not a modern disease. It has been identified in the remains of early societies with different diets, genetics and geographic location, such as Egyptian and Alaskan mummies (c. 3000 BC to c. 1500-2000 AD), suggesting that some risk factors (including smoke inhalation and chronic infection or inflammation) were relevant in ancient societies (Thompson et al., 2013; Zimmerman, 1993). These findings demonstrate that atherosclerosis is a complex disease process that is dependent on multiple risk factors, many of which have yet to be identified.

Atherosclerosis is triggered when the endothelium, a layer of cells lining the arteries, becomes dysfunctional, promoting an inflammatory response. This process can be triggered by several events, including high blood concentrations of low density lipoproteins (LDL), presence of reactive oxygen species (ROS), or hypertension (Bentzon et al., 2014; Libby, 2002; Libby et al., 2019a). When endothelial cells (EC) are activated, proinflammatory cytokines, such as monocyte chemoattractant protein 1 (MCP-1) and tumour necrosis factor (TNF), are secreted, initiating the recruitment of circulating leukocytes to endothelial cells. The expression of leukocyte adhesion molecules on the endothelial surface, including vascular cell adhesion molecule 1 (VCAM-1), endothelial selectin (E-Selectin), platelet selectin (P-Selectin) and intercellular adhesion molecule 1 (ICAM-1), also contribute to the attachment of leukocytes to the vessel wall, leading to the leukocyte adhesion cascade (Libby, 2002; Weber and Noels, 2011). Once the cells have adhered to the activated endothelium, monocytes transmigrate to the innermost layer of the artery, where they acquire characteristics of macrophages and start expressing scavenger receptors, promoting the uptake of oxidised LDL (ox-LDL). Following the uptake of ox-LDL, macrophages differentiate into foam cells, which contain lipid droplets within the cytoplasm (Bentzon et al., 2014; Witztum, 1994). These cells then release cytokines, reactive oxygen species (Rajagopalan et al., 1996) and matrix metalloproteinases (MMPs) (Galis et al., 1995), amplifying the inflammatory response

and initiating the atherosclerotic lesion, leading to the formation of fatty streaks. The inflammatory response generated by foam cells induces further endothelial activation, monocyte infiltration, and also, foam cell proliferation (Libby, 2002). Besides, vascular smooth muscle cells (VSMCs) start migrating from the media to the intima, where they proliferate and start producing extracellular matrix molecules (such as collagen), causing thickening of the intimal layer and forming the fibrous cap (Stoneman and Bennett, 2004).

As the atherosclerotic lesion progresses, foam cells undergo apoptosis and accumulate generating the necrotic core of the atherosclerotic plaque, further sustaining the inflammatory response (figure 1.1) (Bentzon et al., 2014). Over time, the atherosclerotic lesion and the fibrous cap can continue growing, narrowing the vessel lumen (aortic stenosis) or occluding it, and hence, decreasing oxygen supply to downstream tissues. This aortic stenosis caused by a thick fibrous cap could lead to conditions such as angina or abnormal heart rhythm (Bando et al., 2015; Stoneman and Bennett, 2004). Conversely, some atherosclerotic lesions present a thin fibrous cap, which is prone to plaque rupture. Activated leukocytes can release MMPs, resulting in the degradation of extracellular matrix (Galis and Khatri, 2002). In particular, MMP9 and MMP2 have been shown to be relevant to the pathogenesis of atherosclerosis, since their expression is known to correlate with plaque stability (Heo et al., 2011b). In addition, proinflammatory cytokines (including interferon- γ (IFN- γ)) can inhibit collagen production, causing fibrous cap disruption (Libby, 2002). Plaque rupture leads to exposure of the plaque core to the bloodstream, triggering coagulation and thrombus formation due to the presence of tissue factor and activated platelets. This thrombus formation can have severe consequences, occluding the vessel and resulting in acute myocardial infarction, stroke or ischemia. The severity of this last condition is higher than when a more stable plaque is generated, and it can lead to sudden coronary death (Libby et al., 2019a).

The formation of a thrombus can also occur without plaque rupture, and this process involves superficial plaque erosion. Currently, up to one third of acute coronary syndromes could result from plaque erosion instead of plaque rupture (Jia et al., 2013). Lesions that are linked to plaque erosion are morphologically distinct to those that present a thin fibrous cap and are prone to plaque rupture. Although they present a large amount of extracellular matrix and smooth muscle cells, they exhibit low levels of lipids and macrophages, as well as scarce foam cells (Libby et al., 2019b; Virmani et al., 1999). Furthermore, eroded plaques contain high levels of proteoglycans, glycosaminoglycans

and type 3 collagen, whereas ruptured plaques do not present abundant collagen (Falk et al., 2013; Kolodgie et al., 2002; Virmani et al., 2000). It has been suggested that eroded plaques localise to atheroprone regions exposed to disturbed blood flow, and they also present loss of endothelial cells (Franck et al., 2017; Quillard et al., 2015).

Toll-like receptor (TLR)-2 has been suggested to contribute to endothelial dysfunction, causing superficial erosion. Some studies have shown that TLR-2 is upregulated in regions exposed to disturbed flow (Edfeldt et al., 2002; Mullick et al., 2008), and that deletion of TLR-2 reduces atherosclerosis in mouse (Mullick et al., 2005). Hyaluronan, a glycosaminoglycan that is typically found in eroded plaques, can bind to TLR-2 (Scheibner et al., 2006). Both TLR-2 and hyaluronan are known to contribute to endothelial activation by promoting the expression of adhesion molecules, such as E-Selectin and VCAM-1, the production of ROS, and eventually, EC apoptosis (Quillard et al., 2015). Hence, flow disturbance enhances TLR-2 expression and glycosaminoglycan levels, triggering EC dysfunction, apoptosis and desquamation, and ultimately leading to superficial erosion.

Further research should now focus on investigating other mechanisms of superficial plaque erosion. Understanding the underlying biology could lead to novel therapies to treat acute coronary syndromes caused by erosion, which are likely to be different to those provoked by plaque rupture.

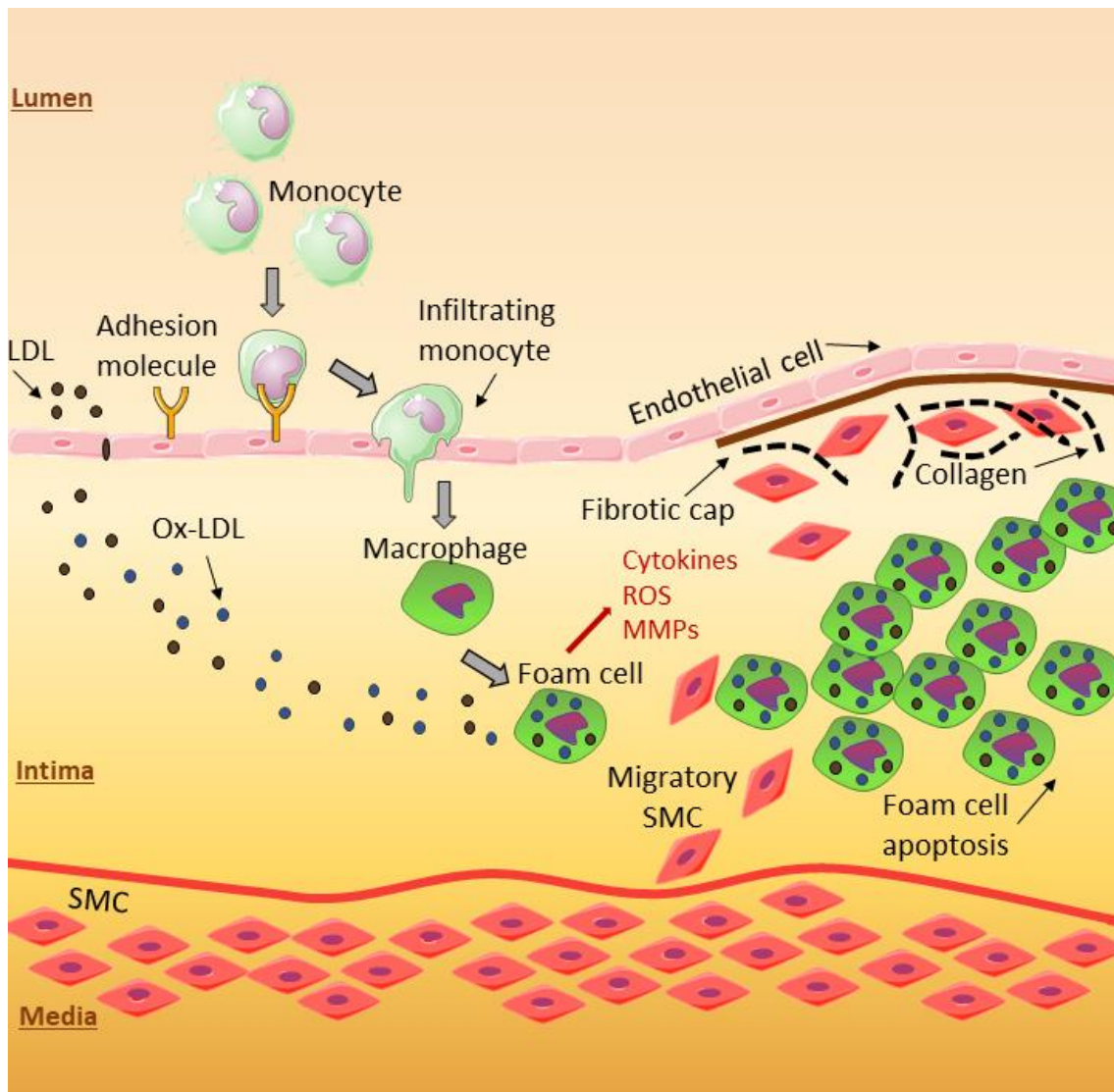


Figure 1.1. Early atherosclerosis and lesion progression. Endothelial cell (EC) dysfunction, which can be triggered by events such as high blood concentrations of LDL, presence ROS, or hypertension, initiates atherosclerosis. When EC are activated, they release cytokines (e.g. MCP-1 and TNF). This, together with the expression of leukocyte adhesion molecules on the endothelial surface (e.g. VCAM-1, ICAM-1, E-Selectin), lead to the adhesion of leukocytes to the EC layer and subsequent monocyte infiltration. In the intima, monocytes acquire characteristics of macrophages and start taking up ox-LDL, leading to macrophage differentiation into foam cells. Foam cells then release cytokines, ROS and MMPs, amplifying the inflammatory response and inducing further endothelial activation, monocyte infiltration, and migration of smooth muscle cells (SMC) into the intima. After SMC migration, SMC proliferate and start producing collagen, generating the fibrous cap. In addition, foam cells undergo apoptosis and accumulate generating the necrotic core of the atherosclerotic plaque, further promoting the inflammatory response.

There are several risk factors that have been associated with the development of atherosclerotic plaques, and most of them have also been linked to endothelial cell dysfunction (Davignon and Ganz, 2004). High cholesterol levels and smoking are both critical for the initiation of atherosclerosis, since high levels of LDL promote the uptake and accumulation of this molecule by macrophages and smoking induces ROS release, leading to LDL oxidation and promoting inflammatory signalling (Csordas and Bernhard, 2013). Other risk factors that contribute to this disease are hypertension, obesity, gender and age. Although these contribute to the progression of atherosclerosis in the entire artery tree, atherosclerosis mainly occurs in specific regions, including curvatures, branches, and arterial bifurcations. On the contrary, straight vessel segments are generally free from the disease (Malek et al., 1999).

1.1.2 Atherosclerosis is a focal disease

In the 15th century, Leonardo da Vinci performed human and animal dissections that allowed him to study the heart and blood vessels. Although the concept of blood circulation was not introduced until 1628 by W. Harvey, da Vinci was already aware of the potential role of haemodynamics in the cardiovascular system. In his numerous drawings, Leonardo compared the blood flow in arteries and veins to the flow of rivers and water around obstacles, and he thought both were subjected to similar forces (Martins e Silva, 2008). In the 19th century, Virchow (Virchow, 1860) and Rokitansky (Rokitansky, 1952) documented that atherosclerosis mainly occurred in specific areas of the arterial tree, suggesting that mechanical forces could play a role in this non-uniform distribution of the disease (Davies, 1995).

In 1969, Caro et al. observed that atheroprone regions and protected regions were exposed to different blood flow patterns. They observed that endothelial cells in atheroprone regions were exposed to non-uniform and disturbed blood flow, whereas straight arterial segments were exposed to steady and unidirectional flow. The fact that atherosclerotic lesions occurred in regions exposed to altered blood flow suggested that haemodynamic forces induced by blood flow influence the distribution of plaques (Caro et al., 1969).

The influence of flow on lesion distribution has been explained by two different but not mutually exclusive mechanisms: mass transport and shear stress theory of atherogenesis.

Mass transport theory: It suggests that the transport of molecules from the bloodstream to the endothelium is different in regions exposed to steady flow and regions with disturbed flow. Several studies have shown that atheroprone regions exposed to disturbed flow have increased endothelial permeability that facilitates the accumulation of lipoproteins and molecules such as nitric oxide (NO), and this is suggested to be due to a prolonged contact between the endothelium and blood (Herrmann et al., 1994; Jo et al., 1991; Staughton et al., 2001).

Shear stress theory: This theory involves the effect of blood flow-dependent forces on the vascular endothelium, since it is directly exposed to flow. It specifically describes the effect of shear stress on the vasculature (Malek et al., 1999).

It has been shown that there is a functional interaction between both mechanisms, and that they affect the development of atherosclerosis. While shear stress is responsible for altering endothelial permeability, this permeability, in turn, controls the transport of molecules (Jo et al., 1991).

1.2 Shear stress

Endothelial cells are exposed to several physical forces that are exerted by blood flow, modulating their response. Some of the forces that have been shown to influence EC function are cyclic circumferential stretch, which depends on cardiac cycle and changes in vessel diameter, hydrostatic pressure, which is also known as compressive stress and is influenced by blood pressure, and shear stress (Papadaki and Eskin, 1997). Shear stress is a frictional force per unit area that is essential for maintaining endothelial physiology. It is exerted by blood flow and its magnitude and direction is dependent on the vascular geometry and cardiac cycle, and it has been suggested to influence atherogenesis (Cunningham and Gotlieb, 2005). This haemodynamic force can be calculated using Poiseuille's equation:

$$\text{Shear stress} = 4\mu Q/\pi r^3$$

This shows that shear stress is directly proportional to blood flow velocity (Q) and viscosity (μ), and inversely proportional to the vessel radius (r) (Malek et al., 1999).

Several computational fluid dynamics models have been generated in the last few years, in order to model how blood flow circulates through vessels. This enables the characterisation of forces generated by flow in different areas of the aorta, producing

shear stress maps in numerous species (Feintuch et al., 2007; Lantz et al., 2012; Serbanovic-Canic et al., 2017). Atheroprone sites, where blood flow is disturbed and slow, are known to be exposed to low shear stress (LSS) (e.g. 4 dynes/cm² or 0.4 Pa). In these regions, in addition to a variation in magnitude, shear stress direction is also altered. In contrast, straight arterial segments that are exposed to unidirectional flow experience a higher magnitude of shear (e.g. 15 dynes/cm² or 1.5 Pa) and are atheroprotected (Davies, 2007) (figure 1.2).

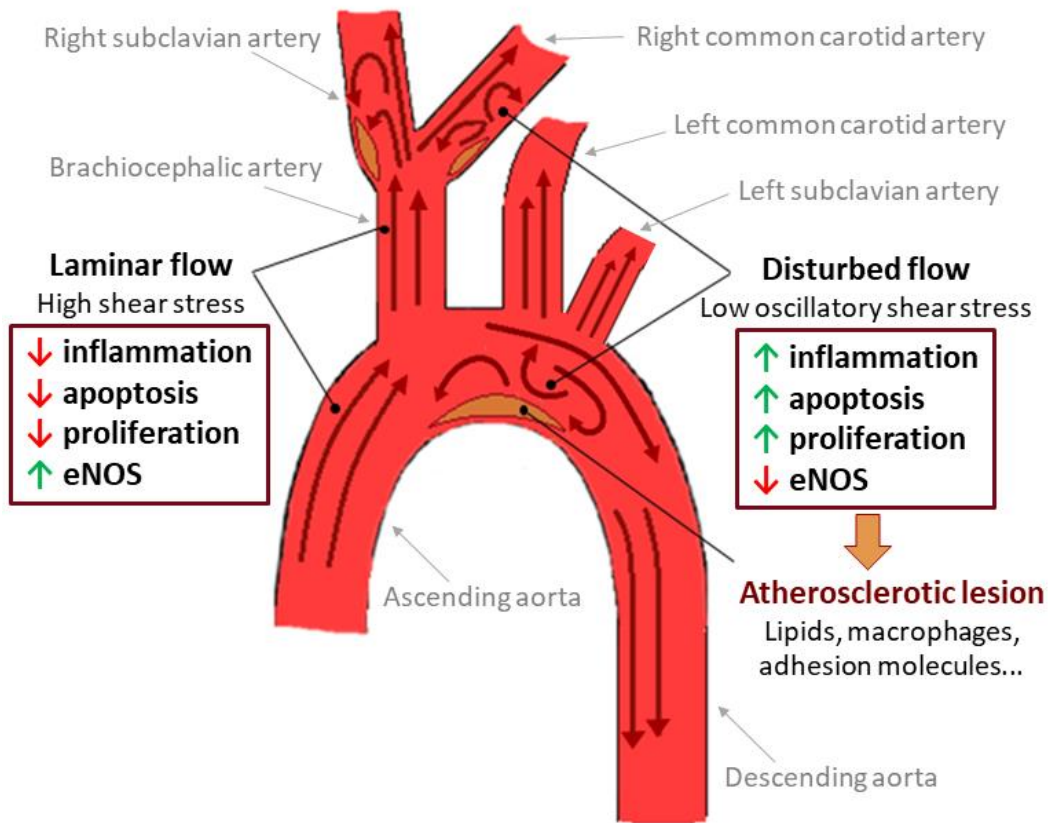


Figure 1.2. Focal distribution of atherosclerosis. Atherosclerosis mainly occurs in specific areas of the vasculature, which include the inner wall of curvatures and the outer wall of bifurcations. Endothelial cells in atheroprone regions are exposed to low shear stress and disturbed flow, and are characterised by low production of eNOS and increased inflammation, apoptosis and proliferation. However, straight arterial segments that are exposed to high shear stress and unidirectional flow are protected from atherogenesis, and they present increased eNOS production and decreased endothelial cell death, proliferation and inflammation.

1.3 Therapeutic targeting of endothelium

Since endothelial dysfunction has an essential role in the initiation of atherogenesis and is an early predictor of this disease, targeting this therapeutically could lead to the treatment and prevention of atherosclerosis and other cardiovascular events. As several studies have shown the importance of endothelial dysfunction in the development of atherosclerosis (Celermajer, 1997; Panza et al., 1990; Vita et al., 1990), many of the current therapies for atherosclerosis are focused on targeting oxidative stress and inflammatory responses, which are critical processes for endothelial function (Davignon and Ganz, 2004; Heitzer et al., 2001). Some of the established drugs that have been shown to improve endothelial dysfunction include angiotensin II type-1 receptor antagonists and angiotensin-converting enzyme inhibitors (Caspritz et al., 1986; Soehnlein et al., 2005; Warnholtz et al., 1999), statins (Laufs et al., 1998) and endothelin-1 receptor antagonists (Clozel, 2003; Thorin and Clozel, 2010). In addition to these, there are a number of new molecules that are currently in preclinical and clinical trials, which have the potential to become new therapeutic options. Some of these, such as canakinumab, which blocks interleukin 1 β (IL-1 β) (Ridker et al., 2017; Ridker et al., 2011), and methotrexate (Everett et al., 2013), target inflammatory markers. Epigenetic approaches have also shown beneficial effects, including microRNA (miR)181b (Sun et al., 2014) and miR92a (Daniel et al., 2014; Loyer et al., 2015). There are other molecules, such as resveratrol (Xia et al., 2017) and sulforaphane (Bai et al., 2015; Evans, 2011) that are naturally occurring compounds and act as antioxidant mediators. Also, targeted antioxidant therapy has become a new attractive therapeutic option. It is characterised by the inhibition of oxidative stress and inflammatory signalling specifically in the endothelium, which can be targeted using antibodies and other ligands that bind to endothelial cell adhesion molecules such as platelet endothelial cell adhesion molecule (PECAM-1) (Hood et al., 2011) and ICAM-1 (Atochina et al., 1998). It has been shown that antioxidant enzymes conjugated to antibodies against the adhesion molecules ICAM-1 and PECAM-1 bind to the endothelium, preventing endothelial dysfunction induced by ROS accumulation (Shuvaev et al., 2007), and also, protecting the endothelium from superoxide (Shuvaev et al., 2007) and H₂O₂ (Sweitzer et al., 2003). The use of these new potential therapies may lead to an improvement of vascular function, and therefore, the prognosis of atherosclerosis. Since the activation of the endothelium is a critical step in numerous

cardiovascular diseases (Celermajer, 1997), targeting endothelial dysfunction is still an interesting approach that could lead to a decline in cardiovascular disease mortality.

1.4 Endothelial responses to shear stress

A large number of studies have yielded evidence supporting the influence of haemodynamic forces upon endothelial physiology and gene expression (Ni et al., 2010; Passerini et al., 2004), which have allowed the identification of new mechanoreceptors and signalling pathways that respond to shear stress. Shear stress is sensed by mechanoreceptors that are expressed by EC, which, in turn, transform mechanical forces to activate signal transduction cascades. Shear stress acts at the apical surface of EC, deforming them in the direction of the flow. There are several molecules that have been proposed to respond to this mechanical force, such as platelet endothelial cell adhesion molecule (PECAM-1), vascular endothelial growth factor receptor (VEGFR) and vascular endothelial cadherin (VE-Cadherin) (which are found on the lateral surface of EC), and the glycocalyx, G proteins and caveolae (at the apical surface). Besides, shear stress can regulate the induction of ion channels, and the cytoskeleton has also been proposed to act as a shear stress sensor, functioning as a link between the apical surface of EC to where the activation of transduction cascades occurs (Hahn and Schwartz, 2009; Li et al., 2014; Tzima et al., 2005). After the activation of signal transduction cascades by these mechanoreceptors, endothelial gene expression is eventually regulated by activating transcription factors (Kwak et al., 2014). While areas exposed to high shear remain disease-free, low magnitudes of this haemodynamic force activate specific mechanoreceptors that trigger the activation of pathways that lead to atherosclerosis (Chatzizisis et al., 2007) (figure 1.3).

Experiments using cultured EC exposed to flow and studies using mice revealed that low shear stress induces endothelial apoptosis, and that this induction is linked with atherosclerosis (Dardik et al., 2005; Zeng et al., 2009). *In vivo* studies showed that prolonged activation of X-box binding protein 1 (XBP1), a molecule with pro-apoptotic properties, led to EC death and atherosclerosis (Zeng et al., 2009). p53 (Heo et al., 2011a), c-Jun N-terminal kinase (JNK) (Chaudhury et al., 2010) and protein kinase C (PKC) ζ (Magid and Davies, 2005), are signalling pathways that have also been revealed to be involved in the induction of apoptosis in low shear areas. In contrast, under high shear stress (HSS), there is an activation of anti-apoptotic signalling pathways, including those

involving endothelial nitric oxide synthase (eNOS) and superoxide dismutase (Dimmeler et al., 1999).

Endothelial proliferation and senescence have also been shown to be induced under disturbed flow (Foteinos et al., 2008; Warboys et al., 2014). Proliferation is regulated by proteins that control the cell cycle, and the relationship between these proteins and shear stress is still not well understood. However, it has been revealed that JNK1 induces proliferation under disturbed flow, whereas EC under laminar flow present a quiescent phenotype that is promoted by the growth arrest and DNA damage inducible gene 45 (GADD45) (Lin et al., 2000).

In high shear areas, proinflammatory responses are inhibited by different molecules, which include transcription factors such as Kruppel-like family 2 (KLF2) (van Thienen et al., 2006) and nuclear factor erythroid 2-related factor (Nrf2) (Zakkar et al., 2009). However, in regions under disturbed flow, inflammation is promoted via increased expression of adhesion molecules (e.g. E-Selectin and VCAM-1), which promote leukocyte recruitment (Hajra et al., 2000; Nagel et al., 1994; Ni et al., 2010; Partridge et al., 2007; Passerini et al., 2004; Zakkar et al., 2008). The main pathways that have been shown to induce inflammatory responses in atherosclerosis are the mitogen-activated protein kinase (MAPK) pathway, and nuclear factor kappa-B (NF- κ B) (Bryan et al., 2014; Cuhlmann et al., 2011).

Blood Flow

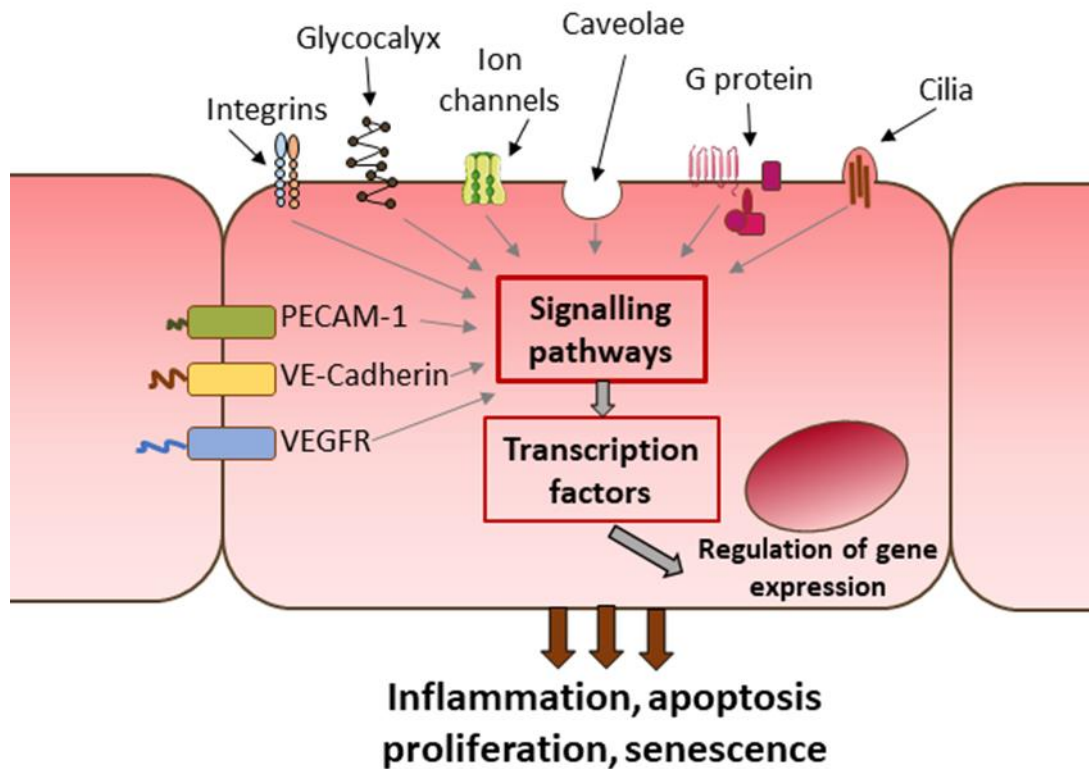


Figure 1.3. Flow-mediated endothelial mechanotransduction. Several molecules have been proposed to act as mechanoreceptors in endothelial cells. These include platelet endothelial cell adhesion molecule (PECAM-1), vascular endothelial growth factor receptor (VEGFR) and VE-Cadherin, which are adhesion molecules that are found on the lateral surface of EC. Others, such as ion channels, integrins, glycocalyx, G proteins, cilia and caveolae, are found at the apical surface. In response to flow, mechanoreceptors activate downstream signalling pathways. These, in turn, activate transcription factors, regulating target genes and modulating processes such as endothelial inflammation, proliferation, senescence and apoptosis.

1.5 MAPK signalling pathway

The MAPK signalling pathway and its regulation of activator protein 1 (AP-1) mediate shear stress-dependent inflammation, and also, they are known to have a critical role in atherogenesis (Cuhlmann et al., 2011; Ricci et al., 2004). Under high shear stress, there is an induction of KLF2 that, in turn, inactivates the proinflammatory AP-1. This inactivation occurs via JNK and its downstream target activated transcription factor 2 (ATF2), by inhibiting their nuclear localisation and phosphorylation (Boon et al., 2010; Fledderus et al., 2007). In addition to this, KLF2 also induces Nrf2 by promoting its nuclear localisation (Fledderus et al., 2008), and Nrf2, in turn, has been shown to have a key role in the regulation of MAPK signalling. One of the mechanism by which Nrf2 has been shown to regulate MAPK signalling is through suppression of the p38 activators MAPK kinase 3 (MAPKK3) and 6 (Zakkar et al., 2009). Also, Nrf2 induces the activity of MAPK phosphatase 1 (MKP-1), which negatively regulates JNK and p38, leading to a reduction in VCAM-1 expression (Zakkar et al., 2009).

Under low shear stress, thioredoxin interacting protein (TXNIP) has also been shown to influence MAPK signalling. TXNIP is induced by low shear stress both *in vitro* and *in vivo*, and it promotes the expression of VCAM-1 in regions under disturbed flow (Wang et al., 2012). One of the mechanisms by which TXNIP induces inflammation in these regions is through transcriptional co-repression of KLF2. Additionally, TXNIP downregulates thioredoxin (TRX), which inhibits the activity of apoptosis signal-regulating kinase 1 (ASK1). ASK1, in turn, is a MAPK kinase kinase that is upstream of JNK and p38, promoting an inflammatory response under low shear stress (Saitoh et al., 1998). Under high shear, TXNIP expression is downregulated in endothelial cells, inhibiting inflammation through repression of MAPK signalling (Yamawaki et al., 2005).

PKC ζ is another shear-dependent molecule that is upregulated by disturbed flow, and it is also known to influence MAPK signalling (Magid and Davies, 2005; Nigro et al., 2010). Under high shear stress, PKC ζ cannot be cleaved into a truncated form that has been shown to promote kinase activity and JNK activation, reducing inflammation (Garin et al., 2007). Also, PKC ζ inhibits eNOS expression in high shear areas, through inhibitory phosphorylation of extracellular receptor kinase 5 (ERK5) (Nigro et al., 2010).

Shear stress has also been shown to influence crosstalk between the MAPK and NF- κ B signalling pathways. One example of this crosstalk is the induction of inflammation by

RelA in low shear stress areas, through activation of JNK signalling (Cuhlmann et al., 2011). Additionally, TNF receptor-associated factors (TRAFs), which are known to be upstream of the NF- κ B signalling pathway and respond to numerous receptors, have been shown to activate both NF- κ B and AP-1 transcription factors, which are directly regulated by the MAPK signalling pathway (Wajant et al., 2001).

1.6 Nuclear factor-kappa B (NF- κ B)

NF- κ B has a critical role in innate and adaptive immunity. This is supported by the fact that the NF- κ B pathway can be induced upon bacterial and viral infections or inflammatory cytokines, among others. In addition to these, this transcription factor also responds to stimuli such as physical stress, including UV-radiation, oxidative stress, and physiological stress (Hayden and Ghosh, 2011). Since NF- κ B has major roles in inflammation (e.g. cytokines and adhesion molecules), cell proliferation and survival (Oeckinghaus and Ghosh, 2009), impaired NF- κ B activity can lead to several disorders, including cancer, inflammatory, metabolic and autoimmune diseases (Baker et al., 2011; Karin, 2006; Kumar et al., 2004).

The NF- κ B transcription factor consists of five family members that are RelA/p65, RelB, c-Rel, p50 and p52. These family members can combine to form homo or heterodimers, which allows them to bind to DNA (Monaco et al., 2004). In EC, the most abundant dimer is p50/RelA (Cuhlmann et al., 2011). NF- κ B subunits are classified into two different groups. p50 and p52, encoded by *NF κ B1* and *NF κ B2*, belong to class I, and class II comprises RelA, RelB and c-Rel (which are encoded by *Rela*, *Relb* and *Rel/c-Rel*, respectively). Class I members are characterised by being synthesised as precursor proteins p105 and p100, and these precursors contain several copies of the ankyrin repeat that allow them to act as inhibitory proteins. P105 and p100 are then processed and the mature proteins p50 and p52 are released, whereas class II members are directly synthesised as active RelA, RelB and c-Rel (Hayden and Ghosh, 2004). All NF- κ B subunits present the Rel homology domain at the N-terminus, which mediates important processes such as dimer formation, DNA binding and nuclear translocation. However, only class II members present a transcription activation domain located at the C-terminus (Perkins, 2007) (figure 1.4).

NF- κ B dimers remain in the cytoplasm in an inactive form due to their association with inhibitor of κ B proteins (I κ B). The I κ B family, which comprises BCL-3, I κ B α , I κ B β ,

I κ B γ , I κ B ϵ , p100 and p105, prevents the translocation of specific NF- κ B dimers into the nucleus by blocking the nuclear localisation sequence (NLS), and therefore, inhibits NF- κ B DNA binding (Perkins, 2007). NF- κ B can be activated via the canonical or non-canonical pathway, and NF- κ B subunits can translocate to the nucleus following ubiquitination and proteasomal degradation of I κ B proteins.

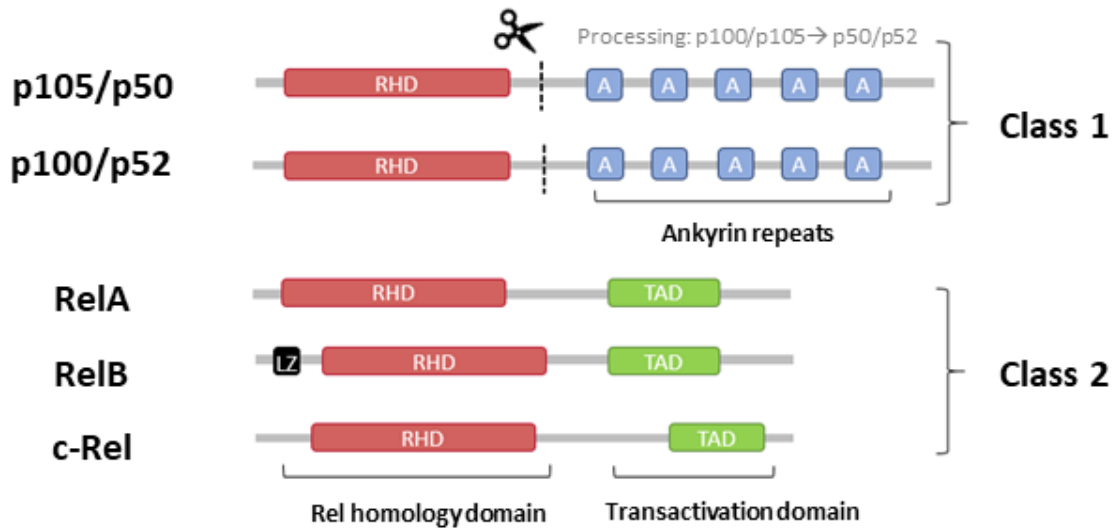


Figure 1.4. Members of the NF-κB family. All NF-κB subunits present the Rel homology domain (RHD) at the N-terminus. This domain mediates dimer formation, DNA binding and nuclear translocation. Additionally, RelA, RelB and c-Rel present a transcription activation domain (TAD), which activates gene transcription and is located at the C-terminus. NF-κB subunits are classified into two groups. p50 and p52 belong to class I, and class II comprises RelA, RelB and c-Rel. p50 and p52 are synthesised as precursor proteins p105 and p100, which include several copies of the ankyrin (A) repeat. p105 and p100 are then processed and they form the mature proteins p50 and p52. On the contrary, class II members are directly synthesised as active RelA, RelB and c-Rel.

1.6.1 Canonical pathway

In response to a cytokine stimulus (e.g. TNF, IL-1), the canonical pathway activates the I κ B kinase complex (IKK), which includes IKK α , IKK β and IKK γ (NEMO). This pathway has been shown to be NEMO and IKK β -dependent, triggering the phosphorylation of I κ B α and targeting it for ubiquitination. Following I κ B α proteasomal degradation, NF- κ B dimers are released into the nucleus, where they can bind to DNA. It is mainly associated with the nuclear translocation of RelA-containing dimers, but it is also involved in the translocation of c-Rel and p50 dimers (Shih et al., 2011) (figure 1.5).

There are numerous receptors that are involved in the activation of the canonical pathway, such as TLR, IL-1 receptors (IL-1R) and TNF receptors (TNFR) (de Winther et al., 2005). Although their mechanisms of activation are slightly different due to the recruitment of different adaptor proteins, they all share the same downstream signalling pathway. When these receptors are activated, they bind to specific adaptor proteins, such as TNFR-associated death domain protein (TRADD), which binds to TNFR; and Toll interacting protein (TOLLIP), myeloid differentiation primary response protein-88 (MyD88) and IL-1R-associated kinase (IRAK), which bind to TLR and IL-1R. Then, TNFR also binds to TRAF2 and receptor-interacting protein 1 (RIP1), whereas TLR and IL-1R activate TRAF6 (Hsu et al., 1996; Hsu et al., 1995; Lomaga et al., 1999; Naito et al., 1999). Both RIP1 and TRAF6 then become ubiquitinated, and it is known that the complex containing TRAF2 and cellular inhibitors of apoptosis 1 and 2 (cIAP-1 and 2) is responsible for the ubiquitination of RIP1 (Bertrand et al., 2008; Vince et al., 2009). The polyubiquitin chains then link NEMO, and hence, the IKK complex, with the receptor, leading to the recruitment and activation of transforming growth factor beta-activated kinase 1 (TAK1) through the adaptor proteins TAK1-binding proteins 1 and 2 (TAB1 and TAB2) (Ninomiya-Tsuji et al., 1999; Wang et al., 2001). TAK1 then phosphorylates IKK β , activating the IKK complex and triggering I κ B α degradation, inducing the nuclear translocation of RelA, p50 and c-Rel containing dimers (Hayden and Ghosh, 2008). This classical pathway has been associated with inflammatory responses and innate immunity, but also, with the regulation of cell survival (Monaco et al., 2004).

1.6.2 Non-canonical pathway

In contrast to the classical pathway, which requires the NEMO regulatory subunit, this alternative pathway seems to be NEMO-independent (Monaco et al., 2004). In addition to this, its activation is also independent on I κ B degradation, and in order for activation

to occur, p100 needs to be processed to generate p52 (Sun and Ley, 2008). Stimuli such as lymphotoxin β and CD40 activate NF- κ B inducing kinase (NIK), which is essential for the activity of non-canonical NF- κ B. IKK α is then activated by NIK, and this activation induces the phosphorylation and proteolytic processing of p100, generating p52 and p52/RelB dimers (Senftleben et al., 2001). The unphosphorylated p100 can also form dimers with RelB, but these dimers localise to the cytoplasm and are not transcriptionally active (Fusco et al., 2009) (figure 1.5).

Although p105 to p50 processing has been shown to be constitutive, p100 to p52 processing barely occurs in the absence of non-canonical activation. This is due to continuous proteasomal degradation of NIK, which maintains NIK levels low. The TRAF2/3/cIAP complex, which is a ubiquitin ligase complex, is responsible for NIK degradation (Skaug et al., 2009). The importance of this regulation has been shown using *Traf3*^{-/-} mice. These mice have increased NIK levels that trigger excessive p100 processing into p52 and constitutive non-canonical activity, leading to mouse death shortly after birth. NIK deletions in mice, however, led to phenotypic rescue (Zarnegar et al., 2008).

There are several receptors that are involved in the activation of the non-canonical pathway, such as the receptor activator of NF- κ B (RANK), CD40 and lymphotoxin- β receptor, which include a TRAF binding site (Sun, 2011). When these receptors are activated, the TRAF2/3/cIAP complex translocate to the receptor cytoplasmic domain, resulting in TRAF3 degradation in a cIAP-dependent manner. Following TRAF3 degradation, the TRAF2/cIAP complex is no longer able to interact with NIK, preventing NIK degradation. Therefore, an upregulation of NIK levels leads to the activation of p100 processing, triggering the formation of RelB and p52 dimers (Vallabhapurapu et al., 2008). The non-canonical NF- κ B pathway has been linked to the regulation of B cell maturation and adaptive immunity, and it has been shown to target proliferative genes and also, to regulate B cell proliferation (Monaco et al., 2004; Ramachandiran et al., 2015; Schumm et al., 2006). In addition to NIK activation of the non-canonical pathway, it has been observed that NIK can phosphorylate c-Rel transactivation domain, leading to its activation (Sanchez-Valdepeñas et al., 2010).

1.6.3 Crosstalk in NF- κ B signalling pathways

There are a number of upstream regulators that modulate both canonical and non-canonical NF- κ B signalling pathways, such as TRAFs and RIPs, which are involved in IKK activation (Ea et al., 2006; Tada et al., 2001). The activity of the canonical and non-canonical signalling pathways involves crosstalk, and one of the mechanisms of crosstalk that has been identified is the upregulation of *NF κ B2* expression by the canonical signalling pathway, producing more p100/p52 (Dejardin et al., 2002). Interestingly, it has also been observed that the activated canonical pathway can inhibit the non-canonical pathway in immune cells (Gray et al., 2014).

In addition to this, there is also crosstalk between NF- κ B signalling pathways and other signalling networks (Oeckinghaus et al., 2011). The IKK complex and its crosstalk with non-NF- κ B pathways has been widely studied. For instance, Notch-1 has been shown to interact directly with IKK α , activating NF- κ B (Song et al., 2008). Also, it is known that the expression of some NF- κ B subunits is Notch-dependent, and that the transcriptional regulation of specific Notch components is dependent on NF- κ B (Osipo et al., 2008). Furthermore, IKK α has been long known to target β -catenin, promoting its stabilisation (Carayol and Wang, 2006). Given the importance of NF- κ B pathways in cell survival, inflammation and immunity, studying the interaction between NF- κ B and other signalling networks will help us elucidate how NF- κ B mediates so many cellular responses.

1.6.4 Negative regulation of NF- κ B

The presence of a negative feedback loop is necessary to prevent long-term NF- κ B activity, and hence, to terminate its response (Lawrence et al., 2005). The negative feedback loops affect all different levels of the NF- κ B signalling pathway, and depending on the level, it will silence the entire NF- κ B signalling cascade or only specific target genes (Natoli and Chiocca, 2008).

At the receptor level, one of the mechanisms that negatively regulates NF- κ B signalling involves the radioprotective 105 (RP105) protein. This protein is a TLR4 homolog and, unlike TLR4, is signalling defective. High levels of TLR4 lead to a temporary upregulation of RP105, and hence, enhanced RP105 levels block the binding between TLR4 and lipopolysaccharide (LPS), inhibiting LPS-dependent NF- κ B activity (Divanovic et al., 2005).

Other negative regulators target post-translational modifications, reversing them. These include the deubiquitinating enzymes A20 and Cezanne, which have been shown to be involved in this process. A20 is synthesised upon NF- κ B stimulation, whereas Cezanne is upregulated in response to TNF stimulation. Both A20 and Cezanne target IKK activity, inhibiting it by deubiquitination. Therefore, when these molecules are induced, NF- κ B cannot be released from I κ B and remains inactive (Enesa et al., 2008; Krikos et al., 1992; Wertz et al., 2004).

There are other negative regulators that target nuclear NF- κ B activity. One example is the I κ B family member I κ B ζ . In contrast to other I κ Bs, which are degraded, this molecule is upregulated by NF- κ B-inducing stimuli (e.g. LPS, TNF and IL-1). Located in the nucleus, I κ B ζ inhibits RelA DNA binding and transactivation (Totzke et al., 2006).

Another regulator that also targets nuclear NF- κ B activity is I κ B α . Transcription of the I κ B α gene, which is dependent on NF- κ B, leads to the removal of NF- κ B from the nucleus, leading to reduced NF- κ B activity (Nelson et al., 2004) (figure 1.5). Although most studies have only studied I κ B α in the negative regulation of NF- κ B activation, I κ B β and I κ B ϵ also play a role (Brown et al., 1993; Budde et al., 2002; Demartin et al., 1993; Scott et al., 1993; Sun et al., 1993). I κ B ϵ has been shown to provide negative feedback on c-Rel and RelA, and it seems to act only on cells on the hematopoietic lineage. This supports the idea that specific I κ Bs generate selective regulation of NF- κ B responses depending on the cellular scenario (Alves et al., 2014; Oeckinghaus and Ghosh, 2009).

Although there are more negative regulators that have already been discovered, we still need to elucidate many of the mechanisms underlying NF- κ B termination. Identifying these mechanisms will be important to better understand the function of the NF- κ B signalling pathway.

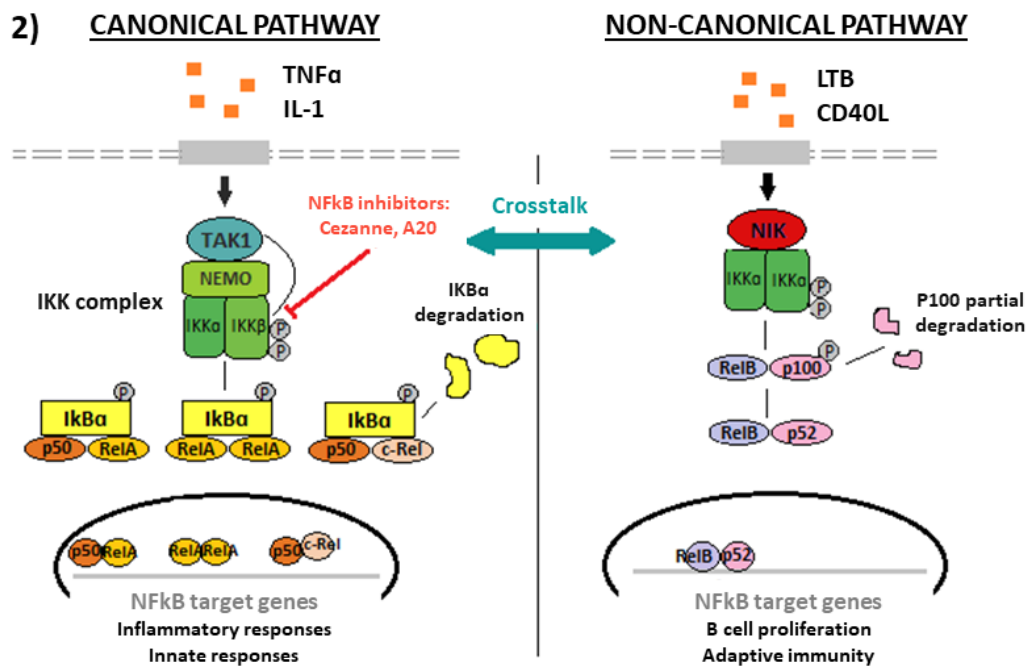


Figure 1.5. Canonical and non-canonical NF- κ B signalling pathways. Stimuli such as TNF α lead to the activation of the canonical pathway. The IKK complex, which includes NEMO, IKK α and IKK β , is then activated and leads to I κ B α degradation. This results in the nuclear translocation of dimers that contain RelA, p50 or c-Rel. The non-canonical pathway is triggered by stimuli such as CD40. NIK and IKK α are then activated, leading to the formation of p52/RelB dimers. Between the canonical and non-canonical signalling pathways, there are also mechanisms of crosstalk, such as upstream regulators that modulate both pathways. Besides, there are negative regulators of NF- κ B (e.g. Cezanne and A20), which inhibit IKK activity by deubiquitination.

1.6.5 NF- κ B and atherosclerosis

There are different lines of evidence that support that NF- κ B plays a role in atherosclerosis. First, NF- κ B can induce the expression of proinflammatory genes that contribute to the initiation and development of atherogenesis, such as cytokines, E-Selectin, VCAM-1 and ICAM-1, and it is also activated by factors that are believed to influence this disease (e.g. angiotensin II, integrin signalling and oxidised lipoproteins) (de Winther et al., 2005). Interestingly, most of the studies that have studied the role of NF- κ B in atherosclerosis have focused on the involvement of the canonical NF- κ B pathway in this disease.

Experiments *in vitro* using human aortic EC (HAEC), have shown that proinflammatory NF- κ B subunits p50 and p65 have increased activation under low shear stress, compared to HAEC exposed to high shear (Mohan et al., 1997). The presence of activated NF- κ B (p65) in atherogenic lesions in humans was first shown in 1996 (Brand et al., 1996), and it was later suggested that NF- κ B activity driving atherogenesis involved p65, p50 and c-Rel (Monaco et al., 2004). Another study demonstrated that the inhibition of NF- κ B activation in the endothelium led to reduced lesion formation in mice. This inhibition was achieved either by depleting the NEMO regulatory subunit or by expressing a dominant negative I κ B α , and it suggested that NF- κ B influences the progression of atherosclerotic lesions (Gareus et al., 2008). It has also been shown that arterial regions exposed to disturbed flow in mice have increased levels of NF- κ B subunit RelA and regulatory subunits I κ B α and I κ B β (Hajra et al., 2000). This induction of p65/RelA under disturbed flow is known to be mediated by c-Jun N-terminal kinase 1 and the downstream ATF2 (Cuhlmann et al., 2011). However, although p65 was shown to be induced under disturbed blood flow, it was inactive in the majority of EC, which suggests that p65 is primed for activation in response to a proinflammatory stimulus in regions susceptible to atherosclerosis.

Although most studies that associate NF- κ B with atherosclerosis have focused on the role of the canonical NF- κ B pathway, Paul Evans' group has recently investigated the effect of shear stress on non-canonical NF- κ B activity. In human umbilical vein EC (HUVEC), they observed that protein levels of p100, p52 and RelB were increased under low shear stress compared to high shear stress, and that the exposure to CD40L, a non-canonical NF- κ B stimulus, dramatically increased the generation of these proteins under low shear stress (Bowden et al., data not published). Furthermore, they reported that depletion of

p100 and p52 led to a decrease in EC proliferation under low shear stress, which suggests that the non-canonical NF- κ B pathway contributes to atherosclerosis by inducing endothelial proliferation. Although p52 had already been described as a regulator of cell proliferation, its role in the endothelium had not been investigated before. In human osteosarcoma cells, it was shown that p52 regulated cell proliferation by modulating Cyclin D expression and repressing p21 (Schumm et al., 2006). Thus, p52 regulation of Cyclin D and p21 could explain the link between p52 and EC proliferation in arteries.

In addition to the regulation of atherosclerosis development by the canonical and non-canonical NF- κ B pathways, negative regulators of NF- κ B have also been shown to play a role in this disease. The expression of the negative regulator Cezanne has been observed to be decreased in regions exposed to disturbed flow in the porcine aorta (Passerini et al., 2004). Also, increased levels of A20, a negative regulator of NF- κ B, have been revealed to decrease lesion size in mice, whereas A20 haploinsufficiency led to increased expression of proinflammatory genes involved in atherogenesis, such as VCAM-1 and ICAM-1 (Wolfrum et al., 2007). Another study showed that suppression of the negative regulator miR-10a in HAEC, promoted inflammation under disturbed blood flow by inducing I κ B α degradation and RelA nuclear localisation (Fang et al., 2010).

Although most studies have described the atherogenic effects of NF- κ B, this family of transcription factors has also been shown to induce anti-apoptotic, cytoprotective and anti-inflammatory genes (Warboys et al., 2011). Experiments using cultured EC showed that NF- κ B induction of anti-apoptotic and cytoprotective molecules such as Bcl-2, A1, manganese superoxide dismutase (MnSOD) and GADD45 β is unaltered by high shear stress, whereas NF- κ B induction of proinflammatory molecules (e.g. VCAM-1, E-Selectin and IL-8) is suppressed by high shear stress (Partridge et al., 2007). Therefore, this suggests that high shear stress prevents inflammation by reducing NF- κ B induction of inflammatory molecules, while NF- κ B-dependent cytoprotection is preserved.

The NF- κ B-mediated suppression of inflammatory responses may be related to the induction of the transcription factor KLF2. In EC exposed to high shear, KLF2 downregulates E-Selectin and VCAM-1, preventing endothelial cell activation. KLF2 has been revealed to sequester cofactors of NF- κ B transcription (e.g. p300), and therefore, it could limit proinflammatory responses by reducing NF- κ B-dependent transcription under high shear stress (SenBanerjee et al., 2004; Wang et al., 2006).

In spite of an increasing amount of data about the role of the transcription factor NF- κ B in the pathogenesis of atherosclerosis, the role of the NF- κ B subunit c-Rel in endothelial cell biology and the effect of shear stress on c-Rel is still unclear.

1.7 c-Rel

1.7.1 Overview of c-Rel biology

c-Rel plays critical roles in mammalian lymphoid cell activity and in different diseases (Gilmore and Gerondakis, 2011), such as cancer and lymphomas, fibrosis and autoimmune diseases. It was first identified as the cellular homologue of v-Rel (Rice et al., 1986), an oncoprotein that is encoded by avian rev-T retrovirus and that generates leukaemia and lymphoma in birds (Zhang et al., 1991). c-Rel, although less aggressive, has also been shown to produce transformation of chicken cells *in vitro*, leading to the formation of tumours (Gilmore et al., 2001).

c-Rel structure is notably similar to both RelA and RelB, since they all present a C-terminal transactivation domain and a N-terminal Rel homology domain (Perkins, 2007). c-Rel also presents a central transactivation inhibitory domain, and human c-REL protein presents 587 amino acids (figure 1.6). It has been shown to form homodimers and heterodimers with RelA and p52, but in most cells, it is associated with p50 (Gilmore and Gerondakis, 2011). Although several protein modifications of c-Rel have been identified, it is still not clear whether these have any effect on c-Rel function. Posttranslational modifications in c-Rel include phosphorylation in both the N-terminus and transactivation domain (Martin and Fresno, 2000; Mosialos et al., 1991), since they contain serine phosphorylation sites, and ubiquitination (Liu et al., 2016). Alternative splicing can also modify c-Rel function by partially removing c-Rel transactivation inhibitory domain, increasing c-Rel activity and DNA-binding (Gilmore and Gerondakis, 2011).

Although c-Rel has many important functions in the regulation of apoptosis and cell growth, *c-Rel* knockout (*c-Rel*^{-/-}) mice are viable and have a seemingly normal development, although they show a deficiency in lymphocyte proliferation and activation (Kontgen et al., 1995a). This allows the study of c-Rel in the immune system and in multiple disease processes.

1.7.2 c-Rel function in B cells and T cells

Upon stimulation, c-Rel induces proliferation and activation of B cells. Consistently, *c-Rel* knockout mice show defects in B cell proliferation that has been associated with a cell cycle arrest in G1 phase (Feng et al., 2004; Grumont et al., 1998). This could be mediated by Irf-4, a protein that binds c-Rel/p50 dimers, induces B cell proliferation, and that is also downregulated in *c-Rel* knockout mice (Grumont and Gerondakis, 2000). Other molecules that could regulate c-Rel-induced proliferation include E2F3a and cyclin E (Feng et al., 2004). c-Rel also regulates B cell apoptosis by inducing expression of A1, a Bcl-2 homologue (Grumont et al., 1999b). Bcl-2 and Bcl-xL can also rescue *c-Rel* knockout B cells from apoptosis (Grumont et al., 1998; Owyang et al., 2001). In conclusion, c-Rel protects B cells from cell death via A1, Bcl-2 and Bcl-xL and promotes proliferation via Irf-4, E2F3a and cyclin E.

Upon stimulation, c-Rel regulates proliferation and activation of T cells (Bunting et al., 2007). IL-2, a cytokine involved in T cell activation, is upregulated by c-Rel by enhancing IL-2 transcription (Kontgen et al., 1995a; Rao et al., 2003), and therefore, *c-Rel* knockout mice present impaired IL-2 production and immunodeficiency (Kontgen et al., 1995a). c-Rel has also been involved in the development of Th17 cells. This can occur via IL-21 (Chen et al., 2010), although other mechanisms that involve c-Rel but not IL-21 have also been observed (Ruan et al., 2011a). Besides, c-Rel has been involved in the regulation of Foxp3 transcription in regulatory T cells (Tregs), by increasing Foxp3 expression together with Jun B (Son et al., 2011).

Since c-Rel is important for both T cells and B cells, abnormal expression of c-Rel might lead to immunological disorders such as lymphomas. The *REL* gene is located at chromosome 2p13, and this region has been shown to be amplified in many different B cell lymphomas (Barth et al., 2003; Li et al., 2015; Weniger et al., 2007). Besides, higher levels of nuclear c-REL have been associated with a worse outcome in specific subsets of patients with this disorder (Li et al., 2015) (figure 1.6).

Furthermore, recent analyses using conditional knockout mice have provided new insights into the functions of NF- κ B subunits in B and T-cell subsets. In B cells, B cell-specific *c-Rel* deletion has been demonstrated to impair the formation of germinal centres (GC), which produce memory B cells and plasma cells that generate high-affinity antibodies (Maja et al., 2016). GC-specific deletion of *c-Rel* triggered the collapse of GC,

due to impaired activation of metabolic programmes that induce cell growth. On the contrary, while RelA is not necessary for GC maintenance, it was shown to be required for the generation of GC-derived plasma cells (Heise et al., 2014). GC-specific deletion of both *NF-κB2* and *RelB*, but not of the single genes, also triggered the collapse of GC (De Silva et al., 2016), which is similar to what happens when *c-Rel* is deleted. These studies show that individual NF-κB subunits have different roles in GC and B cells, and therefore, understanding these roles could provide an insight into how individual NF-κB subunits contribute to the development of B cell tumours.

In T cells, conditional deletion of *c-Rel* in Tregs has been shown to compromise thymic Treg development, whereas RelA is critical for mature Treg identity (Oh et al., 2017). Also, Treg-specific *c-Rel* deletion has been observed to impair the maintenance of activated Tregs, a subset of cells that is present at sites of tumours, leading to a reduction in melanoma growth (Grinberg-Bleyer et al., 2017). Conditional deletion of *NF-κB2* in Tregs, however, has revealed a critical role of NF-κB2 in maintaining Treg homeostasis, achieved through the inhibition of RelB-containing complexes (Grinberg-Bleyer et al., 2018). Altogether, these studies show that an appropriate balance of NF-κB activity is necessary for the maintenance of Treg cell function and activity, demonstrating its importance for an adequate immune response.

1.7.4 c-Rel and autoimmune diseases

There is some evidence that suggests that c-Rel plays a role in various autoimmune diseases. In a mouse model of inflammatory bowel disease, it has been shown that *c-Rel* knockout mice do not develop the disease due to a lack of production of IL-23 (Wang et al., 2008). c-Rel has also been suggested to contribute to some types of rheumatoid arthritis by inducing IL-21, which promotes cell proliferation (Niu et al., 2010). On the other hand, overexpression of c-Rel protects against diabetes by inducing miR-21, which decreases islet apoptosis (Mokhtari et al., 2009; Ruan et al., 2011b) (figure 1.6).

1.7.5 c-Rel and cancer

c-Rel may influence some types of breast cancer. This disease has been associated with increased c-Rel expression and nuclear localisation (Belguise and Sonenshein, 2007). c-Rel has also been shown to increase proliferative genes that can lead to aberrant proliferation, such as cyclin D1 (Belguise and Sonenshein, 2007). Also, in some head and neck carcinomas, the expression of ΔNp63α (a p53 family member) and Tap73 (tumour

suppressor) is decreased by c-Rel, leading to uncontrolled proliferation (Lu et al., 2011). However, c-Rel has also been suggested to inhibit tumour formation. In specific types of gastric cancer, *c-Rel* knockout mice are more susceptible to tumorigenesis, developing lesions that showed increased proliferation (Burkitt et al., 2013). This was also observed in some colon adenocarcinomas, where *c-Rel* knockout mice presented more and larger lesions compared to wildtype (WT) mice, and they also had increased proliferation (Burkitt et al., 2015). The molecular mechanisms underlying the tumour-promoting versus tumour-protecting effects of c-Rel remain unknown (figure 1.6).

1.7.6 *c-Rel* and fibrosis

c-Rel has been implicated in fibrosis in several systems, including liver, heart and skin. After chronic liver injury, *c-Rel* knockout mice have been observed to present reduced fibrosis (Gielsing et al., 2010). Also, hepatocyte proliferation was decreased in these mice following toxic liver injury, due to decreased generation of FoxM1, Cdc25 and cyclin B1 (Gielsing et al., 2010). Altogether, these results suggest that c-Rel plays a role in both liver fibrosis and regeneration after an injury.

In the heart, c-Rel has been shown to influence fibrosis and cardiac hypertrophy after chronic treatment with angiotensin in mice, by controlling both Gata4 and myocyte enhancer factor 2A (Mef2A) (Gaspar-Pereira et al., 2012). Correspondingly, it has also been observed that c-REL nuclear localisation increases in failing human hearts (Gaspar-Pereira et al., 2012).

c-Rel has also been implicated in the induction of skin fibrosis in mice, by inducing keratinocyte proliferation. In this study, skin samples from humans with psoriasis and systemic sclerosis also showed altered expression of c-REL compared to healthy samples (Fullard et al., 2013) (figure 1.6).

1.7.7 *c-Rel* and the nervous system

c-Rel has been shown to play a role in neuronal survival and neuroinflammation. Unlike RelA, which contributes to neuronal apoptosis (Ingrassia et al., 2012), c-Rel has protective effects by preventing neuronal cell death, by inducing Bcl-xL and the transcription of MnSOD (Bernard et al., 2001; Sarnico et al., 2009). Also, c-Rel has been observed to limit ischemic injury, and its deficiency has led to neurodegeneration in mice (Bauguera et al., 2012). Besides, some studies have shown that c-Rel is important for long

term memory, as well as other genes to which c-Rel can bind, such as Fos, Egr1 and Mkp-3 (Ahn et al., 2008; Levenson et al., 2004) (figure 1.6).

1.7.8 c-Rel and atherosclerosis

In 2012, a study using *ApoE* knockout mice suggested that suppression of *c-Rel* expression by small interfering RNA (siRNA) led to reduced stress-induced atherosclerotic lesions by inhibiting proinflammatory gene expression (Djuric et al., 2012). However, the authors did not validate siRNA-suppression of *c-Rel* in vascular tissue, which complicates the interpretation of their data. Thus, the siRNAs effects observed in this study could be due to off-target effects, and/or gene-silencing could be affecting other tissues (e.g. liver) and influencing atherosclerosis indirectly. This study does however generate numerous questions about the role of c-Rel in atherosclerosis, and hence, further investigation is clearly needed to determine whether c-Rel is involved in this disease.

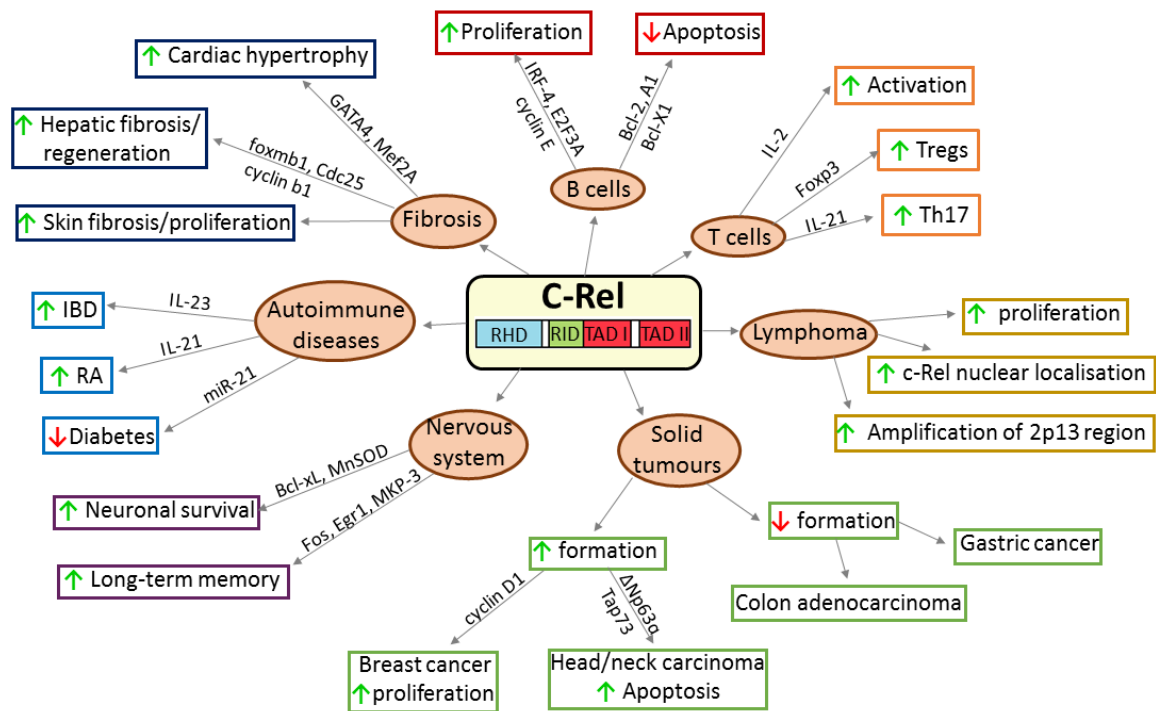


Figure 1.6. The role of c-Rel in the immune system and disease. c-Rel presents a N-terminal Rel homology domain (RHD), a Rel inhibitory domain (RID), and a C-terminal transactivation domains (TADI/TADII). It controls proliferation and activation of B and T cells, and it has been shown to have a key role in the development of Tregs and the generation of Th17. C-Rel is also involved in a number of autoimmune diseases, such as rheumatoid arthritis and inflammatory bowel disease, as well as in several B cell lymphomas. Moreover, it has been linked to different types of cancer, by suppressing (e.g. gastric cancer) and promoting tumour formation (e.g. breast cancer, head/neck adenocarcinoma). In the nervous system, it is essential for long-term memory and it induces neuronal survival. c-Rel also plays a role in several fibrotic processes, contributing to hepatic/skin fibrosis and cardiac hypertrophy by promoting cell proliferation.

1.8 Project rationale and hypothesis

Here, I have analysed how shear stress regulates the expression and activity of NF- κ B transcription factors in EC during atherosclerosis. Although various studies have implicated NF- κ B in the development of atherosclerosis (Brand et al., 1996; Cuhlmann et al., 2011; Monaco et al., 2004) not all NF- κ B subunits have been studied in detail. The role of RelA and p50 in this disease has been extensively studied (Cuhlmann et al., 2011; Mohan et al., 1997), and also, our group has recently reported that p52 and p100 induce proliferation under low shear stress (Bowden et al., data not published). However, I have focused on the potential role of c-Rel in endothelial mechanobiology and atherosclerosis, a subject that was poorly understood.

Since several NF- κ B subunits respond to shear stress and contribute to atherosclerosis, and c-Rel plays a role in the control of proatherogenic processes such as cell proliferation, apoptosis and inflammation in numerous cell types, I hypothesise that c-Rel is regulated by shear stress in the endothelium, and that it influences EC physiology and atherogenesis by altering EC survival and inflammation.

1.9 Project aims

The aims of the project are to:

- 1. Investigate the effect of shear stress on c-Rel expression *in vitro* using cultured EC.
- 2. Define the effect of shear stress on c-Rel expression *in vivo* in murine and porcine models.
- 3. Elucidate c-Rel function in EC exposed to shear stress *in vitro* and *in vivo*.
- 4. Assess whether c-Rel influences atherosclerosis by genetic deletion approaches using a murine model.

Chapter 2. Methods

2.1 Mouse licensing

All animal work was performed in the UK under the Animal (Scientific Procedures) Act 1986 (ASPA). The experiments were licensed by the UK Home Office (Project License Number P5395C858).

2.2 *En face* staining of murine vascular endothelium

2.2.1 *Mouse sacrifice*

C57BL/6J mice between 6-12 weeks of age were given intraperitoneal injections of 100 µl pentobarbital. When animals stopped showing pedal withdrawal reflex, the mouse chest was dissected using forceps and scissors in order to reveal the heart and other organs. The vasculature was then perfused with 10 ml phosphate buffered saline (PBS) and then fixed by injecting 4% (w/v) paraformaldehyde (PFA) (VWR Chemicals) in PBS through the left ventricle by cardiac puncture. After perfusion fixation, a cut was made around the ribcage and through the diaphragm, and the ribcage was placed into a bijoux tube containing 4% (w/v) PFA for 30 minutes.

2.2.2 *Aortic dissection*

Using fine forceps, the murine aorta was gently lifted and detached from the spinal cord, moving along the spine towards the top of the ribcage. Surrounding organs such as lungs, oesophagus, trachea, thymus and heart were removed by blunt dissection, using a Petri dish containing PBS. Fat and connective tissue were then removed in order to expose the aortic arch, and the vena cava was also separated from the aorta. Once cleaned, intercostal vessels were cut using spring scissors, and the adventitia layer was also removed. The aorta was dissected into two segments, the aortic arch and the descending aorta. The brachiocephalic artery was cut from the aortic arch segment making a V-shaped cut, and the aortic arch was then opened by cutting along the outer curvature. After opening the aortic segments, they were stored in PBS at 4°C until staining (figure 2.1).

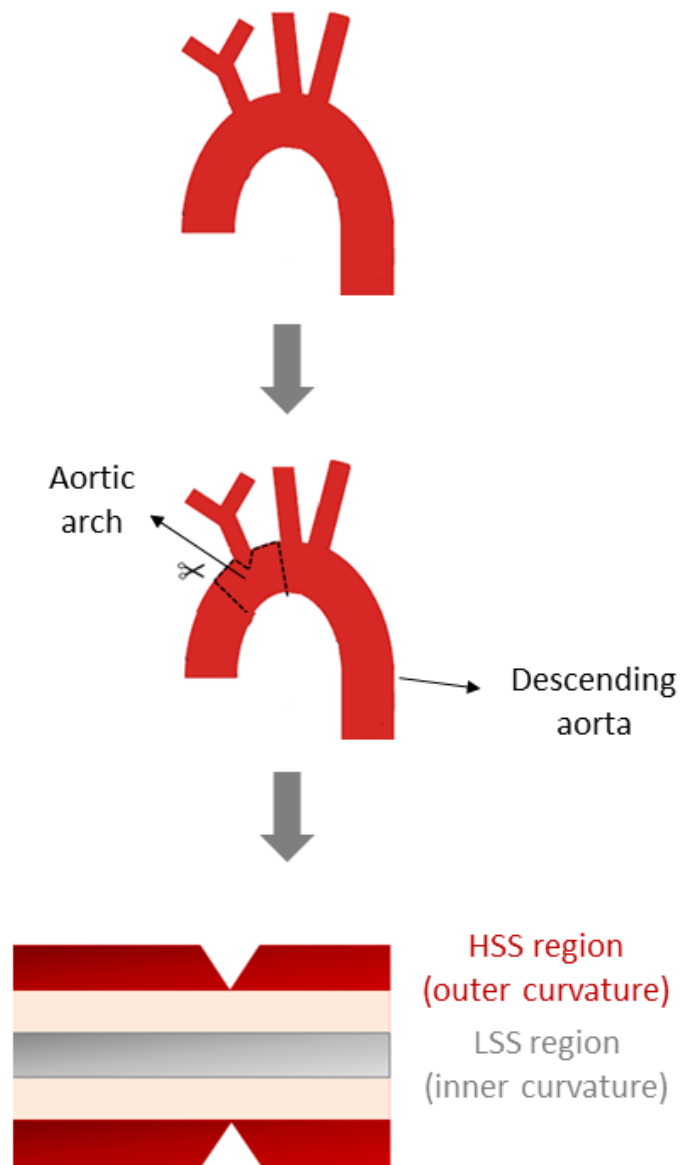


Figure 2.1. Aortic opening/dissection for *en face* staining of the murine endothelium. After aortic dissection, the brachiocephalic artery was removed from the aortic arch. The aortic arch, which presents an inner curvature exposed to disturbed flow and low shear stress (LSS) and an outer curvature exposed to high shear stress (HSS), was then opened by cutting along the outer curvature. Once opened, aortic segments were stained using antibodies and mounted for confocal microscopy.

2.2.3 En face staining of murine vascular endothelium

Aortic segments were placed within separate wells of a 96-well plate, and they were permeabilised using 0.5% (v/v) triton-X (Sigma-Aldrich)/ 20% (v/v) goat serum (Sigma-Aldrich) in PBS at 4°C overnight. The segments were then washed three times in PBS for 10 minutes, and they were incubated with 1 µg/µl of the selected primary antibody (see appendix 1) and 1 µg/µl CD31 antibody in 5% (w/v) bovine serum albumin (BSA) (Sigma-Aldrich)/ 0.1% (v/v) triton-X/PBS at 4°C for three days. Simultaneously, other segments were incubated with 1 µg/µl isotype IgG control antibodies (Sigma-Aldrich), to control for unspecific binding. Segments were washed three times in PBS for 10 minutes, and they were incubated with the selected secondary antibody (Alexa Fluor 568 goat anti-rabbit IgG and Alexa Fluor 488 donkey anti-rat IgG) (Life Technologies) diluted 1:300 in 5% (w/v) BSA/0.1% (v/v) triton-X/PBS at 4°C overnight, protected from light. Aortic segments were then washed three times in PBS for 10 minutes, and stained with TO-PRO-3 iodide (Life Technologies) diluted 1:300 in PBS for 2 h at room temperature for nuclear staining. By using Prolong gold anti-fade reagent (Thermo Fisher Scientific), aortic segments were mounted on a microscopy slide and covered with a coverslip, and nail polish was applied on each corner of the glass coverslip. Microscopy slides were left overnight at 4°C weighted with a small weight in order to keep aortic segments flat while drying. A Confocal LSM510 NLO inverted microscope (Zeiss) with a 63x (numerical aperture 1.4) oil immersion objective was then used to image Alexa Fluor 568 (543 laser), Alexa Fluor 488 (488 laser) and TO-PRO-3 nuclear stain (633 laser) at the outer and inner curvature and the descending aorta. Results were normalised to the isotype IgG control. ImageJ software was used to calculate mean fluorescence intensity in various cells in different fields of view.

2.3 Mouse breeding

2.3.1 Genotyping

DNA was extracted from ear tissue in order to analyse the genotype of mice. To do this, 50 µl of ear clip lysis reagent (1M Tris-HCl (pH 8.5), 10% (v/v) Tween 20, 0.5M EDTA (pH 8.0)) and 300 µg/ml proteinase K (Thermo Fisher Scientific) were added to each ear notch, followed by incubation at 56°C overnight. After incubation at 56°C, ear notches were incubated at 100°C for 10 minutes to inactivate the proteinase K. 600 µl of sterile distilled water was added to the samples, and a standard polymerase chain reaction (PCR) was then carried out. The PCR reaction mix had a total volume of 25 µl, and it contained

1X PCR buffer (Qiagen), 100 μ M dNTPs (Thermo Fisher Scientific), 0.15 μ M of forward and reverse gene-specific primers (table 2.1), 0.75 units/25 μ l Taq DNA polymerase (Qiagen) and a variable volume of earclip DNA and sterile distilled water. Using a thermal cycler (Veriti™ 96-well Thermal Cycler, Thermo Fisher Scientific) the reaction mix was incubated at 95°C for 5 minutes, which was followed by thermal cycling (35 repeats) at 95°C for 30 s, an annealing stage at 56°C for 30 s and an extension stage at 72°C for 1 minute. The final step consisted of 10 minutes at 72°C. PCR product was analysed by electrophoresis using an agarose gel (2% (w/v) agarose in 1x Tris-acetate-EDTA (TAE) buffer with ethidium bromide (Sigma)) submerged in TAE buffer. Samples were loaded using DNA loading dye (Thermo Fisher Scientific) and ran alongside quick-Load Purple Low Molecular Weight DNA Ladder (New England BioLabs). The gel was run for 80 minutes using the following settings: Voltage- 85, Current- 200 mA, Watt- 200. It was then imaged using the InGenius3 gel imaging system (Syngene) and analysed using the Genesys software (Syngene).

Primer name	Primer sequence	Expected product size
<i>c-Rel</i> WT forward	GTACTGCATCAACTGCATGAC	<i>c-Rel</i> floxed: 661 bp <i>c-Rel</i> WT: 324 bp
<i>c-Rel</i> WT Reverse	CAGAGACTAACACGTGGTA	
<i>c-Rel</i> floxed reverse	GACCACTACCAGCAGAACAC	
<i>Cdh5-Cre</i> forward	AGTGCGTTCGAACGCTAGAG	Cre positive \approx 350 bp
<i>Cdh5-Cre</i> reverse	TCGATGCAACGAGTGATGAG	

Table 2.1. PCR genotyping information. After extracting DNA from ear tissue, gene-specific primers were used to analyse the genotype of mice.

2.3.2 *Cdh5-Cre-ER^T* transgenic model

The *Cdh5-Cre-ER^T* transgenic mouse model was generated in Ralf Adams' laboratory (London Research Institute) (Sorensen et al., 2009). In order to generate this transgenic model, a transgene which included a *Cdh5* promoter fragment fused to a *Cre-ER^T* cDNA was injected into mouse C57BL/6J embryos, and these were then backcrossed with C57BL/6J to develop heterozygous mice for the *Cdh5-Cre-ER^T* gene. *Cdh5*, which is also known as VE-cadherin, is an endothelial cell-specific gene. Therefore, in order to obtain mice expressing tamoxifen-inducible *Cre-ER^T* recombinase specifically in the

endothelium, a model expressing a Cre recombinase ER^T under the control of the *Cdh5* gene promoter was used. 50 μ l of 40 mg/ml tamoxifen (T5698, Sigma-Aldrich) dissolved in 9:1 corn oil (C8267, Sigma-Aldrich): ethanol mixture ratio was then given to the mice by intraperitoneal injection for 5 days, leading to the activation of $Cre-ER^T$. The activation of $Cre-ER^T$ leads to a Cre-mediated excision at the LoxP sites.

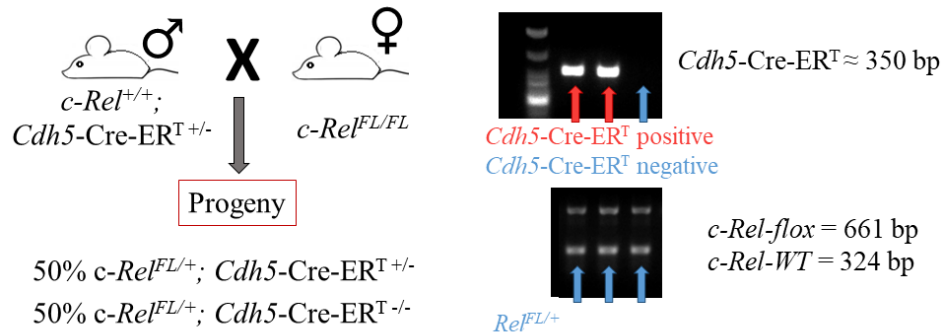
2.3.3 Breeding of *Cdh5-c-Rel^{KO}* (*c-Rel-EC^{KO}*) mice

To generate conditional EC-specific *c-Rel* knockout (KO) mice, *c-Rel* floxed homozygous female mice (*c-Rel^{FL/FL}*), which contains loxP and FRT sites flanking exon 1 of the *Rel* gene (from Ulf Klein's laboratory) were bred with heterozygous *Cdh5-Cre-ER^T* male mice (*c-Rel^{+/+}; Cdh5-Cre-ER^T +/-*). Genotyping of these mice (as above 2.3.1) revealed that this breeding step generated 50% of *c-Rel^{FL/+}; Cdh5-Cre-ER^T +/-* mice, which are mice that are heterozygous for the *c-Rel* allele and also for the *Cdh5-Cre-ER^T* allele, and 50% of *c-Rel^{FL/+}; Cdh5-Cre-ER^T -/-* mice. *c-Rel^{FL/+}; Cdh5-Cre-ER^T +/-* male mice were then used for the second breeding step (figure 2.2A).

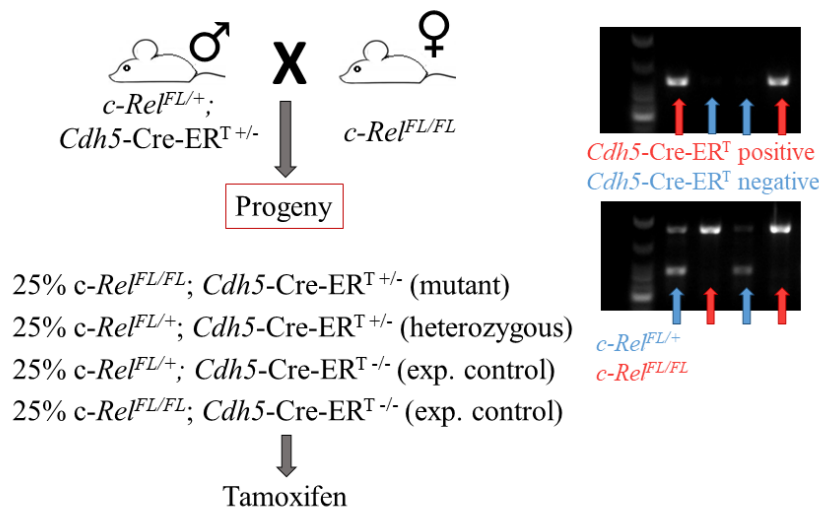
In the second breeding step, *c-Rel^{FL/+}; Cdh5-Cre-ER^T +/-* male mice were back crossed with *c-Rel* floxed homozygous female mice (*c-Rel^{FL/FL}*) in order to obtain mice containing both *Rel* alleles floxed, and hence, to ensure loss of c-Rel function in the endothelium. The progeny generated was 25% *c-Rel^{FL/FL}; Cdh5-Cre-ER^T +/-* mice (mutants), 25% *c-Rel^{FL/+}; Cdh5-Cre-ER^T +/-* mice (heterozygous); 25% *c-Rel^{FL/+}; Cdh5-Cre-ER^T -/-* mice (experimental controls) and 25% *c-Rel^{FL/FL}; Cdh5-Cre-ER^T -/-* mice (experimental controls) (figure 2.2B).

Once these mice were generated, *c-Rel^{FL/FL}; Cdh5-Cre-ER^T +/-* mice and experimental controls were treated with tamoxifen as explained in 2.3.2, leading to the activation of $Cre-ER^T$. Since the LoxP sites flank exon 1 of the *Rel* gene, LoxP sites deletion generated an endothelial-specific *c-Rel* null allele, giving rise to *Cdh5-c-Rel^{KO}* mice (*c-Rel-EC^{KO}*) (figure 2.2C).

A Breeding step 1



B Breeding step 2



C

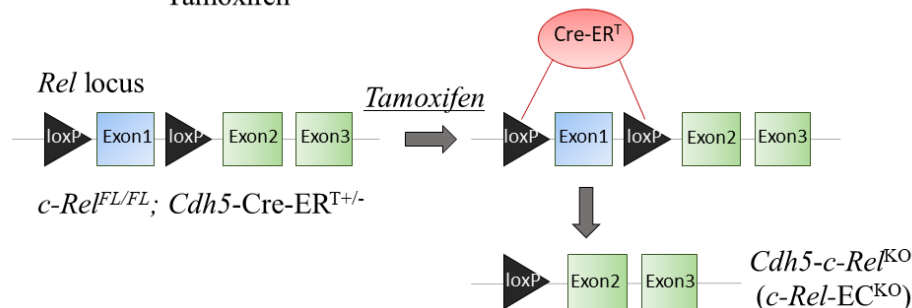


Figure 2.2. Generation of *Cdh5-c-Rel*^{KO} (*c-Rel-EC*^{KO}) mice. **A)** $c-Rel^{FL/+}; Cdh5-Cre-ER^{T+/-}$ males were crossed with $c-Rel^{FL/FL}$ females, generating an expected progeny of 50% $c-Rel^{FL/+}; Cdh5-Cre-ER^{T+/-}$ mice and 50% $c-Rel^{FL/+}; Cdh5-Cre-ER^{T-/-}$ mice. Genotyping of this mice revealed that all mice were heterozygote for the *c-Rel* floxed allele, containing the WT allele (324 bp) and the *c-Rel* floxed allele (661 bp). Approximately 50% of the progeny expressed *Cdh5-Cre-ER*^T (≈ 350 bp). **B)** When the second breeding step was performed, $c-Rel^{FL/+}; Cdh5-Cre-ER^{T+/-}$ males were backcrossed with $c-Rel^{FL/FL}$ females, giving rise to 25% $c-Rel^{FL/FL}; Cdh5-Cre-ER^{T+/-}$ (mutants), 25% $c-Rel^{FL/+}; Cdh5-Cre-ER^{T+/-}$ (heterozygous), 25% $c-Rel^{FL/+}; Cdh5-Cre-ER^{T-/-}$ (experimental controls) and 25% $c-Rel^{FL/FL}; Cdh5-Cre-ER^{T-/-}$ (experimental controls). **C)** Following tamoxifen injections, *Cdh5-Cre-ER*^T activity was switched on. This led to a Cre-mediated excision at the LoxP sites flanking exon 1 of the *Rel* gene, deleting *c-Rel* specifically in endothelial cells and generating *c-Rel-EC*^{KO} mice.

2.4 Induction of hypercholesterolemia in C57BL/6J mice

12 week old C57BL/6J mice were injected 6×10^{12} pfu of an adeno-associated virus (AAV) which contained mutated proprotein convertase subtilisin/kexin type 9 (rAAV8-D377Y-mPCSK9) by a single intraperitoneal injection. This version of PCSK9 contained a gain-of-function mutation, leading to the induction of hypercholesterolemia. 5 days after the single intraperitoneal injection, C57BL/6J mice were exposed to a high fat Western diet (SDS, 829100) for 6 weeks (diet content is described in table 2.2).

Diet components	Weight percentage
Sucrose	33.9
Anhydrous milk fat	20.0
Casein	19.5
Maltodextrin	10.0
Cellulose	5.0
Corn starch	5.0
AIN-76A-MX	3.5
AIN-76A-VX	1.0
Corn oil	1.0
Calcium carbonate	0.4
L-cysteine	0.3
Choline bitartrate	0.2
Cholesterol	0.15
Antioxidant	0.01

Table 2.2. Western diet composition. C57BL/6J mice were given a high fat Western diet for 6 weeks, following injection of an adeno-associated virus containing PCSK9.

2.5 Analysis of plasma lipids

C57BL/6J mice treated with AAV-PCSK9 were killed by intraperitoneal injections of 100 μ l pentobarbital. Following this, cardiac puncture was performed to collect blood using a heparin-coated syringe, and it was kept in individual 1.5 ml Eppendorf tubes until plasma collection was performed. To obtain plasma samples from the collected blood, 1.5 ml Eppendorf tubes were centrifuged at 2000 g for 5 minutes. After centrifugation, the supernatant (plasma) was collected and kept at -80°C until analysis of triglycerides and cholesterol was performed at the Clinical Chemistry Department at the Royal Hallamshire Hospital (Sheffield).

2.6 Oil red O staining and lesion analysis

C57BL/6J mice treated with AAV-PCSK9 were killed using pentobarbital as above. After mouse and aortic dissection (as described in 2.2), the aortas were cut along the outer curvature, they were fixed in 2% (w/v) PFA overnight, and they were kept in PBS at 4°C until oil red O staining was performed to analyse lesion coverage. To prepare Oil Red O stock solution, 0.3 g ORO powder (Sigma-Aldrich) was dissolved in 100 ml 100% (v/v) isopropanol. The solution was filtered using Whatman number 1 filter paper and 0.22 µm filter, and it was kept in the fridge until the working solution was prepared. To prepare Oil Red O working solution (which should be used within two hours of preparation), the stock solution was diluted 6:4 using sterile distilled water and it was left at room temperature for 10 minutes. Once this was prepared, each aorta was incubated with 60% (v/v) isopropanol for 2 minutes and then stained using 60% (v/v) Oil Red O working solution for 10-15 minutes. Aortas were then rinsed in 60% (v/v) isopropanol for 2 minutes, followed by distilled water. Aortas were stored in PBS at 4°C until imaging was performed. To perform imaging, aortas were placed on plates covered with wax, and they were imaged through a Stemi 2000 C microscope (Zeiss) using a Canon PowerShot A650 IS digital camera. Once the images were taken, the lesion area of the aorta was measured using the imaging software NIS-Elements BR (Nikon).

2.7 Partial ligation of the left carotid artery (LCA) in *ApoE* knockout mice

Partial ligation was carried out by Andreas Schober's laboratory (Ludwig-Maximilians University of Munich, Munich, Germany).

In order to establish causal relationships between flow and genes of interest *in vivo*, partial ligation of the left carotid artery was performed in *ApoE* knockout C57BL/6J mice between 6-8 weeks of age as previously described (Nam et al., 2009). Mice were given intraperitoneal injections of 10 mg/kg xylazine/80 mg/kg ketamine, and after disinfecting the area of interest, a ventral incision of 5 mm was made in the mouse neck. Partial ligation of the left carotid artery was carried out by closing the external, internal and the occipital artery impeding blood outflow with silk suture, whereas the superior thyroid artery was left open. The right carotid artery was used as a control and was sham-operated, and the ventral incision was then closed (figure 2.3). Mice were fed a high-cholesterol (0.15%) diet for 6 weeks and they were killed by CO₂ inhalation. After perfusion with PBS with 10 U/ml heparin (Sigma-Aldrich) through the left ventricle of the heart, the left

and right carotid artery were cleaned from surrounding adipose tissue. 150 µl of QIAzol lysis reagent (Qiagen) was then injected into the carotid lumen for several seconds, and miRNeasy mini kit (Qiagen) was then used to isolate mRNA following manufacturer's protocol. *C-Rel* mRNA expression in the left and right carotid artery was then compared and assessed by quantitative reverse transcriptase PCR (qRT-PCR). *c-Rel* mRNA expression was normalised by measurement of hypoxanthine-guanine phosphoribosyltransferase (*Hprt*).

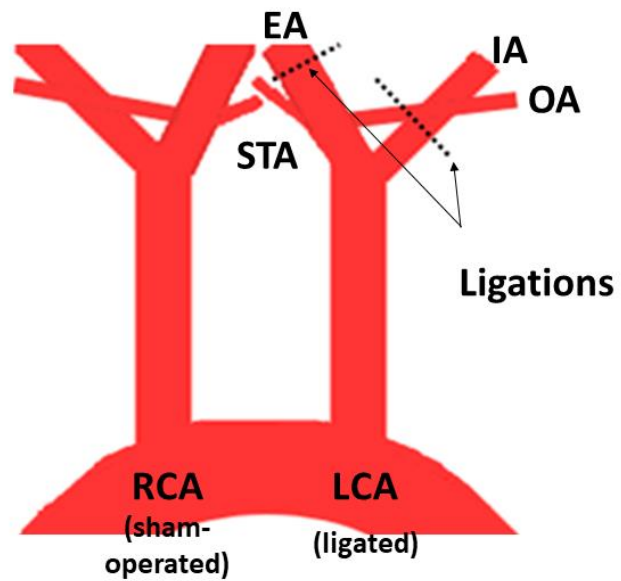


Figure 2.3. Partial ligation of the left carotid artery (LCA) in *ApoE* knockout mice. The external (EA), internal (IA) and occipital (OA) carotid artery on the LCA were ligated and closed, whereas the superior thyroid artery (STA) was left open. Partial ligation induces disturbed flow and low shear stress in the LCA. However, the sham-operated right carotid artery (RCA) is exposed to high shear stress.

2.8 Endothelial cell isolation from porcine aortas

Porcine aortas from approximately 6 month old pigs were collected from a local abattoir within 30 minutes of slaughter. They were immediately transported to the laboratory in ice-cold transport media, which contained 500 ml of Dulbecco Modified Eagle Medium (DMEM) (Lonza), 100 U/ml penicillin (Gibco), 100 µg/ml streptomycin (Gibco) and 100 µg/ml gentamycin (Gibco).

Prior to aortic dissection, RNaseZap Solution (Thermo Fisher Scientific) and 70% (v/v) industrial methylated spirit (IMS) (Fisher Scientific) were sprayed onto laboratory surfaces and dissection tools. Porcine aortas were washed in ice-cold PBS, and they were then cleaned from surrounding adipose and connective tissue using forceps and scissors, avoiding direct manipulation to prevent aortic damage. The aortic arch was then cut along the outer curvature in order to expose the lumen, and a shear stress map generated in the Evans laboratory (Serbanovic-Canic et al., 2017) was used to identify low and high shear stress areas. Low and high shear stress regions were dissected using a scalpel blade, and they were put lumen-side down onto 1 mg/ml collagenase (Roche) in M199 medium for 10 minutes at room temperature. The collagenase solution was then collected into a tube and the endothelial layer was scraped from the lumen using a scalpel blade (Figure 2.4).

After transferring the scrapes into the tube containing the collagenase solution, EC were centrifuged for 6 minutes at 1000 rpm and supernatant was then removed. Trizol reagent (Thermo Fisher Scientific) was used to isolate total RNA from the EC pellet, according to manufacturer's protocol.

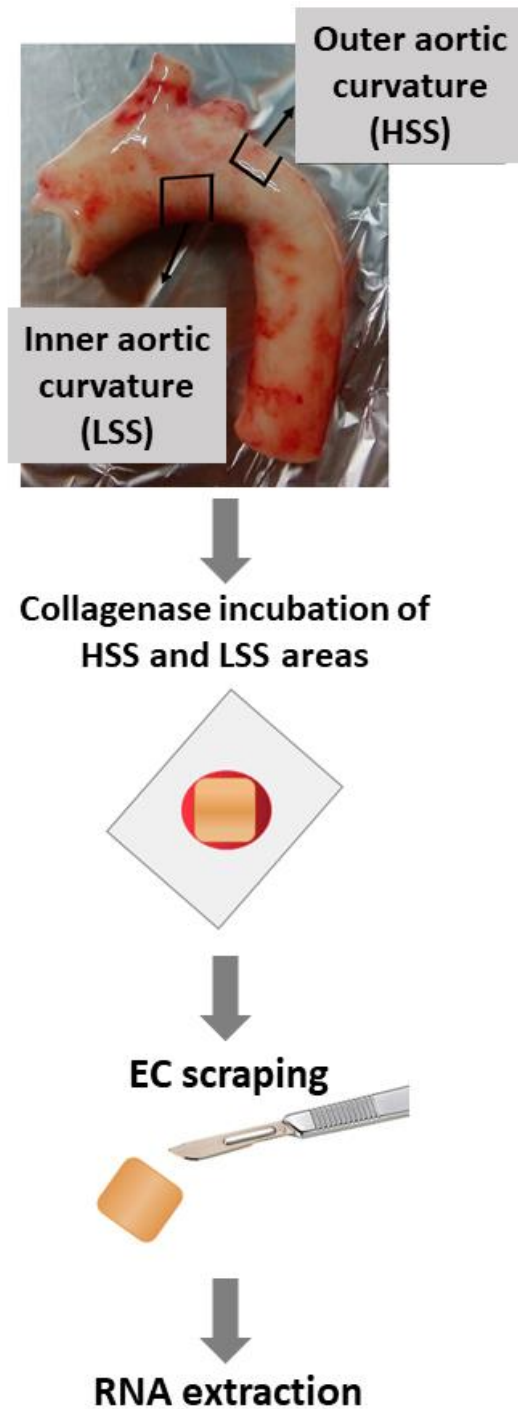


Figure 2.4. EC isolation from porcine aortas. Shear stress maps were used to identify high shear (HSS) and low shear (LSS) regions of the porcine aorta. After this, regions exposed to different shear patterns were dissected using a scalpel blade. Arterial segments exposed to HSS and LSS were incubated in 1 mg/ml collagenase solution in M199 media for 10 minutes. Endothelial cells were then isolated from LSS and HSS areas by scraping the endothelial layer from the aortic lumen.

2.8.1 RNA extraction from porcine endothelial cells

Porcine endothelial cells were lysed immediately after collection using Trizol reagent (Thermo Fisher Scientific). After pipetting up and down to homogenise the samples, cells were incubated for 5 minutes at room temperature and 100% (v/v) chloroform (Fisher Chemicals) was added to the tube. The sample was then incubated for 3 minutes at room temperature and centrifuged at 13000 rpm for 15 minutes at 4°C. This generated an aqueous phase with RNA, which was transferred into another tube and 100% (v/v) isopropanol (Sigma-Aldrich) was then added. Following incubation for 10 minutes at room temperature, the sample was centrifuged at 14000 rpm for 10 minutes at 4°C. After centrifugation, the supernatant was discarded and 75% (v/v) ethanol was used to wash the pellet (Sigma-Aldrich), and after this, it was vortexed and centrifuged at 8000 rpm for 5 minutes at 4°C. Following centrifugation, the supernatant was discarded and RNA pellet was let to air-dry for 5-10 minutes. It was then resuspended in Rnase-free water (Qiagen) and incubated at 57°C for 12 minutes.

RNA purity and concentration were then determined using a NanoDrop ND-1000 (Thermo Scientific), and samples were stored at -80°C until cDNA synthesis was performed.

2.9 Primary endothelial cells

2.9.1 Isolation of Human Umbilical Vein Endothelial Cells (HUVEC)

HUVEC were isolated from umbilical cords or purchased from PromoCell. Umbilical cords were collected from the Maternity Ward at the Royal Hallamshire Hospital (Sheffield, UK, ethical approval REC 10/H1308/25) and kept in HBSS (Sigma-Aldrich) at 4°C before HUVEC isolation. Prior to isolation, AzoWipe® wipes were used to clean umbilical cords. The umbilical vein was cannulated using a 2.0 x 45 mm cannula (BD Venflon), which was secured using clamps. To remove blood clots, 10 ml of M199 (Sigma-Aldrich) was flushed through the umbilical vein. After clamping the distal end of the cord, 10 ml of sterile filtered 1mg/ml type IV collagenase (Roche) in M199 (Sigma-Aldrich) was injected into the vein and incubated for 15 minutes. Following incubation, the clamp was removed. The isolated cells were collected in a 50 ml tube and centrifuged at 12000 rpm for 5 minutes prior to cell seeding in T75 flasks coated with 1% (w/v) gelatin.

2.9.2 Human endothelial cell culture and maintenance

T75 flasks and 6-well plates were coated with 1% (w/v) gelatin (Sigma-Aldrich) before cell seeding. After isolation from umbilical cords or purchase from PromoCell (c-12200), HUVEC were maintained in M199 (Sigma-Aldrich) supplemented with 20% (v/v) foetal bovine serum (Sigma-Aldrich), 100 µg/ml streptomycin (Gibco), 100 U/ml penicillin (Gibco), 4 mmol/L L-glutamine (Gibco), 10 U/ml heparin (Sigma-Aldrich) and 30 µg/ml EC growth supplement (Sigma-Aldrich). Human coronary artery EC (HCAEC) were purchased from PromoCell (C-12221) and they were maintained in endothelial cell growth medium MV2 (PromoCell) supplemented with 0.05 ml/ml foetal calf serum, 10 ng/ml basic fibroblast growth factor, 5 ng/ml epidermal growth factor, 20 ng/ml insulin-like growth factor, 1 µg/ml ascorbic acid, 0.5 ng/ml vascular endothelial growth factor 165 and 0.2 µg/ml hydrocortisone (all from PromoCell). HUVEC and HCAEC were incubated at 37°C in 5% CO₂ incubators (Leec, Touch 190 S), and the media was changed every 2 or 3 days. Cells were split 1:3 using trypsin-EDTA (Serox) when they reached confluence and they were used at passages 3-7.

2.10 Flow systems

2.10.1 Orbital shaker system

In order to assess the effect of flow on EC, HUVEC or HCAEC were seeded onto a 6-well plate coated with 1% (w/v) gelatin, at a density of 250,000 cells/well. Cells were then incubated overnight at 37°C and 5% CO₂ to reach confluence, using 2 ml of complete M199/well. Media was changed the next morning and 3 ml of complete M199 (Sigma-Aldrich) was added. Cells in the 6-well plate were then exposed to flow for 72 h using an orbital shaker (Grant-Bio PSU-10i) set at 210 rpm in a 37°C and 5% CO₂ incubator. The orbital shaker was used to generate non-disturbed flow and high shear stress (~13 dynes/cm²) at the periphery of the wells, and oscillatory flow/low shear stress (~5 dynes/cm²) at the centre of the wells. Sheared cells were assessed for cell alignment to flow and they were washed in ice-cold PBS twice. Using a shear stress map generated by Evans laboratory (Warboys et al., 2014), cells were then scraped from the centre and periphery of the well with the end of a 1ml syringe piston (BD) (Figure 2.5). They were collected in PBS and centrifuged for 5 minutes at 1500 rpm.



Figure 2.5. Orbital shaker system. Human endothelial cells were seeded on 6-well plates. An orbital shaker set at 210 rpm was then used to generate flow. Endothelial cells at the periphery of the wells were exposed to laminar flow/high shear stress ($\sim 13 \text{ dynes/cm}^2$), and endothelial cells in the centre of the wells were subjected to oscillatory flow/low shear stress ($\sim 5 \text{ dynes/cm}^2$). After 72 h of flow, cells were scraped from the centre and periphery of the wells using the end of a 1ml syringe piston.

2.10.2 Parallel plate system (Ibidi® system)

An Ibidi® pump system was used to test the effect of flow magnitude and frequency on human endothelial cells. After coating the Ibidi® slides with 150 µl of 1% (w/v) gelatin for 30 minutes, cells from a confluent T75 flask were trypsinised using trypsin-EDTA and they were centrifuged at 1500 rpm for 5 minutes at room temperature. 250000 cells in 100 µl of M199 were seeded onto 0.4 µm Ibidi® slides, and 250000 cells in 150 µl of M199 were seeded on the 0.6 µm ones. Cells were incubated overnight in a 37°C and 5% CO₂ incubator and M199 media was then replaced. Cells were exposed to flow using Ibidi® syringe pump system for the next 72 h. The flow parameters were set as follows: Laminar high shear stress (13 dynes/cm²) and low shear stress (5 dynes/cm²). After 72 h, pumps were stopped and cells were collected from the µ-slides using PBS. They were then centrifuged for 5 minutes at 1500 rpm.

2.11 Immunofluorescence staining of HUVEC

Glass coverslips were adhered to 6-well plates using DPX mounting medium (VWR chemicals), and they were left overnight in a 37°C incubator. Once DPX mounting medium was dry, wells were coated with 1% (w/v) gelatin and after 30 minutes, cells were seeded. After 72 h of flow, cells were washed three times for 5 minutes with ice-cold PBS, and fixed with 4% (w/v) PFA (Alfa Aesar) for 12 minutes at room temperature. Cells were washed three times for 5 minutes in PBS and permeabilised with 0.1% (v/v) triton-X (Sigma-Aldrich) in PBS at room temperature for 15 minutes, and then, cells were blocked with 20% (v/v) goat serum (Sigma-Aldrich) in PBS for 1 hour, to prevent non-specific interactions. To allow dual staining of VE-cadherin (EC marker) and a protein of interest, cells were stained stepwise with mouse anti-VE-cadherin antibody, then goat anti-mouse secondary antibodies and then with another primary antibody followed by an appropriate secondary antibody. In detail, cells were incubated with anti VE-cadherin antibody (1:300) in 5% (v/v) goat serum in PBS overnight at 4°C, and cells were washed three times for 5 minutes in PBS. Cells were incubated with Alexa Fluor 488 goat anti-mouse IgG (1:300; Life technologies) in 5% (v/v) goat serum in PBS for 3 h at room temperature protected from light. After staining for VE-Cadherin and washing three times for 5 minutes, selected primary antibodies (see appendix 1) were diluted at the desired concentration in 5% (v/v) goat serum/PBS and applied to cells. Alternatively, cells were incubated with isotype IgG control antibodies (Sigma-Aldrich) to control for non-specific binding. Primary antibodies were incubated overnight at 4°C, and after washing the cells

three times for 5 minutes with PBS, they were incubated with appropriate secondary antibodies in 5% (v/v) goat serum/PBS for 3 h at room temperature protected from light. Cells were then washed three times for 5 minutes, and they were incubated with 4 ug/ml DAPI for 15 minutes at room temperature. Prolong gold anti-fade reagent (Invitrogen) was used to mount coverslips on microscopy slides. A Leica DMI4000B inverted microscope with a 20x objective was then used to image the cells.

2.12 Western Blotting

2.12.1 Protein isolation

EC were isolated from the centre and periphery of 6-well plates as described in 2.10.1. They were centrifuged at 14000 rpm for 5 minutes and resuspended in 40 µl (centre) and 200 µl (periphery) of 1x loading buffer (62.5 mM Tris-HCl pH 6.8, 10% (v/v) glycerol (GPR Rectapur), 2% (w/v) sodium dodecyl sulfate (SDS) (GE Healthcare), 0.002% (w/v) bromophenol blue (Sigma-Aldrich)) with 10% (v/v) β-mercaptoethanol. Lysates were incubated at 100°C for 10 minutes, transferred on ice for 5 minutes, and centrifuged for 8 minutes at 14000 rpm at 4°C. Lysates were then stored at -80°C.

2.12.2 Gel preparation and electrophoresis

In order to cast gels, cassette sandwiches were made using mini-PROTEAN® 1 mm spacer plates and short plates (Bio-Rad, 1653311), and a casting frame and stand were used to ensure alignment between the two. H₂O was then poured into the cassette sandwich to detect potential leaks. A separating gel was then made (0.375 M Tris-HCl pH 8.8, 7.5% (v/v) acrylamide (Bio-Rad), 0.1% (w/v) SDS (GE Healthcare), 0.1% (w/v) ammonium persulphate solution (APS) (Sigma-Aldrich) and 0.01% (v/v) tetramethylethylenediamine (TEMED) (Sigma-Aldrich)). It was poured into the cassette sandwich using a Pasteur pipette once the H₂O was removed, and 80% (v/v) isopropanol (Sigma-Aldrich) was added on top of the separating gel in order to remove bubbles. To polymerise, it was incubated at 37°C for 10 minutes, and a stacking gel was then made (0.15 M Tris-HCl pH 6.8, 4% (v/v) acrylamide (Bio-Rad), 0.1% (w/v) SDS (GE Healthcare), 0.1% (w/v) APS (Sigma-Aldrich) and 0.01% (v/v) TEMED (Sigma-Aldrich)). After removing 80% (v/v) isopropanol (Sigma-Aldrich) from the cassette sandwich, the stacking gel was poured over the separating gel, a comb was inserted to form the wells, and it was incubated at 37°C for 10 minutes. When the gel was set, the cassette sandwich was inserted into the electrophoresis chamber, adding 1 L of running

buffer (200 mM glycine (Sigma-Aldrich), 25 mM TRIS base (Fisher Scientific), 0.1% (w/v) SDS (GE Healthcare)). The comb was then removed and protein samples were pipetted into the electrophoresis wells. Precision Plus Protein Dual Color Standard (Bio-Rad) was used as a molecular weight marker. The chamber was connected to a PowerPac power supply (Bio-Rad) and it was run at 100 V for 1.5 h.

2.12.3 Membrane transfer

A nitrocellulose membrane (Immobilon-P) was activated using 100% (v/v) methanol (VWR chemicals) for 2 minutes, washed and kept in distilled water until use. After the electrophoresis, the gel was removed from the cassette sandwich and it was placed over one piece of sponge and one piece of filter paper, soaked in transfer buffer (20% (v/v) methanol (VWR chemicals), 200 mM glycine (Sigma-Aldrich), 25 mM TRIS base (Fisher Scientific)). The activated membrane was then put on top of the gel, covered by one piece of filter paper and a sponge, avoiding bubbles. Transfer was induced by application of 90-100 V for 60 minutes (PowerPac power supply (Bio-Rad)).

2.12.4 Antibody staining

After blocking the membrane in 10% (w/v) milk in TBST (20 mM Tris-HCl, 137 mM NaCl and 0.1% (v/v) Tween20 (Sigma-Aldrich)) for 1 hour at room temperature, membrane segments were incubated in 1:1000 selected primary antibody (see appendix 1) and 1:3000 PDHX or Calnexin antibody (control) in 5% (w/v) milk in TBST overnight at 4°C. Membrane segments were then washed four times in TBST for 5 minutes and they were incubated in secondary goat anti-rabbit- Horseradish Peroxidase (HRP) antibody (P0448, Dako) or goat anti-mouse-HRP antibody (P0447, Dako) in 5% (w/v) milk powder in TBST for 1 hour at room temperature. Membrane segments were washed four times in TBST for 5 minutes, and, in order to visualise protein bands, they were placed onto chemoluminescence blotting substrate (ECL) reagent (Roche) or high sensitivity ECL (GE Healthcare) for 3 minutes. In a dark room, membrane segments were placed in a film cassette and after exposing the membrane to the film (GE Healthcare), the film was developed using developing solution (Ilford PQ Universal), washed with water and fixed with Ilford Hypam fixer. Alternatively, membranes were imaged using the ChemiDoc Imaging system (Bio-Rad).

2.13 RNA extraction from cultured ECs

Cells were centrifuged at 1500 rpm for 5 minutes and RNA was isolated using the RNeasy Mini Kit (Qiagen). After removing the supernatant, cells were lysed with 350 μ l of buffer RLT containing 10 μ l/ml of β -mercaptoethanol (Sigma-Aldrich). 350 μ l of 70% (v/v) ethanol (Sigma-Aldrich) was then added to the lysate. After transferring the sample to an RNeasy spin column and centrifuging for 15 s at 13000 rpm, 350 μ l of buffer RW1 was added and centrifuged for 15 s at 13000 rpm. 10 μ l of DNase I (Roche) was then mixed with 70 μ l of buffer RDD, and the lysate was incubated with the mixture for 15 minutes at room temperature. After DNase I incubation, 350 μ l of buffer RW1 was added to the column and it was centrifuged for 15 s at 13000 rpm. 500 μ l of buffer RPE was added and centrifuged for 15 s at 13000 rpm, and after this, an extra 500 μ l of buffer RPE was added and centrifuged for 2 minutes at 13000 rpm. The column was then transferred into a 1.5 ml tube and the sample was eluted in 30-50 μ l of RNase-free water. RNA purity and concentration were determined using a NanoDrop ND-1000 (Thermo Scientific). RNA samples were stored at -80°C.

2.14 cDNA synthesis

cDNA Synthesis Kit (Bio-Rad) was used for cDNA synthesis of 75-500 ng of RNA in a total volume of 20 μ l. In addition to a variable amount of RNA, the reaction mix also contained 5% (v/v) iScript reverse transcriptase (Bio-Rad), 20% (v/v) 5x iScript reaction mix (Bio-Rad), and nuclease-free water. The reaction mix was then incubated at 25°C for 5 minutes, 46°C for 20 minutes, and 95°C for 1 minute. The cDNA generated was stored at -20°C and it was used to perform qRT-PCR.

2.15 Primer design

Ensembl (<https://www.ensembl.org/index.html>) and the Primer3web <http://primer3.ut.ee/> were used to design all PCR primers. In order to test for primer specificity and to prevent binding in other places of the genome, the primer-BLAST web (<http://www.ncbi.nlm.nih.gov/tools/primer-blast/>) was also used. qRT-PCR was first performed to test primer efficiency and primers were purchased from Integrated DNA Technologies. The table 2.3 shows the primers used in this study.

Organism	Gene	Forward primer (5'-3')	Reverse primer (3'-5')	Purpose
<i>H. sapiens</i>	<i>HPRT</i>	TTGGTCAGGCAGTATAATCC	GGGCATATCCTACAACAAAC	Housekeeper qRT-PCR
<i>H. sapiens</i>	<i>c-REL/REL</i>	CTCCTGTGTCTCGAACCCAA	CCTCCTCTGACACTTCCACAAT	EC expression: qRT-PCR
<i>H. sapiens</i>	<i>ENOS</i>	TGAAGCACCTGGAGAATGAG	TTGACCATCTCCTGATGGAA	
<i>H. sapiens</i>	<i>MCP-1</i>	GCAGAAGTGGGTTCAGGATT	TGGGTGTGGAGTGAGTGTT	
<i>H. sapiens</i>	<i>KLF4</i>	GAACCCACACAGGTGAGAAA	CCCGTGTGTTTACGGTAGTG	
<i>H. sapiens</i>	<i>VCAM-1</i>	CATTGACTTGCAGCACCACA	AGATGTGGTCCCCTCATTCTG	
<i>H. sapiens</i>	<i>ICAM-1</i>	CACAAGCCACGCCTCCCTGAACCTA	TGTGGGCCTTTGTGTTTTGATGCTA	
<i>H. sapiens</i>	<i>E- SELECTIN</i>	GCTCTGCAGCTCGGACAT	GAAAGTCCAGCTACCAAGGGAAT	
<i>H. sapiens</i>	<i>TXNIP</i>	CCTTCGGGTTCAGAAGATCA	TTGGATCCAGGAACGCTAAC	
<i>H. sapiens</i>	<i>p38/ MAPK14</i>	TGATTGGTCTGTTGGACGTT	CCATGAGATGGGTCACCAG	
<i>H. sapiens</i>	<i>RANK/ TNFRSF11A</i>	TTCTGCTTCTCTTCGCGTCT	CTCATTGATCCAGTGCCACA	
<i>H. sapiens</i>	<i>TWEAK/ TNFSF12</i>	ATCAACAGCTCCAGCCCTCT	AGCCTTCCCCTCATCAAAGT	
<i>H. sapiens</i>	<i>JNK2/ MAPK9</i>	GTCATCCTGGGTATGGGCTA	CAACCTTCCACCAGCTCTCC	
<i>H. sapiens</i>	<i>ERK1/ MAPK3</i>	ATCTTCCCTGGCAAGCACTA	AGGTAGTTTCGGGCCTTCAT	
<i>H. sapiens</i>	<i>ERK2/ MAPK1</i>	CATTATTGAGCACCAACCA	TGGTCATTGCTGAGGTGTTG	
<i>H. sapiens</i>	<i>p21</i>	GATGTCCGTCAGAACCCATG	TTAGGGCTTCTCTTGAGAGA	
<i>H. sapiens</i>	<i>NFKB2</i>	GCCGAAAGACCTATCCCACT	TTAGTCACATGCAGGACACCC	
<i>H. sapiens</i>	<i>NIK/ MAP3K14</i>	GGAATACCTCCACTCACGAAGG	CTGTGAGCAAGGACTTCCAG	
<i>S. scrofa</i>	<i>B2M</i>	GGTTCAGGTTTACTCACGCCAC	CTTAACTATCTTGGGCTTATCG	Housekeeper qRT-PCR
<i>S. scrofa</i>	<i>REL</i>	TGGAAGTGTCTAGAGGAGGAGAT	GGGTGACATCGGCTTGTGAA	EC expression: qRT-PCR
<i>S. scrofa</i>	<i>ENOS</i>	CGCTACAACATTCTGGAGGA	ACTTGGCCAGCTGGTAACT	
<i>S. scrofa</i>	<i>MCP-1</i>	TCACCTGCTGCTATACACTTAC	ATCACTGCTTCTTAGGACACTTG	
<i>S. scrofa</i>	<i>CD31</i>	TCAATGCTCCGTGAAAGAAG	CCTGGGTGTCATTCAAAGTG	
<i>S. scrofa</i>	<i>SMA</i>	CGATGAAGGAGGGCTGGAACAGGG	CGTGACCACTGCCGAGCGTGAGAT	
<i>M. musculus</i>	<i>Hprt</i>	AGTCCAGCGTCGTGATTAG	TCTCGAGCAAGTCTTTCAGTCC	Housekeeper qRT-PCR
<i>M. musculus</i>	<i>Rel</i>	TGCCGTGTGAACAAGAAGT	GGCTTCCCAGTCATTCAACA	EC expression: qRT-PCR

Table 2.3. PCR primer sequences. Gene-specific primers were used for qRT-PCR. Gene expression was assessed in endothelial samples from *Homo sapiens*, *Sus scrofa*, and *Mus musculus*.

2.16 Quantitative RT-PCR (qRT-PCR)

CFX384 Touch™ Real-Time PCR Detection System (Bio-Rad) was used to assess mRNA expression by using gene-specific primers. cDNA was combined with SsoAdvanced SYBR Green Supermix (56% (v/v); Bio-Rad) and 10 μM reverse and forward primer.

The qRT-PCR process was initiated with a denaturation of 3 minutes at 95°C, and the cDNA was then amplified for 40 cycles. These cycles consisted of 5 seconds at 95°C and 45 seconds at 60°C. The final dissociation stage consisted on a gradual 0.5°C increment, from 65°C to 95°C. *HPRT* was used as a house-keeping gene in murine and human samples, whereas expression of porcine samples was normalised to beta-2-microglobulin (*B2M*) expression. In order to assess primer quality and non-specific binding, primer dissociation curves were used. Relative mRNA expression was quantified using the $\Delta\Delta C_t$ method, which starts with cDNA normalisation. The normalisation process consists on subtracting the C_t value (number of cycles that are necessary to cross a threshold amount of PCR product) of the house-keeping gene from the C_t value of specific genes (ΔC_t). Then, in order to compare cDNA samples from two different experimental conditions and express them relative to each other, the ΔC_t of one condition was subtracted from the second ($\Delta\Delta C_t$). The fold change was then obtained following the formula $2^{-\Delta\Delta C_t}$.

2.17 HUVEC siRNA electroporation using Neon transfection system

siRNA oligonucleotides were used to knockdown specific genes in order to assess gene function (table 2.4). Confluent HUVEC from a T75 flask were washed twice with PBS and trypsinised using trypsin/EDTA. Following trypsin neutralisation using complete growth media, HUVEC were centrifuged at 1500 rpm for 5 minutes at room temperature. Cells were then resuspended in PBS and centrifuged at 1500 rpm for 5 minutes, and this process was repeated further two times. After the last centrifugation, HUVEC pellet was resuspended in R buffer. HUVEC were transfected with 50 nM c-Rel and scrambled non-targeting control siRNAs using the Neon Transfection System (Voltage: 1200 V, Pulse width: 40 ms, pulse number: 1 pulse) following the manufacturer's protocol (https://tools.thermofisher.com/content/sfs/manuals/neon_device_man.pdf).

Gene	siRNA	Company purchased from
<i>Scrambled</i>	ON-TARGET plus Non-targeting Control siRNA D-001810-01-05	Dharmacon
<i>c-REL</i>	StealthRNAi siRNA RELHSS109157	Thermo Fisher Scientific
<i>c-REL</i>	StealthRNAi siRNA RELHSS109158	Thermo Fisher Scientific

Table 2.4. siRNA oligonucleotide information. siRNA oligonucleotides were used to knockdown specific genes to assess gene function.

2.18 RNA microarray in HUVEC

HUVEC from different donors were electroporated and transfected with *SCR* and *c-REL* siRNA as described in 2.17. Following siRNA transfection, cells were seeded on 6-well plates coated with 1% (w/v) gelatin, and incubated overnight at 37°C and 5% CO₂. After addition of 3 ml of complete M199 (Sigma-Aldrich), cells were exposed to flow for 72 h using an orbital shaker (Grant-Bio PSU-10i). RNA extraction was performed as described in 2.13, and the integrity, purity and concentration of the RNA generated was assessed using a NanoDrop ND-1000 (Thermo Scientific). RNA samples were then stored at -80°C until the microarray was performed. To confirm *c-REL* silencing in *c-REL* siRNA-treated HUVEC, qRT-PCR was carried out before performing RNA microarray. RNA samples were labelled and hybridised to the Human Clariom™ S Assay (Affymetrix) and data were then analysed using Transcriptome Analysis Console Software (Affymetrix). Once this was performed, functional annotation using DAVID (<http://david.abcc.ncifcrf.gov>) was used to reveal gene enrichment. Differential expression of specific genes was then validated by qRT-PCR, western blotting, and *en face* staining.

2.18 Statistical analysis

The average of at least three independent experiments is shown with the standard error of the mean. When qRT-PCR is used to measure gene expression between low and high shear stress areas, the expression at low shear stress regions was expressed relative to that at high shear regions (High shear stress=1); When qRT-PCR is used to measure gene expression between *SCR* and *c-REL*-treated HUVEC, expression in *c-REL* siRNA-treated cells was expressed relative to that in *SCR*-treated HUVEC (*SCR* siRNA=1). Differences between two or more groups that are normally distributed were assessed by performing two-tailed paired Student t-test, one or two way ANOVA. Statistical tests were carried out using the software GraphPad Prism (La Jolla, California, USA). A p-value<0.05 was considered significant.

Chapter 3. c-Rel protein levels are enriched at low shear stress regions

3.1 Introduction

Numerous studies have shown the influence of haemodynamic forces upon endothelial cell physiology and gene expression, and also, their contribution to the development of atherosclerosis (Caro et al., 1969; Malek et al., 1999; Ni et al., 2010; Passerini et al., 2004). Atherosclerosis is known to occur at specific regions, including curvatures and arterial bifurcations, which are areas exposed to disturbed blood flow and low shear stress. In atherosusceptible areas, low shear stress alters endothelial cell physiology, priming EC for proliferation, apoptosis and inflammation. However, EC in atheroprotected regions remain in a quiescent state, due to the influence of high shear stress and unidirectional flow on the endothelium (Malek et al., 1999).

Different patterns of shear stress are sensed by mechanoreceptors that are expressed by EC. These mechanoreceptors, in turn, lead to the activation of signalling cascades, which eventually activate specific transcription factors that are responsible for the regulation of gene expression (Kwak et al., 2014). Among the multiple transcriptional programs altered by shear stress, this haemodynamic force has been shown to regulate the activation of the NF- κ B family of transcription factors (Cuhlmann et al., 2011; Petzold et al., 2009). NF- κ B is critical for the regulation of numerous cell responses, since it controls genes involved in inflammation, cell proliferation and survival (Oeckinghaus and Ghosh, 2009), but also, there are different lines of evidence that support that NF- κ B contributes to the development of atherosclerosis (Brand et al., 1996; Cuhlmann et al., 2011; Gareus et al., 2008).

Some studies demonstrating the influence of shear stress on NF- κ B include experiments *in vitro* using HAEC, which show that the proinflammatory NF- κ B subunits RelA and p50 have enhanced activation under low shear stress (Mohan et al., 1997). Other studies have revealed that arterial sites under low shear stress in mice present high levels of RelA and the inhibitory components I κ B α and I κ B β (Hajra et al., 2000), and that RelA overexpression under low shear is mediated by JNK1 and its downstream target ATF2 (Cuhlmann et al., 2011).

Despite most studies have investigated the effect of mechanical forces on the canonical NF- κ B pathway, Paul Evans' group has also studied the influence of this haemodynamic force on non-canonical NF- κ B. In HUVEC, they reported that protein levels of p100 and

p52 were upregulated in EC under low shear stress compared to high shear stress (Bowden et al., data not published).

Although there are several studies that show that shear stress plays a role in the activation of NF- κ B subunits, including RelA, p50 and p100/p52, the influence of this haemodynamic force on c-Rel in endothelial cells has not been described. Identifying a potential regulation of c-Rel by haemodynamic forces will help us gain a better understanding of the molecular mechanisms underlying EC responses to shear stress.

3.2 Hypothesis and aims

Since shear stress is known to activate the NF- κ B signalling pathway and several NF- κ B subunits are already known to respond to shear stress, I hypothesise that shear stress differentially regulates the expression of c-Rel in ECs.

To test this hypothesis, I aim to:

1. Investigate the effect of shear stress on c-Rel protein levels in the mouse aorta by *en face* staining.
2. Investigate the expression of *c-REL* at the transcript level at low and high shear stress regions in the porcine aorta.
3. Investigate the effect of shear stress on *c-Rel* mRNA expression by performing partial ligation of the left carotid artery (LCA) in *ApoE* knockout mice.
4. Investigate the effect of shear stress on c-REL transcript and protein levels in cultured EC (HUVEC and HCAEC), using *in vitro* flow systems.

3.3 c-Rel protein levels are enriched at low shear stress regions of the murine aorta

The localisation of atherosclerotic lesions has been widely studied. Within the murine vasculature, atherosclerosis has been shown to develop at the inner curvature of the aortic arch, where cells are exposed to disturbed blood flow and low shear stress (VanderLaan et al., 2004). In order to investigate whether c-Rel protein levels are controlled by shear stress *in vivo*, *en face* staining of the murine aortic arch was performed. After aortic dissection of 6-9 weeks old C57BL/6J mice, areas exposed to different patterns of shear at the aortic arch were stained for c-Rel using a specific antibody. CD31, an EC marker, determined high shear and low shear regions, revealing that cells under high shear (outer curvature) are aligned and elongated, whereas cells at the inner curvature present a cobblestone appearance. When c-Rel expression was assessed, it was found that c-Rel protein levels were significantly upregulated at the inner curvature (low shear) compared to the outer curvature (high shear stress) of the murine aorta. However, c-Rel signals were heterogeneous. Under disturbed flow, some cells showed nuclear staining, whereas others showed perinuclear and cytoplasmic staining (figure 3.1).

In order to validate these results and to assess c-Rel deletion and the specificity of c-Rel antibody, a new batch of wildtype and *c-Rel* knockout mice were stained for c-Rel. This revealed that fluorescent signals were absent in *c-Rel* knockout mice, validating the specificity of c-Rel antibody (figure 3.2). c-Rel fluorescence intensity from wildtype mice was then normalised against background signal from non-specific antibody binding in *c-Rel* knockout mice, confirming that c-Rel protein levels are enriched at low shear/disturbed flow regions of the murine aorta compared to regions exposed to high shear (figure 3.2C). An isotype rabbit IgG antibody was also used for staining as a negative control in wildtype and *c-Rel* knockout mice (figure 3.3). From these results, I conclude that c-Rel protein levels are upregulated at low shear regions compared to high shear regions of the murine endothelium.

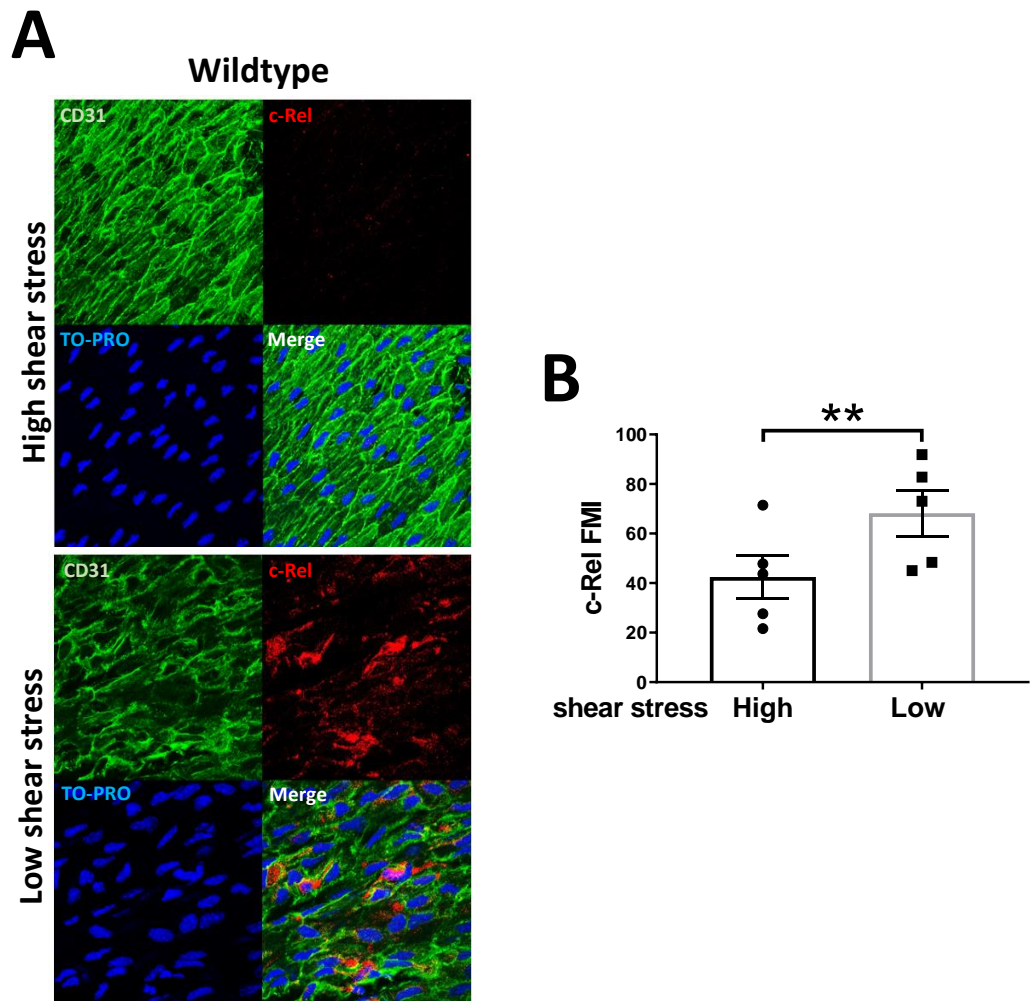


Figure 3.1. c-Rel protein levels are enriched at low shear stress regions of the murine aorta. **A)** *En face* staining at low shear and high shear stress regions of the mouse aorta was performed in C57BL/6J female wildtype mice between 6-9 weeks of age, in order to assess c-Rel protein levels (red) by confocal microscopy. Anti-CD31 antibody (green) was used as an endothelial marker and TO-PRO 3 was used for nuclear staining. **B)** Quantification of c-Rel fluorescence intensity at the inner (low shear stress) and outer (high shear stress) curvature of the mouse aorta after normalisation against the isotype rabbit IgG antibody. Mean values are shown with standard error of the mean; n=5 independent experiments. **p<0.01, using paired T-test.

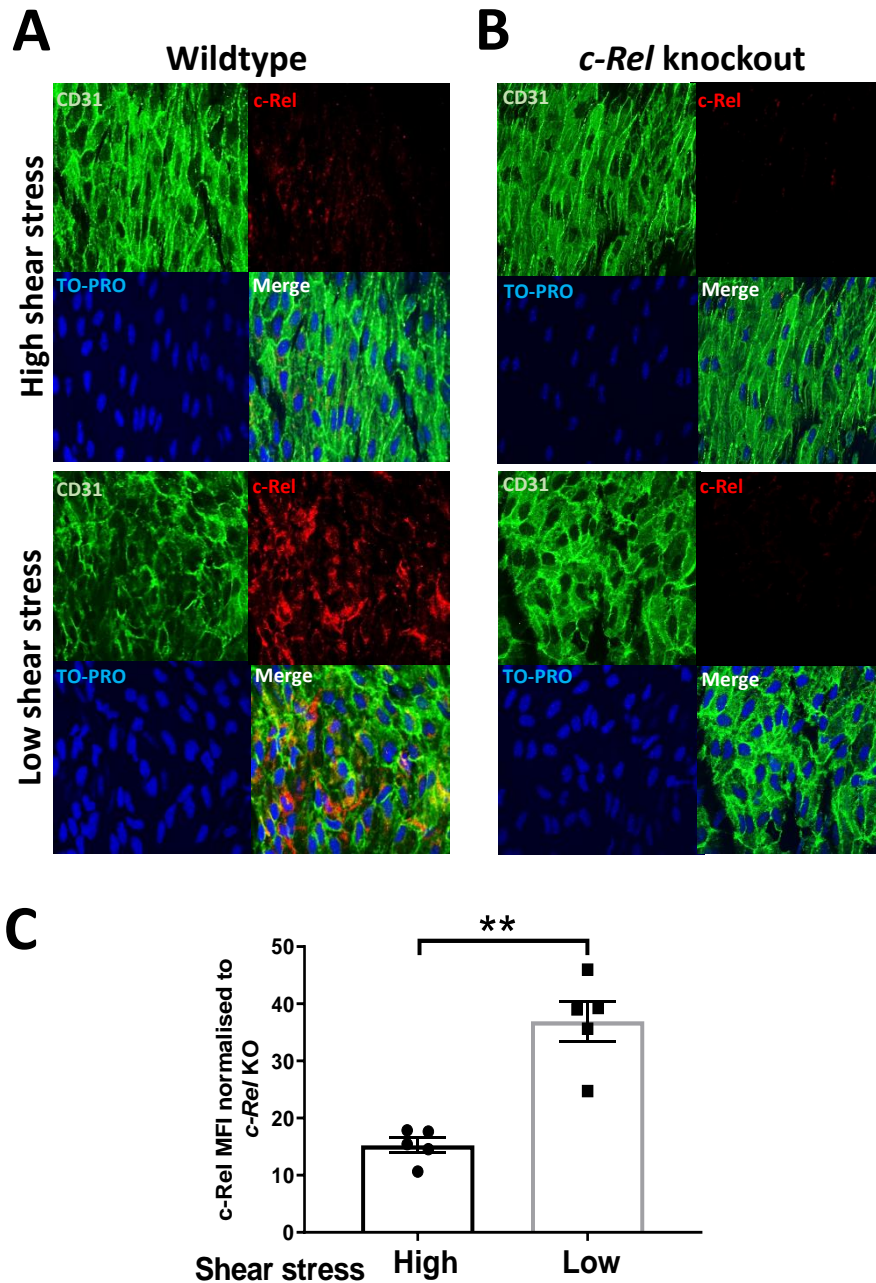


Figure 3.2. Validation of *c-Rel* deletion in mouse. *En face* staining at low and high shear stress regions of the mouse aorta was performed in C57BL/6J female **A)** wildtype and **B)** *c-Rel* knockout (KO) mice between 6-9 weeks of age, in order to assess the specificity of *c-Rel* antibody. Anti-CD31 antibody (green) was used as an endothelial marker and TO-PRO 3, for nuclear staining. **C)** Quantification of *c-Rel* fluorescence intensity at the inner (low shear stress) and outer (high shear stress) curvature of the mouse aorta after normalisation against *c-Rel* knockout mice. Mean values are presented with standard error of the mean; n=5 independent experiments. ***p<0.001, using paired T-test.

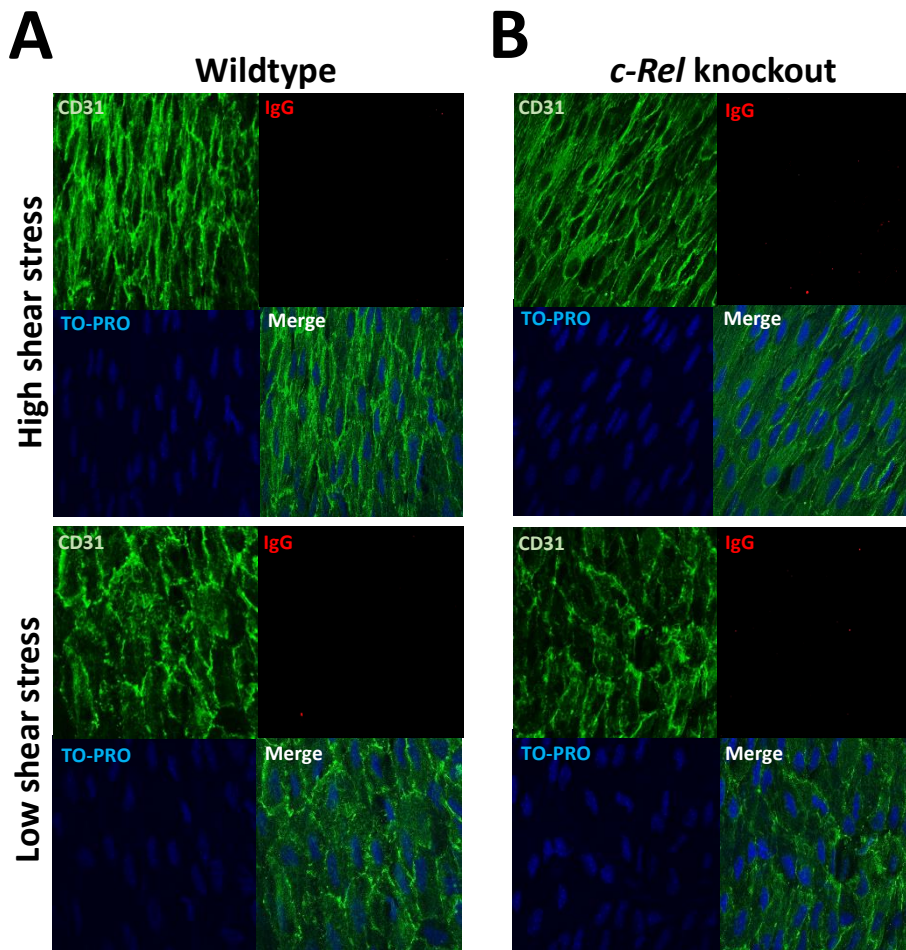


Figure 3.3. Negative control for *en face* staining of the mouse aorta. Isotype rabbit IgG antibody was used to control for non-specific binding at low and high shear stress regions of the mouse aorta, using **A)** wildtype and **B)** *c-Rel* knockout mice. Anti-CD31 antibody (green) was used as an endothelial marker and TO-PRO 3 was used for nuclear staining.

3.4 Shear stress does not regulate *c-REL* mRNA expression in porcine aortas

In order to assess whether shear stress regulation of c-Rel is conserved between porcine and murine models, porcine EC were isolated from regions exposed to high shear and low oscillatory shear stress using collagenase. Following RNA extraction, cDNA was synthesised and a series of quality controls were performed.

To control for selection of mechanically-distinct regions, the expression of two established shear stress-induced genes was investigated. The expression of *MCP-1* and *eNOS*, which are genes induced by low and high shear stress respectively (Bao et al., 1999), was assessed. qRT-PCR analysis revealed that *MCP-1* expression is enriched at disturbed flow/low shear regions of the porcine aorta, whereas *eNOS* expression is enhanced at the outer curvature exposed to high shear stress, confirming that the regions selected are exposed to the defined shear stress patterns (figure 3.4A). Samples that showed enrichment of *eNOS* at high shear regions and *MCP-1* under low shear stress were selected for analysis of *c-REL*.

In order to test whether RNA predominantly originated from the endothelium and not from smooth muscle cells, *CD31*, an endothelial marker, and smooth muscle actin (*SMA*), a VSMC marker, were measured and compared by qRT-PCR. qRT-PCR results revealed that *CD31* levels were higher than *SMA* levels, suggesting that cells isolated originated from the endothelium (figure 3.4B).

Subsequently, qRT-PCR analysis using porcine gene-specific primers did not reveal significant differences between *c-REL* mRNA expressions at low shear compared to high shear stress regions of the adult porcine aorta (figure 3.4C), due to a high variability among different samples. Hence, the upregulation of c-Rel protein at low shear stress regions of the murine aorta is not conserved in pigs at the mRNA level, but c-REL protein levels at the porcine aorta have not been assessed.

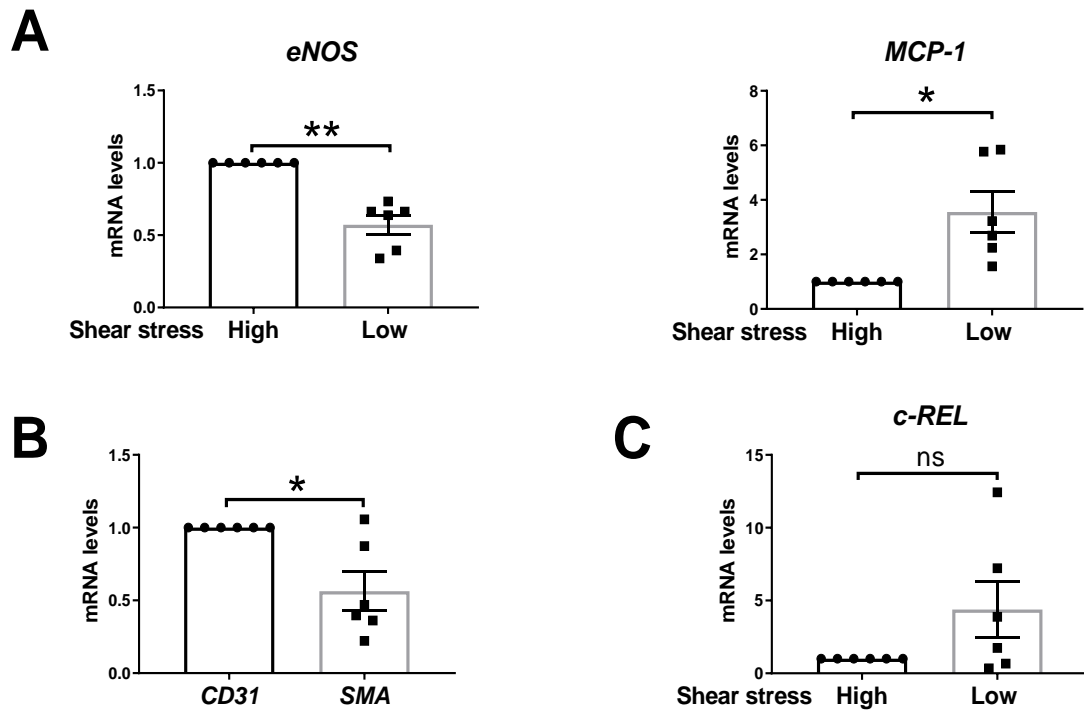


Figure 3.4. Shear stress does not regulate *c-REL* mRNA expression in porcine aortas. EC were isolated from high and low shear stress regions of the porcine aorta to perform qRT-PCR. **A)** qRT-PCR analysis of the flow-responsive genes *MCP-1* and *eNOS* to control for mechanically-distinct regions. **B)** qRT-PCR analysis and comparison of *CD31*, an EC marker, and *SMA*, a SMC marker. *SMA* expression was expressed relative to *CD31* levels. **C)** qRT-PCR analysis of *c-Rel* mRNA expression at high and low shear stress regions of the porcine aorta. *B2M* was used as a house-keeping gene. Mean values at low shear stress are presented with standard error of the mean, and the expression at low shear regions was expressed relative to that at high shear regions (High shear stress=1); n=6 independent experiments. **p<0.01, *p<0.05, ns: non-significant, using paired T-test.

3.5 *c-Rel* mRNA expression is reduced by partial ligation of murine carotid arteries

To determine whether flow and c-Rel have a causal relationship *in vivo*, I examined whether flow reduction in the murine carotid artery altered *c-Rel* transcript levels.

To achieve this, the left carotid artery in *ApoE* knockout mice was partially ligated prior to high fat feeding for 6 weeks, imposing disturbed flow and low shear stress on the left carotid artery and leading to atherosclerosis (Nam et al., 2009). The right carotid artery, however, was sham-operated, and therefore, exposed to high shear stress.

When mRNA expression of *c-Rel* was assessed at the partially ligated left carotid artery and sham-operated right carotid artery by qRT-PCR, I observed that the mRNA expression of *c-Rel* was enhanced at the right carotid artery (RCA) compared to the partially ligated left carotid (LCA) exposed to low shear stress and disturbed flow (figure 3.5). The enhancement of *c-Rel* at the RCA exposed to high shear does not reflect the results obtained by *en face* staining, where c-Rel protein was upregulated at low shear regions on the murine aorta. However, c-Rel protein levels using this model still need to be assessed, since I have only investigated the effect of flow reduction on *c-Rel* mRNA levels.

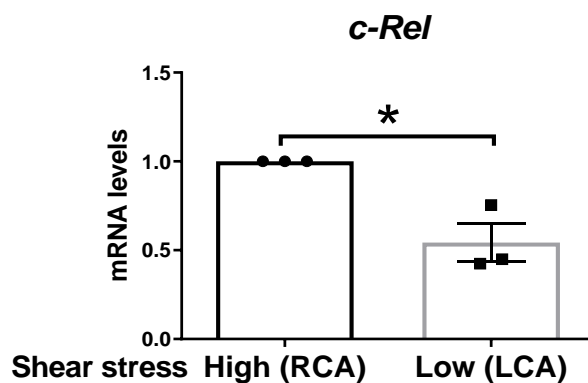


Figure 3.5. *c-Rel* mRNA expression is reduced by partial ligation of carotid arteries in *ApoE* knockout mice. Partial ligation of the left carotid artery (LCA) was performed in *ApoE* knockout mice, imposing disturbed flow and low shear stress. The right carotid artery (RCA) was sham-operated and exposed to high shear stress. After surgery, mice were exposed to a high-fat diet for 6 weeks. mRNA expression of *c-Rel* was assessed by qRT-PCR. Mean values at LCA are presented with SEM, and *c-Rel* expression at LCA was expressed relative to that at RCA (RCA=1); n=3 independent experiments. *p<0.05, using paired T-test.

3.6 c-REL protein levels are enriched in HUVEC and HCAEC exposed to low shear stress using the orbital shaker

Although there is an upregulation of c-Rel protein levels at low shear regions in the mouse aorta, this upregulation might not only be due to the effect of shear stress, since there are other factors, such as inflammation, that could also be contributing to this process. Therefore, in order to determine whether c-Rel is directly regulated by different shear stress patterns, c-REL expression was assessed in cultured endothelial cells (HUVEC and HCAEC) exposed to flow using the orbital shaker system.

After culturing EC on 6-well plates, these were exposed to different flow patterns for 72 h. By using computational fluid dynamics, it has been established that the orbital shaker (set at 210 rpm) generates a high pulsatile shear stress in the periphery of the well (13 dynes/cm²), which presents a relatively constant direction but fluctuations in the magnitude of the force. However, in the centre, it generates a shear stress that changes direction very quickly, but this generated shear also presents a relatively uniform low magnitude (5 dynes/cm²) (Dardik et al., 2005; Warboys et al., 2010; Warboys et al., 2014).

When EC morphology at the periphery and centre of the wells was assessed in HCAEC and HUVEC by fluorescence microscopy, I observed that EC were aligned at the periphery of the well, which are regions exposed to high shear stress and unidirectional flow. However, EC at the centre of the wells were poorly aligned and became more polygonal in shape, due to the effect of multidirectional and complex flow (figure 3.6). Therefore, this confirmed that the orbital shaker generates different haemodynamic conditions that lead to distinct EC responses, making this system suitable to study EC responses to shear stress.

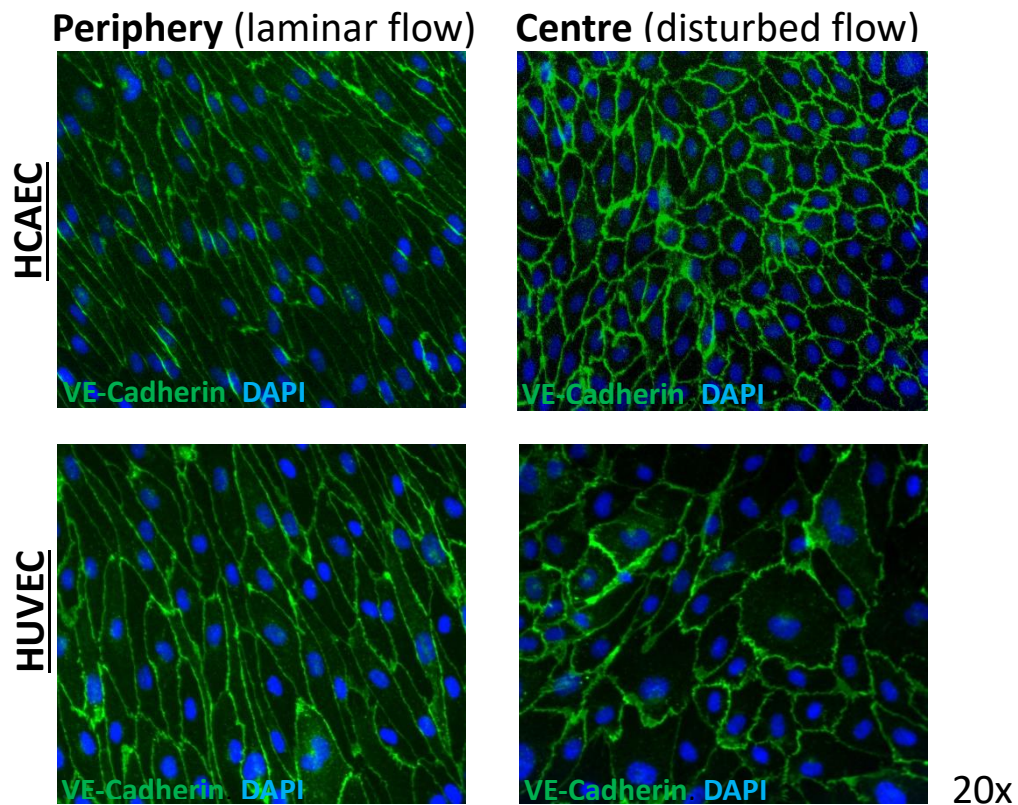


Figure 3.6. HUVEC sensing of flow patterns. After exposing HUVEC and HCAEC to flow for 72 h using the orbital shaker, endothelial cells were fixed using 4% (w/v) paraformaldehyde and stained against EC marker CD144, followed by Alexa Fluor 488 secondary antibody and DAPI for nuclear staining. Cell morphology was analysed by fluorescence microscopy using a 20x objective. This figure shows a representative image from three independent experiments.

I next used the orbital shaker system to determine whether c-REL protein levels can be directly regulated by shear stress *in vitro*. HUVEC and HCAEC were seeded on 6-well plates and they were then exposed to continuous flow for 72 h using the orbital shaker (Warboys et al., 2014). Cultured endothelial cells from the centre and periphery of the wells were isolated, and c-REL protein levels at these regions were quantified by Western blot.

When c-REL protein levels were assessed in HUVEC, it was observed that c-REL was upregulated at the centre (low shear and disturbed flow) compared to the periphery of the wells (high shear stress and unidirectional flow) (figure 3.7A).

Similarly, when c-REL protein levels were assessed in HCAEC, c-REL was significantly upregulated under disturbed flow (centre), compared to laminar flow (periphery) (figure 3.7B). Therefore, these results indicate that low shear stress directly increases c-REL protein levels in HUVEC and HCAEC, which is consistent with the results obtained by *en face* staining of mouse aortas, where c-Rel protein levels were also upregulated in EC exposed to low shear stress.

c-REL protein levels were also assessed by immunofluorescence. However, the signal obtained was very weak and comparable to that of the IgG control, and therefore, it could not be quantified. This could be due to low c-REL expression levels (data not shown).

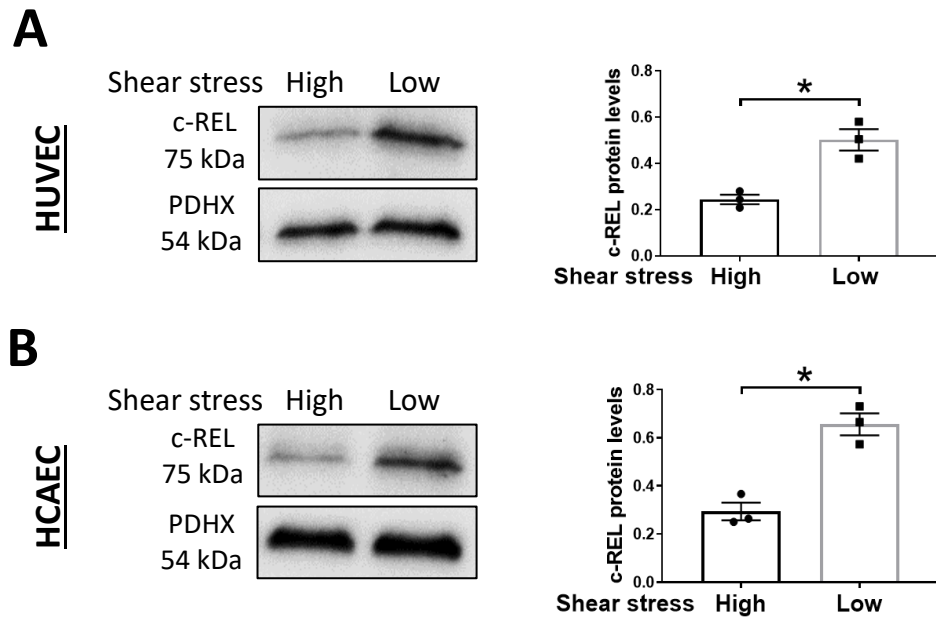


Figure 3.7. c-REL protein levels are enriched in HUVEC and HCAEC exposed to disturbed flow using the orbital shaker system. HUVEC and HCAEC were seeded on 6-well plates and exposed to different patterns of flow for 72 h using the orbital shaker system. Protein lysates from the high and low shear stress areas of the wells were generated and analysed using an anti-c-REL antibody. PDHX was used as a house-keeper gene, and it was detected on the protein lysates using an anti-PDHX antibody. Representative blot and quantification of c-REL protein expression levels under high shear (periphery) or low oscillatory shear stress (centre) in **A**) HUVEC or **B**) HCAEC are shown. ImageJ software was used to quantify the relative c-REL protein expression levels by densitometry. Mean values are presented with standard error of the mean, and c-REL protein levels were expressed relative to PDHX protein levels; n=3 independent experiments *p<0.05, using paired T-test.

3.7 c-REL protein levels are enriched in HUVEC exposed to low shear stress using the Ibidi® system

After testing c-REL protein levels in HUVEC and HCAEC exposed to flow using the orbital system, another *in vitro* system, the Ibidi® parallel plate system, was used to confirm the regulation of c-REL by shear stress.

These two complimentary *in vitro* systems generate different shear stress patterns. The flow generated in the centre of the wells using the orbital shaker is multidirectional and entails a temporal variation. However, the Ibidi® system generates well-defined shear stress magnitudes and directions, exposing cultured EC to specific flow patterns.

To test c-REL protein levels using the Ibidi® system, HUVEC were seeded on Ibidi® slides and they were exposed to high laminar shear stress (13 dynes/cm²), and low shear stress (5 dynes/cm²) for 72 h. After cell isolation, c-REL protein levels were measured by Western blot.

When the Ibidi® system was used, c-REL protein levels were upregulated under low shear stress compared to high shear stress in HUVEC (figure 3.8). This is consistent with the results obtained in HUVEC and HCAEC using the orbital shaker system, and also, with the ones obtained by *en face* staining of the murine endothelium. Hence, this confirms that c-REL protein is directly upregulated by low shear stress *in vitro*.

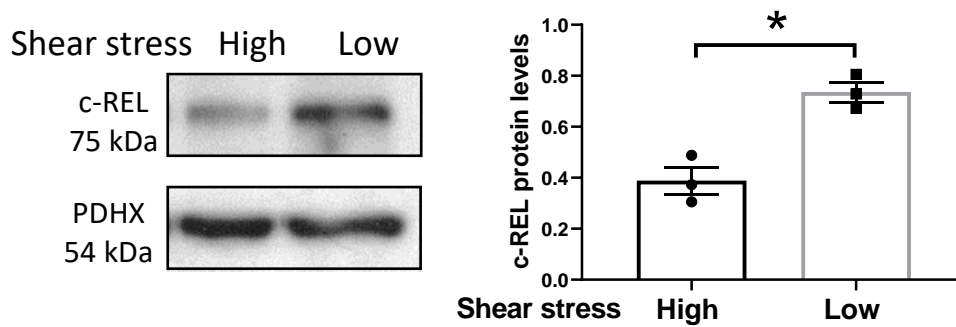


Figure 3.8. c-REL protein levels are enriched in HUVEC exposed to low shear stress using the Ibidi® parallel plate system. HUVEC were seeded on Ibidi® slides and they were exposed to high shear (13 dynes/cm²), and low shear stress (5 dynes/cm²) for 72 h using the Ibidi® parallel plate system. Protein lysates from cells exposed to high and low shear stress were generated and analysed using an anti-c-REL antibody. PDHX was used as a house-keeper gene, and it was detected on the protein lysates using an anti-PDHX antibody. Representative blot and quantification of c-REL protein levels under high and low shear stress are shown. ImageJ software was used to quantify the relative c-REL protein expression levels by densitometry. Mean values are presented with standard error of the mean, and c-REL protein levels were expressed relative to PDHX protein levels; n=3 independent experiments *p<0.05, using paired T-test.

3.8 *c-REL* mRNA expression does not reflect c-REL protein expression using the orbital shaker system

To test whether the induction of c-REL at low shear stress regions also involves an increase in *c-REL* mRNA levels, the expression of various genes in HCAEC or HUVEC exposed to flow for 72 h were assessed by qRT-PCR.

The flow-responsive genes *MCP-1* and *eNOS* were used as a control for mechanically-distinct regions. *MCP-1* transcript levels were enriched at the centre of the well exposed to disturbed flow in HUVEC and HCAEC, which is consistent with previous findings ((Hsiai et al., 2003). Again, in agreement with previous publications (Davis et al., 2001), the expression of *eNOS* was upregulated in HUVEC and HCAEC at the periphery of the wells exposed to high shear stress (figure 3.9A/C).

When endothelial *c-REL* expression was measured, I observed that the mRNA expression of *c-REL* in both HUVEC and HCAEC was significantly increased at the periphery of wells exposed to high shear stress compared to the centre (low shear and disturbed flow) (figure 3.9B/D), which differs with the results obtained at the protein level by *en face* staining of the mouse aorta and Western blotting in HUVEC and HCAEC. This suggests that c-REL protein induction at low shear stress regions does not involve an upregulation in *c-REL* mRNA levels.

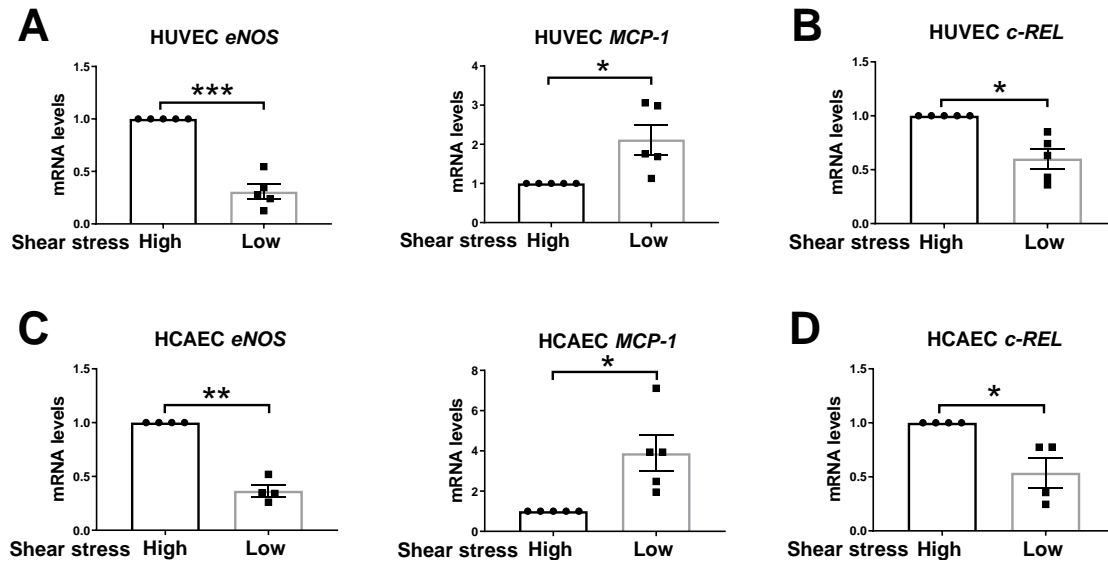


Figure 3.9. *c-REL* mRNA expression does not reflect c-REL protein expression using the orbital shaker system. Cells were exposed to flow for 72 h on a 6-well plate using the orbital system and RNA was extracted to perform qRT-PCR. Relative expression of *eNOS* and *MCP-1* in **A**) HUVEC and **C**) HCAEC. Relative expression of *c-REL* in **B**) HUVEC and **D**) HCAEC. *HPRT* was used as a house-keeping gene. Mean values at low shear stress are presented with standard error of the mean, and the expression at low shear stress areas was expressed relative to that at high shear stress regions (high shear stress=1); n=5 (HUVEC) or n=4-5 (HCAEC) independent experiments. ***p<0.001, **p<0.01, *p<0.05, using paired T-test.

3.9 *c-REL* mRNA expression does not reflect c-REL protein expression using the Ibidi® system

c-REL expression was further tested by exposing HCAEC to different shear stress patterns using the Ibidi® system. To determine the expression of genes of interest by qRT-PCR, HCAEC were exposed to laminar high shear stress (13 dynes/cm²) and low shear stress (5 dynes/cm²) for 72 h.

First, HCAEC response to flow was analysed by measuring the expression of *MCP-1* and *KLF4*, which control for mechanically-distinct regions. *MCP-1* transcript levels are known to be upregulated in EC exposed to low oscillatory shear stress compared to high shear stress (Hsiai et al., 2003), and *KLF4* has been previously shown to be downregulated under low shear stress (Hamik et al., 2007). In agreement with these studies, the results obtained using the Ibidi® system show that *KLF4* expression is elevated in HCAEC exposed to high shear stress, whereas *MCP-1* is upregulated in cells exposed to low shear stress (figure 3.10A).

The expression of *c-REL* in HCAEC exposed to high or low shear stress was then tested by qRT-PCR. *c-REL* expression in HCAEC was not significantly different between cells exposed to high and low shear stress (figure 3.10B), which again, differs with the results obtained at the protein level by *en face* staining of the mouse aorta and Western blot in HUVEC and HCAEC. Therefore, I conclude that c-REL protein is enhanced in EC exposed to low shear stress compared to high shear stress, but this regulation does not occur at the mRNA level.

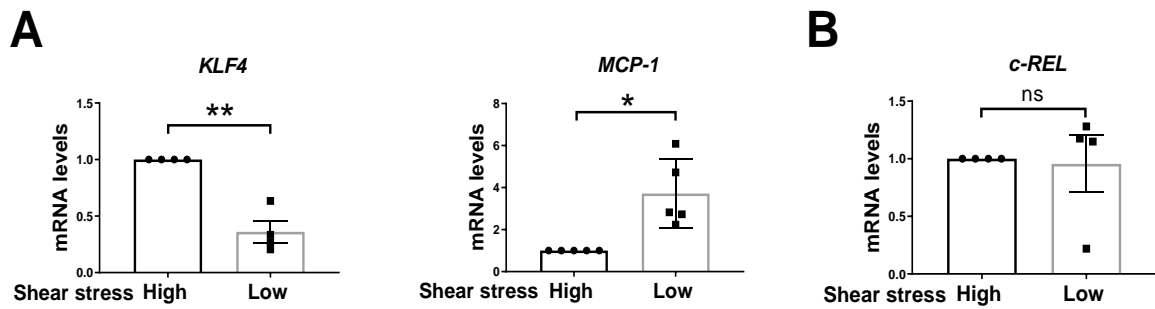


Figure 3.10. *c-REL* mRNA expression does not reflect c-REL protein expression using the Ibidi® system. HCAEC were exposed to laminar high shear stress (13 dynes/cm²) and low shear stress (5 dynes/cm²) for 72 h, and mRNA was extracted to perform qRT-PCR. **A)** Relative expression of *KLF4* and *MCP-1* in HCAEC. **B)** Expression of *c-REL* in HCAEC. *HPRT* was used as a house-keeping gene. Mean values at low shear are presented with standard error of the mean, and the expression at low shear areas was expressed relative to that at high shear (high shear stress=1); n=4-5 independent experiments.*p<0.05, ns: non-significant, using paired T-test.

3.10 Conclusions

I conclude that:

- c-Rel protein levels are upregulated at low shear stress regions exposed to disturbed flow, compared to high shear regions of the murine aorta *in vivo*.
- The induction of c-Rel protein at low shear regions of the murine aortic arch is not conserved in pigs at the mRNA level, but c-REL protein levels still need to be assessed.
- *c-Rel* mRNA expression is downregulated by partial ligation of murine carotid arteries *in vivo*, but c-Rel protein levels using this model still need to be assessed.
- c-REL protein levels are induced by low shear stress and disturbed flow compared to high shear stress in HUVEC and HCAEC.
- *c-REL* mRNA levels are not induced by low shear stress and disturbed flow in cultured EC *in vitro*, and therefore, the regulation of c-Rel induction at low shear regions does not occur at the mRNA level.

The enrichment of c-Rel protein levels at low shear stress areas *in vivo* and *in vitro* supports the idea that c-Rel is controlled by shear stress. However, the data presented in this chapter suggest that this regulation does not occur at the mRNA level. Hence, c-Rel may be subject to translational or posttranslational regulation. This warrants further investigation into the mechanism by which shear stress controls c-Rel expression.

3.11 Discussion

Although shear stress has been previously shown to regulate the expression of several NF- κ B subunits, the effect of haemodynamics on the NF- κ B subunit c-Rel had not been investigated yet. To address this, I have assessed the expression of c-Rel at mechanically-distinct regions using *in vitro* and *in vivo* models. In this chapter, I have shown that c-Rel protein levels are upregulated at low shear stress regions compared to high shear regions *in vivo* and *in vitro*, by performing *en face* staining of the murine endothelium and Western blot in HUVEC and HCAEC. However, these data suggest that the regulation of c-Rel induction at low shear regions exposed to disturbed flow does not occur at the mRNA level.

3.11.1 c-Rel expression analysis using *in vivo* models

When c-Rel protein was assessed in the murine endothelium, an enrichment of c-Rel was observed at low shear regions. Additionally, staining of EC in the murine aorta revealed that c-Rel localisation is heterogeneous, since some cells showed nuclear staining and others showed perinuclear and cytoplasmic expression. Therefore, this indicates that the induction of c-Rel in atheroprone regions does not only affect its expression, it also alters c-Rel activation. Whereas c-Rel nuclear localisation shows that c-Rel is active in some EC in atherosusceptible areas, c-Rel is only primed for further activation in those cells that present cytoplasmic and perinuclear c-Rel staining. Consistent with this, other NF- κ B subunits, such as RelA, have also been shown to be primed for activation in regions under disturbed flow, showing elevated expression but low nuclear localisation (Hajra et al., 2000).

After observing that c-Rel protein is upregulated in EC under low shear stress by performing *en face* staining of the murine aortic arch, I investigated whether this shear stress-dependent induction of c-Rel is conserved between porcine and murine models. To do this, EC were isolated from low and high shear regions of the porcine aorta.

Pigs were chosen for these expression studies for various reasons. First, the mechanically-distinct regions present in the porcine vasculature show similarities with the ones in the human arterial tree (LaMack et al., 2010). Also, both humans and pigs share a great amount of signalling pathways, as well as anatomic and physiologic characteristics within the cardiovascular system. Therefore, pigs provide a suitable model for the study of human atherogenesis (Artinger et al., 2009). Finally, pigs are large animals, and thus, it

is possible to extract a relatively high amount of RNA from regions exposed to different shear stress patterns to study gene expression.

After the isolation of porcine EC from mechanically-distinct regions, it was observed that *c-REL* expression was not significantly different between low/disturbed and high shear stress regions, which suggested that the upregulation of c-Rel protein level at low shear stress regions of the murine aorta is not conserved in pigs at the mRNA level. We further attempted to test c-REL protein levels in porcine aortas by performing immunofluorescence staining. However, the antibody used (sc71, Santa Cruz Biotechnology) did not seem to work in pigs and the signal obtained was very weak (data not shown). Therefore, other antibodies or techniques (e.g. Western blotting) could be used to assess c-REL expression at the protein level using this model. When *c-REL* mRNA expression was tested, it was observed that *c-REL* expression in low and high shear regions varied greatly among samples, which generated difficulties in the interpretation of the results. This variation could be due to smooth muscle cell (SMC) contamination. Thus optimisation of the endothelial cell scraping technique could potentially reduce SMC contamination from RNA samples, minimising *c-REL* variation among porcine aortas. Variation in *c-REL* expression could also relate to an age and size variation. Indeed, age affects haemodynamics in pigs of the same breed, by regulating, among other factors, heart rate (Swindle et al., 2012). Moreover, when cells were isolated, it was observed that different aortas presented significantly different sizes, potentially affecting our results.

Altogether, this suggests that the large variation of *c-REL* expression among different aortas may have been affected by several factors, including SMC contamination and RNA quality, age, and size variation.

Studies using partial carotid ligation as a model of disturbed flow and low shear in *ApoE* knockout mice were also performed. These studies can show causal relationships between flow and genes of interest *in vivo*, and also, this model allows the isolation of RNA in sufficient quantity, whereas naturally occurring areas of disturbed flow are small areas in which endothelial RNA isolation is more challenging. Although no quality controls were presented for this model due to limited cDNA availability, another member in our group had previously tested these samples, showing that the expression of the shear-sensitive inflammatory molecules *Vcam-1* and *Icam-1* were enhanced in partially ligated LCA

compared to sham-operated RCA (Feng et al., 2017), and therefore, controlling for mechanically-distinct areas (Walpolo et al., 1995). Using this model, it was shown that *c-Rel* expression was upregulated in high shear stress areas, which does not reflect the enrichment of c-Rel protein at low shear regions on the murine aorta. However, our study using partial carotid ligation was performed at the mRNA level, and therefore, c-Rel protein levels using this model still need to be assessed. In addition to this, the variations between both experiments could be due to biological differences. These include the time EC were exposed to flow, and also, anatomic and physiological differences in vascular beds and fluid dynamics between aorta and carotid arteries.

3.11.2 c-Rel expression analysis using in vitro flow systems

Although I have shown that c-Rel protein levels are upregulated at atheroprone regions in the mouse aorta, this upregulation could be influenced by many different factors. In addition to different shear stress patterns due to vessel geometry, c-Rel expression could be affected by the presence of inflammatory molecules, which are known to be increased in atheroprone areas due to enhanced mass transport (Tarbell, 2003). Also, atheroprone areas present low oxygen tension (hypoxia), which may alter gene expression (Silvola et al., 2011). Besides, a different embryonic origin of different regions of the aorta could also have an impact on gene regulation (Trigueros-Motos et al., 2013). To investigate whether c-Rel protein induction in atherosusceptible regions is directly regulated by shear stress, two complementary *in vitro* platforms were used, the orbital shaker system and the parallel plate or Ibidi® system.

When c-REL protein levels were assessed in HUVEC and HCAEC exposed to flow using the orbital shaker, it was observed that the expression of c-REL was promoted in the centre of the wells (low shear stress) compared to the periphery (high shear stress). By using computational fluid dynamics, it has been shown that the orbital shaker system generates complex and multidirectional flow in the centre of the well, with multiple changes in direction and constant low magnitude. In the periphery, the flow generated is relatively unidirectional, and although the magnitude of shear stress generated is relatively high, it presents temporal fluctuations (Warboys et al., 2014).

Despite the fact that the orbital system generates a multidirectional and complex flow in the centre of the wells that partly reproduces the flow in atheroprone areas of the mouse aorta, the orbital shaker system still has some limitations. It generates high and low shear

stress in the same well, which could affect the regulation of c-Rel expression, and therefore, could lead to difficulties in determining whether shear stress is directly controlling c-Rel expression. For instance, it has been shown that shear stress influences the release of endothelial microvesicles and cytokines (Vion et al., 2013). The release of these molecules by cells in the centre of the wells could affect endothelial cells located in the periphery, and similarly, cells in the centre could be influenced by the release of particles by cells in the periphery. Additionally, cells could migrate from different regions of the well, potentially affecting c-REL expression in HUVEC or HCAEC exposed to flow using the orbital system.

To overcome this limitation, we also tested c-REL expression in HUVEC under flow using the Ibidi® parallel plate system. The Ibidi® system generates steady flow conditions, generating high (13 dynes/cm²) and low (5 dynes/cm²) unidirectional shear stress in cells seeded on different Ibidi® slides. Again, it was revealed that c-REL protein levels were upregulated under low shear stress compared to high shear stress, therefore confirming that low wall shear stress directly upregulates c-REL protein levels.

To assess whether the induction of c-REL protein at low shear stress areas involves an increase in *c-REL* mRNA levels, cultured ECs were exposed to different flow patterns by using the orbital shaker (HUVEC and HCAEC) and the parallel plate or Ibidi® system (HCAEC). When cells were exposed to flow using the orbital system, it was observed that the expression of *c-REL* was enhanced under high shear stress compared to low shear stress in both HUVEC and HCAEC. However, when cells were exposed to flow using the Ibidi® system, the mRNA expression of *c-REL* did not change in HCAEC exposed to low and high shear stress. As explained above, the Ibidi® system generates steady flow conditions, generating high and low unidirectional shear stress. This contrasts with the multidirectional flow generated by the orbital shaker, and therefore, it suggests that the orbital and Ibidi® systems generate different mechanical environments that might influence gene expression, leading to variations in *c-REL*.

The orbital shaker and the Ibidi® system partly reproduce the physiological mechanics that endothelial cells are exposed to *in vivo*. However, there are a number of caveats that need to be acknowledged when using these systems. *In vivo*, cells in atheroprone regions are exposed to a complex flow that transports cells, inflammatory molecules and secreted proteins, and these factors could enhance the effect shear stress has on c-Rel expression.

This effect could also be altered by mechanical stretch of the arterial wall (Jufri et al., 2015). When cells are cultured *in vitro*, they are not exposed to this force. Additionally, the extracellular matrix that is present in the vasculature differs from the one used in *in vitro* systems. HUVEC and HCAEC are attached to 6-well plates or Ibidi® slides using gelatin, whereas cells in the vasculature are exposed to a more complex extracellular matrix. Differences in matrix composition have been shown to alter the activation of certain signalling pathways, leading to alterations in gene expression (Orr et al., 2005). Since there is no *in vitro* system that mimics the complexity of temporal and spatial flow variations *in vivo*, using several experimental models is critical to reproduce some of the physiological mechanics.

Despite the differences in *c-REL* transcript levels between the orbital shaker and the Ibidi® system, *c-REL* mRNA expression was not enhanced at low shear stress regions. This suggests that although c-REL protein is upregulated in EC under low shear stress, this regulation does not occur at the mRNA level.

3.11.3 Regulation of c-Rel protein levels

In this chapter, I have shown that there is a lack of correlation between the results obtained at the protein level and the studies performed at the mRNA level. This could be due to c-Rel protein half-life, which can be affected by protein stability of c-Rel, or posttranslational modifications, which alter c-Rel protein levels. Although posttranslational modifications in c-Rel have not been studied in detail and their functional relevance *in vivo* is, in most cases, unknown, c-Rel has been shown to undergo several of these modifications (Gilmore and Gerondakis, 2011).

Phosphorylation by PKA has been revealed to occur within the RHD, but further studies are still required to determine whether this process also occurs *in vivo* (Mosialos et al., 1991). It has also been shown that both PKC ζ and NIK phosphorylate the c-Rel TAD, promoting c-Rel transactivation activity (Martin and Fresno, 2000; Sanchez-Valdepenas et al., 2006). Moreover, c-Rel is susceptible to ubiquitination, undergoing degradation through lysines (Chen et al., 1998).

Interestingly, it has also been reported that miR-155 can repress Pellino1 (Peli1) in T cells, which is a ubiquitin ligase that induces c-Rel degradation (Liu et al., 2016). Altogether, this shows that there are multiple levels of regulation that can affect the correlation between c-Rel transcript and protein. Although understanding the mechanism

by which both transcripts and proteins are regulated is important, the protein expression is what determines the activity and function of transcription factors such as c-Rel.

3.11.4 A hypothesis for shear stress-induction of c-Rel

The data presented here suggest a model where low shear stress enhances c-Rel at the protein level, but not at the mRNA level. Among several mechanisms that could alter protein stability, miR-155 has been shown to repress T cell expression of Peli1, a ubiquitin ligase that induces c-Rel degradation (Liu et al., 2016).

Victoria Ridger's laboratory has recently shown that neutrophil-derived microvesicles are internalised by endothelial cells preferentially at areas prone to atherosclerosis, where they deliver miR-155 and induce plaque formation (Gomez et al., 2020). This suggests that miR-155 could regulate c-Rel protein levels in the endothelium, promoting the expression of c-Rel protein at areas exposed to disturbed flow by preventing its degradation.

I hypothesise that c-Rel is induced under low shear stress and disturbed flow through miR-155, which inhibits Peli1 expression and, therefore, inhibits c-Rel degradation in these regions (figure 3.11). Although this hypothesis could explain the induction of c-Rel under low shear stress *in vivo*, it is still unclear whether it could explain the *in vitro* results. Future studies are required to assess this potential mechanism.

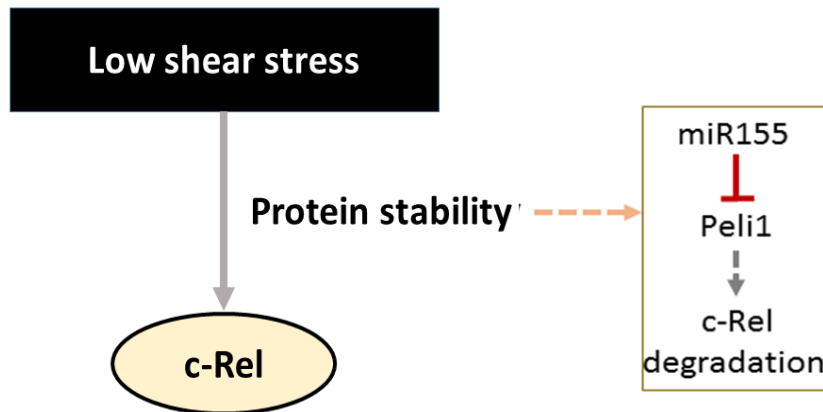


Figure 3.11. A hypothesis for shear stress-induction of c-Rel. c-Rel is enriched at regions exposed to low shear stress. Among several mechanisms that could alter protein stability, miR155 could potentially regulate c-Rel protein in the endothelium, enhancing it under low shear stress.

Chapter 4. c-Rel controls
proliferation and inflammation in
cells exposed to low shear stress *in*
vitro

4.1 Introduction

In atheroprone regions, low shear stress is sensed by endothelial cells, altering endothelial cell phenotype and function. Shear stress alters multiple transcriptional programmes that promote the initiation of atherosclerosis by regulating inflammation, proliferation and apoptosis, among other important processes.

In the previous chapter, it was shown that low shear stress induces c-Rel protein levels. Hence, this suggests that c-Rel could have a role in the modulation of signalling events that contribute to atherosclerosis development.

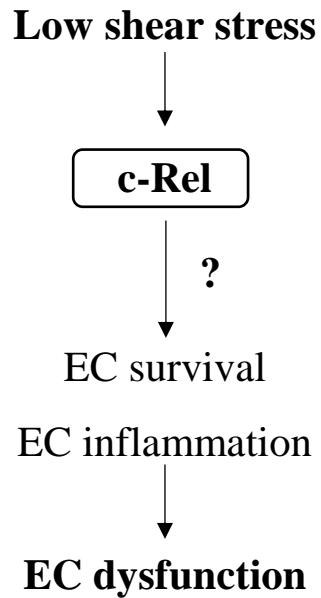
c-Rel has been shown to control proliferation, apoptosis and inflammation in several immune and non-immune cells. However, the role of c-Rel in endothelial cell function and atherosclerosis remains poorly understood. In B cells and neurons, c-Rel is known to contribute to the inhibition of cell death (Grumont et al., 1999b; Ruan et al., 2011b; Sarnico et al., 2009). Additionally, c-Rel has been reported to induce tumour growth by promoting proliferation in various types of cancer, such as lymphoma, melanoma and breast cancer, and autoimmune diseases, such as rheumatoid arthritis. It also promotes B and T cell proliferation, contributing to the development of germinal centres in B cells; and it has been involved in several fibrotic processes, including the induction of cardiac hypertrophy via upregulation of Gata4 and Mef2A (Bunting et al., 2007; Fullard et al., 2013; Gaspar-Pereira et al., 2012; Gieling et al., 2010; Grinberg-Bleyer et al., 2017; Grumont et al., 1998; Heise et al., 2014). Moreover, c-Rel has been shown to have a major role in inflammation, by inducing cytokine production in the immune system (Chen et al., 2010; Kontgen et al., 1995b; Rao et al., 2003; Wang et al., 2008).

Furthermore, other NF- κ B subunits are already known to regulate cell survival and inflammation in the endothelium. Since RelA is known to induce EC inflammation in atheroprone sites (Cuhlmann et al., 2011), and the non-canonical NF- κ B subunit p52/p100 has been reported to promote EC proliferation under disturbed flow (Bowden et al., data not published), it would be interesting to determine the extent to which c-Rel is involved in the regulation of these processes in the endothelium.

Since endothelial proliferation, apoptosis and inflammation are proatherogenic processes in endothelial cells (Foteinos et al., 2008; Zeng et al., 2009) and c-Rel is involved in the control of these processes in several cell types, c-Rel could potentially regulate these in the endothelium, influencing atherosclerosis.

4.2 Hypothesis and aims

I hypothesise that c-Rel regulates EC dysfunction under low shear stress by altering EC survival and inflammation.



To test this hypothesis, I aim to:

1. Study c-Rel function in EC exposed to low shear stress by assessing inflammation, proliferation and apoptosis.
2. Characterise c-Rel downstream targets involved in the regulation of these processes by performing RNA microarray in HUVEC.

4.3 c-Rel promotes inflammation in HUVEC exposed to low shear stress

Since inflammation is known to be a proatherogenic process in endothelial cells (Hajra et al., 2000; Passerini et al., 2004), the role of c-Rel in this process was investigated. To assess the role of c-Rel in the regulation of endothelial inflammation, siRNA-mediated *c-REL* knockdown was first performed. HUVEC were transfected with two specific *c-REL* siRNAs (RELHSS109157 and RELHSS109158, designated i and ii, respectively) and scrambled (*SCR*) siRNA by using electroporation, and cells were then exposed to flow for 72 h using the orbital shaker. In order to validate *c-REL* silencing, cells exposed to high and low shear areas were collected, and *c-REL* silencing in *c-REL* siRNA-treated cells was confirmed at the transcript level (figure 4.1A and C) and at the protein level (figure 4.1B and D).

After confirming *c-REL* knockdown, the role of *c-REL* in the control of EC inflammation was studied. *SCR* and *c-REL* siRNA-treated HUVEC were exposed to flow for 72 h using the orbital shaker, and qRT-PCR was then performed to assess mRNA expression of the inflammatory markers *VCAM-1*, *ICAM-1* and *E-SELECTIN*. Knockdown of *c-REL* using two different siRNAs (figure 4.2A and E) led to a significant decrease of *VCAM-1*, *ICAM-1* and *E-SELECTIN* expression in cells under low shear stress (figure 4.2B and F). However, under high shear stress, *c-REL* knockdown (figure 4.2C and G) significantly decreased the expression of *E-SELECTIN* but did not have major effects on *VCAM-1* or *ICAM-1* (figure 4.2D and H).

After observing that *c-REL* promotes inflammation under low shear stress in HUVEC, the role of *c-REL* in the control of VCAM-1 and E-SELECTIN protein levels was investigated. *SCR* and *c-REL* siRNA-treated HUVEC were exposed to flow for 72 h, and Western blotting was carried out to assess VCAM-1 and E-SELECTIN protein levels. *c-REL* silencing resulted in a significant reduction of VCAM-1 (figure 4.3A) and E-SELECTIN (figure 4.3B) in cells under low shear stress, whereas this reduction was not significant in cells under high shear stress (figure 4.3). Therefore, these results indicate that c-Rel promotes inflammation in HUVEC under low shear stress, at both the mRNA and protein level.

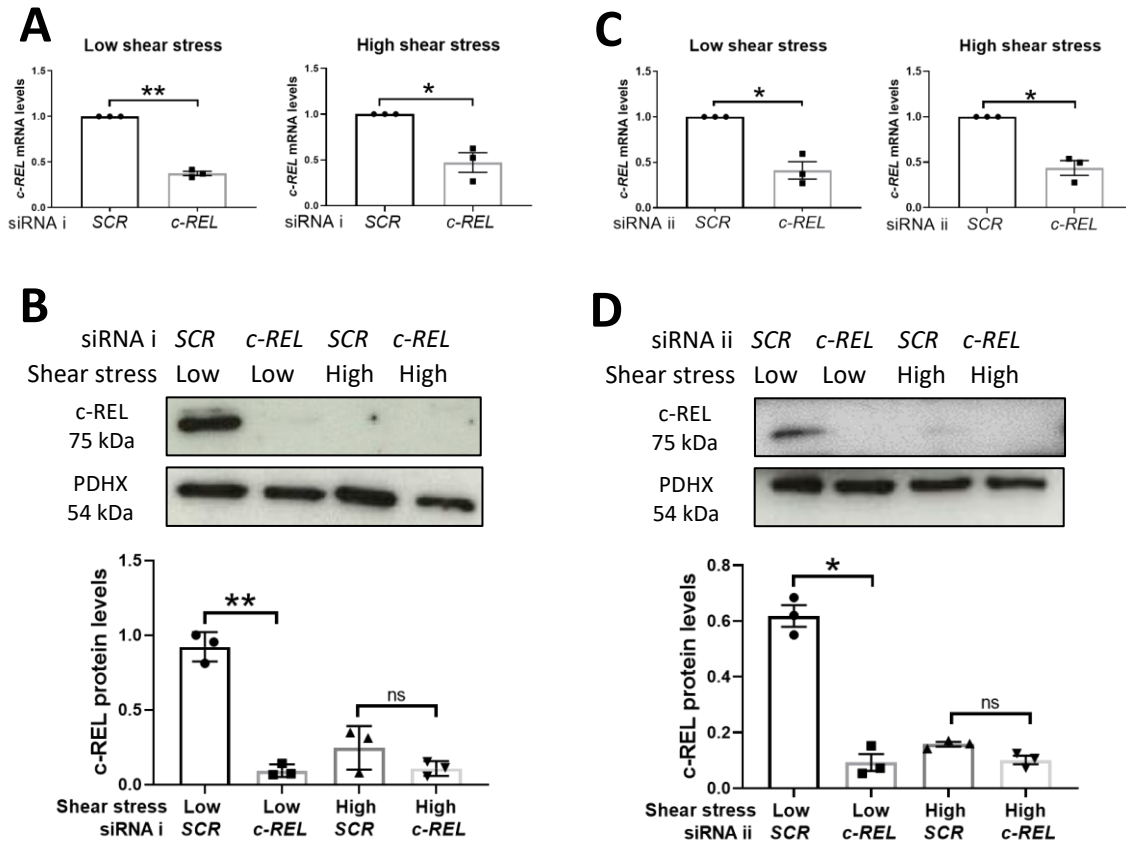
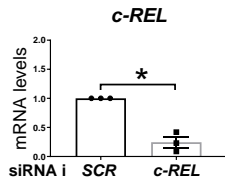
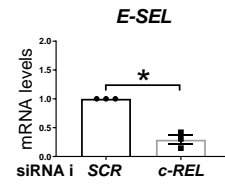
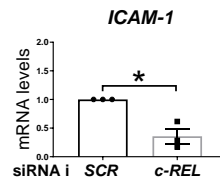
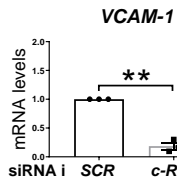


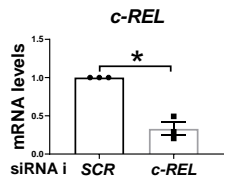
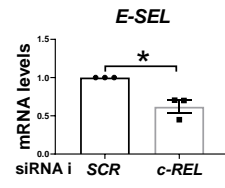
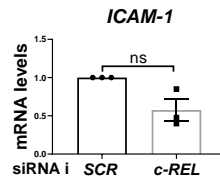
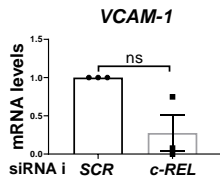
Figure 4.1. Validation of *c-REL* silencing expression in HUVEC exposed to flow using the orbital shaker. HUVEC were transfected with a non-targeting siRNA or two different *c-REL* siRNAs (RELHSS109157 (i) or RELHSS109158 (ii)) using electroporation. Cells were then exposed to flow for 72 h using the orbital plate system. To assess *c-REL* silencing using RELHSS109157, *c-REL* expression was assessed by **A**) qRT-PCR and **B**) Western blotting. To assess *c-REL* silencing using RELHSS109158, *c-REL* expression was measured by **C**) qRT-PCR and **D**) Western blotting. When qRT-PCR was performed, *HPRT* was used as a house-keeping gene. Mean values are presented with standard error of the mean, and the expression in *c-REL* siRNA-treated cells is expressed relative to that in *SCR* siRNA-treated cells (*SCR* siRNA=1). When Western blotting was performed, PDHX was used as a house-keeper gene. Representative blot and quantification of *c-REL* protein levels in HUVEC are shown. ImageJ software was used to quantify the relative *c-REL* protein expression levels by densitometry. n=3 independent experiments. *p<0.05, **p<0.01, ns: non-significant, using **A**), **C**) paired T-test or **B**), **D**) one-way ANOVA with post-hoc Tukey's test.

A

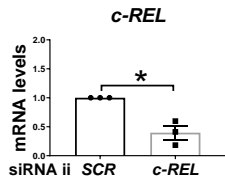
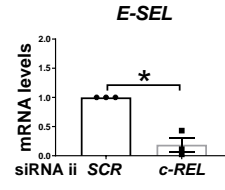
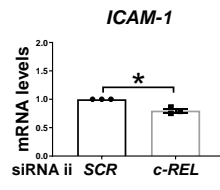
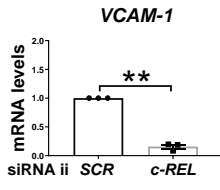
Low shear stress

**B****C**

High shear stress

**D****E**

Low shear stress

**F****G**

High shear stress

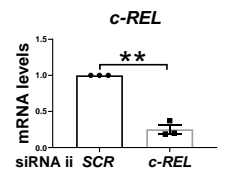
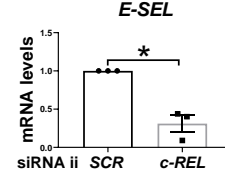
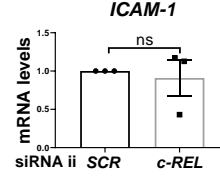
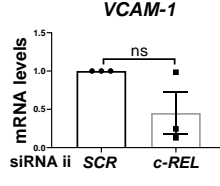
**H**

Figure 4.2. c-Rel promotes the expression of VCAM-1, ICAM-1 and E-SELECTIN in HUVEC exposed to low shear stress. HUVEC were transfected with a non-targeting siRNA or two different *c-REL* siRNAs (RELHSS109157 (i) or RELHSS109158 (ii)) using electroporation. Cells were then exposed to flow for 72 h using the orbital plate system and mRNA was extracted to perform qRT-PCR. When *c-REL* was silenced using RELHSS109157, *c-REL* expression was assessed under **A)** low and **C)** high shear stress, and the inflammatory markers *VCAM-1*, *ICAM-1* and *E-SELECTIN* (*E-SEL*) were assessed under **B)** low and **D)** high shear stress. When *c-REL* was silenced using RELHSS109158, *c-REL* expression was assessed under **E)** low and **G)** high shear stress, and the inflammatory markers *VCAM-1*, *ICAM-1* and *E-SEL* were assessed under **F)** low and **H)** high shear stress. *HPRT* was used as a house-keeping gene. Mean values are presented with standard error of the mean, and the expression in *c-REL* siRNA-treated cells is expressed relative to that in *SCR* siRNA-treated cells (*SCR* siRNA=1); n=3 independent experiments. *p<0.05, **p<0.01, ns: non-significant, using paired T-test.

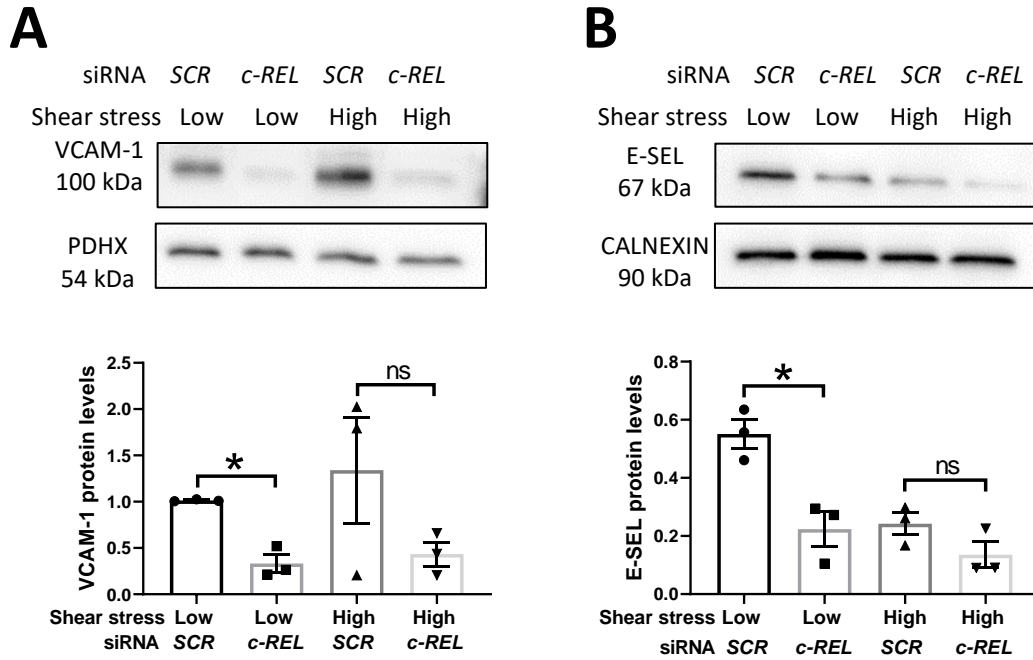


Figure 4.3. *c-Rel* promotes VCAM-1 and E-SELECTIN protein levels in HUVEC exposed to low shear stress. HUVEC were transfected with a non-targeting siRNA or a *c-REL* siRNA (RELHSS109157) using electroporation. Cells were then exposed to flow for 72 h using the orbital plate system. Protein lysates from *SCR* and *c-REL* siRNA-treated HUVEC under low and high shear stress were generated and protein expression was analysed using **A**) anti-VCAM-1 and **B**) anti-E-SELECTIN (E-SEL) antibodies. **A**) HPRT and **B**) CALNEXIN were used as house-keeping genes. Representative blot and quantification of VCAM-1 and E-SEL protein levels in HUVEC are shown. ImageJ software was used to quantify relative protein expression levels by densitometry. Mean values are presented with standard error of the mean, and protein levels are expressed relative to the house-keeping gene. n=3 independent experiments.*p<0.05, ns: non-significant, using one-way ANOVA with post-hoc Tukey's test.

4.4 c-Rel promotes proliferation in HUVEC exposed to low shear stress

Endothelial proliferation has been shown to be induced under disturbed flow, contributing to atherosclerosis (Foteinos et al., 2008; Warboys et al., 2014). Therefore, after assessing the role of c-Rel in inflammation, the contribution of c-Rel to endothelial proliferation was also investigated. *SCR* and *c-REL* siRNA-treated HUVEC were exposed to flow for 72 h using the orbital shaker system, and EC proliferation was assessed by immunofluorescence staining for proliferating cell nuclear antigen (PCNA).

Consistent with previous studies, EC proliferation was significantly increased in HUVEC exposed to low shear stress than high shear stress (figure 4.4, compare A and B, and C and D). Knockdown of *c-REL* using two different siRNAs led to a significant decrease of PCNA positive cells under low shear stress (figure 4.4A and C), indicating that c-Rel promotes EC proliferation under low shear stress. *c-REL* silencing using both siRNAs also led to a reduction in proliferation under high shear stress (figure 4.4B and D), but this reduction was more modest than the one observed under low shear stress.

In order to confirm that c-Rel promotes proliferation in HUVEC, immunofluorescence staining for Ki67 was also performed. After confirming that EC proliferation was increased in HUVEC exposed to low shear stress (figure 4.5, compare A and B), it was observed that *c-REL* silencing led to a decrease in Ki67 staining under low shear stress (figure 4.5A). Again, *c-Rel* knockdown also led to a modest decrease in proliferation under high shear stress (figure 4.5B). These data are consistent with the immunofluorescence staining for PCNA, and therefore, confirm that c-Rel induces proliferation in HUVEC, particularly under low shear stress.

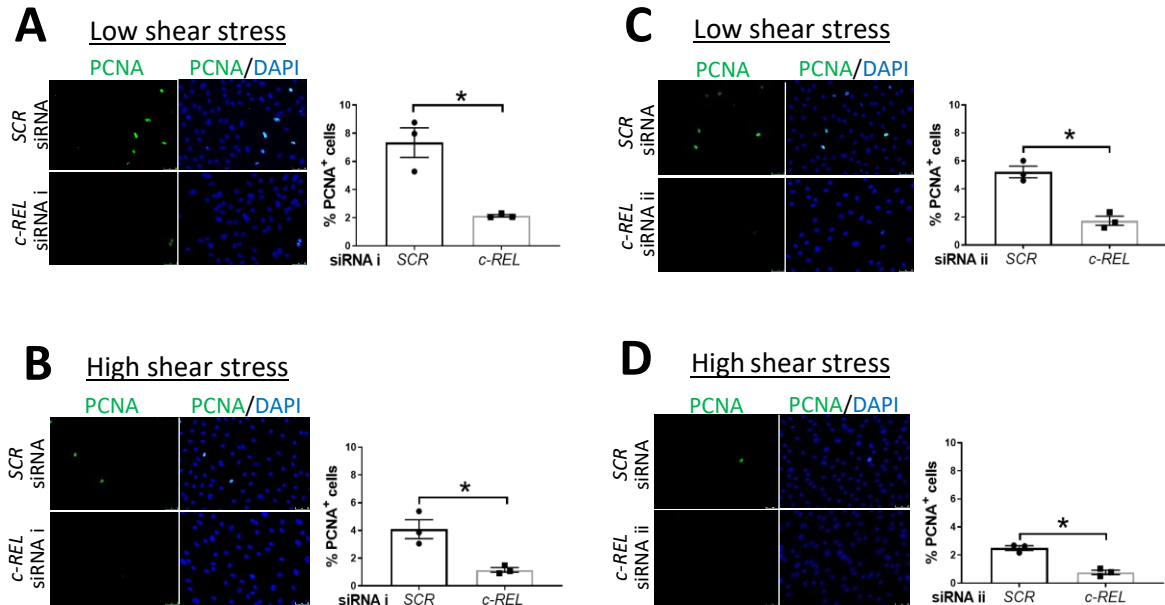


Figure 4.4. c-Rel promotes EC proliferation by PCNA staining in HUVEC exposed to low shear stress. HUVEC were transfected with a non-targeting siRNA or two different *c-REL* siRNAs (RELHSS109157 (i) or RELHSS109158 (ii)) using electroporation. Cells were then exposed to flow for 72 h using the orbital plate system. Anti-PCNA antibody (green) was used to stain for proliferative cells and DAPI (blue) for nuclear staining. When *c-REL* was silenced using RELHSS109157, immunofluorescence staining for PCNA was assessed under **A**) low and **B**) high shear stress. Similarly, when *c-REL* was silenced using RELHSS109158, immunofluorescence staining for PCNA was assessed under **C**) low and **D**) high shear stress. Representative images and quantification of PCNA positive cells are shown. Mean values are presented with standard error of the mean; n=3 independent experiments. *p<0.05, using paired T-test.

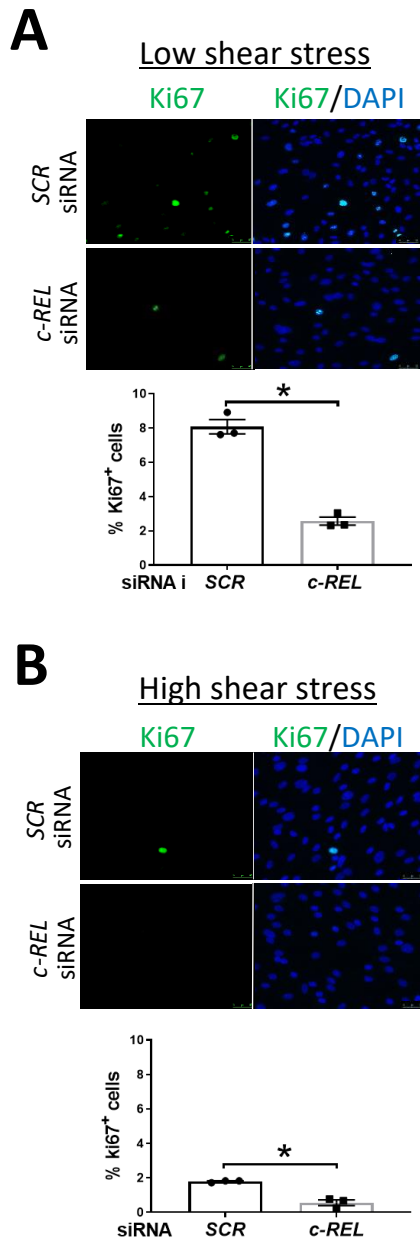


Figure 4.5. c-Rel promotes EC proliferation by Ki67 staining in HUVEC exposed to low shear stress. HUVEC were transfected with a non-targeting siRNA or a *c-REL* siRNA (RELHSS109157) using electroporation. Cells were then exposed to flow for 72 h using the orbital plate system. Anti-Ki67 antibody (green) was used to stain for proliferative cells and DAPI (blue) for nuclear staining. When *c-REL* was silenced using RELHSS109157, immunofluorescence staining for Ki67 was assessed under **A**) low and **B**) high shear stress. Representative images and quantification of Ki67 positive cells are shown. Mean values are presented with standard error of the mean; n=3 independent experiments. *p<0.05, using paired T-test.

4.5 c-Rel does not have a major role in EC apoptosis

After confirming that c-Rel has a role in controlling EC inflammation and proliferation under low shear stress, the potential role of c-Rel in EC apoptosis, another proatherogenic process, was investigated. *SCR* and *c-REL* siRNA-treated HUVEC were exposed to flow for 72 h using the orbital shaker system, and EC apoptosis was assessed by immunofluorescence staining for active caspase 3.

Consistent with previous studies, EC apoptosis was increased in HUVEC exposed to low shear stress compared to high shear stress (figure 4.6, compare A and B, and C and D). Knockdown of *c-REL* using the *c-REL* siRNA RELHSS109157 led to a significant but very modest increase of active caspase 3 positive cells under low shear stress (figure 4.6A), whereas it did not affect apoptosis under high shear stress (figure 4.6B). Similarly, knockdown of *c-REL* using RELHSS109158 *c-REL* siRNA led to a slight but non-significant increase in apoptosis under low shear stress (figure 4.6C), whereas, again, it did not affect apoptosis under high shear stress (figure 4.6D). The proportion of apoptotic cells observed under low shear stress is around 1%, and the difference in apoptosis between *SCR* and *c-REL* siRNA-treated HUVEC is minimal and might not be biologically relevant. Therefore, these data suggest that c-Rel does not have a major role in the control of EC apoptosis.

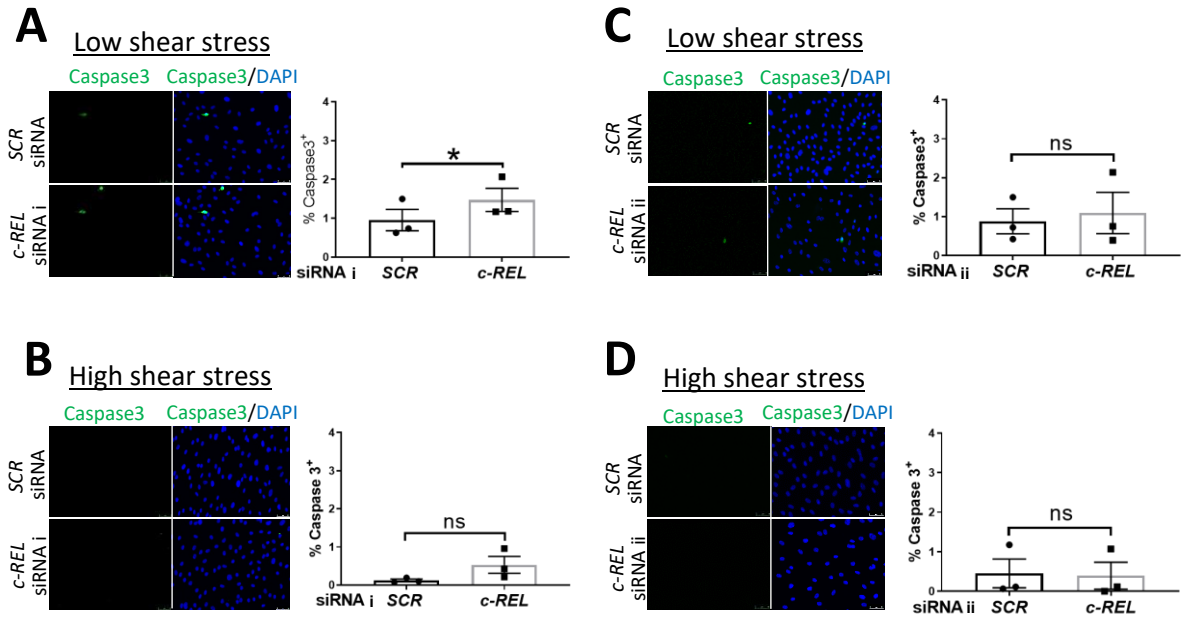


Figure 4.6. c-Rel does not have a major role in EC apoptosis. HUVEC were transfected with a non-targeting siRNA or two different *c-REL* siRNAs (RELHSS109157 (i) or RELHSS109158 (ii)) using electroporation. Cells were then exposed to flow for 72 h using the orbital plate system. Anti-active caspase 3 antibody (green) was used to stain for apoptotic cells and DAPI (blue) for nuclear staining. When *c-REL* was silenced using RELHSS109157, immunofluorescence staining for active caspase 3 was assessed under **A**) low and **B**) high shear stress. Similarly, when *c-REL* was silenced using RELHSS109158, immunofluorescence staining for active caspase 3 was assessed under **C**) low and **D**) high shear stress. Representative images and quantification of active caspase 3 positive cells are shown. Mean values are presented with standard error of the mean; n=3 independent experiments. *p<0.05, ns: non-significant, using paired T-test.

4.6 Characterisation of genes downstream of c-Rel using a RNA microarray: c-Rel positively regulates TXNIP, p38 and RANK

Although I have previously shown that c-Rel promotes EC inflammation and proliferation under low shear stress, the mechanisms by which c-Rel controls these processes are still unknown. In order to investigate this, a RNA microarray was performed in HUVEC under low shear stress. *SCR* and *c-REL* siRNA-treated HUVEC were exposed to flow for 72 h using the orbital shaker system. After extracting RNA from cells exposed to low shear stress, RNA samples from three different HUVEC donors were labelled and hybridised against Human Clariom™ S Assay (Affymetrix). Data were then analysed using Transcriptome Analysis Console Software (Affymetrix), which revealed that, under low shear stress, 2398 genes were altered by *c-REL* silencing ($p < 0.05$, fold change > 1.2). Out of these 2398 differentially expressed genes, 1030 were downregulated when *c-REL* was silenced (positive regulation) (see appendix 2), and 1368 were upregulated following *c-REL* knockdown (negative regulation).

Once this was performed, genes positively regulated by c-Rel were selected for further analysis. A functional gene set enrichment analysis using DAVID Functional Annotation Analysis Software (<http://david.abcc.ncifcrf.gov>) was carried out, which revealed multiple enriched molecular functions (table 4.1).

Some of these enriched molecular functions were mitochondrion, ribosome and translation, cell-cell adhesion, presplicesome, and protein ubiquitination, among others. Interestingly, the MAPK signalling cascade and the NIK/NF- κ B signalling pathway, which have a known role in the regulation of inflammation and proliferation, also showed high enrichment scores (table 4.1).

Gene Ontology	Number of genes	Enrichment Score
Mitochondrion	121	7.11
Ribosome and translation	70	4.70
Cell-cell adhesion	35	2.94
Presplicesosome	7	2.61
Protein ubiquitination	95	2.45
DNA damage recognition, nucleotide excision repair	11	2.33
proteasome-mediated ubiquitin-dependent protein catabolic process	33	2.31
MAPK cascade	31	2.31
NIK/NF- κ B signalling	10	2.31
Mitochondrial respiratory chain complex I assembly	10	2.03
Nucleosome	19	1.78
Protein heterodimerisation activity	41	1.78
Innate immune response	28	1.73
Carbohydrate binding	12	1.67
Zinc ion binding	84	1.54
Response to interferon	7	1.51

Table 4.1. Functional annotation of differentially expressed genes. After performing RNA microarray, A functional enrichment analysis of genes positively regulated by c-Rel was carried out using DAVID Functional Annotation Bioinformatics Microarray Analysis Software.

A total of seven genes involved in the MAPK signalling cascade and the NIK/NF- κ B signalling pathway were selected for further analysis, due to their known or inferred implication in the control of inflammation and proliferation. Of these, five are components (*MAPK1 (ERK2)*, *MAPK3 (ERK1)*, *MAPK9 (JNK2)* and *MAPK14 (p38)*) or regulators (*TXNIP*) of the MAPK cascade, whereas two of them (*TNFSF12 (TWEAK)* and *TNFRSF11A (RANK)*) are involved in the regulation of the NF- κ B pathway, and in particular, the non-canonical NF- κ B signalling pathway. The expression of these selected genes was visualised using a volcano plot (figure 4.7).

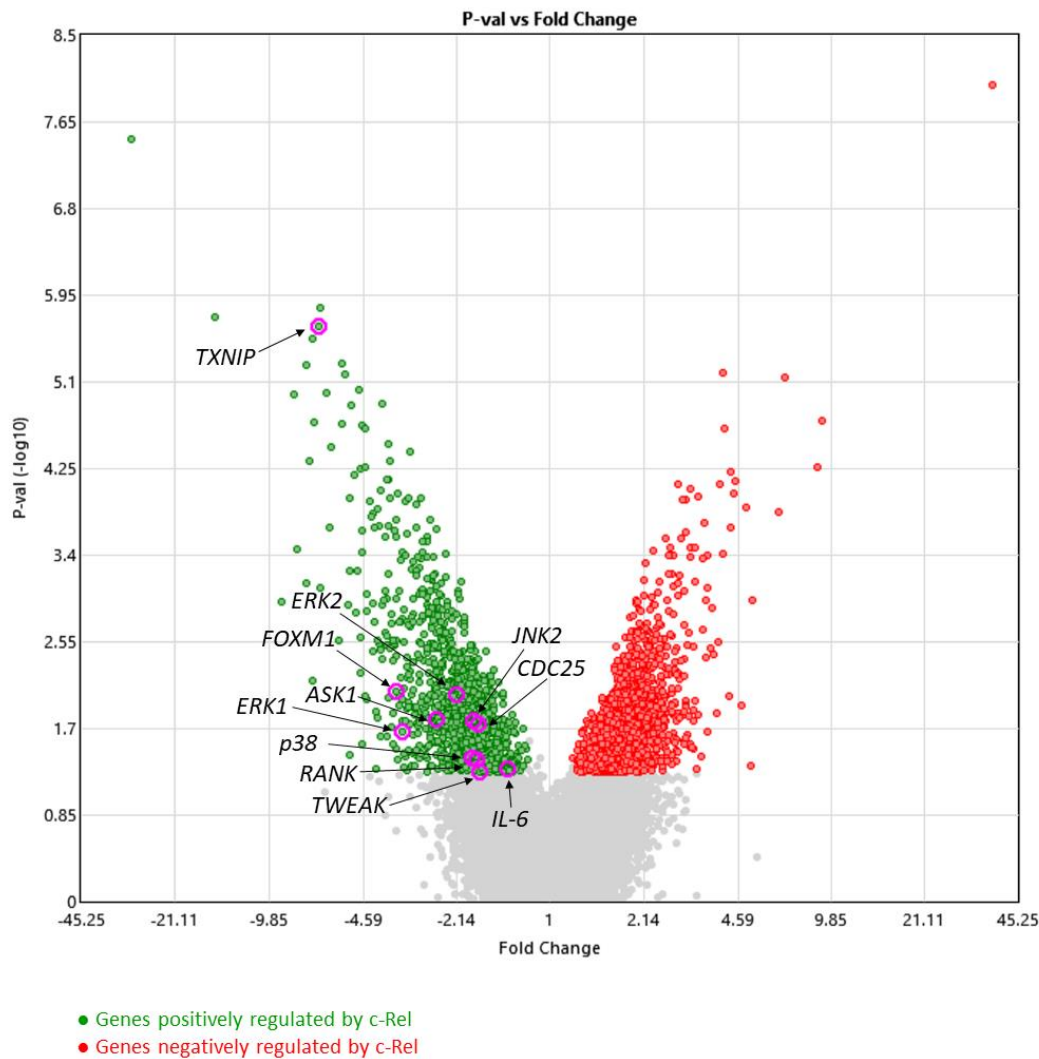


Figure 4.7. RNA microarray in HUVEC under low shear stress. HUVEC from three different donors were transfected with a non-targeting siRNA or a *c-REL* siRNA (RELHSS109157) using electroporation. Cells were then exposed to flow for 72 h using the orbital plate system. RNA samples were labelled and hybridised against Human Clariom™ S Assay (Affymetrix). Transcriptome Analysis Console Software (Affymetrix) was used to analyse the data generated, which revealed 2398 genes to be differentially expressed ($p < 0.05$, fold change > 1.2). The data are visualised as a volcano plot. 1030 genes were positively regulated by c-Rel (green), whereas 1368 were negatively regulated (red). Selected genes involved in the MAPK cascade and the NIK/NF- κ B pathway, as well as other genes potentially involved in inflammation and proliferation are highlighted in pink.

To validate differential expression of these seven genes, qRT-PCR was first performed in HUVEC using three different donors. The expression of *TXNIP*, *MAPK1 (ERK2)*, *MAPK3 (ERK1)*, *MAPK9 (JNK2)*, *MAPK14 (p38)*, *TNFSF12 (TWEAK)* and *TNFRSF11A (RANK)* was assessed in *SCR* and *c-REL* siRNA-treated HUVEC, after exposing them to flow for 72 h using the orbital shaker system. Knockdown of *c-REL* in HUVEC under low shear stress led to a significant decrease of *TXNIP* and *MAPK14 (p38)*, which are components of the MAPK cascade, and *TNFRSF11A (RANK)*, which is an activator of the NIK/NF- κ B signalling pathway. However, *c-REL* knockdown had inconsistent effects on *MAPK1 (ERK2)*, *MAPK3 (ERK1)*, *MAPK9 (JNK2)* and *TNFSF12 (TWEAK)* (figure 4.8A and B). Therefore, these results validate *TXNIP*, *p38* and *RANK* as c-Rel target genes.

To further validate *TXNIP*, *p38* and *RANK* as c-Rel target genes, Western blotting was performed in HUVEC. After exposing *SCR* and *c-REL* siRNA-treated HUVEC to 72 h of flow using the orbital shaker, *TXNIP*, *p38* and *RANK* protein levels were assessed. *c-REL* silencing in cells under low shear stress resulted in a significant reduction of *TXNIP* (figure 4.9A), *p38* (figure 4.9B) and *RANK* (figure 4.9C), and therefore, these results confirm that *TXNIP*, *p38* and *RANK* are positively regulated by c-Rel.

TXNIP and *p38* have been previously shown to mediate the proinflammatory effects of shear stress (Yamawaki et al., 2005; Zakkar et al., 2008), and thus, c-Rel positive regulation of *TXNIP* and *p38* provides a potential mechanism for c-Rel proinflammatory effects. *RANK* is known to promote proliferation (Kukita and Kukita, 2013) and is an activator of non-canonical NF- κ B (Novack et al., 2003). Interestingly, our group has recently reported that the non canonical NF- κ B subunit p52/p100 induces EC proliferation in response to low shear stress (Bowden et al., data not published). Hence, c-Rel-dependent activation of *RANK*, and therefore, the non-canonical NF- κ B pathway, could also provide a potential mechanism for c-Rel pro-proliferative effects.

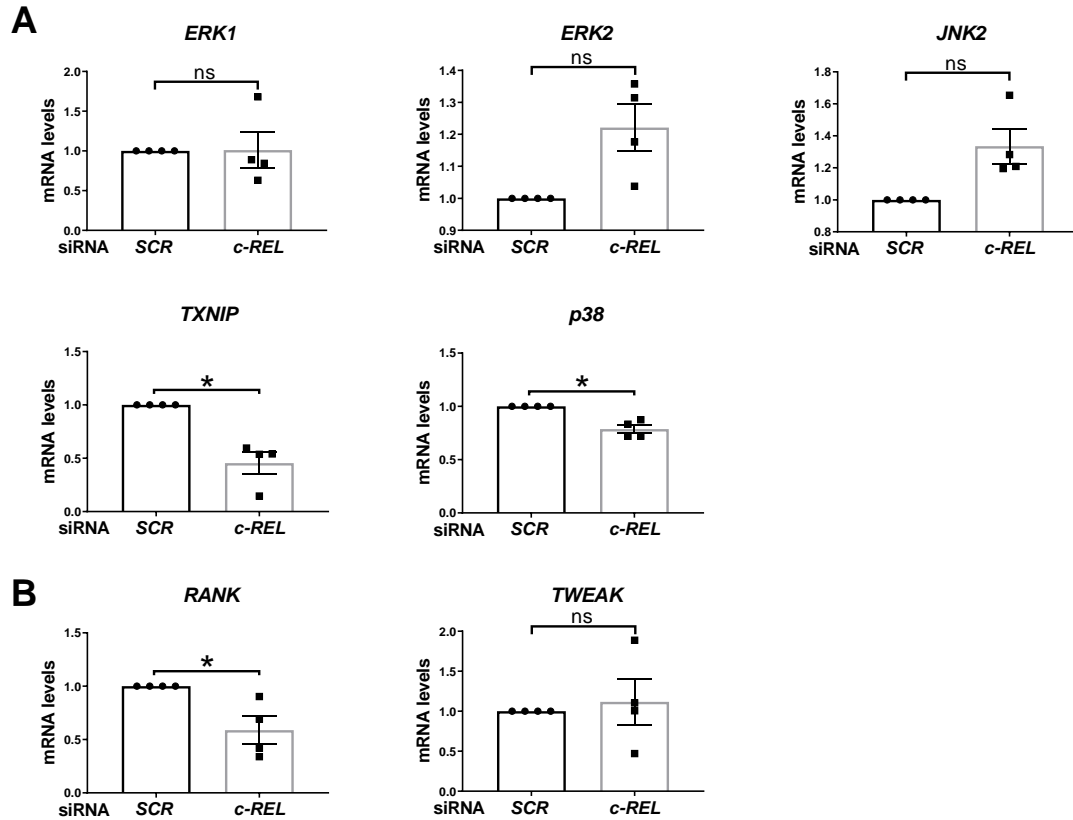


Figure 4.8. Validation of microarray data by qRT-PCR. HUVEC from three different donors were transfected with a non-targeting siRNA or a *c-REL* siRNA (RELHSS109157) using electroporation. Cells were then exposed to flow for 72 h using the orbital plate system and RNA was extracted to perform qRT-PCR. Relative expression of **A**) MAPK cascade components *TXNIP*, *MAPK1* (*ERK2*), *MAPK3* (*ERK1*), *MAPK9* (*JNK2*), *MAPK14* (*p38*) and **B**) NIK/NF- κ B signalling pathway components *TNFSF12* (*TWEAK*) and *TNFRSF11A* (*RANK*) was measured in HUVEC. *HPRT* was used as a house-keeping gene. Mean values are presented with standard error of the mean, and the expression in *c-REL* siRNA-treated cells is expressed relative to that in *SCR* siRNA-treated cells (*SCR* siRNA=1); n=3 independent experiments. *p<0.05, ns: non-significant, using paired T-test.

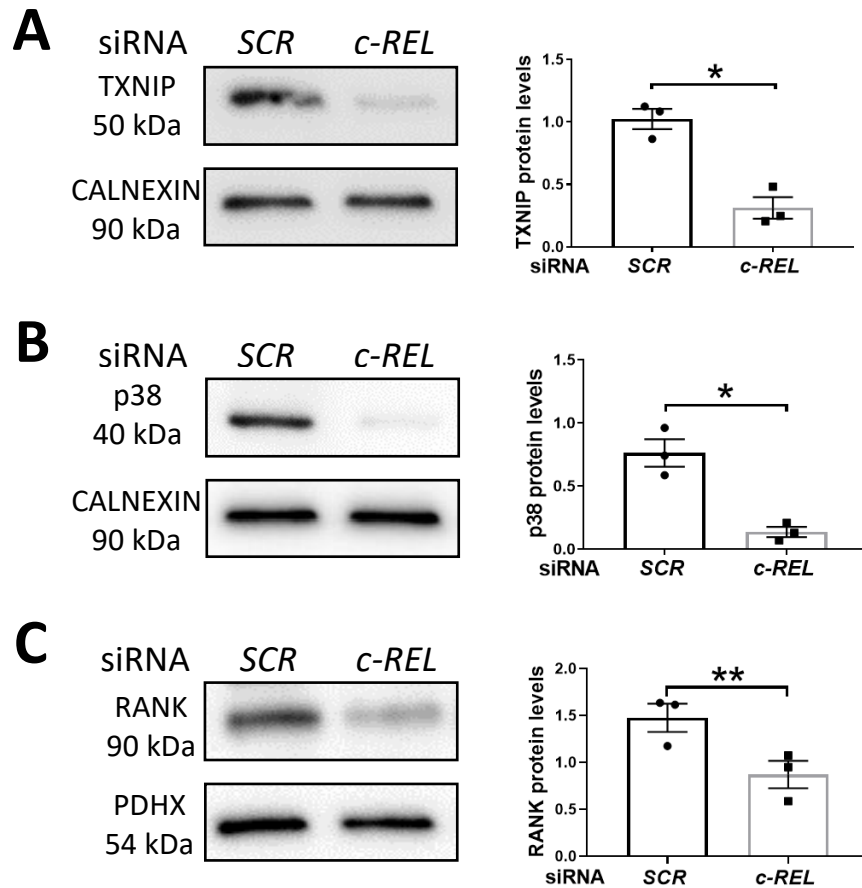


Figure 4.9. Validation of TXNIP, p38 and RANK as c-Rel target genes by Western blotting. HUVEC from three different donors were transfected with a non-targeting siRNA or a *c-REL* siRNA (RELHSS109157) using electroporation. Cells were then exposed to flow for 72 h using the orbital plate system. Protein lysates from *SCR* and *c-REL* siRNA-treated HUVEC under low shear stress were generated and analysed using anti-TXNIP, anti-p38 and anti-RANK antibodies. HPRT and CALNEXIN were used as house-keeping genes. Representative blots and quantification of **A**) TXNIP **B**) p38 and **C**) RANK protein expression levels under low shear stress in *SCR* and *c-REL* siRNA-treated HUVEC are shown. ImageJ software was used to quantify the relative TXNIP, p38 and RANK protein expression levels by densitometry. Mean values are presented with standard error of the mean, and TXNIP, p38 and RANK were expressed relative to the house-keeping gene; n=3 independent experiments, **p<0.01, *p<0.05, using paired T-test.

4.7 c-Rel positively regulates the non-canonical NF- κ B subunits NIK, p52 and p100 to promote proliferation

In the previous section, I have demonstrated that RANK is regulated by c-Rel, by performing microarray studies and subsequent qRT-PCR and Western blotting experiments. RANK is known to promote proliferation (Kukita and Kukita, 2013) and it also activates the non-canonical NIK/NF- κ B signalling pathway in other cell types (Novack et al., 2003). Since it has been recently reported that the non canonical NF- κ B subunits p52/p100 induce EC proliferation in response to low shear stress (Bowden et al., data not published), a potential role of c-Rel in the regulation of the non-canonical NIK/NF- κ B pathway was investigated.

As NIK activates p100 processing to p52 and is essential for non-canonical NF- κ B activity (Xiao et al., 2001), the potential regulation of NIK, p100 and p52 by c-Rel was first studied by qRT-PCR. The mRNA expression of *NIK* and *NFKB2* (*p52/p100*) was assessed in *SCR* and *c-REL* siRNA-treated HUVEC, after exposing them to flow for 72 h using the orbital shaker system. Knockdown of *c-REL* in HUVEC under low shear stress led to a significant decrease of *NIK* mRNA levels, indicating that c-Rel positively regulates *NIK* at the transcript level. However, *c-REL* silencing did not significantly affect *NFKB2* mRNA levels (figure 4.10A).

To assess whether c-Rel has a role in the regulation of p52 and p100 protein levels, Western blotting was performed in HUVEC. After exposing *SCR* and *c-REL* siRNA-treated HUVEC to 72 h of flow using the orbital shaker, p52 and p100 protein levels were assessed. *c-REL* silencing resulted in a significant decrease of p52 (figure 4.10B) and p100 (figure 4.10C), indicating that c-Rel positively regulates p52 and p100 protein levels, but showing that this regulation does not occur at the mRNA level.

Altogether, these data indicate that c-Rel positively regulates the non-canonical NF- κ B components RANK, NIK and p52/p100, thereby providing a potential mechanism for the pro-proliferative effects of c-Rel.

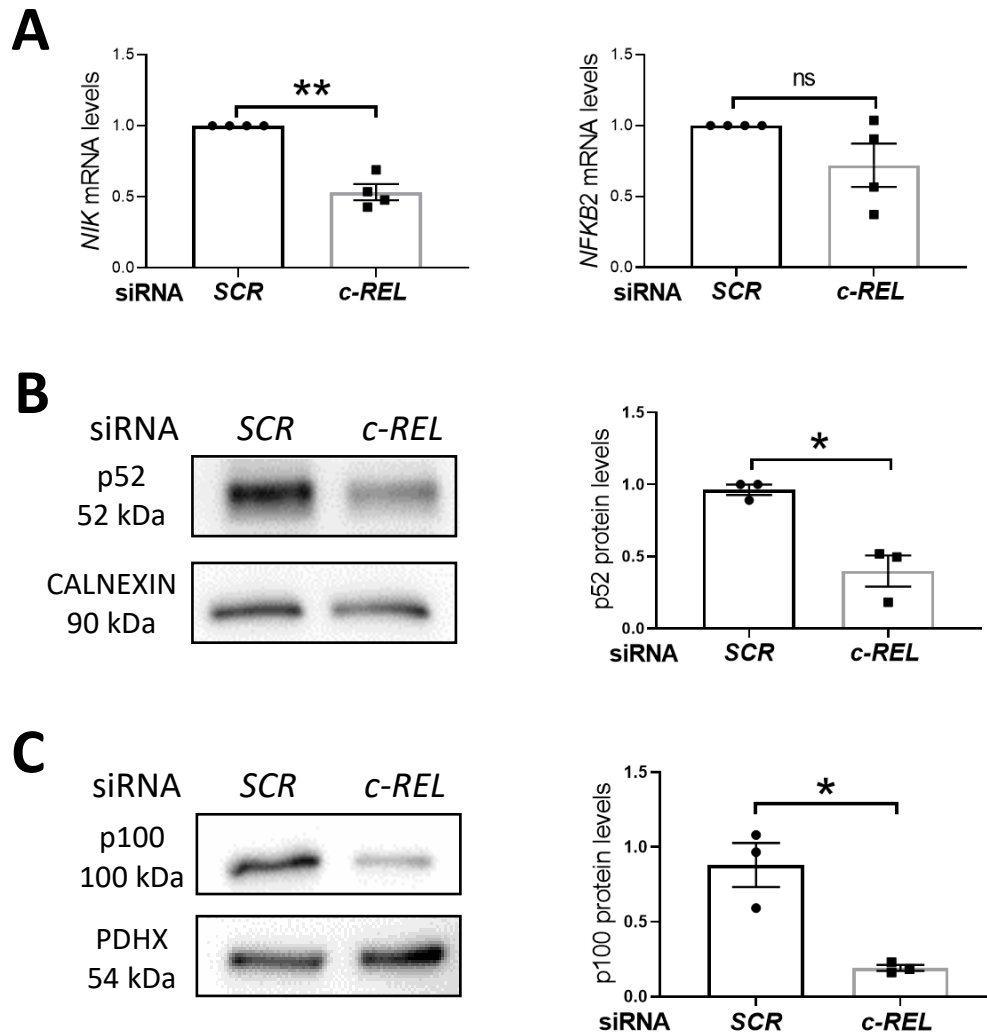


Figure 4.10. c-Rel promotes EC proliferation by inducing the non-canonical NF- κ B subunits NIK, p52 and p100. HUVEC were transfected with a non-targeting siRNA or a *c-REL* siRNA (RELHSS109157) using electroporation. Cells were then exposed to flow for 72 h using the orbital plate system. **A**) qRT-PCR was performed to assess the relative expression of *NIK* and *NFKB2*. *HPRT* was used as a house-keeping gene. Mean values are presented with standard error of the mean, and the expression in *c-REL* siRNA-treated cells is expressed relative to that in *SCR* siRNA-treated cells (*SCR* siRNA=1). **B**), **C**) Protein lysates from *SCR* and *c-REL* siRNA-treated HUVEC under low shear stress were generated and analysed using anti-p52 and anti-p100 antibodies. CALNEXIN and PDHX were used as house-keeping genes. Representative blots and quantification of **B**) p52 and **C**) p100 protein expression levels under low shear stress in *SCR* and *c-REL* siRNA-treated HUVEC are shown. ImageJ software was used to quantify the relative p52 and p100 protein levels by densitometry. p52 and p100 were expressed relative to the house-keeping gene. Mean values are presented with standard error of the mean; n=3-4 independent experiments, **p<0.01, *p<0.05, ns: non-significant, using paired T-test.

4.8 c-Rel negatively regulates p21 to promote proliferation

p52 has been previously shown to induce cell proliferation via inhibition of the anti-proliferative protein p21 in human osteosarcoma cells (Schumm et al., 2006). Interestingly, this process has been recently studied in our lab, suggesting that p52 promotes EC proliferation under low shear stress through repression of p21 (Bowden et al., data not published). Therefore, after showing that c-Rel is involved in the regulation of the non-canonical NF- κ B subunits p100 and p52, the potential role of c-Rel in the control of p21 in endothelial cells was also investigated.

p21 mRNA expression was assessed in *SCR* and *c-REL* siRNA-treated HUVEC by qRT-PCR, after exposing cells to flow for 72 h using the orbital shaker system. *c-REL* silencing in HUVEC under low shear stress led to a significant upregulation of *p21* mRNA levels, indicating that c-Rel negatively regulates *p21* at the transcript level (figure 4.11A).

Similarly, when Western blotting was performed in *SCR* and *c-REL* siRNA-treated HUVEC to assess p21 protein levels, *c-REL* knockdown also resulted in a significant increase of p21 protein levels, confirming that c-Rel represses p21 expression (figure 4.11B).

To further validate the negative regulation of p21 by c-Rel, p21 was assessed by immunofluorescence staining in *SCR* and *c-REL* siRNA-treated HUVEC exposed to low shear stress. Consistent with the previous data, *c-REL* silencing led to a 8-fold increase of p21 (figure 4.11C). Therefore, these results indicate that c-Rel inhibits the anti-proliferative p21 in HUVEC under low shear stress.

Altogether, these data show that c-Rel promotes endothelial proliferation by inducing the non-canonical NF- κ B components RANK, NIK and p52/p100, and also, through repression of p21.

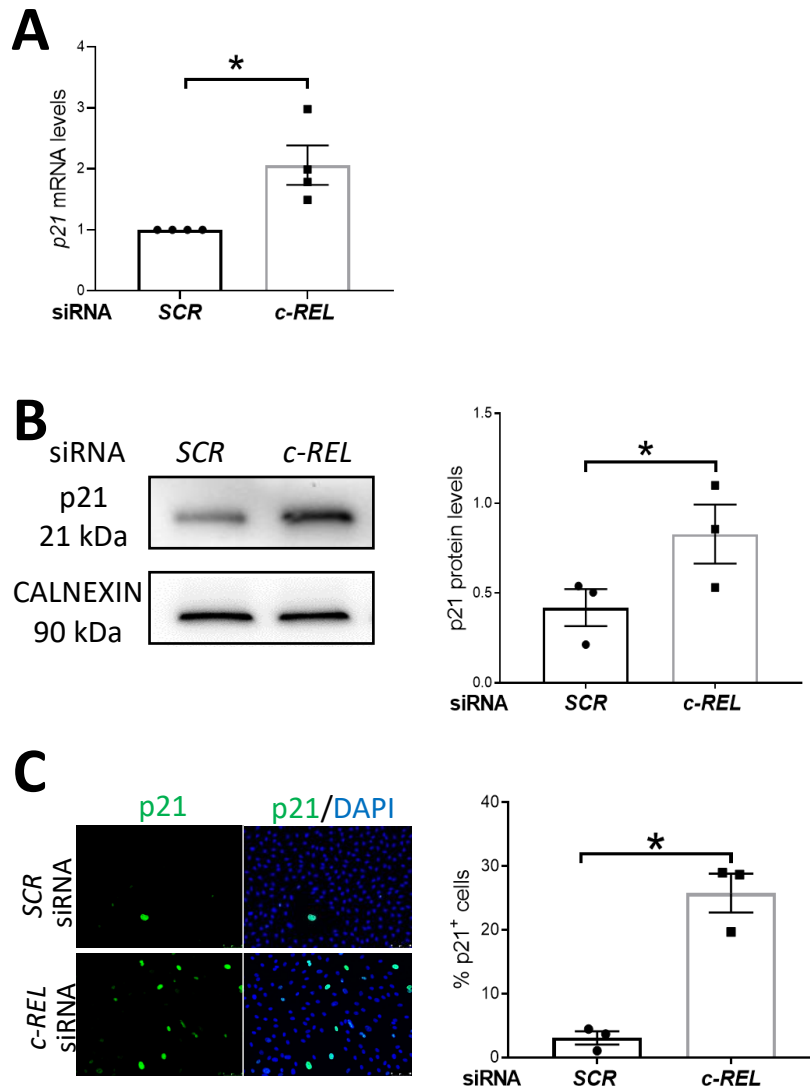


Figure 4.11. c-Rel promotes EC proliferation via inhibition of p21. HUVEC were transfected with a non-targeting siRNA or a *c-REL* siRNA (RELHSS109157) using electroporation. Cells were exposed to flow for 72 h using the orbital plate system. **A**) qRT-PCR was performed to assess the relative expression of *p21*. *HPRT* was used as a house-keeping gene. Mean values are presented with standard error of the mean, and the expression in *c-REL* siRNA-treated cells is expressed relative to that in *SCR* siRNA-treated cells (*SCR* siRNA=1). **B**) Protein lysates from *SCR* and *c-REL* siRNA-treated HUVEC under low shear stress were generated and analysed using an anti-p21 antibody. CALNEXIN was used as a house-keeping gene. Representative blot and quantification of p21 protein levels in HUVEC are shown. ImageJ software was used to quantify the relative p21 protein levels by densitometry. p21 levels were expressed relative to CALNEXIN. **C**) Immunofluorescence staining for p21 was performed using an anti-p21 antibody (green), and DAPI (blue) was used for nuclear staining. Representative images and quantification of p21 positive cells are shown. Mean values are presented with standard error of the mean; n=3-4 independent experiments, *p<0.05, using paired T-test.

4.9 Conclusions

In this chapter I have shown that c-Rel promotes EC dysfunction, by promoting both inflammation and proliferation in EC exposed to low shear stress. Furthermore, I have elucidated the mechanism by which c-Rel controls these processes, by performing RNA microarray and subsequent validation experiments.

Specifically, I conclude that:

- c-Rel promotes inflammation and proliferation in endothelial cells exposed to low shear stress.
- c-Rel does not have a major role in apoptosis in endothelial cells exposed to flow.
- c-Rel positively regulates the MAPK cascade components TXNIP and p38, providing a potential mechanism for c-Rel proinflammatory effects.
- c-Rel induces the expression of the non-canonical NIK/NF- κ B signalling pathway components RANK, NIK and p52/p100, and also, it represses the expression of the anti-proliferative p21. Therefore, this provides a potential mechanism for c-Rel pro-proliferative effects.

4.10 Discussion

c-Rel has been shown to regulate inflammation, proliferation and apoptosis in several cell types (Chen et al., 2010; Fullard et al., 2013; Gaspar-Pereira et al., 2012; Grumont et al., 1999a; Kontgen et al., 1995b; Sarnico et al., 2009). However, c-Rel function in the endothelium has not been studied. The data presented in this chapter indicates that c-Rel promotes EC proliferation and inflammation, suggesting that c-Rel expression in low shear stress areas regulates endothelial cell physiology.

c-REL silencing markedly reduced the percentage of proliferative cells under low shear stress, reducing their levels to those of control cells under high shear stress. Hence, this indicates that c-Rel could be involved in controlling the transition between a proliferative and a quiescent phenotype in sheared cells. Similarly, *c-REL* silencing also decreased E-SELECTIN protein levels under low shear stress to the levels observed under high shear stress, and thus, this could again indicate a role of c-Rel in regulating the switch between a proinflammatory phenotype in low shear areas and an anti-inflammatory one in regions exposed to high shear stress. After showing for the first time that c-Rel is involved in the regulation of low shear stress-induced endothelial dysfunction by promoting EC proliferation and the expression of inflammatory and adhesion molecules (VCAM-1, ICAM-1 and E-SELECTIN), the mechanisms by which c-Rel promotes these processes were investigated.

RNA microarray in HUVEC and subsequent experiments revealed that c-Rel promotes inflammation via induction of the MAPK regulator TXNIP and its downstream target p38, whereas the mechanism underlying c-Rel-dependent induction of proliferation involves the non-canonical NF- κ B signalling pathway and the anti-proliferative molecule p21. I have shown that c-Rel induces the NF- κ B activator RANK, its downstream target NIK, and the non-canonical NF- κ B subunits p100/p52, eventually leading to an increase in proliferation by inhibiting the anti-proliferative molecule p21 (figure 4.12). The function of c-Rel in EC exposed to flow and other data shown in this chapter will now be discussed in further detail.

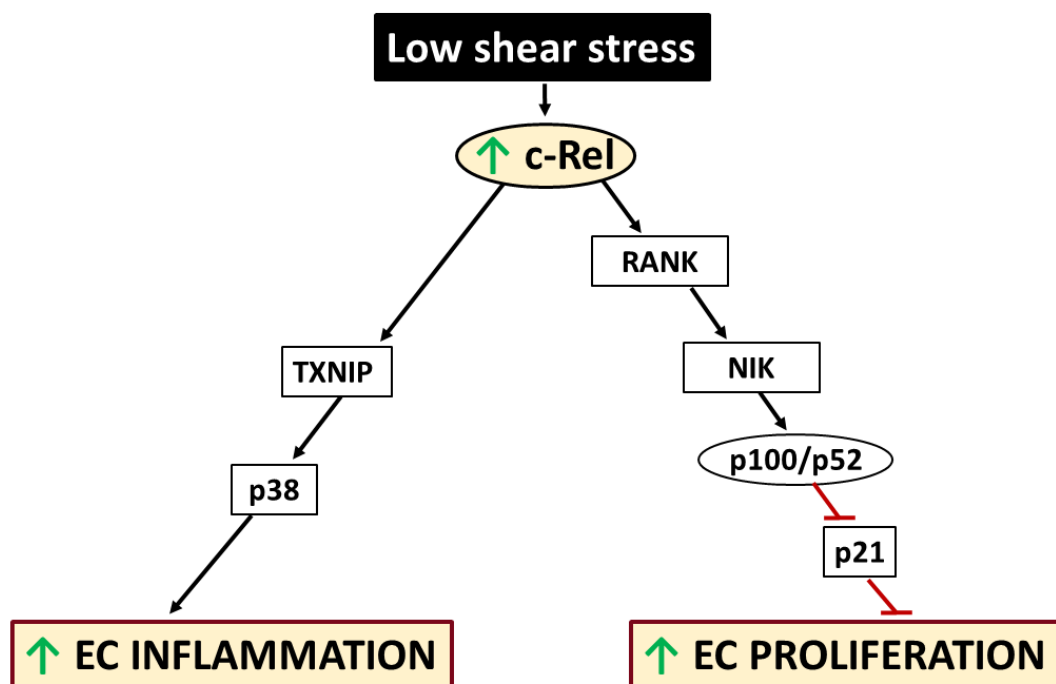


Figure 4.12. c-Rel promotes EC inflammation and proliferation in regions exposed to low shear stress. c-Rel is enhanced in EC exposed to low shear stress, promoting EC inflammation and proliferation. c-Rel-dependent induction of EC inflammation occurs via TXNIP and its downstream target p38. To promote EC proliferation, c-Rel increases the expression of RANK, NIK and p100/p52, and inhibits the anti-proliferative molecule p21.

4.10.1 Low shear stress increased EC proliferation, apoptosis and E-SELECTIN expression, but it did not regulate VCAM-1 protein levels

In this chapter, I have shown that cell proliferation and apoptosis are upregulated in HUVEC exposed to low shear stress compared to high shear stress, which supports previous observations (Chaudhury et al., 2010; Dardik et al., 2005; Obikane et al., 2010; Zeng et al., 2009). An upregulation of endothelial apoptosis and proliferation under low shear stress causes a high EC turnover in these regions of the aorta, whereas this process is markedly reduced in areas protected from the disease (Davies et al., 1986). These differences in EC turnover may substantially contribute to endothelial dysfunction, promoting the development of atherosclerosis in sites exposed to low shear stress.

Similarly, when endothelial inflammation was tested in HUVEC under flow, E-SELECTIN protein levels were enriched in cells exposed to low shear stress and disturbed flow. This is consistent with previously published data that show an increase of inflammatory markers in atherosusceptible regions, indicating that increased expression of adhesion molecules by EC contributes to atherosclerosis (Chappell et al., 1998; Hajra et al., 2000; Partridge et al., 2007). However, when VCAM-1 protein levels were assessed by Western blotting after exposing HUVEC to flow using the orbital shaker for 72 h, it was observed that disturbed flow did not induce VCAM-1 protein levels. There are numerous reasons that could give an explanation to this. First, the orbital shaker system generates different patterns of shear stress within one well, and communication between cells exposed to high and low shear stress can potentially influence their physiology. For example, shear stress is known to influence the release of endothelial microvesicles, cytokines and other factors (Vion et al., 2013), and the release of these molecules by cells that are exposed to high shear stress could affect the expression of VCAM-1 and other genes in endothelial cells exposed to low shear stress, and vice versa. Besides, EC migration also occurs between different areas of the well, which could also have an effect on the regulation of VCAM-1 protein levels. This limitation could be overcome in future studies using the Ibidi® system, which generates specific magnitudes of shear stress (Bowden et al., 2016). Furthermore, the magnitude and duration of shear stress could also influence VCAM-1 levels. The response of EC to mechanical stimuli varies depending on the magnitude, and a certain threshold not exceeded in the orbital system may need to be reached for cells to trigger VCAM-1 upregulation (DeVerse et al., 2013). Shear stress duration could also affect the levels of this adhesion molecule, and shorter or longer

periods of flow exposure might be required for its upregulation. Importantly, the lack of cytokine stimulation, such as TNF stimulation, might affect VCAM-1 protein, preventing a synergistic upregulation under low shear stress. Previous studies have revealed a shear stress-dependent upregulation of VCAM1 in response to TNF, whereas shear stress alone did not affect VCAM-1 levels in the absence of TNF stimulation (DeVerse et al., 2013). Therefore, this suggests that an upregulation of VCAM-1 levels under low shear stress in cultured EC may require a previous stimulation with TNF or other factors, such as LPS. Because of these considerations, future work will include the assessment of VCAM-1 levels in stimulated cells exposed to different patterns of flow, as well as the assessment of c-Rel function in EC in response to cytokine stimulation.

4.10.2 c-Rel controls endothelial proliferation before the onset of S-phase

For the assessment of proliferation, two different proliferation markers were used, PCNA and Ki67. Interestingly, *c-REL* silencing reduced the percentage of both PCNA and Ki67 positive cells, providing a better understanding of the mechanisms underlying the decrease in cell proliferation. PCNA and Ki67 are expressed in proliferative cells, but their expression peaks at different phases of the cell cycle. Ki67 is expressed in every non-G0 phase of the cell cycle, reaching its expression peak during G2 and M phase (Jurikova et al., 2016). PCNA expression, however, reaches its peak during S phase (Jurikova et al., 2016; Zerjatke et al., 2017) (figure 4.13). The fact that *c-REL* silencing reduced both proliferation markers in a similar way, suggests that c-Rel controls endothelial proliferation before the onset of S-phase and not during later stages. Interestingly, it has been previously shown that *c-Rel* knockout mice present defects in B cell proliferation, and this has been associated with a cell cycle arrest in G1 phase (Feng et al., 2004; Grumont et al., 1998), suggesting that this process could also occur in the endothelium.

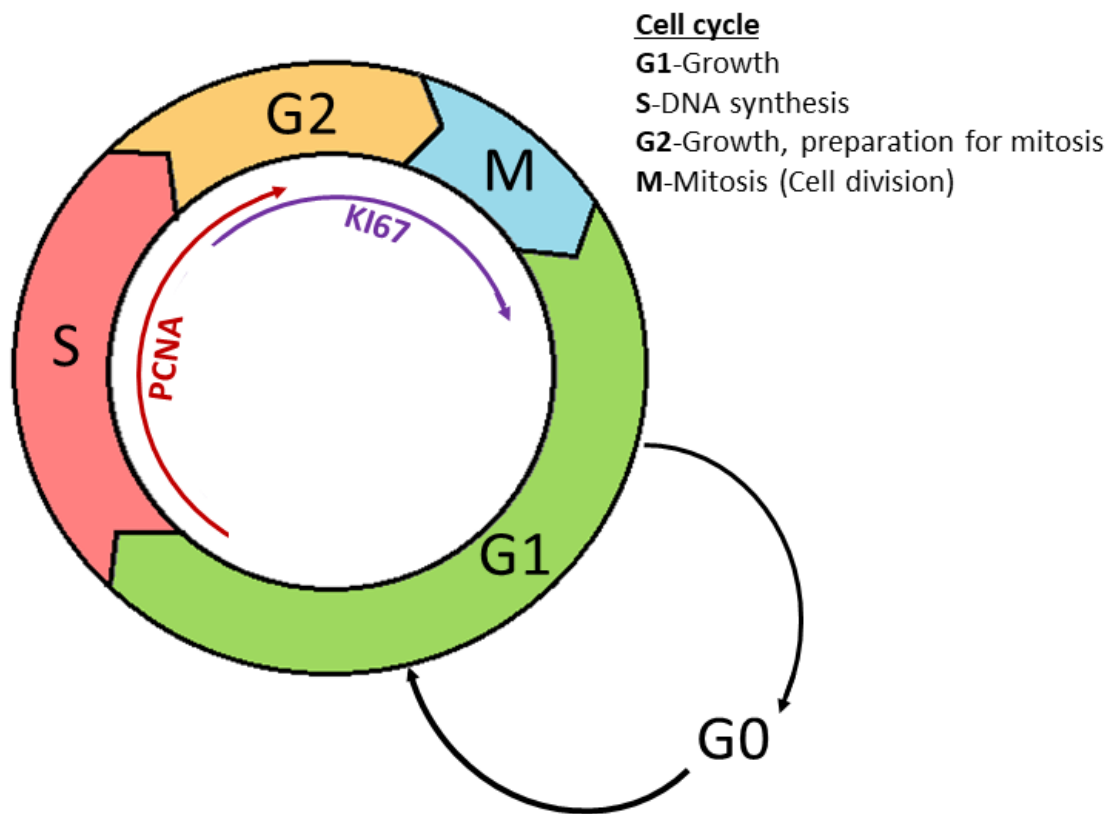


Figure 4.13. The expression of PCNA and Ki67 proliferation markers peaks at different stages of the cell cycle. Diagram showing the cell cycle and its different stages, including their relative length (G1: Growth, S: DNA synthesis, G2: Growth and preparation for mitosis, M: Mitosis (cell division), G0: Cell cycle arrest). The proliferation marker PCNA reaches its peak during S phase, whereas Ki67 reaches its expression peak during G2 and M phase.

4.10.3 c-REL silencing has modest effects in endothelium exposed to high shear stress

In addition to a reduction in proliferation under low shear stress, *c-REL* silencing also decreased proliferation under high shear stress by immunostaining with PCNA and Ki67. Although in the previous chapter it was shown that the protein levels of c-Rel were higher under low shear stress than high shear stress, c-Rel is still expressed in atheroprotected regions. Therefore, the low expression that c-Rel exhibits in these areas may be enough to trigger c-Rel function, leading to a modest but significant induction of EC proliferation under high shear stress. In terms of EC inflammation, *c-REL* silencing also led to reduced E-Selectin and VCAM-1 protein levels under high shear stress, but this reduction, measured by Western blot, did not reach significance. Again, this suggests that although c-Rel activity mainly occurs at low shear stress regions, where this transcription factor is preferentially expressed, c-Rel might also have moderate effects on cell proliferation and inflammation in EC exposed to high shear stress.

4.10.4 c-Rel does not have a major role in EC apoptosis

When the role of c-Rel in EC apoptosis was assessed by immunostaining for active caspase-3, it was observed that *c-REL* silencing led to a significant but very modest increase of apoptosis under low shear stress using RELHSS109157 *c-REL* siRNA. However, a different c-Rel siRNA (RELHSS109158) did not cause a significant increase of active caspase-3-positive cells under low shear stress. The proportion of apoptotic cells observed under low shear stress is remarkably low (~1%), which is approximately equivalent to one active caspase 3-positive cell per field of view. The difference in apoptosis between *SCR* and *c-REL* siRNA-treated HUVEC using RELHSS109157 is minimal (~0.5%), and, even though it is statistically significant, it may not imply biological relevance. Moreover, when a 2nd c-Rel siRNA was used, there were not significant differences in apoptosis between *SCR* and *c-REL* siRNA-treated HUVEC, further supporting that c-Rel does not have a major role in the control of EC apoptosis. However, further experiments are still required. EC apoptosis could be enhanced by serum starvation (Li et al., 2007), which may provide additional information on the role of c-Rel in EC apoptosis. The role of c-Rel in EC apoptosis *in vivo* could also be investigated to validate the *in vitro* studies.

4.10.5 RNA microarray in HUVEC: Characterisation of genes downstream of c-Rel

When RNA microarray was performed in HUVEC, a total of seven genes involved in the MAPK signalling cascade and the NIK/NF- κ B signalling pathway were selected due to

their known or inferred implication in the control of inflammation and proliferation. Selected genes were *MAPK1 (ERK2)*, *MAPK3 (ERK1)*, *MAPK9 (JNK2)*, *MAPK14 (p38)* and *TXNIP*, which are involved in the MAPK cascade; and *TNFSF12 (TWEAK)* and *TNFRSF11A (RANK)*, which regulate the non-canonical NF- κ B signalling pathway. However, when qRT-PCR was performed to validate differential expression of these genes, only *TXNIP*, *MAPK14 (p38)* and *TNFRSF11A (RANK)* were validated.

Multiple factors could explain the discrepancy between RNA microarray and qRT-PCR results. First, biological variability may have contributed to this. Three HUVEC donors were used for RNA microarray, and three different donors were then used for qRT-PCR validation. Hence, biological differences between samples inevitably affect both microarray and qRT-PCR results (Morey et al., 2006). Additionally, technical issues could have an impact on the results obtained. RNA quality is critical to get accurate results, and contaminating factors, such as alcohols, influence the activity of reverse transcriptases used in these procedures (Freeman et al., 1999). Also, different priming methods and the formation of primer dimers could influence the data generated (Bustin, 2002; Freeman et al., 1999). Furthermore, microarrays can generate errors, including non-specific cross-hybridisation of the targets that are fluorescently labelled to the array probes (Chuaqui et al., 2002). Another source of error is data normalisation. Whereas a global normalisation is carried out when microarrays are performed, qRT-PCR uses a house-keeping gene against which the rest of the genes are normalised (Morey et al., 2006). Finally, lower correlations between microarrays and qRT-PCR have been shown for genes that exhibit less than 2-fold changes, whereas this correlation is higher when they show greater fold-changes. Therefore, any of these factors, alone or in combination, could have contributed to the differences observed, explaining the discrepancy between the data obtained using a microarray or qRT-PCR analysis.

4.10.6 Potential mechanism for the regulation of inflammation by c-Rel

In spite of the differences between the RNA microarray results and qRT-PCR validation in HUVEC, two genes involved in inflammation and atherosclerosis, *TXNIP* and *p38*, were validated as c-Rel target genes.

TXNIP is a protein that interacts and inhibits the expression and function of TRX, a thiol oxidoreductase that controls cellular redox status and suppresses oxidative stress (Lu and Holmgren, 2014). In the endothelium, TRX has been suggested to increase in response to

inducible NOS (iNOS), representing a protective mechanism against cytotoxic NO production and protecting against atherosclerosis (Takagi et al., 1998). Besides, loss of TRX is associated with EC dysfunction and a prothrombotic and proinflammatory phenotype, further supporting TRX protective role in atherogenesis (Kirsch et al., 2016). TRX has also been shown to directly interact with ASK1 (*MAP3K5*), inhibiting ASK1 kinase activity (Saitoh et al., 1998). This indicates that both TXNIP and ASK1 interact with TRX, and when TXNIP binds to TRX, it releases ASK1 from TRX inhibition (Yamawaki et al., 2005).

TXNIP has been shown to be enriched at low shear stress regions, by performing experiments *in vivo* and *in vitro* (Wang et al., 2012). Under low shear stress, the induction of TXNIP leads to inhibition of TRX, resulting in increased activity of ASK1. ASK1 is a MAP kinase kinase kinase that is upstream of JNK and p38, and p38, in turn, has been shown to promote VCAM-1 expression under low shear stress (Yamawaki et al., 2005; Zakkar et al., 2008). Hence, the upregulation of TXNIP under low shear stress generates an inflammatory response, increasing ASK1, JNK, p38 and VCAM-1 levels and repressing TRX (Saitoh et al., 1998; Wang et al., 2012; Yamawaki et al., 2005). On the contrary, TXNIP expression is downregulated in EC under high shear stress, inhibiting inflammation through repression of the MAPK signalling cascade (Yamawaki et al., 2005) (figure 4.14). Altogether, this demonstrates that both TXNIP and p38 regulate inflammation in EC exposed to low shear stress, and also, that p38 is a downstream target of TXNIP. Thus, the regulation of TXNIP and p38 by c-Rel could explain the proinflammatory activity of c-Rel.

Interestingly, in addition to the reduction in TXNIP and p38 levels in *c-REL* siRNA-treated HUVEC, the RNA microarray also revealed a significant 2.5-fold downregulation of ASK1 (*MAP3K5*, $p=0.016$). Therefore, this finding further supports the involvement of c-Rel in the regulation of this system.

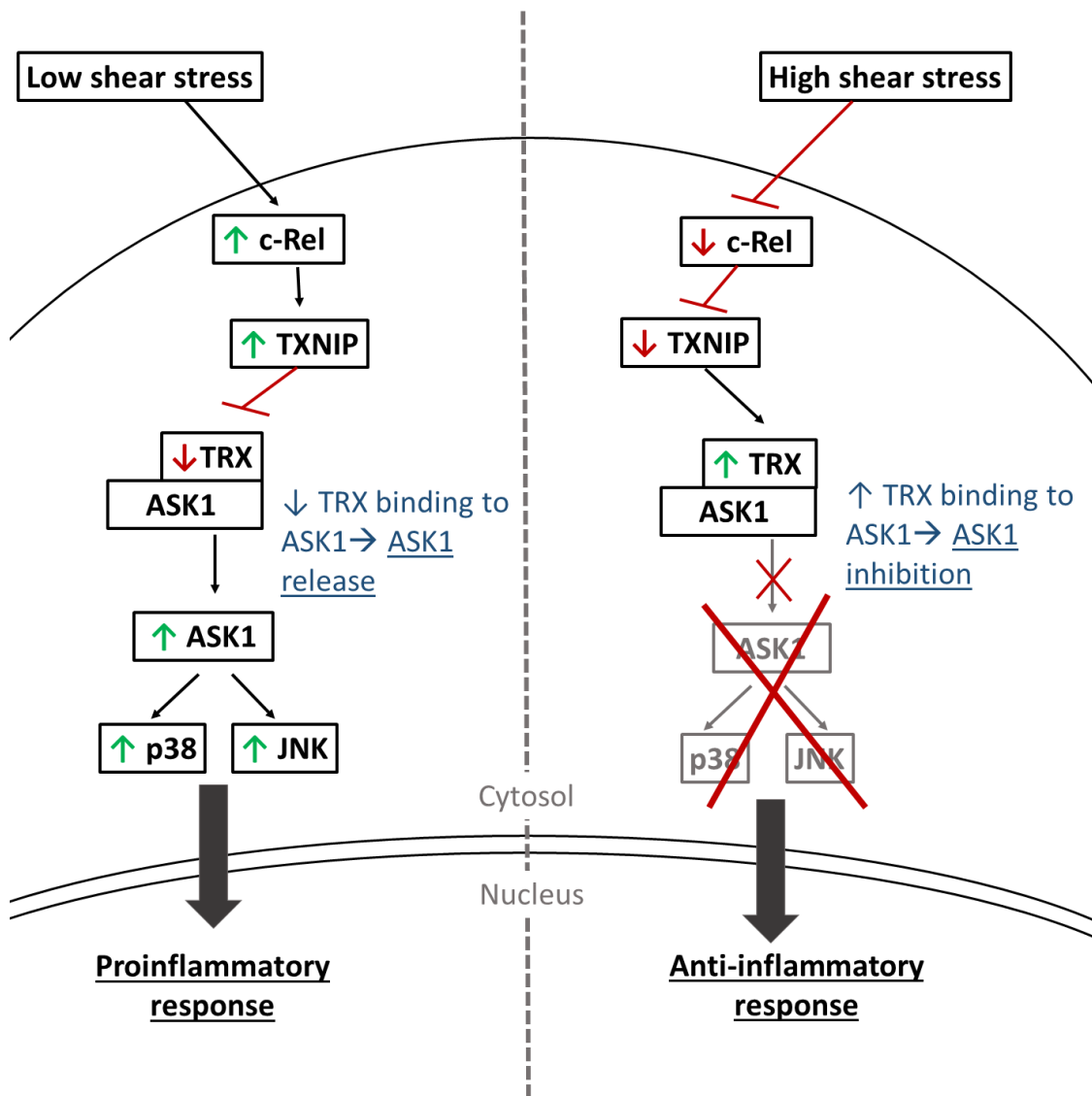


Figure 4.14. Potential mechanism for the regulation of inflammation by c-Rel. Under low shear stress, c-Rel promotes the induction of TXNIP. TXNIP then binds to TRX, inhibiting its activity and leading to ASK1 release. ASK1 is a MAPK kinase kinase that is upstream of JNK and p38, and therefore, its release leads to a proinflammatory response. On the contrary, high shear stress downregulates c-Rel and TXNIP levels. This increases TRX activity and TRX binding to ASK, suppressing p38 and JNK expression and inducing an anti-inflammatory response.

Although I have shown that the regulation of TXNIP and p38 by c-Rel could explain c-Rel proinflammatory effects, c-Rel could still be regulating other genes to induce this process. In other cell types, c-Rel has been shown to regulate a number of cytokines, such as IL-21, IL-23 (Chen et al., 2010; Niu et al., 2010; Wang et al., 2008), that have previously been shown to contribute to atherosclerosis (Erbel et al., 2011). Interestingly, the RNA microarray in HUVEC revealed that IL-6 was a c-Rel target gene, since it was downregulated in *c-REL* siRNA-treated HUVEC. IL-6 is known to contribute to endothelial dysfunction and activation (Wassmann et al., 2004; Wung et al., 2005), and it has recently been shown that modulation of IL-6 pathway using canakinumab is associated with a reduction of atherosclerotic and cardiovascular events (Ridker et al., 2018). Hence, the regulation of IL-6 by c-Rel could be an additional mechanism that could explain c-Rel proinflammatory effects.

Low shear stress enhances the expression of RelA, another NF- κ B subunit, via activation of JNK MAP kinase (Cuhlmann et al., 2011). Therefore, c-Rel could potentially regulate RelA levels via the TXNIP-ASK1-JNK pathway activation. Moreover, since NF- κ B subunits form dimers in order to bind to gene promoters and activate transcription, c-Rel could potentially form dimers with RelA in the endothelium, leading to an increase in inflammation under low shear stress. Future work will involve assessing the interactions between NF- κ B subunits in EC exposed to flow, in order to determine the effect of c-Rel on the expression and function of other NF- κ B subunits.

4.10.7 Potential mechanism for the regulation of proliferation by c-Rel

4.10.7.1 RANK

The RNA microarray and subsequent validation by qRT-PCR and Western blotting showed that *TNFRSF11A* (*RANK*) is a c-Rel downstream target. RANK belongs to the TNFR superfamily, and it is one of the best characterised non-canonical NF- κ B receptors. It is well known for its role in osteoclastogenesis (Theill et al., 2002), but it is also known to promote T cell proliferation (Anderson et al., 1997) and proliferation of epithelial cells during mammary gland development (Fata et al., 2000; Gonzalez-Suarez et al., 2007). Interestingly, RANK is also involved in angiogenesis, as well as in endothelial cell proliferation and migration. It is upregulated in response to VEGF and its upregulation has been shown to increase vascular permeability (Benslimane-Ahmim et al., 2011; Kim et al., 2002; Min et al., 2007). In addition to the specific role of RANK in cell

proliferation, its role as an activator of the non-canonical NF- κ B signalling pathway further supports this proliferative effect.

The activity of NIK, a key component of non-canonical NF- κ B signalling, is triggered by signalling through several TNFR superfamily members, including RANK. NIK then activates IKK α , leading to the phosphorylation and processing of p100 to p52 (Sun, 2011). Since our lab has recently reported that the non canonical NF- κ B subunits p52/p100 induce EC proliferation in response to low shear stress (Bowden et al., data not published), c-Rel-dependent regulation of RANK and other components of the non-canonical pathway, NIK, p100 and p52, supports c-Rel pro-proliferative effects (figure 4.15).

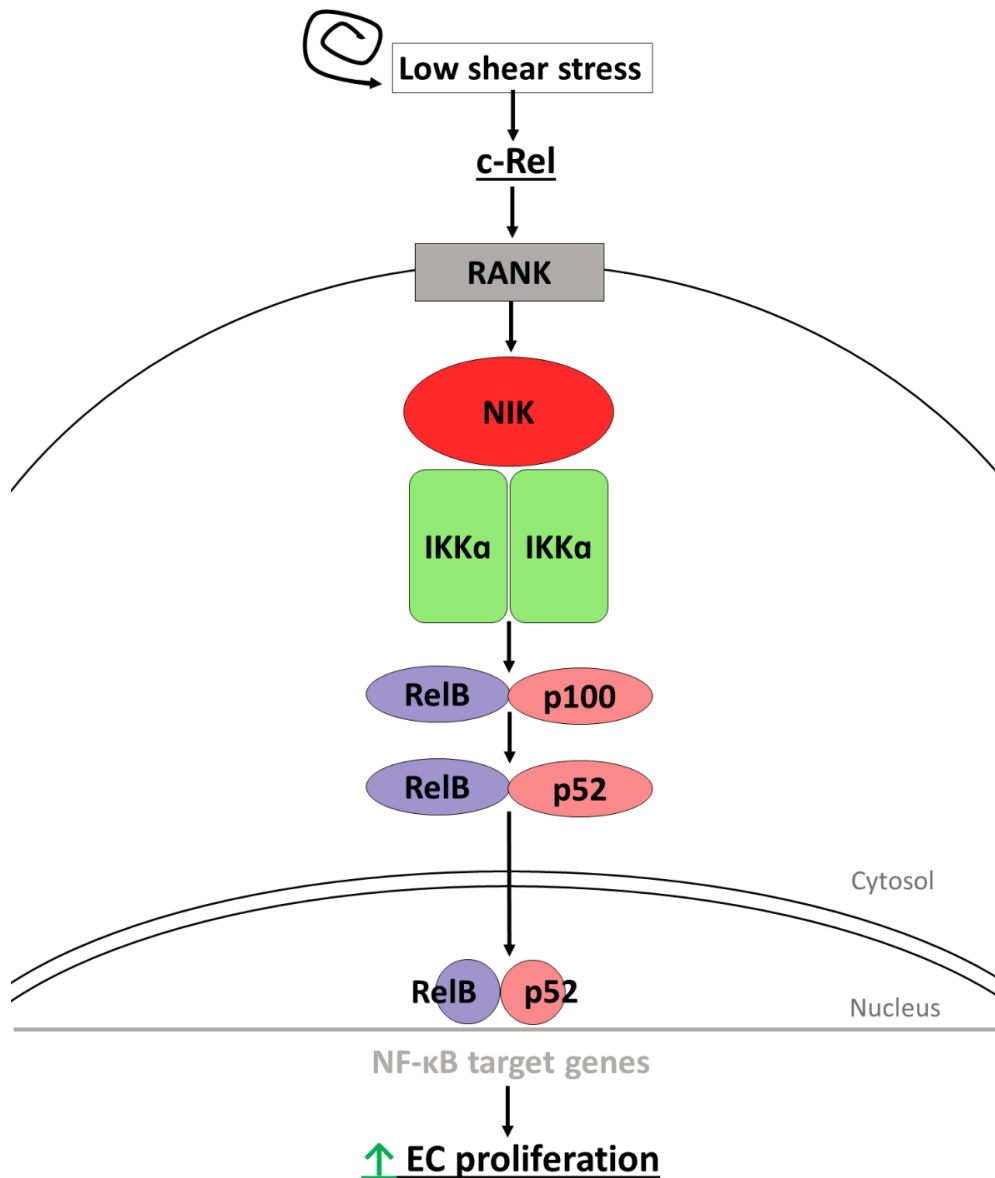


Figure 4.15. Potential mechanism for the regulation of proliferation by c-Rel. Under low shear stress, c-Rel promotes the induction of RANK and the non-canonical NF- κ B components NIK, p100 and p52. RANK, a non-canonical NF- κ B receptor that is known to promote proliferation in several cell types, induces the activity of NIK. This, in turn, promotes phosphorylation and processing of p100 to p52 through activation of IKK α , leading to increased endothelial proliferation at disturbed flow regions.

4.10.7.2 c-Rel-RANK-p52-p21 signalling

In addition to the data generated in our lab that links p100 and p52 with low shear-induced EC proliferation, previous studies have also shown that the non-canonical NF- κ B pathway can trigger proliferation in other cell types. For instance, it has been shown that silencing of *NFKB2* or *NIK (MAP3K14)* in melanoma cells markedly reduces tumour growth and increases senescence (De Donatis et al., 2016). Also, CD40, which is known to activate non-canonical NF- κ B signalling, has been shown to induce proliferation and angiogenesis in endothelial cells (Leroyer et al., 2008). Furthermore, using human osteosarcoma cells, it was revealed that p52 inhibits the anti-proliferative molecule p21 to promote cell proliferation (Schumm et al., 2006). The regulation of p21 by p52 was further investigated in our lab, and it was reported that under low shear stress, p52 represses p21 to induce EC proliferation (Bowden et al., data not published). Since c-Rel promotes proliferation under low shear stress and it also induces RANK, NIK, p100 and p52 levels, the potential role of c-Rel in the regulation of p21 was studied, demonstrating that c-Rel, as well as p52, suppresses p21 levels to promote EC proliferation.

p21 or cyclin-dependent kinase inhibitor 1 (CDK1) is an anti-proliferative protein that binds to cyclins and CDKs to inhibit cell proliferation. Specifically, p21 can block G1 to S-phase progression, leading to a quiescent state in G0. The p21-dependent inhibition of G1/S transition requires p53, and they can act together to induce cell senescence (Abbas and Dutta, 2009). As I have previously shown, the fact that c-Rel regulates the expression of both PCNA and Ki67 suggests that c-Rel controls endothelial proliferation before the onset of S-phase, inhibiting cell cycle progression in G0 or G1 phase. Therefore, this suggests that in *c-Rel*-siRNA treated HUVEC, the reduction of EC proliferation could be due to an increase in p21 levels, which would inhibit EC proliferation before the onset of S-phase and would maintain EC in a quiescent state. Enhanced c-Rel levels under low shear stress would suppress p21 expression, leading to high levels of proliferation in atheroprone areas exposed to low shear stress. These data are consistent with a previously published study, which shows that high shear stress leads to enhanced p21 protein levels, reducing EC proliferation in HUVEC (Akimoto et al., 2000).

The interaction of p53 with p21 and their role in senescence could be important to understand this pathway. p53 levels have been shown to be upregulated at low shear stress areas of the murine aortic arch, and they have been shown to promote senescence in areas of disturbed flow. Besides, higher levels of p53 in cells exposed to low shear stress

correlated with high levels of p21, supporting the idea that they are involved in the same pathway (Warboys et al., 2014). However, as seemingly against this, a different study revealed that high shear stress leads to enhanced p21 expression (Akimoto et al., 2000). A different cell fate could explain this discrepancy. Whereas a p53-dependent induction of p21 results in EC quiescence under high shear stress, p53 and p21 promote senescence in endothelial cells exposed to low shear stress. Work by Warboys et al. showed that levels of p53 and p21 in cells under low shear stress were heterogeneous. Senescent cells in low shear areas presented high expression of p53 and p21, but the rest of the cells under low shear did not show p21 or p53 expression (Warboys et al., 2014). Therefore, this further supports the idea that the regulation of p21 and p53 depends on the context and varies in response to different stimuli (figure 4.16). Future work will assess the role of c-Rel in senescence in the sheared endothelium. Moreover, the mechanisms that regulate p53-p21 decision-making in endothelial cells exposed to flow still need to be investigated.

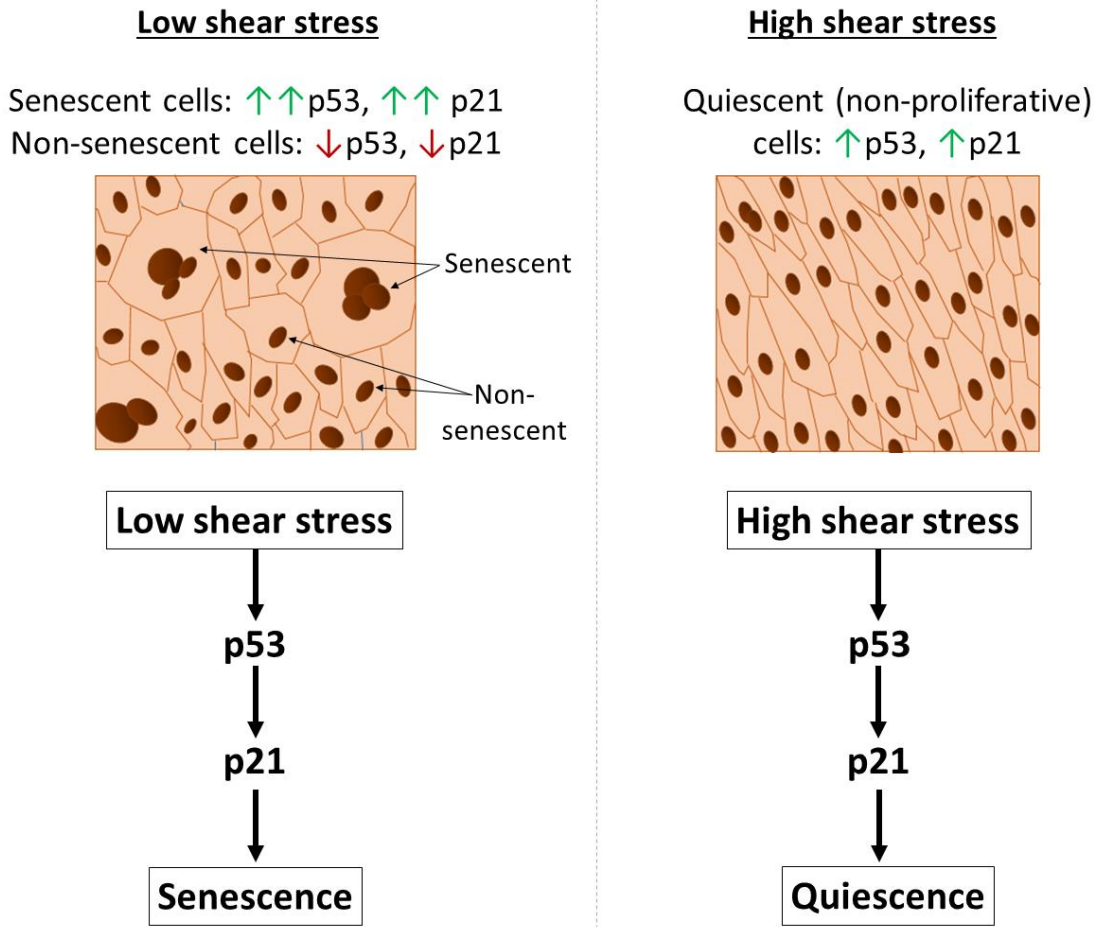


Figure 4.16. Pleiotropic nature of p53 and p21 in endothelial cells exposed to flow. Under low shear stress, the expression p53 and p21 is heterogeneous. Senescent cells have high levels of p53 and p21, whereas non-senescent cells do not express p53 or p21. Under high shear stress, the expression of p53 and p21 is more homogeneous. Endothelial cells at these regions show relatively high p53 and p21 levels, leading to a quiescent, non-proliferative phenotype. Therefore, this shows that different shear patterns affect the pleiotropic effects of p53 and p21: whereas p53 and p21 promote senescence in endothelial cells exposed to low shear stress, they promote quiescence under high shear stress.

4.10.7.3 Other c-Rel proliferative mechanisms

Aside from non-canonical NF- κ B signalling to p21, there may be other c-Rel-dependent mechanisms that could also be contributing to EC proliferation. An interesting candidate would be GATA4. c-Rel has been shown to promote fibrosis and cardiac hypertrophy after chronic treatment with angiotensin in mice, by direct upregulation of Gata4 (Gaspar-Pereira et al., 2012). Interestingly, GATA4 is known to induce proliferation in EC exposed to low shear stress, and it has also been involved in the induction of endothelial to mesenchymal transition (EndoMT) (Mahmoud et al., 2016; Mahmoud et al., 2017). Therefore, the potential interaction between c-Rel and GATA4 in the endothelium will be interesting to study, as well as the potential role of c-Rel in EndoMT.

Besides, the RNA microarray performed in HUVEC revealed that *FOXM1* and its downstream target *CDC25* are c-Rel target genes. Interestingly, c-Rel has been shown to promote proliferation in other cell types by inducing these molecules. c-Rel is known to be required for the normal proliferative regeneration of hepatocytes, and *c-Rel* knockout mice present a hepatocyte proliferation defect following toxic liver injury, due to impaired generation of *FoxM1* and *Cdc25* (Gielsing et al., 2010). In endothelial cells, *FoxM1* and *Cdc25* have also been shown to mediate EC proliferation (Zhao et al., 2006), and therefore, it will be interesting to investigate the role of c-Rel in the regulation of these molecules in the endothelium.

In summary, cell proliferation and inflammation are known to be proatherogenic processes in endothelial cells. In this chapter, I have shown for the first time that c-Rel alters endothelial physiology by inducing both EC proliferation and inflammation under low shear stress. The mechanisms by which c-Rel promote inflammation involve the induction of TXNIP and its downstream target p38, whereas c-Rel promotes proliferation via induction of the non-canonical NF- κ B components RANK, NIK, p100/p52, and through repression of p21. More experiments are required to assess whether c-Rel controls these molecules directly, and also, to assess c-Rel function *in vivo*. The potential regulation of EC inflammation and proliferation by c-Rel and the role of c-Rel in atherosclerosis will be addressed in the next chapter.

Chapter 5. c-Rel promotes
atherosclerosis and controls EC
dysfunction at atheroprone sites *in*
vivo

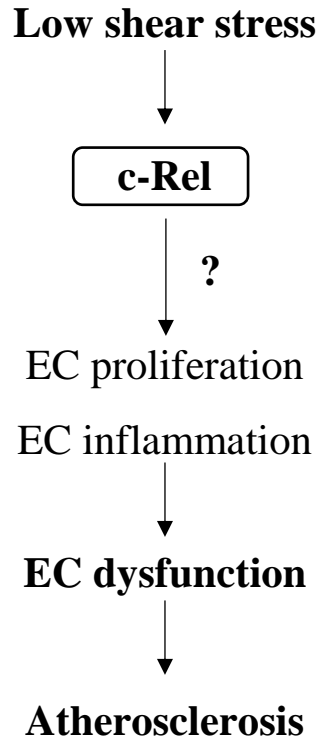
5.1 Introduction

In the previous chapters, I have shown that c-Rel protein is enriched at atheroprone areas *in vivo* and *in vitro*, and also, that c-Rel promotes endothelial proliferation and inflammation under low shear stress in cultured endothelial cells. However, the role of c-Rel in EC proliferation and inflammation has only been investigated using *in vitro* systems, and in particular, the orbital shaker system. This system partly reproduces the physiological mechanics endothelial cells are exposed to *in vivo*, but it also presents a number of limitations. As there is no *in vitro* system that can mimic the complexity of spatial and temporal flow fluctuations *in vivo*, it is essential to validate the experiments performed *in vitro* using an *in vivo* model. An *in vivo* model will help us get a better understanding of the function of c-Rel in endothelial cells exposed to low shear stress.

Although my results suggest that c-Rel promotes endothelial dysfunction, which is known to contribute to atherosclerosis, the role of c-Rel in this disease still needs to be elucidated. The NF- κ B pathway has been previously shown to be involved in the development of atherosclerotic lesions. Inhibition of NF- κ B activation in EC, achieved by depletion of NEMO or generation of a dominant negative I κ B α , resulted in decreased formation of atherosclerotic plaques in mice (Gareus et al., 2008). Also, expression of RelA and the inhibitory components I κ B α and I κ B β has been reported to be enhanced in atherosusceptible regions in mice (Hajra et al., 2000). Besides, a study using *ApoE* knockout mice suggested that inhibition of *c-Rel* expression by siRNA led to decreased stress-induced atherosclerosis (Djuric et al., 2012). However, siRNA-depletion of *c-Rel* in this study was not validated in vascular tissue, and hence, the effects observed might be caused by off-target effects. Also, siRNA-silencing could be targeting *c-Rel* in other tissues, indirectly affecting atherosclerosis. Since this study raises questions about the involvement of c-Rel in atherosclerosis, it is still necessary to determine whether c-Rel and endothelial c-Rel contribute to the development of this disease.

5.2 Hypothesis and aims

I hypothesise that c-Rel induces focal EC dysfunction and atherosclerosis by altering EC proliferation and inflammation.



To test this hypothesis, I aim to:

1. Study c-Rel function in EC exposed to low shear stress by assessing inflammation and proliferation in the murine aortic arch of wildtype and *c-Rel* knockout mice.
2. Characterise the role of c-Rel in atherosclerosis by using wildtype and *c-Rel* knockout mice treated with AAV-PCSK9.
3. Assess the role of c-Rel in atherosclerosis by using EC-specific *c-Rel* knockout mice and experimental controls treated with AAV-PCSK9.

5.3 c-Rel promotes EC inflammation at low shear stress regions in the mouse aortic arch

EC inflammation is known to be enhanced at low shear stress areas in the vasculature, and also, it has been shown to be a key driver of EC dysfunction and atherosclerosis. In the previous chapter, it was shown that c-Rel induces the expression of the inflammatory markers VCAM-1, ICAM-1 and E-SELECTIN in cultured endothelial cells exposed to flow. However, the role of c-Rel in inflammation *in vivo* has not been determined yet.

In order to investigate the role of c-Rel in EC inflammation *in vivo*, *en face* staining of the murine endothelium was performed, using C57BL/6J wildtype and *c-Rel* knockout mice. Regions exposed to high shear and low oscillatory shear stress at the aortic arch were stained for E-Selectin and Vcam-1, using specific antibodies.

The data indicated that the expression of the inflammatory markers E-Selectin and Vcam-1 was enhanced at low shear stress compared to high shear stress regions in wildtype mice (figure 5.1A and B), which is consistent with previously published studies (Hajra et al., 2000; Nam et al., 2009; Ni et al., 2010). After testing this, it was observed that E-Selectin and Vcam-1 expression levels at low shear areas of the murine aorta were markedly downregulated in *c-Rel* knockout mice compared to wildtype mice (figure 5.1A and B). Again, this is consistent with the data shown in the previous chapter, which showed that *c-REL* silencing leads to a decrease in inflammation in HUVEC under low shear stress. Although *c-Rel* deletion also reduced E-Selectin expression in atheroprotected areas (high shear stress) of the mouse aorta, it did not affect Vcam-1 levels, suggesting that the effects of c-Rel on inflammation are more modest under high shear stress. Altogether, these observations indicate that c-Rel induces inflammation at low shear stress sites, contributing to focal endothelial dysfunction.

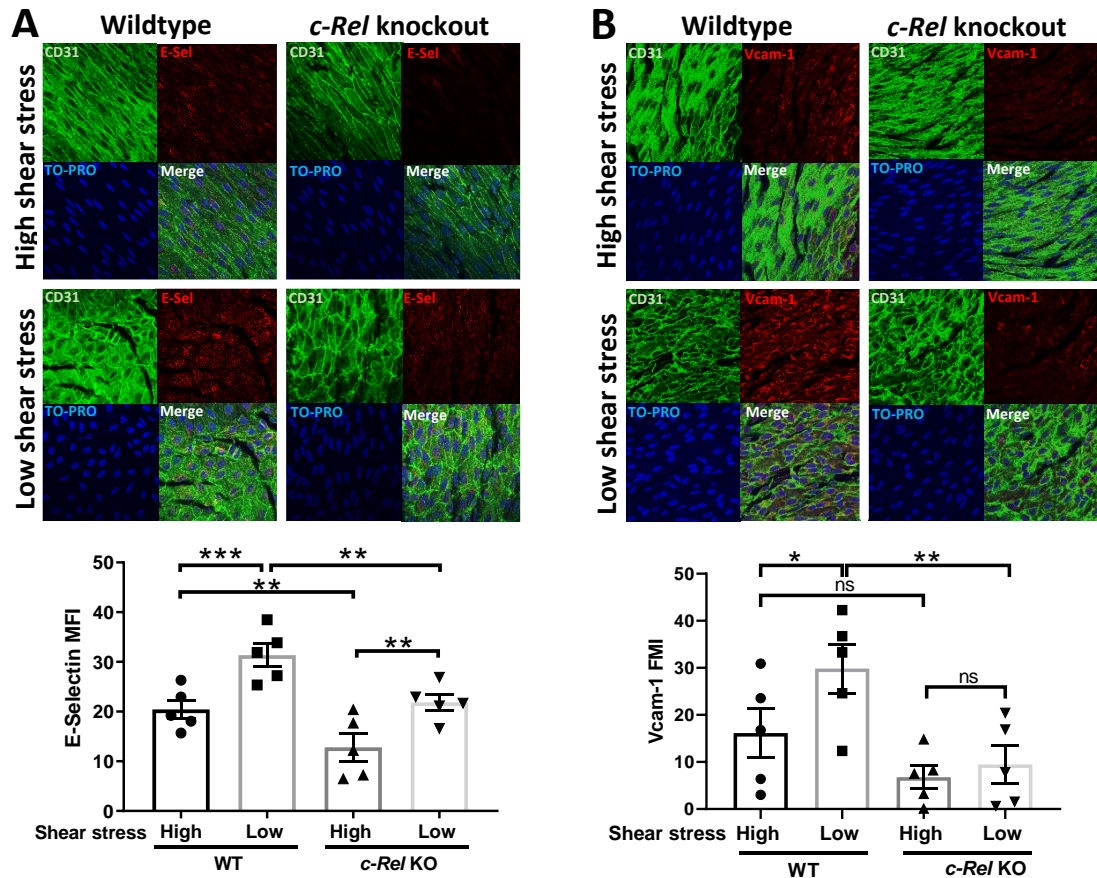


Figure 5.1. *c-Rel* promotes EC inflammation at low shear stress regions of the murine aorta. *En face* staining at low shear (inner curvature) and high shear stress (outer curvature) regions of the mouse aorta was performed in C57BL/6J wildtype (WT) and *c-Rel* knockout (KO) mice between 6-9 weeks of age. **A)** E-Selectin and **B)** Vcam-1 protein levels (red) were quantified by confocal microscopy. Anti-CD31 antibody (green) was used as an endothelial marker and TO-PRO 3 was used for nuclear staining. Representative images and quantification of **A)** E-Selectin and **B)** Vcam-1 mean fluorescence intensity are shown. Mean values are shown with standard error of the mean; n=5 independent experiments. *p<0.05, **p<0.01, ***p<0.001, ns: non-significant, using 2-way ANOVA with post-hoc Tukey's test.

5.4 c-Rel promotes EC proliferation at low shear stress regions in the mouse aortic arch

After elucidating the role of c-Rel in EC inflammation, the role of c-Rel in EC proliferation *in vivo* was investigated. EC proliferation, which is known to be enhanced at atheroprone regions exposed to disturbed flow, has been shown to be involved in the development of atherosclerotic lesions (Akimoto et al., 2000; Davies et al., 1986; Foteinos et al., 2008). Furthermore, c-Rel has been shown to promote proliferation in several cell types, including B cells (Feng et al., 2004; Grumont et al., 1998), T cells (Bunting et al., 2007) and cardiomyocytes (Gaspar-Pereira et al., 2012).

Although I have previously shown that c-Rel promotes cell proliferation under low shear stress by using anti-PCNA and Ki67 in HUVEC, the role of c-Rel in EC proliferation using *in vivo* models is unknown. Hence, *en face* staining of the murine endothelium was performed in C57BL/6J wildtype and *c-Rel* knockout mice, and the expression of the proliferative marker Ki67 was assessed in high shear and low shear regions of the murine aortic arch.

Staining of Ki67, a marker of cell proliferation, indicated that EC proliferation is higher at the inner curvature of the mouse aorta (low shear stress), compared to the outer curvature (high shear) in wildtype mice (figure 5.2). When Ki67 was quantified at low shear stress areas of wildtype and *c-Rel* knockout mice, it was shown that *c-Rel* deletion leads to a significant decrease in EC proliferation (figure 5.2), suggesting that c-Rel promotes proliferation under low shear stress. This supports the data generated *in vitro*, which showed that siRNA-mediated silencing of *c-REL* significantly reduces proliferation in cultured EC. Under high shear stress, however, EC proliferation is not reduced in *c-Rel* knockout mice compared to wildtype mice, indicating that c-Rel promotes EC proliferation only in atheroprone areas of the mouse aorta.

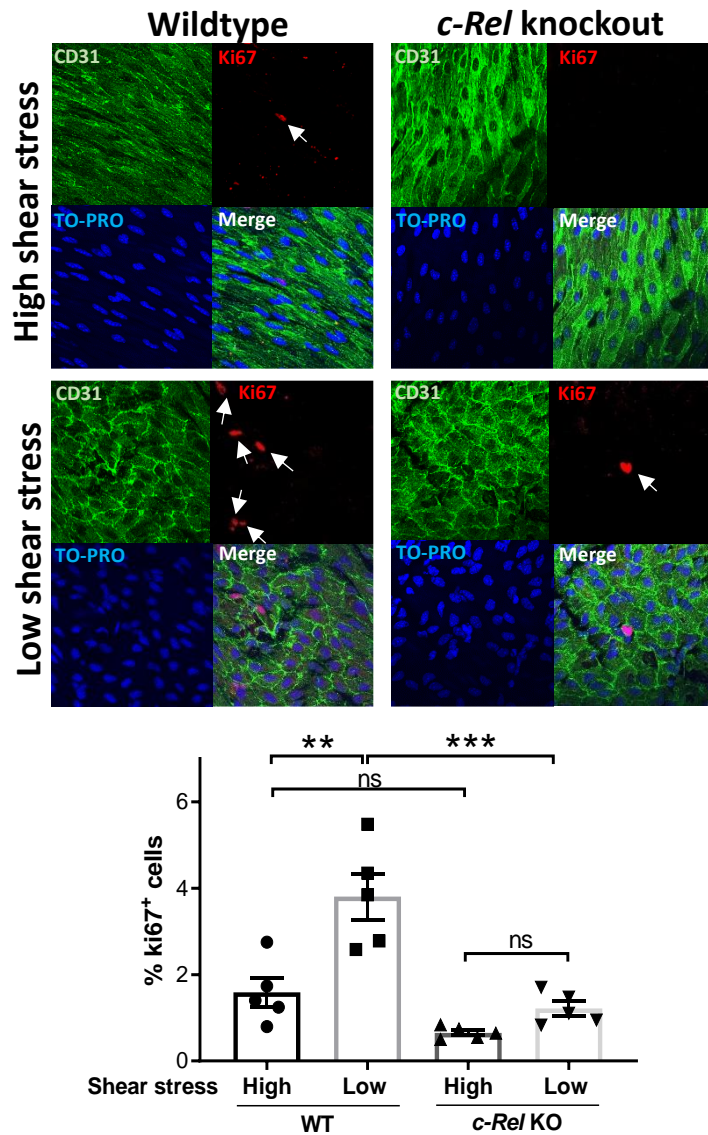


Figure 5.2. *c-Rel* promotes EC proliferation at low shear stress regions of the murine aorta. *En face* staining at low shear (inner curvature) and high shear stress (outer curvature) regions of the mouse aorta was performed in C57BL/6J wildtype (WT) and *c-Rel* knockout (KO) mice between 6-9 weeks of age. Expression levels of Ki67 (red), a marker for cell proliferation, were assessed by confocal microscopy. Anti-CD31 antibody (green) was used as an endothelial marker and TO-PRO 3 was used for nuclear staining. Representative images and quantification of Ki67 are shown. Proliferative cells were represented as % of cells positive for Ki67. Number of cells per field of view were quantified. Mean values are shown with standard error of the mean; n=5 independent experiments. **p<0.01, ***p<0.001, ns: non-significant, using 2-way ANOVA with post-hoc Tukey's test.

5.5 c-Rel induces the expression of the MAPK cascade components Txnip and p38 to promote EC inflammation in the mouse aortic arch

In the previous chapter, a RNA microarray was performed in HUVEC to elucidate the mechanisms by which c-Rel controls EC inflammation and proliferation *in vitro*. Interestingly, several components of the MAPK signalling pathway, which are known to mediate the proinflammatory effects of shear stress and to contribute to atherosclerosis (Cuhlmann et al., 2011; Ricci et al., 2004; Yamawaki et al., 2005), were shown to be positively regulated by c-Rel.

By performing subsequent qRT-PCR and Western blotting experiments, the MAPK components TXNIP and p38 were validated as c-Rel target genes in HUVEC exposed to low shear stress, providing a potential mechanism for c-Rel proinflammatory activity. However, these have not yet been validated as c-Rel target genes using an *in vivo* model. To get a better understanding of this process, the role of c-Rel in the regulation of Txnip and p38 was investigated in wildtype and *c-Rel* knockout mice by performing *en face* staining of the murine aorta.

By using Txnip and p38 specific antibodies, *en face* staining revealed that the expression of these MAPK components was enhanced at low shear stress compared to high shear stress regions in wildtype mice, although for p38, this increase did not reach significance (figure 5.3A and B). When the expression of Txnip and p38 was compared between wildtype and *c-Rel* knockout mice, it was observed that both Txnip and p38 levels under low shear stress were significantly downregulated in *c-Rel* knockout mice (figure 5.3A and B). This is consistent with the *in vitro* data that were previously shown, and therefore, it indicates that c-Rel positively regulates the expression of Txnip and p38 in cells exposed to low shear stress *in vitro* and *in vivo*. Altogether, these results show that c-Rel promotes EC inflammation through the induction of the MAPK regulator Txnip and the MAPK component p38.

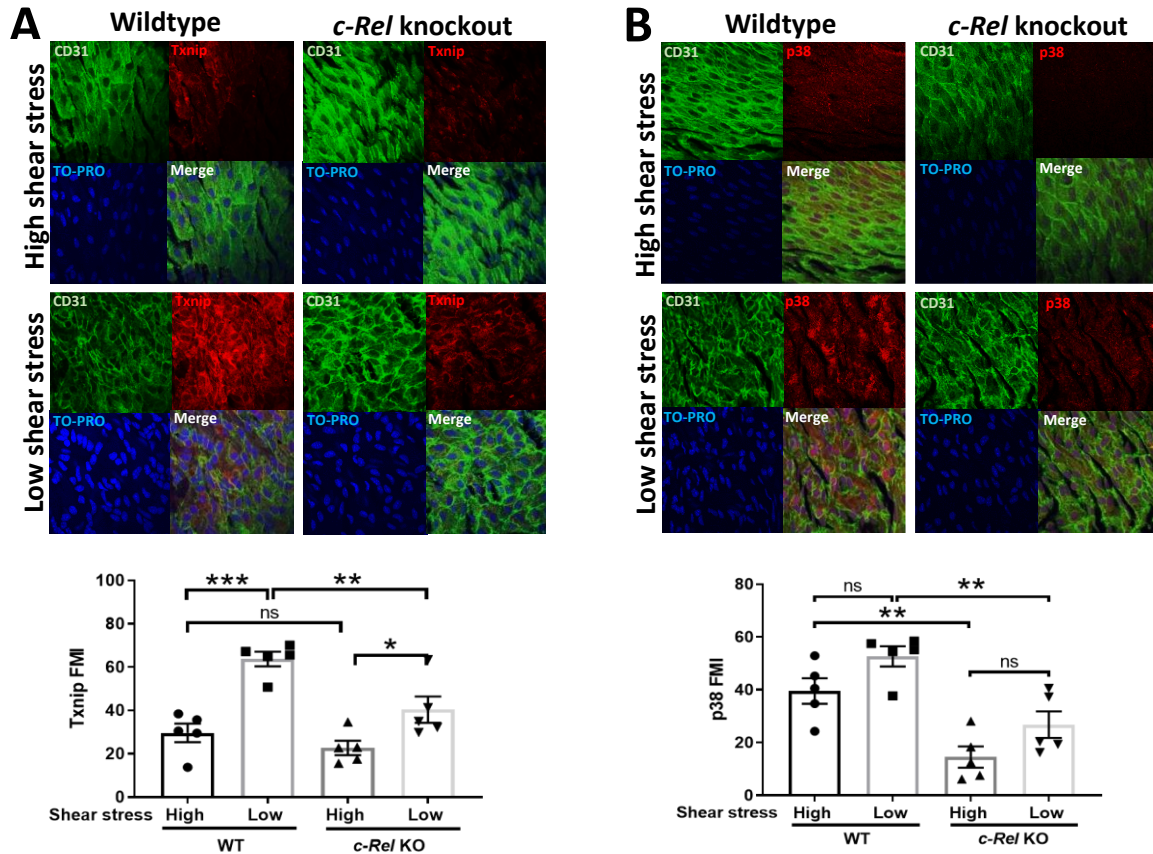


Figure 5.3. *c-Rel* promotes expression of the MAPK components Txnip and p38 at low shear stress regions of the murine aorta. *En face* staining at low shear (inner curvature) and high shear stress (outer curvature) regions of the mouse aorta was performed in C57BL/6J wildtype (WT) and *c-Rel* knockout (KO) mice between 6-9 weeks of age. **A**) Txnip and **B**) p38 protein levels (red) were assessed by confocal microscopy. Anti-CD31 antibody (green) was used as an endothelial marker and TO-PRO 3 was used for nuclear staining. Representative images and quantification of **A**) Txnip and **B**) p38 mean fluorescence intensity are shown. Mean values are shown with standard error of the mean; n=5 independent experiments. *P<0.05, **p<0.01, ***p<0.001, ns: non-significant, using 2-way ANOVA with post-hoc Tukey's test.

5.6 c-Rel induces the expression of the non-canonical NF- κ B pathway components RANK and NIK to promote EC proliferation in the mouse aortic arch

As shown in the previous chapter, the RNA microarray performed in *SCR* and *c-REL* siRNA-treated HUVEC revealed that the NIK/NF- κ B signalling pathway, which is known to be involved in the regulation of cell proliferation and survival, is positively regulated by c-Rel. Subsequent validation experiments *in vitro* revealed that RANK, an activator of the non-canonical NF- κ B signalling pathway (Novack et al., 2003) that is known to promote proliferation (Kukita and Kukita, 2013), is a c-Rel target gene.

Since other non-canonical NF- κ B members have also been reported to promote EC proliferation under low shear stress (Bowden et al., data not published), the protein and mRNA levels of the non-canonical NF- κ B members NIK, p100 and p52 were also assessed. These *in vitro* experiments showed that c-Rel induced the expression of the non-canonical NF- κ B activator RANK, which triggered the activity of NIK, a key component of non-canonical NF- κ B signalling. This activation, in turn, led to the induction of the precursor protein p100, promoting the formation of the mature protein p52. Although these experiments revealed that RANK, NIK, p100 and p52 were regulated by c-Rel *in vitro*, it has not yet been determined whether these molecules are downstream of c-Rel *in vivo*.

In order to investigate this, the role of c-Rel in the regulation of the non-canonical NF- κ B activators Rank and Nik was studied in wildtype and *c-Rel* knockout mice by performing *en face* staining of the murine aorta. When the expression of Rank and Nik was compared at low shear stress areas in wildtype and *c-Rel* knockout mice, it was found that Rank and Nik protein levels were significantly downregulated in *c-Rel* knockout mice (figure 5.4A and B). This supports the *in vitro* data previously generated, indicating that c-Rel regulates the non-canonical NF- κ B pathway in cells exposed to low shear stress, both *in vitro* and *in vivo*. Altogether, this suggests that c-Rel promotes EC proliferation through the induction of the non-canonical NF- κ B signalling pathway.

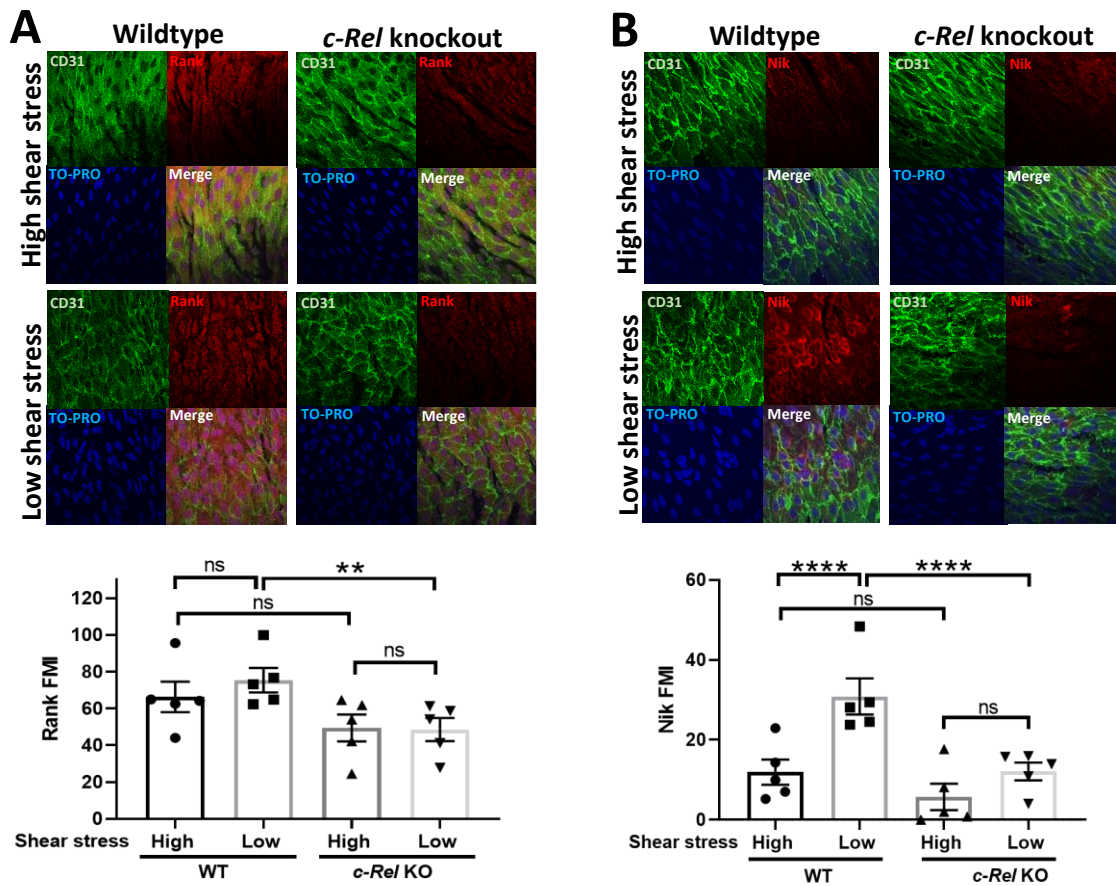


Figure 5.4. *c-Rel* promotes expression of the non-canonical NF- κ B components Rank and Nik at low shear stress regions of the murine aorta. *En face* staining at low shear (inner curvature) and high shear stress (outer curvature) regions of the mouse aorta was performed in C57BL/6J wildtype (WT) and *c-Rel* knockout (KO) mice between 6-9 weeks of age. **A)** Rank and **B)** Nik protein levels (red) were assessed by confocal microscopy. Anti-CD31 antibody (green) was used as an endothelial marker and TO-PRO 3 was used for nuclear staining. Representative images and quantification of **A)** Rank and **B)** Nik mean fluorescence intensity are shown. Mean values are shown with standard error of the mean; n=5 independent experiments. **p<0.01, ****p<0.0001, ns: non-significant, using 2-way ANOVA with post-hoc Tukey's test.

5.7 c-Rel promotes the development of atherosclerosis

Since c-Rel has a role in the regulation of EC dysfunction by inducing inflammation and proliferation in cells exposed to low shear stress, it was hypothesised that c-Rel may contribute to the formation of atherosclerotic lesions. To investigate whether c-Rel is involved in the development of atherosclerosis, an *in vivo* mouse model of atherosclerosis was used.

Atherosclerotic plaques were studied by promoting hypercholesterolemia in 12 week old C57BL/6J wildtype and *c-Rel* knockout mice using an adenovirus containing PCSK9. The injection of a gain-of-function PCSK9 mutant causes degradation of the LDL receptor, targeting it for destruction in the lysosome and therefore, increasing total cholesterol levels in plasma (Shapiro and Fazio, 2017). One week after the AAV-PCSK9 injection, mice were fed a high fat diet for 6 weeks and atherosclerotic lesions were stained using Oil Red O, which stains triglycerides and lipoproteins.

In wildtype mice, it was observed that lesions localised predominantly to atheroprone areas exposed to low shear stress as expected, such as the inner curvature of the arch and carotid bifurcations. Smaller lesions were also observed in the descending aorta, and most of these localised to intercostal branches of the aorta due to changes in haemodynamics. When lesion coverage in wildtype and *c-Rel* knockout mice was compared, it was observed that *c-Rel* deletion markedly reduced lesion area in the aorta, indicating that c-Rel promotes the development of atherosclerosis at low shear stress sites (figure 5.5).

Analysis of plasma revealed that *c-Rel* deletion led to a reduction in circulating lipids. *c-Rel* knockout mice presented reduced levels of triglycerides, total cholesterol, non-high-density lipoprotein (HDL) cholesterol, HDL cholesterol and LDL cholesterol, compared to wildtype mice (figure 5.6). Therefore, this suggests that the decrease in atherosclerosis in *c-Rel* knockout mice might not be only due to vascular c-Rel. c-Rel might be playing a role in the liver or in other cell types, such as macrophages, altering lipid metabolism and influencing cholesterol and triglycerides levels in plasma.

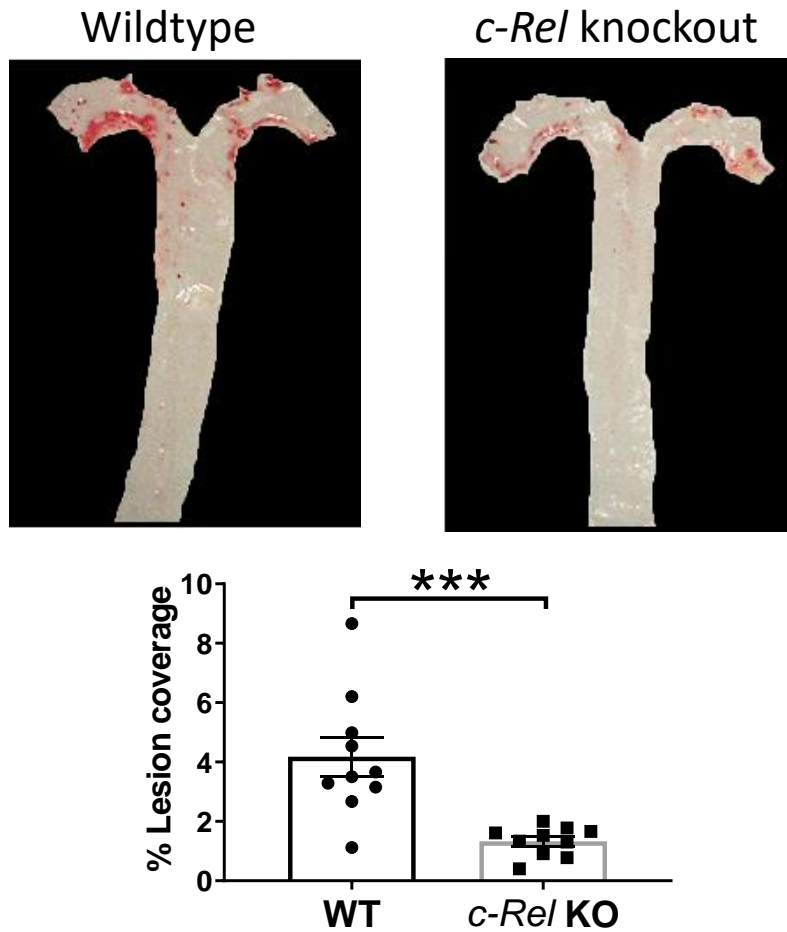


Figure 5.5. *c-Rel* promotes the development of atherosclerotic lesions at low shear stress regions of the mouse aorta. 12 week old female C57BL/6J wildtype (WT) and *c-Rel* knockout (KO) mice were treated with AAV-PCSK9 to induce hypercholesterolemia. After one week, they were fed a high fat diet for 6 weeks. Atherosclerotic lesions were analysed using Oil Red O after fixation with 2% (w/v) paraformaldehyde. Representative images and quantification of lesion coverage are shown. The percentage of lesion coverage of the mouse aorta was measured using the imaging software NIS-Elements BR (Nikon). Mean values are shown with standard error of the mean; n=10 mice per group. ***p<0.001, using unpaired T-test.

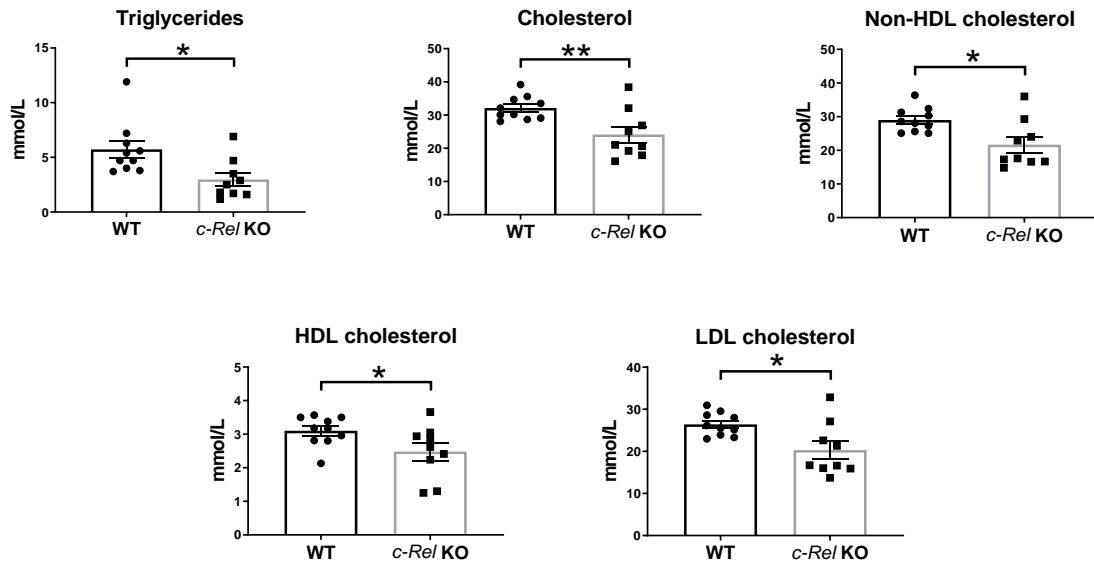


Figure 5.6. c-Rel increases plasma triglycerides and cholesterol levels in mouse. 12 week old female C57BL/6J wildtype (WT) and *c-Rel* knockout (KO) mice were treated with AAV-PCSK9 to induce hypercholesterolemia. After one week, they were fed a high fat diet for 6 weeks. The levels of triglycerides, total cholesterol, non-HDL cholesterol, HDL cholesterol and LDL cholesterol in plasma were measured. Mean values are shown with standard error of the mean; n=9-10 mice per group. ***p<0.001, using unpaired T-test.

5.8 Endothelial c-Rel promotes the development of atherosclerosis

Although total *c-Rel* deletion in mice reduced atherosclerotic lesions, it also led to a reduction in lipids levels in plasma. Therefore, the specific role of endothelial c-Rel in atherosclerosis was investigated.

c-Rel expression was deleted from the endothelium by crossing mice containing loxP sites (which flanked exon 1 of the *Rel* gene) with mice with a tamoxifen-inducible form of Cre driven by the endothelial *Cdh5* gene. *c-Rel*^{FL/FL}; *Cdh5*-Cre-ER^{T+/-} mice and experimental controls (*c-Rel*^{FL/+}; *Cdh5*-Cre-ER^{T-/-} and *c-Rel*^{FL/FL}; *Cdh5*-Cre-ER^{T-/-} mice) were then treated with tamoxifen to generate EC-specific *c-Rel* knockout mice (*c-Rel* EC^{KO}). Successful deletion of *c-Rel* in ECs (*Cdh5*⁺ cells) was visualised by eGFP signal, since the conditional *c-Rel* allele is constructed such that, upon Cre-mediated recombination, the promoter region and the ATG-containing exon of *c-Rel* are deleted together with the activation of eGFP (data not shown) (Heise et al., 2014). Besides, tamoxifen-induced *Cdh5*-Cre-ER^T mice have previously shown high levels of Cre-mediated deletion in vascular ECs (>90%) (Monvoisin et al., 2006; Sorensen et al., 2009).

When the mice were 12 week old, hypercholesterolemia was induced using an adenovirus containing PCSK9. One week after a single AAV-PCSK9 intraperitoneal injection, mice were fed a high fat Western diet for 6 weeks and atherosclerotic lesions were stained using Oil Red O.

When lesion coverage in *c-Rel* EC^{KO} mice and experimental controls was quantified, it was observed that genetic deletion of *c-Rel* in EC significantly decreased lesion area in the aorta, indicating that endothelial c-Rel promotes the development of atherosclerosis. As it was previously shown, experimental controls showed atherosclerotic lesions that localised preferentially to the inner curvature of the arch and carotid bifurcations, which are regions exposed to low shear stress. Lipid deposition was also found at intercostal artery branch points of the descending aorta (figure 5.7).

Although this indicates that endothelial c-Rel induces atherosclerotic development, the cholesterol or triglycerides levels in plasma have not yet been tested, and endothelial c-Rel could still be promoting atherosclerosis by altering lipid metabolism. Therefore, the role of EC-c-Rel in atherosclerosis requires further investigation.

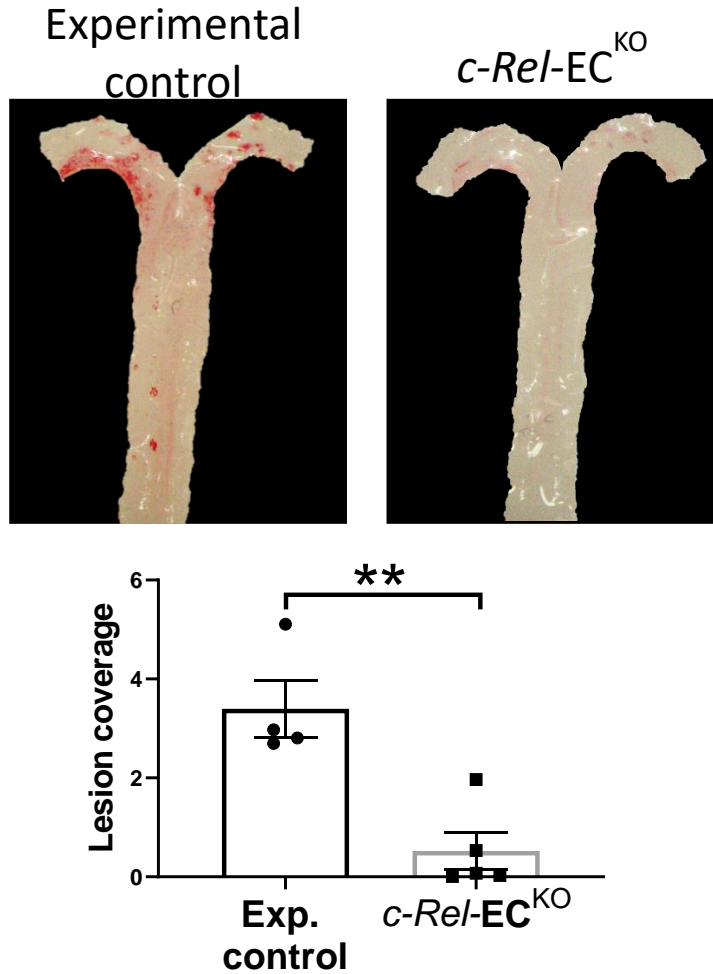


Figure 5.7. Endothelial *c-Rel* promotes the development of atherosclerotic lesions at low shear stress regions of the mouse aorta. 12 week old male C57BL/6J experimental controls and *c-Rel-EC^{KO}* (EC-specific *c-Rel* knockout) mice were treated with AAV-PCSK9 to induce hypercholesterolemia. After one week, they were fed a high fat diet for 6 weeks. Atherosclerotic lesions were analysed using Oil Red O after fixation with 2% (w/v) paraformaldehyde. Representative images and quantification of lesion coverage are shown. The percentage of lesion coverage of the mouse aorta was measured using the imaging software NIS-Elements BR (Nikon). Mean values are shown with standard error of the mean; n=4-5 mice per group. **p<0.01, using unpaired T-test.

5.9 Conclusions

In this chapter I have shown that c-Rel promotes EC dysfunction *in vivo*, by inducing both EC inflammation and proliferation at sites of disturbed flow in the mouse aorta. Furthermore, I have shown that c-Rel controls EC inflammation via Txnip and p38, and that it regulates EC proliferation via activation of the non-canonical NF- κ B pathway (Rank and Nik). Finally, I have shown that total c-Rel and endothelial c-Rel promote lesion formation at low shear regions of the vasculature.

Specifically, I conclude that:

- c-Rel drives EC inflammation and proliferation at sites of low shear stress in the murine aorta, contributing to EC dysfunction.
- c-Rel drives EC inflammation at atheroprone sites in the murine aorta by promoting the expression of the MAPK regulator Txnip and the MAPK component p38.
- c-Rel drives EC proliferation at atheroprone sites in the murine aorta by promoting the expression of the non-canonical NIK/NF- κ B signalling pathway components Rank and Nik.
- c-Rel promotes atherosclerosis, but it also induces cholesterol and triglycerides levels in plasma, suggesting that c-Rel is involved in altering lipid metabolism.
- Endothelial c-Rel promotes atherosclerosis, but further investigation of the potential role of endothelial c-Rel in lipid metabolism is still required.

5.10 Discussion

Atherosclerosis preferentially occurs at bends and branches of the vasculature. It is a disease that is triggered by EC dysfunction, which involves the induction of EC inflammation and proliferation at regions exposed to low shear stress (Warboys et al., 2011). Although several studies have revealed a number of genes that are associated with the development of this disease, the mechanisms underlying focal endothelial dysfunction are still not completely understood.

In this chapter, I have investigated the function of c-Rel in endothelial cells *in vivo*, as well as the role of c-Rel and endothelial c-Rel in atherosclerosis. I have shown that c-Rel promotes EC proliferation and inflammation *in vivo*, which is consistent with the results previously obtained *in vitro*. Besides, I have shown that c-Rel positively regulates Txnip and p38 in the mouse aorta, providing a potential mechanism for c-Rel proinflammatory effects under low shear stress. Also, c-Rel has been suggested to regulate the expression of the non-canonical NF- κ B activators Rank and Nik in atheroprone regions of the murine endothelium, further supporting the role of c-Rel in the regulation of EC proliferation. Finally, after elucidating the role of c-Rel in EC dysfunction *in vitro* and *in vivo*, it was observed that c-Rel promotes atherosclerosis and, importantly, it was shown for the first time that endothelial c-Rel is associated with the development of atherosclerosis. Further details about the role of c-Rel in atherosclerosis and EC dysfunction will now be discussed.

5.10.1 c-Rel promotes EC proliferation and inflammation *in vivo*

By performing *en face* staining of the mouse aorta, I have first shown that EC proliferation measured by Ki67 and the inflammatory markers Vcam-1 and E-Selectin are induced in atheroprone compared to atheroprotected regions of the murine vasculature. This is consistent with the data obtained *in vitro* (presented in chapter 4), and with previously published studies that indicate that low shear regions have higher proliferation rates and expression of adhesion molecules (Akimoto et al., 2000; Davies et al., 1986; Hajra et al., 2000; Nam et al., 2009; Ni et al., 2010).

In addition to this, I have observed that c-Rel induces EC proliferation and inflammation at low shear regions in the mouse aorta, which, again, correlates with the *in vitro* results shown in the previous chapter. However, there are remarkable differences between the *in vivo* and *in vitro* model used.

Although the overall magnitude of shear stress in the periphery and centre of the wells generated by the orbital shaker is similar to arterial magnitudes of shear stress, the *in vivo* flow is much more complex. The flow generated by the orbital shaker is pulsatile, but this pulsatility is different to the one in the vasculature, which is determined by the cardiac cycle and the presence of bends and branches in the arterial tree. Besides, the cardiac cycle generates cyclic stretch and differences in pressure that result in vessel and cell deformation *in vivo* (Han et al., 2016), whereas cells *in vitro* are cultured on plastic and are not affected by these forces. In addition to the differences in haemodynamics, the composition of the extracellular matrix *in vivo* is very different from the one in *in vitro* models. *In vivo*, the extracellular matrix contains collagen, laminin, fibronectin, and a number of glycoproteins and proteoglycans that can affect the regulation of gene expression (Chiang et al., 2009; Orr et al., 2005). However, cultured EC *in vitro* are attached to the wells using only gelatin and endogenously-produced matrix. Another difference between both models is the presence of multiple cell types *in vivo*, such as macrophages, monocytes and smooth muscle cells. These cells can release cytokines and metalloproteinases, among other molecules, and influence gene expression, and also they can cooperate with each other to carry out their functions (Yurdagul et al., 2016).

Despite all the differences between the orbital shaker system and the mouse model, c-Rel promotes EC proliferation and inflammation both *in vivo* and *in vitro*. Although it is difficult to disentangle the relative contributions of each factor to the function of c-Rel, this suggests that the magnitude of shear stress could be the main factor triggering c-Rel activity. This hypothesis could be tested using a flow-altering cuff in the mouse carotid, which could be used to establish a causal link between different patterns of shear stress and gene function *in vivo* (Kuhlmann et al., 2012).

5.10.2 Does increased EC proliferation lead to atherosclerosis?

EC proliferation has been shown to be enhanced in atheroprone areas, contributing to EC dysfunction and the development of atherosclerosis (Akimoto et al., 2000; Davies et al., 1986; Foteinos et al., 2008; Mahmoud et al., 2016; Obikane et al., 2010).

However, EC proliferation at low shear stress regions has also been suggested to be atheroprotective. miR-126-5p, a microRNA that inhibits the anti-proliferative molecule Dlk1, leads to enhanced proliferation under low shear stress. A study by Schober et al. showed that deletion of miR-126-5p blocked EC repair in response to injury, and it also

led to increased atherosclerotic development in *miR126/ApoE* double knockout mice (Schober et al., 2014). Therefore, this study suggests that EC proliferation at low shear regions is atheroprotective, as proliferative cells replace dead or lost cells after injury.

Although this study shows that EC proliferation could function as a repair mechanism, c-Rel-dependent induction of proliferation at low shear stress areas seems to be promoting EC dysfunction. Since c-Rel has also been shown to contribute to EC inflammation and the development of atherosclerosis, the induction of proliferation by c-Rel is likely to contribute to these detrimental effects.

5.10.3 c-Rel promotes the development of atherosclerosis: possible mechanisms include altered lipid metabolism

When the development of atherosclerosis was compared in wildtype and *c-Rel* knockout mice, it was observed that *c-Rel* deletion markedly reduced lesion area in the aorta, indicating that c-Rel promotes the development of atherosclerosis. Moreover, analysis of plasma revealed that *c-Rel* deletion led to a reduction in circulating lipids, decreasing levels of triglycerides and cholesterol in plasma. This suggests that the decrease in atherosclerosis in *c-Rel* knockout mice is not only due to vascular c-Rel, and that c-Rel might be playing a role in other cell types. For example, c-Rel could be targeting the liver, altering lipid metabolism.

c-Rel is known to be highly expressed in cells of hematopoietic origin, such as B cells, T cells and macrophages, and the expression of c-Rel in these cell types could influence the development of the disease. A recent study has shown that silencing of c-Rel in macrophages inhibits the expression of several proinflammatory cytokines, including IL-1 β , IL-12 and IL-23, leading to a further decrease in IFN- γ and IL-17A (Zhang et al., 2017). Interestingly, all these cytokines have been shown to play a role in the development of atherosclerosis. IL-1 β is a proinflammatory cytokine that has been linked to atherosclerosis, and the CANTOS study has revealed its therapeutic relevance as a target for atherosclerosis (Ridker et al., 2017). IL-12 consists of a 35 kDa (p35) light chain and a 40 kDa (p40) heavy chain that is expressed by macrophages and B cells, among others (Trinchieri, 2003). It has been shown that *IL-12 p40/ApoE* knockout mice have less atherosclerotic lesions compared to controls (Davenport and Tipping, 2003), and also, that administration of IL-12 protein induces atherogenesis in *ApoE* knockout mice (Lee et al., 1999). IL-17A and its positive regulator IL-23 have been shown to be expressed in

atherosclerotic lesions, and IL-17A has also been linked to increased inflammation and plaque vulnerability (Erbel et al., 2011). IFN- γ , in turn, is a proinflammatory cytokine that is highly expressed in atherogenic lesions (Tedgui and Mallat, 2006), and it is known to induce ROS release and lipid uptake in macrophages. Administration of exogenous IFN- γ has also been found to promote atherosclerosis in *ApoE* knockout mice (Whitman et al., 2000). Furthermore, c-Rel is known to have a key role in the immune response, regulating B and T cell responses. Since both B and T cells have been shown to have a role in atherosclerotic lesion development (Ammirati et al., 2015), c-Rel function in B and T cells could be contributing to this disease. Altogether, this supports the idea that c-Rel is promoting atherosclerosis through several cell types, and therefore, the generation of an EC-specific *c-Rel* knockout is required to specifically assess the role of vascular c-Rel in this disease.

In addition to the potential induction of atherosclerosis through several cell types, *c-Rel* deletion also reduced circulating lipids. The role of c-Rel in the liver has been studied in the context of liver fibrosis, and it has been shown to regulate liver inflammation, regeneration, and hepatocyte proliferation in this context (Gieling et al., 2010). However, the role of c-Rel in lipid metabolism has not been studied. Cholesterol and triglycerides are insoluble in water, and hence, they need to be associated to specific lipoprotein particles to be transported in the plasma. These lipoprotein particles contain apoproteins, which, in addition to being carrier proteins, they also act as co-factors for enzymes that have a role in lipoprotein metabolism (Shepherd, 2001). Cholesterol can be synthesised by all types of cells from acetyl coenzyme A (which is produced in the mitochondria) or obtained from the diet, although the liver is the main place for *de novo* synthesis (Repa and Mangelsdorf, 2000). Triglycerides, in turn, can be synthesised by the liver or obtained from dietary sources (Hubacek, 2016). Once this occurs, triglycerides and cholesterol need to be transported into the plasma using apoproteins, and this process is mediated by two different pathways: if the lipids have been obtained from the diet they follow an exogenous route, which begins with intestinal absorption of cholesterol and triglycerides. Then, they enter the bloodstream as components of chylomicrons. However, cholesterol and triglycerides synthesised by the liver follow an endogenous route, and they enter the circulation as components of lipoproteins (Shepherd, 2001). The key enzyme that mediates triglyceride degradation is lipoprotein lipase (Hassing et al., 2012), whereas cholesterol degradation to bile acids is mediated by CYP7A1 (Pikuleva, 2008). When the

levels of triglycerides and cholesterol are abnormal, it is usually due to problems in the synthesis and degradation of triglycerides and cholesterol, or in the transport of associated apoproteins (Shepherd, 2001). Therefore, this suggests that c-Rel targets one of these processes to modulate the levels of circulating lipids.

Although the role of c-Rel in the synthesis, degradation and transport of cholesterol and triglycerides has not been studied, the RNA microarray in HUVEC that was presented in the previous chapter showed some potential c-Rel targets. Using DAVID Functional Annotation Analysis Software (<http://david.abcc.ncifcrf.gov>), a KEGG pathway annotation of genes positively regulated by c-Rel was carried out, revealing the following enriched KEGG pathways (table 5.1).

KEGG pathway	Number of genes	P-Value
Ribosome	27	3.9E-6
Lysosome	23	4.9E-5
Alcoholism	27	4.1E-4
Parkinson's disease	23	5.4E-4
Huntington's disease	28	6.4E-4
Viral carcinogenesis	29	8.2E-4
Oxidative phosphorylation	20	3.3E-3
HIF-1 signalling pathway	15	9.1E-3
Proteasome	9	1.3E-2
Sphingolipid signalling pathway	17	1.3E-2
Endocytosis	28	1.5E-2
Systemic lupus erythematosus	18	1.7E-2
Valine, leucine and isoleucine degradation	9	1.9E-2
Ubiquitin mediated proteolysis	18	2.0E-2
Non-alcoholic fatty liver disease	19	2.5E-2
Fatty acid elongation	7	3.1E-2

Table 5.1. KEGG pathway annotation of differentially expressed genes. After performing RNA microarray, A KEGG pathway analysis of genes positively regulated by c-Rel was carried out using DAVID Functional Annotation Bioinformatics Microarray Analysis Software.

These results suggest that c-Rel could be involved in lipid metabolism, since they show that c-Rel is targeting genes involved in processes such as sphingolipid signalling pathway, fatty acid elongation or non-alcoholic fatty liver disease. Besides, the role of c-Rel in oxidative phosphorylation and the lysosome could also influence lipid availability. Oxidative phosphorylation is very important for lipid biosynthesis, since some of the enzymes involved in this process, such as acetyl CoA, are synthesised in the mitochondria through an oxidation reaction (Coskun et al., 2013; Maltese and Aprille, 1985). The lysosome, in turn, has been shown to play a key role in lipid transport and biogenesis. Cholesterol and triglycerides are processed by the lysosome following their uptake by endocytosis, and these molecules are then transported to other cell locations, such as the plasma membrane, endoplasmic reticulum or the Golgi apparatus (Goldstein and Brown, 2015; Thelen and Zoncu, 2017). Also, the lysosome plays a role in *de novo* synthesis of lipids, and it is also involved in lipid catabolism (Thelen and Zoncu, 2017). Altogether, these data show that c-Rel may be involved in the synthesis, transport and degradation of lipids, and therefore, it could modulate the levels of circulating lipids. However, this RNA microarray was performed using endothelial cells, and it is still necessary to determine whether c-Rel also controls these genes in other cell types. Future work will be needed to assess the role of c-Rel in the liver, in order to elucidate the mechanism by which c-Rel is regulating circulating lipids.

Furthermore, in addition to reducing LDL cholesterol, *c-Rel* deletion also led to a decrease in HDL cholesterol. Numerous studies have shown that high HDL cholesterol levels protect from cardiovascular disease (Cockerill et al., 1995; Gordon et al., 1989; Gordon et al., 1977; Nofer et al., 2001), whereas LDL cholesterol has been associated with elevated risk of cardiovascular disease (Castelli et al., 1986). However, although it has been shown that decreasing LDL levels therapeutically can reduce the risk of cardiovascular disease (Baigent et al., 2005), the causal relationship between low HDL levels and high cardiovascular disease events is still under debate (Hausenloy and Yellon, 2008; Wild and Byrne, 2008). Moreover, it has recently been shown that very high levels of HDL cholesterol (>60 mg/dl) in humans are associated with a higher risk of cardiovascular events, suggesting that very high levels of HDL cholesterol might not be beneficial. Since very high levels of HDL lead to more cardiovascular events instead of protecting from cardiovascular disease, this could explain why *c-Rel* deletion decreases both LDL and HDL levels and also, reduces atherosclerosis.

5.10.4 Endothelial c-Rel promotes the development of atherosclerosis

Although total *c-Rel* deletion in mice inhibited the development of atherosclerosis, it also led to a reduction in lipids levels in plasma. Since *c-Rel* is expressed in numerous cell types, the effects seen on atherosclerosis could be due to expression of *c-Rel* outside the endothelium. Therefore, the specific role of endothelial *c-Rel* in atherosclerosis was investigated. When endothelial *c-Rel* was deleted, it was observed that atherosclerotic lesions were markedly reduced, hence, indicating that endothelial *c-Rel* specifically promotes atherosclerosis.

However, the levels of circulating lipids have not been measured yet. If the levels of cholesterol and triglycerides in plasma are not significantly different between *c-Rel-EC*^{KO} mice and experimental controls, it would be unlikely for EC *c-Rel* to induce atherosclerosis by modifying lipid metabolism. However, if they are significantly different, EC *c-Rel* could be affecting the liver, and atherosclerosis development could be promoted due to lipid alterations. Future work will investigate the role, if any, of EC *c-Rel* in the control of lipid metabolism.

Chapter 6. General discussion

6.1 c-Rel drives atherosclerosis at sites of disturbed blood flow by activating inflammatory and proliferative transcriptional programmes in endothelium

Before the completion of this project, several NF- κ B subunits had been studied in the context of shear stress. RelA was known to promote EC inflammation in atheroprone sites (Cuhlmann et al., 2011), and recent data from the lab suggests that the non-canonical NF- κ B subunit p52/p100 induces EC proliferation under disturbed flow (Bowden et al., data not published). However, the influence of shear stress on c-Rel had not been investigated.

Similarly, c-Rel had been shown to control proliferation, apoptosis and inflammation in several immune and non-immune cells (Bunting et al., 2007; Chen et al., 2010; Gaspar-Pereira et al., 2012; Grumont et al., 1999a; Kontgen et al., 1995b; Sarnico et al., 2009), but the function of c-Rel in the endothelium and its potential contribution to EC dysfunction and atherosclerosis had not been elucidated.

Here, I have shown that low shear stress upregulates c-Rel protein levels *in vivo* by performing *en face* staining of mouse aortas, and *in vitro* using HUVEC and HCAEC exposed to flow. Furthermore, silencing of *c-REL* in HUVEC led to a reduction in EC proliferation and the expression of the inflammatory markers VCAM-1, ICAM-1 and E-SELECTIN under low shear stress, and these observations were later observed *in vivo* by *en face* staining of mouse aortas.

After showing the role of c-Rel in EC inflammation and proliferation, a RNA microarray was performed in HUVEC to elucidate the mechanisms by which c-Rel controls these processes. Microarray data and subsequent validation by qPCR and Western blotting indicated that c-Rel positively regulates TXNIP and p38, and this regulation was further validated *in vivo*. Since TXNIP and p38 have been shown to mediate the proinflammatory effects of shear stress (Yamawaki et al., 2005; Zakkar et al., 2008), this provides a potential mechanism for c-Rel proinflammatory effects in EC. The RNA microarray and experiments *in vitro* also indicated that c-Rel induces RANK, which was later shown *in vivo*. RANK is an activator of the non-canonical NF- κ B pathway and it is known to promote cell proliferation (Anderson et al., 1997; Fata et al., 2000). As the non-canonical NF- κ B subunits p52 and p100 have been reported to promote EC proliferation by suppression of p21 (Bowden et al., unpublished), the role of c-Rel in this pathway was investigated. My studies suggest that c-Rel promotes the expression of NIK, p52/p100 and inhibits p21 expression to induce EC proliferation.

After showing the importance of c-Rel in EC dysfunction, the potential role of c-Rel in regulating the development of atherosclerosis was investigated. Total *c-Rel* knockout mice and *c-Rel-EC^{KO}* mice showed a significant reduction in atherosclerotic lesions compared to controls, therefore indicating that c-Rel and EC c-Rel promote the initiation of atherosclerosis. Altogether, these results show that c-Rel is important for EC dysfunction and atherogenesis, potentially providing a new therapeutic target for the treatment and prevention of this disease (figure 6.1).

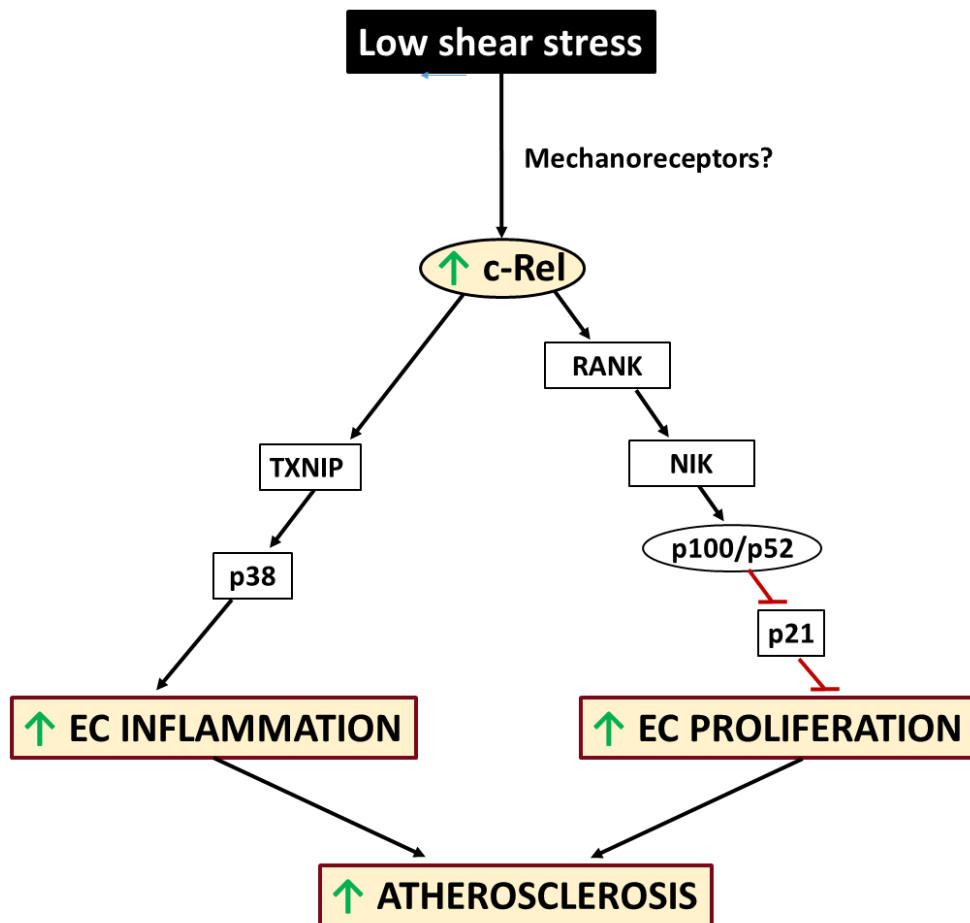


Figure 6.1. c-Rel drives atherosclerosis at sites of disturbed blood flow by activating inflammatory and proliferative transcriptional programmes in endothelium. c-Rel is enhanced in EC exposed to low shear stress, promoting atherosclerosis by inducing EC inflammation and proliferation. The induction of EC inflammation occurs via TXNIP and its downstream target p38, whereas c-Rel promotes EC proliferation via induction of RANK, NIK and p100/p52 and through suppression of the anti-proliferative p21. The mechanisms by which shear stress regulates c-Rel still need to be elucidated. Additionally, it would be interesting to study whether c-Rel induces EC inflammation and proliferation at the same time, or whether these pathways are mutually exclusive. Furthermore, c-Rel could potentially activate other pathways to induce EC activation, which will also need to be investigated.

6.2 Translating results to human atherosclerosis

6.2.1 Emerging therapeutic strategies to inhibit c-Rel induction of atherosclerosis

c-Rel is a protooncogene that has been shown to play a role in the regulation of tumorigenesis, including B cell lymphomas and a number of solid tumours (Fullard et al., 2012). Besides, it has been shown that genetic deletion of c-Rel in Tregs leads to a drastic reduction in melanoma growth, which also occurs when c-Rel is chemically inhibited (Grinberg-Bleyer et al., 2017). Therefore, therapeutic targeting of c-Rel is currently attracting interest, since it could result in clinical benefit.

IT-603 and IT-901 are c-Rel inhibitors that are currently available, and they have successfully been used in preclinical trials. They were discovered by performing screening of a library that contained 15000 small molecules, and they both present high specificity for c-Rel (Shono et al., 2016). These two small-molecule hydrophobic inhibitors function as direct NF- κ B inhibitors, as they prevent DNA binding of the c-Rel protein directly. Thiohydantoin IT-603 was the first c-Rel-specific inhibitor used, and its effects have been tested *in vitro*. It has been shown that treatment of T cells with this inhibitor promotes c-Rel deficiency and leads to inhibition of T cell alloactivation. However, it does not affect T cell activation in response to viral or tumor-associated antigens, showing its safety (Shono et al., 2014) (table 6.1).

Naphthalenethiobarbiturate IT-901 has also shown efficacy *in vivo*, using mouse models and a xenograft model of human B cell lymphoma. Treatment with this inhibitor has led to suppression of graft versus host disease, and also, it has been shown to have antilymphoma activity (Shono et al., 2016) (table 6.1). Although both IT-603 and IT-901 appear to be effective c-Rel inhibitors, IT-901 presents higher efficacy and a better pharmacokinetic profile. Intraperitoneal injection of IT-901 has also been shown to be the preferred method of administration, compared to subcutaneous injection and oral administration. Although this inhibitor is well tolerated, concentrations above 10 μ mol/L become progressively toxic (Shono et al., 2016). Since IT-901 has been shown to be well tolerated and to have high efficacy, and it also presents a good pharmacokinetic profile, this inhibitor is a promising drug candidate that could be tested in clinical trials. Therefore, this drug could potentially be used to inhibit c-Rel-dependent endothelial cell dysfunction, which could lead to the treatment of atherosclerosis.

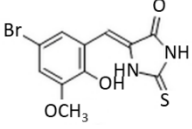
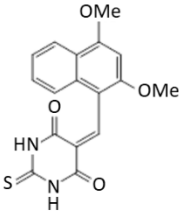
c-Rel Inhibitor	Biological Activity	Chemical Structure and Formula	Reference
IT-603	Diminishes graft-versus-host disease and reduces alloactivation in T cells, but does not impair T-cell activation in response to viral or tumor-associated antigens.	 $C_{11}H_9BrN_2O_3S$	Shono et al., 2014.
IT-901	Reduces severity of graft-versus-host disease. Inhibits growth of human B-cell lymphoma xenografts in mice.	 $C_{17}H_{14}N_2O_4S$	Shono et al., 2016.

Table 6.1. Summary of c-Rel-specific inhibitors. IT-603 and IT-901 are c-Rel specific inhibitors. Their biological activity, chemical structure and formula are summarised on this table.

However, c-Rel is not only expressed in endothelial cells, it also shows high expression in cells of hematopoietic origin. Since EC c-Rel specifically promotes atherosclerosis, the endothelium should be the target for a therapeutic intervention. It has recently been shown that endothelial mRNA molecules can be targeted using nanoparticles loaded with siRNA, for example, this technology was used to suppress TGF- β signalling specifically in EC, reducing plaque growth (Chen et al., 2019). Therefore, this could potentially be used as a therapeutic strategy, and targeting EC c-Rel using siRNAs could lead to plaque regression and a reduction in plaque growth.

In addition to this, another study has shown that endothelial cells at low shear regions can be targeted using lipoparticles (Kheiriloom et al., 2015). As c-Rel has been shown to be predominantly expressed at low shear areas that are prone to atherosclerosis, deleting c-Rel from EC under low shear stress would be desired. Since VCAM-1 levels are increased in the endothelium exposed to low shear stress, this study targeted VCAM-1 using cationic lipoparticles (CCLs) that were coated with VCAM-1-targeting peptides. The CCLs also contained anti-miR-712, and when these were delivered to low shear

regions, they successfully reduced shear-mediated atherosclerosis (Kheirilomoom et al., 2015). Therefore, CCLs could also be used to deliver c-Rel specific inhibitors, such as IT-901, to EC exposed to low shear stress. The use of CCLs might then become a new therapeutic strategy that could potentially lead to the prevention or treatment of atherosclerosis.

6.2.2 Assessment of c-Rel in human atherosclerosis

Although I have shown that c-Rel promotes atherosclerosis in mice, the role of c-Rel in human atherosclerosis has not been investigated. Human plaques have been classified according to their severity, and the atherosclerotic severity grades are as follows: grade I includes aortic wall intimas with no or minimal intimal thickening, grade II refers to aortic walls with extensive intimal thickening and no atheroma, grade III indicates the presence of a immobile atheroma that protrudes <5mm into the lumen, grade IV refers to an immobile atheroma that protrudes >5mm into the lumen, and grade V indicates mobile or ulcerated atheromas (Montgomery et al., 1996).

Previous studies have investigated the expression of EndoMT markers in human coronary arteries of different grades, showing that EC TGF- β signaling, NOTCH3, SM22 α , collagen and fibronectin increase in patients with moderate or severe coronary artery disease (CAD) compared to patients with no or mild CAD (Chen et al., 2015). Similarly, immunofluorescence staining of human coronary arteries of different severity grades could be performed using c-Rel antibodies, which would determine the role of this transcription factor in the progression and growth of atherosclerotic plaques.

6.3 Future work

6.3.1 Functional analysis of c-Rel in vitro using the Ibidi® system

After assessing the function of c-Rel *in vitro* using the orbital shaker system, the function of c-Rel should also be studied using the Ibidi® system. It is known that the orbital shaker generates different patterns of shear stress within one well, and therefore, cells under low shear could migrate to regions under high shear and vice versa, potentially affecting the function of c-Rel. Similarly, the release of microvesicles, cytokines and other factors by cells under different flow patterns could have an influence on c-Rel activity. The Ibidi® system could then be used to overcome this limitation, since all cells in an Ibidi® chamber are exposed to the same shear stress patterns.

6.3.2 Expression and functional analysis of c-Rel in vivo using a flow-altering constrictive cuff

Although the expression of c-Rel has been shown to be higher at low shear stress compared to high shear stress regions of the mouse aorta, this did not determine whether there is a causal relationship between haemodynamic forces and c-Rel expression. To overcome this limitation, a constrictive cuff could be inserted into the carotid artery (Kuhlmann et al., 2012), which generates areas exposed to low unidirectional shear stress (upstream of the cuff constriction), areas of oscillatory shear (downstream of the cuff constriction), and areas of high shear stress (within the cuff constriction). Using this, a causal relationship between different patterns of shear stress and c-Rel expression could be determined. Furthermore, the constrictive cuff model could be used to determine the role of c-Rel in the regulation of EC inflammation and proliferation by comparing responses in wildtype and *c-Rel* knockout mice.

6.3.3 Role of c-Rel in senescence

Since c-Rel has been shown to inhibit the anti-proliferative molecule p21 via p52, and p21 is also known to be involved in senescence in EC (Warboys et al., 2014), c-Rel could play a potential role in this process. Previous reports have also shown that p52 inhibits p21, and this has been revealed to be dependent on p53 (Schumm et al., 2006). Besides, p53 has been shown to promote senescence in areas of disturbed flow, and high levels of p53 in these regions correlated with high p21 levels (Warboys et al., 2014). Therefore, the interaction between p52, p21 and p53 in EC cells needs to be investigated, as well as the role that c-Rel plays in this process. In addition to this, the potential role of c-Rel in senescence will be studied by assessing the expression of the senescence marker senescence-associated β -Galactosidase in c-Rel siRNA-treated cells compared to controls.

6.3.4 Validation of c-Rel function in vitro and in vivo

To validate whether c-Rel promotes EC inflammation via TXNIP and p38, overexpression studies could be performed to assess whether TXNIP or p38 can rescue the anti-inflammatory phenotype of c-Rel silencing. Similarly, these overexpression studies could also be used to test whether RANK, NIK and p52/p100 could rescue the anti-proliferative phenotype of c-Rel silencing. In addition to this, generation of gene specific knockout mice would be useful to assess c-Rel target genes, in order to

investigate whether its deletion mimics the anti-proliferative and anti-inflammatory phenotypes of *c-Rel* knockout mice.

6.3.5 Does c-Rel regulate its target genes directly?

Although I have shown that c-Rel regulates the expression of several genes involved in EC inflammation and proliferation, it has not been studied whether c-Rel regulates these genes directly or indirectly. Hence, chromatin immunoprecipitation (ChIP) experiments could be carried out to identify novel c-Rel interactions with promoters of these genes, modulating their expression.

6.3.6 Effect of c-Rel signalling on other NF- κ B family members

Since other NF- κ B members, such as RelA, have also been shown to have a role in EC inflammation and the distribution of atherosclerosis (Brand et al., 1996; Cuhlmann et al., 2011), it will be interesting to investigate the effects of c-Rel silencing on RelA, and similarly, whether RelA silencing influences c-Rel expression in EC. c-Rel and RelA could be forming heterodimers to contribute to this disease, and therefore, the interaction between these subunits could be investigated. Moreover, it has been reported that p50 inhibits c-Rel expression in other cell types (Gaspar-Pereira et al., 2012), and hence, the study of the interaction between these two NF- κ B transcription factors in the endothelium will be of interest.

6.3.7 Mechanosensitive signalling pathways upstream of c-Rel

Although I have determined potential signalling pathways downstream of c-Rel that control EC inflammation and proliferation, it is still unknown how shear stress regulates c-Rel. PI3K, PKC ζ and TGF- β signalling pathways are known to be upstream of c-Rel in different cell types (Grumont et al., 2002; Mendoza et al., 2006; Piera-Velazquez et al., 2010; Sanchez-Valdepenas et al., 2007) and they have also been shown to respond to shear stress (Chen et al., 2015; Dimmeler et al., 1998; Magid and Davies, 2005; Nigro et al., 2010; Tseng et al., 1995). Therefore, it will be investigated whether these signalling pathways are upstream of c-Rel in EC. In addition to this, Notch-1 has been shown to be a mechanosensor (Mack et al., 2017) and it is also known to be upstream of c-Rel in T cells and hematopoietic cells (Cheng et al., 2001; Shin et al., 2006). Hence, it will be interesting to determine the role of Notch-1 in the regulation of c-Rel expression. Moreover, a mechanosensory complex that comprises VE-cadherin, PECAM-1 and VEGFR-2 has been shown to be important for the activation of NF- κ B/Rel in sheared EC,

however, the specific role of this complex in the activation of c-Rel still needs to be elucidated. Finally, c-Rel could also be regulated by siRNAs. miR-155 has been shown to inhibit c-Rel degradation in T cells via repression of the ubiquitin ligase peli1 (Liu et al., 2016). Also, Victoria Ridger's lab has recently shown that miR-155 is delivered to EC by neutrophil-derived microvesicles preferentially at atheroprone regions (Gomez et al., 2020), and miR-155 expression has been observed to be increased in both human and mouse atherosclerotic plaques (Du et al., 2014). Therefore, studying the potential regulation of c-Rel by a miR155-Peli1 pathway in EC cells could provide an explanation for the differences in c-Rel protein stability at low and high shear stress areas.

6.3.8 Assessment of c-Rel function and lipid levels using c-Rel-EC^{KO}

Although the role of c-Rel in the regulation of EC inflammation and proliferation has been tested *in vivo* using total *c-Rel* knockout mice, *c-Rel-EC^{KO}* mice will be used to validate the regulation of proliferation (Ki67), inflammatory markers (Vcam-1, E-Selectin) and c-Rel target genes (Txnip, p38, Rank, Nik, p100/p52, p21). This will be done by performing immunohistochemistry in the aortic root of *c-Rel-EC^{KO}* mice and experimental controls.

The cholesterol and triglycerides levels in plasma still need to be determined in *c-Rel-EC^{KO}* mice and experimental controls. If the lipid levels are not significantly different between both groups, no further experiments will be performed. However, if the lipid levels vary significantly between experimental controls and *c-Rel-EC^{KO}* mice, vascular c-Rel may be altering lipid metabolism. To assess this potential regulation of lipid metabolism by c-Rel, a RNA-seq using the livers from these animals will be performed, which will help determine differences in the synthesis, transport and degradation of cholesterol and triglycerides.

6.3.9 Effect of c-Rel inhibitor in atherosclerosis

Although *c-Rel* deletion has been shown to prevent the development of atherosclerosis, it is still unknown whether targeting c-Rel could lead to the regression of atherosclerosis. There are two c-Rel inhibitors that have been shown to be specific, IT-603 and IT-901, and these inhibitors could be used to assess the potential role of c-Rel in atherosclerosis regression. Mice treated with AAV-PCSK9 will be exposed to a high fat diet for 6 weeks, and half of these mice will then be injected with a specific c-Rel inhibitor for 2 weeks. This will help determine the effect of c-Rel in plaque regression, and it will potentially identify c-Rel as a potential therapeutic target for the treatment of atherosclerosis.

6.3.10 Contribution of non-vascular c-Rel to atherosclerosis

c-Rel is expressed in several cell types, such as T cells, macrophages and smooth muscle cells. Therefore, c-Rel could be contributing to atherosclerosis and plaque formation through different cell types. It will be interesting to determine whether c-Rel promotes inflammation and proliferation in non-vascular cells, or whether this phenotype is specific to EC c-Rel.

6.3.11 Assessment of c-Rel expression at low shear stress regions of AAV-PCSK9-treated mice and human coronary tissue sections

I have shown that c-Rel is upregulated at low shear regions of wildtype mouse aortas, however, c-Rel signals in these mice were heterogeneous. Under low shear stress, some cells showed nuclear staining, whereas others showed perinuclear and cytoplasmic staining. Hence, it will be interesting to determine whether c-Rel expression becomes more nuclear in hypercholesterolemic mice treated with PCSK9/*ApoE* knockout mice compared to controls. Similarly, the role of c-Rel in human coronary tissue sections will be used to study c-Rel expression, by performing immunofluorescence staining of plaques of different severity grades (I-V). This will determine the relationship between c-Rel and plaque severity, and it will establish the role of c-Rel in the progression and growth of atherosclerotic plaques.

Chapter 7. Appendix

Appendix 1. Antibodies used

Primary Antibody	Host	Company purchased from
Calnexin (610524)	Mouse	BD Biosciences
PDHX (sc-393644)	Mouse	Santa Cruz Biotechnology
RANK (sc-374360)	Mouse	Santa Cruz Biotechnology
RANK(AF546 sc-374360)	Mouse	Santa Cruz Biotechnology
VE-Cadherin (555661)	Mouse	BD Biosciences
Active Caspase 3 (9661)	Rabbit	Cell Signalling
c-Rel (SC71)	Rabbit	Santa Cruz Biotechnology
E-Selectin (nbp1-45545)	Rabbit	Novus Biologicals
Ki67 (ab15580)	Rabbit	Abcam
NIK (ab216409)	Rabbit	Abcam
PCNA (ab18197)	Rabbit	Abcam
p21 (2947)	Rabbit	Cell Signalling
p38 (9212)	Rabbit	Cell Signalling
p52/p100 (ab109440)	Rabbit	Abcam
TXNIP (18243-1-AP)	Rabbit	Proteintech
VCAM-1 (ab134047)	Rabbit	Abcam
CD31 (102514)	Rat	BioLegend

Appendix 2. RNA microarray in HUVEC: Genes downregulated by c-REL silencing

Gene symbol	Average expression levels (log2) in SCR siRNA-treated HUVEC	Average expression levels (log2) in c-REL siRNA-treated HUVEC	Fold change	ID
TSPAN7	12.23	8.08	-17.86	TC0X00011279.hg.1
LGALS9	13.28	9.63	-12.52	TC1700012216.hg.1
AQP1	10.53	7.21	-9.97	TC0700013347.hg.1
PDLIM1	11.59	8.32	-9.64	TC1000011485.hg.1
MEIS2	12.66	9.57	-8.51	TC1500009036.hg.1
HACD2	11.38	8.39	-7.93	TC0300012208.hg.1
CD34	13.36	10.43	-7.61	TC0100017142.hg.1
PLSCR4	10.51	7.64	-7.32	TC0300012720.hg.1
SLCO2A1	9.82	6.99	-7.11	TC0300012484.hg.1
MATN2	10.11	7.29	-7.09	TC0800008324.hg.1
RPL18A	14.29	11.54	-6.74	TC1200008677.hg.1
LDB2	14.24	11.51	-6.63	TC0400010141.hg.1
ZFPL1	8.72	6	-6.6	TC1100007996.hg.1
RBMS2	13.34	10.7	-6.2	TC1200007844.hg.1
CYB5A	8.85	6.23	-6.15	TC1800009029.hg.1
HTR2B	11.73	9.14	-6.05	TC0200016006.hg.1
CGNL1	10.42	7.83	-6.04	TC1500007346.hg.1
CHTOP	7.95	5.41	-5.83	TC0100010044.hg.1
ACKR4	10.09	7.62	-5.53	TC0300008847.hg.1
TCN2	11.44	9	-5.42	TC2200009257.hg.1
IMP4	7.94	5.51	-5.38	TC0200009299.hg.1
ENTPD1	13.11	10.69	-5.36	TC1000012482.hg.1
LRR32	12.2	9.78	-5.35	TC1100011694.hg.1
HLA-C	8.88	6.46	-5.33	TC0600014257.hg.1
GIPC2	9.69	7.29	-5.27	TC0100018239.hg.1
BAG3	11.01	8.66	-5.11	TC1000009090.hg.1
TXNIP	11.09	8.74	-5.1	TC0100015598.hg.1
APOL1	10.73	8.39	-5.09	TC2200007242.hg.1
ZFYVE21	9.76	7.43	-5.05	TC1400008415.hg.1
TNFSF10	13.63	11.32	-4.95	TC0300013146.hg.1
NDUFC1	9.03	6.74	-4.88	TC0400012968.hg.1
CMKLR1	9.57	7.29	-4.87	TC1200011838.hg.1
SORT1	9.15	6.9	-4.76	TC0100015194.hg.1
EHD3	9.28	7.03	-4.75	TC0200007155.hg.1
ABCG2	8.47	6.24	-4.69	TC0400011279.hg.1
BMP4	15.05	12.82	-4.69	TC1400009214.hg.1

HIGD2A	10.51	8.3	-4.64	TC050009587.hg.1
TMEM123	15.94	13.74	-4.6	TC1100012121.hg.1
IL18BP	12.35	10.16	-4.58	TC1100008330.hg.1
WWC3	8.33	6.16	-4.51	TC0X00006590.hg.1
IFITM2	16.15	14	-4.44	TC1100012948.hg.1
KCTD3	7.36	5.21	-4.43	TC0100011592.hg.1
IRF1	7.95	5.81	-4.41	TC0500012017.hg.1
TGFBR3	9.57	7.46	-4.33	TC0100014910.hg.1
LGALS9C; LGALS9B	10.37	8.26	-4.31	TC1700007127.hg.1
FAXDC2	11.34	9.24	-4.3	TC0500012567.hg.1
TSG101	9.82	7.72	-4.28	TC1100010268.hg.1
BCAM	10.14	8.04	-4.28	TC1900008286.hg.1
RNF125	6.7	4.6	-4.27	TC1800009222.hg.1
C1orf21	12.46	10.38	-4.22	TC0100010887.hg.1
PUS7	9.54	7.46	-4.22	TC0700012159.hg.1
SCARA3	11.33	9.26	-4.21	TC0800007114.hg.1
ENPP4	9.45	7.37	-4.21	TC0600008156.hg.1
MANSC1	12.7	10.64	-4.15	TC1200009964.hg.1
APOL3	9.09	7.04	-4.14	TC2200008588.hg.1
LRRFIP1	8.49	6.45	-4.11	TC0200016603.hg.1
LMO2	9.66	7.62	-4.11	TC1100010495.hg.1
LIPA	10.67	8.65	-4.08	TC1000012577.hg.1
PLPP3	14.96	12.93	-4.08	TC0100018443.hg.1
PLA2G16	10.71	8.74	-3.92	TC1100011126.hg.1
EPAS1	15.86	13.89	-3.92	TC0200007458.hg.1
KIAA0100	12.72	10.75	-3.92	TC1700010202.hg.1
F11R	14.67	12.71	-3.9	TC0100018519.hg.1
MAPK3	13.74	11.78	-3.9	TC1600009954.hg.1
FDFT1	10.2	8.25	-3.86	TC0800006760.hg.1
SDPR	15.29	13.34	-3.86	TC0200015264.hg.1
IER3	14.26	12.31	-3.85	TC0600011386.hg.1
KLF9	8.52	6.61	-3.78	TC0900010366.hg.1
PDE7B	10.75	8.84	-3.77	TC0600009545.hg.1
CXorf36	13	11.09	-3.76	TC0X00009507.hg.1
HIST1H1B	9.82	7.92	-3.74	TC0600011232.hg.1
PIK3C2B	9.68	7.79	-3.73	TC0100017029.hg.1
NUMA1	11.43	9.53	-3.73	TC1100011539.hg.1
ANXA11	13.1	11.21	-3.71	TC1000011203.hg.1
HIP1R	8.26	6.38	-3.68	TC1200009221.hg.1
FAM101B	9.58	7.7	-3.67	TC1700009318.hg.1
ACP5	8.12	6.25	-3.67	TC1900009684.hg.1
PI16	9.25	7.37	-3.66	TC0600007854.hg.1

TLK1	7.78	5.93	-3.62	TC0200014893.hg.1
RBM8A	10.22	8.37	-3.61	TC0100018477.hg.1
HEG1	10.78	8.93	-3.6	TC0300012238.hg.1
MMRN2	12.97	11.13	-3.59	TC1000012573.hg.1
GLB1; TMPPE	11.6	9.76	-3.58	TC0300010664.hg.1
CTDSPL2	9.74	7.9	-3.56	TC1500007091.hg.1
WWP2	8.97	7.14	-3.55	TC1600008239.hg.1
CDON	7.63	5.81	-3.53	TC1100012722.hg.1
CPXM2	11.81	9.99	-3.53	TC1000012108.hg.1
FBL	10.22	8.42	-3.49	TSUnmapped00000427.hg.1
ATP2B1	8.75	6.95	-3.49	TC1200011474.hg.1
VAMP5	11.06	9.26	-3.48	TC0200008261.hg.1
RPSA; SNORA62; SNORA6	16.26	14.46	-3.48	TC0300007101.hg.1
RNF170; MIR4469	7.01	5.22	-3.47	TC0800010299.hg.1
UBE2L6	11.42	9.63	-3.45	TC1100010897.hg.1
MRPS18B	8.92	7.15	-3.42	TC0600014097.hg.1
MCAM; MIR6756	11.52	9.74	-3.42	TC1100012520.hg.1
LAMTOR5	10.45	8.68	-3.4	TC0100015236.hg.1
EPB41L2	10.2	8.43	-3.4	TC0600013165.hg.1
HIST1H1E	12.08	10.32	-3.39	TC0600007273.hg.1
HIST1H2AG	8.99	7.24	-3.37	TC0600014083.hg.1
SNRPD3	12.44	10.69	-3.36	TC2200009235.hg.1
SLC9A9	6.19	4.46	-3.33	TC0300012686.hg.1
RPL35	14.26	12.52	-3.33	TC0900011510.hg.1
CTNNAL1	9.55	7.83	-3.31	TC0900011148.hg.1
FAU	10.41	8.69	-3.3	TC1100013185.hg.1
EVI5	9.44	7.72	-3.3	TC0100014927.hg.1
AP3D1	9.04	7.32	-3.29	TC1900009208.hg.1
LAP3	13.02	11.31	-3.28	TC0400006987.hg.1
NR3C2	8.65	6.94	-3.27	TC0400012078.hg.1
NR3C1	7.14	5.44	-3.24	TC0500012340.hg.1
RPS18	15.95	14.25	-3.24	TC0600007693.hg.1
HLA-E	12.55	10.85	-3.23	TC0600007530.hg.1
ATP11C	12.84	11.16	-3.22	TC0X00010966.hg.1
CFB	7.15	5.46	-3.21	TC0600014106.hg.1
FYTDD1	10.08	8.4	-3.19	TC0300010066.hg.1
GIMAP6	10.02	8.36	-3.16	TC0700013043.hg.1
ACSS2	6.78	5.13	-3.15	TC2000007202.hg.1
NXN	11.45	9.8	-3.14	TC1700009333.hg.1
TEAD4	6.63	4.99	-3.13	TC1200006515.hg.1
LGALS9B	11.01	9.37	-3.12	TC1700010050.hg.1

CHSY1	10.23	8.59	-3.12	TC1500010655.hg.1
AGPAT5	9.83	8.19	-3.12	TC0800006566.hg.1
HDAC1	10.39	8.75	-3.12	TC0100007678.hg.1
ELOVL5	13.61	11.97	-3.12	TC0600012072.hg.1
TCTEX1D1	7.13	5.49	-3.11	TC0100008637.hg.1
RPL27A; SNORA3A; SNORA3B	10.41	8.78	-3.09	TC1100006791.hg.1
EDEM2	11.09	9.47	-3.08	TC2000008960.hg.1
NFKBIA	11.98	10.36	-3.08	TC1400008940.hg.1
SUCLG1	7.9	6.28	-3.08	TC0200013232.hg.1
LTA4H	13.24	11.62	-3.07	TC1200011599.hg.1
TXNDC11	10.34	8.72	-3.06	TC1600009412.hg.1
SLC39A6	8.69	7.08	-3.05	TC1800008474.hg.1
CSNK2A2	13.64	12.03	-3.04	TC1600010476.hg.1
ST8SIA6	12.31	10.71	-3.04	TC1000009927.hg.1
CORO1C	13.08	11.48	-3.04	TC1200011846.hg.1
NELFCD	9	7.39	-3.04	TC2000007923.hg.1
GLT8D2	8.13	6.53	-3.03	TC1200011752.hg.1
MKRN1	11.45	9.85	-3.03	TC0700012812.hg.1
SPECC1L- ADORA2A	11.74	10.14	-3.03	TC2200009234.hg.1
CLDN5	10.26	8.67	-3.02	TC2200007987.hg.1
RIT1	10.52	8.93	-3.02	TC0100015975.hg.1
PEBP1	10.3	8.7	-3.01	TC1200009071.hg.1
CEP350	7.87	6.28	-3.01	TC0100010793.hg.1
SH3BP5	12.01	10.43	-3	TC0300010399.hg.1
NAAA	8.21	6.63	-3	TC0400012933.hg.1
MEX3C	8.45	6.86	-3	TC1800008707.hg.1
CTSH	6	4.41	-3	TC1500010160.hg.1
ACP2	8.95	7.36	-3	TC1100010730.hg.1
DUSP1	8.9	7.32	-2.98	TC0500012842.hg.1
PPT1	11.36	9.78	-2.98	TC0100013818.hg.1
H1FO	11.72	10.15	-2.97	TC2200007318.hg.1
IFT80	9.42	7.85	-2.97	TC0300014074.hg.1
LMNB1	9.12	7.55	-2.97	TC0500008544.hg.1
CDC23	8.09	6.52	-2.96	TC0500012163.hg.1
FBL	9.84	8.28	-2.96	TSUnmapped00000349.hg.1
MTMR10	12.56	11	-2.96	TC1500008893.hg.1
LZTFL1	9.45	7.89	-2.95	TC0300010931.hg.1
ZNF366	8.33	6.78	-2.93	TC0500011100.hg.1
FBXL3	8.78	7.24	-2.91	TC1300010048.hg.1
KLRG1	9.48	7.94	-2.91	TC1200006738.hg.1
METTL7A	8.83	7.29	-2.9	TC1200007626.hg.1

RPS13; SNORD14B	15.3	13.77	-2.9	TC1100013147.hg.1
TPRA1	9.01	7.47	-2.9	TC0300012315.hg.1
RHOBTB1	8.16	6.63	-2.9	TC1000010737.hg.1
HDAC5	8.22	6.68	-2.89	TC1700010811.hg.1
ETFDH	7.62	6.09	-2.89	TC0400009132.hg.1
CTNS	8.99	7.47	-2.88	TC1700006585.hg.1
YIF1B	11.19	9.67	-2.88	TC1900010597.hg.1
UQCC2	6.16	4.64	-2.87	TC0600011560.hg.1
BTF3	13.54	12.01	-2.87	TC0500007772.hg.1
FAM107A	7.47	5.95	-2.87	TC0300011311.hg.1
TNS2	8.56	7.04	-2.87	TC1200007690.hg.1
CDK16	9.73	8.22	-2.85	TC0X00007132.hg.1
ALDH2	11.66	10.15	-2.85	TC1200012707.hg.1
HSD17B11	11.7	10.2	-2.84	TC0400012945.hg.1
GSTP1	13.96	12.46	-2.84	TC1100008144.hg.1
EFNA1	7.72	6.21	-2.83	TC0100010111.hg.1
TEX264	8.85	7.35	-2.83	TC0300013835.hg.1
CYB5D2	9.66	8.17	-2.83	TC1700006611.hg.1
PEPD	12.09	10.6	-2.82	TC1900010391.hg.1
CDC25B	11.89	10.4	-2.81	TC2000006559.hg.1
LYVE1	14.87	13.39	-2.8	TC1100010090.hg.1
NSD1	8.21	6.72	-2.8	TC0500009610.hg.1
LGALS3	8.85	7.38	-2.79	TC1400007227.hg.1
POLR3E	6.94	5.46	-2.79	TC1600007193.hg.1
RASSF9	6.27	4.79	-2.79	TC1200011435.hg.1
WDR6	8.47	7	-2.78	TC0300013827.hg.1
MTIF3	8.93	7.45	-2.77	TC1300008439.hg.1
ZNF233	6.39	4.92	-2.77	TC1900008259.hg.1
ADGRA2	10.48	9.01	-2.76	TC0800007311.hg.1
PPP1CC	14.81	13.35	-2.75	TC1200011916.hg.1
IL13RA1	10.54	9.08	-2.75	TC0X00008230.hg.1
KLF2	12.72	11.27	-2.74	TC1900007270.hg.1
WRNIP1	8.77	7.32	-2.73	TC0600006611.hg.1
GRB10	9.46	8.01	-2.73	TC0700011054.hg.1
UBB	15.43	13.99	-2.72	TC1700007014.hg.1
GLUD1	10.72	9.28	-2.72	TC1000011323.hg.1
HMGB2	10.28	8.84	-2.72	TC0400012432.hg.1
PMPCB	10.74	9.31	-2.7	TC0700008666.hg.1
SETDB2	6.24	4.81	-2.7	TC1300007164.hg.1
FBXO25	7.79	6.35	-2.7	TC0800006447.hg.1
TSN	8.21	6.78	-2.7	TC0200009134.hg.1
KCTD12	8.87	7.44	-2.69	TC1300009288.hg.1

CIPC	6.08	4.65	-2.69	TC1400010634.hg.1
TSPAN18	13.68	12.25	-2.69	TC1100007400.hg.1
GMPR	6.13	4.7	-2.69	TC0600007068.hg.1
SERPINB6	13.03	11.6	-2.69	TC0600010542.hg.1
RAB15	11.57	10.15	-2.68	TC1400009422.hg.1
PIR	12.6	11.18	-2.68	TC0X00011355.hg.1
GABARAPL2	8.59	7.16	-2.68	TC1600008454.hg.1
RGL2	11.4	9.98	-2.68	TC0600011535.hg.1
SERTAD4	7.88	6.46	-2.67	TSUnmapped00000211.hg.1
GNAQ	12.16	10.74	-2.67	TC0900010485.hg.1
MPZL2	11.23	9.82	-2.66	TC1100012474.hg.1
CYBRD1	10.83	9.42	-2.65	TC0200009955.hg.1
BFSP1	7.4	6	-2.64	TC2000008493.hg.1
MARK2	8.19	6.79	-2.64	TC1100007913.hg.1
PSMB4	11.35	9.95	-2.63	TC0100009955.hg.1
TMEM135	6.48	5.09	-2.63	TC1100008673.hg.1
LYRM1	9.4	8.01	-2.63	TC1600007143.hg.1
SORBS3	6.62	5.22	-2.63	TC0800012279.hg.1
C1orf131	7.99	6.6	-2.62	TC0100017722.hg.1
RPS15	16.2	14.81	-2.62	TC1900006532.hg.1
NDRG1	8.5	7.11	-2.62	TC0800011881.hg.1
PRKAR1A	10.85	9.46	-2.62	TC1700012297.hg.1
RBM22	10.97	9.58	-2.61	TC0500012485.hg.1
RNF34	9.51	8.13	-2.61	TC1200009164.hg.1
HLA-B	10.22	8.83	-2.61	TC0600014258.hg.1
SHARPIN	8.57	7.18	-2.61	TC0800012190.hg.1
TRNP1	7	5.61	-2.61	TC0100007493.hg.1
NET1	11.38	10	-2.61	TC1000006617.hg.1
BST2	8.02	6.63	-2.61	TC1900009970.hg.1
FAM43A	9.53	8.15	-2.6	TC0300009944.hg.1
SLC9A3R2	13.58	12.2	-2.6	TC1600006585.hg.1
DNM2	9.41	8.04	-2.6	TC1900006994.hg.1
PPA1	8.07	6.69	-2.6	TC1000010914.hg.1
MFAP2	12.13	10.76	-2.59	TC0100013071.hg.1
HDGF	8.71	7.34	-2.59	TC0100016022.hg.1
DNAJB4	13.86	12.49	-2.59	TC0100018238.hg.1
NSMCE1	8.92	7.55	-2.59	TC1600009829.hg.1
GUCY1A3	6.51	5.13	-2.59	TC0400009086.hg.1
BTBD9	5.07	3.69	-2.59	TC0600011723.hg.1
RBBP8; MIR4741	6.88	5.51	-2.58	TC1800009221.hg.1
ORAI1	6.71	5.34	-2.58	TC1200009172.hg.1
HIST1H4C	11.4	10.03	-2.58	TC0600007268.hg.1

HPCAL1	8.79	7.42	-2.58	TC0200006687.hg.1
CCDC93	9.21	7.85	-2.57	TC0200014004.hg.1
ATP5D	8.7	7.34	-2.57	TC1900006520.hg.1
CAMK2D	10.89	9.53	-2.57	TC0400011643.hg.1
EMP2	11.88	10.51	-2.57	TC1600009362.hg.1
ISY1-RAB43	7.78	6.42	-2.57	TC0300014047.hg.1
ZFP36L2	12.35	11	-2.56	TC0200012404.hg.1
HLA-A	11.72	10.37	-2.56	TC0600007495.hg.1
SLC25A27	6.99	5.63	-2.56	TC0600008166.hg.1
PLSCR1	9.97	8.62	-2.55	TC0300012728.hg.1
MAP3K5	7.87	6.52	-2.55	TC0600013280.hg.1
NCOA4	12.22	10.87	-2.55	TC1000010515.hg.1
PSMD4	11.24	9.9	-2.54	TC0100009949.hg.1
SEMA6A	9.04	7.69	-2.54	TC0500011775.hg.1
EBAG9	9.58	8.24	-2.54	TC0800008550.hg.1
GBP4	9.95	8.61	-2.54	TC0100014855.hg.1
ACAT1	8.77	7.44	-2.53	TC1100008983.hg.1
PRKCH	13.63	12.29	-2.53	TC1400010617.hg.1
CFI	11.56	10.22	-2.53	TC0400011580.hg.1
HEXA	11.27	9.94	-2.52	TC1500010890.hg.1
HIST1H2BI	5.4	4.07	-2.52	TC0600007293.hg.1
APIAR	9.03	7.7	-2.52	TC0400008427.hg.1
CEP70	7.55	6.23	-2.51	TC0300012572.hg.1
GLMP	11.58	10.26	-2.51	TC0100018510.hg.1
TRIM34	6.76	5.43	-2.51	TC1100012955.hg.1
HIST2H2AAA4; HIST2H2AA3	9.14	7.82	-2.5	TC0100018482.hg.1
DDR2	10.43	9.11	-2.5	TC0100010387.hg.1
DIRAS3	6.58	5.26	-2.5	TC0100014528.hg.1
PROS1	9.21	7.89	-2.49	TC0300011757.hg.1
MIER1	8.39	7.07	-2.49	TC0100008641.hg.1
LGALSL	6.68	5.38	-2.48	TC0200007803.hg.1
FOXM1	8.46	7.15	-2.48	TC1200009621.hg.1
CPE	15.37	14.06	-2.48	TC0400009223.hg.1
GBP1	8.57	7.26	-2.47	TC0100014852.hg.1
NXT2	8.03	6.72	-2.47	TC0X00008097.hg.1
UBE2H	13.29	11.99	-2.47	TC0700012584.hg.1
MED15	13.51	12.21	-2.47	TC2200009194.hg.1
MKNK2	9.35	8.05	-2.46	TC1900009201.hg.1
FOXP1	13.29	11.99	-2.46	TC0300011485.hg.1
CLDN12	7.58	6.28	-2.46	TC0700013396.hg.1
GTF2A1L; STON1- GTF2A1L; STON1	6.76	5.46	-2.45	TC0200007536.hg.1

TIMP1	14.01	12.72	-2.45	TC0X00007149.hg.1
LIFR	8.71	7.42	-2.45	TC0500010540.hg.1
SC5D	7.45	6.16	-2.44	TC1100009306.hg.1
COBL1	10.04	8.76	-2.44	TC0200014792.hg.1
TMEM127	12.7	11.41	-2.44	TC0200013516.hg.1
ZNF160	8.1	6.81	-2.44	TC1900011327.hg.1
RAMP2	9.11	7.83	-2.43	TC1700007913.hg.1
LIMCH1	7.76	6.48	-2.43	TC0400007345.hg.1
FNDC3A	9.59	8.31	-2.43	TC1300007152.hg.1
PSMB5	9.72	8.44	-2.43	TC1400008689.hg.1
THRA	10.37	9.09	-2.43	TC1700007777.hg.1
MSRB3	10.88	9.6	-2.43	TC1200008028.hg.1
ETS2	12.27	10.99	-2.43	TC2100007140.hg.1
SNAPC2	7.76	6.48	-2.42	TC1900006866.hg.1
PNPLA2	7.03	5.76	-2.42	TC1100006492.hg.1
SPRY4	6.82	5.55	-2.42	TC0500012312.hg.1
GTPBP8	9.8	8.53	-2.42	TC0300008352.hg.1
EDEM1	9.68	8.4	-2.42	TC0300006491.hg.1
C1orf115	8.02	6.75	-2.41	TC0100011663.hg.1
KXD1	13.13	11.86	-2.41	TC1900007396.hg.1
GOLGA8N	8.06	6.79	-2.41	TC1500010712.hg.1
ADGRG6	10.64	9.37	-2.4	TC0600009669.hg.1
IGFBP4	12.42	11.17	-2.39	TC1700007796.hg.1
ADRBK1	7.84	6.59	-2.39	TC1100008123.hg.1
TPCN1	8.27	7.01	-2.39	TC1200008933.hg.1
PLTP	11.13	9.87	-2.39	TC2000009250.hg.1
ST6GAL1	12.02	10.77	-2.39	TC0300009789.hg.1
KRAS	10.25	9	-2.39	TC1200010158.hg.1
CARHSP1	6.67	5.41	-2.39	TC1600009322.hg.1
EXOC6	9.93	8.68	-2.38	TC1000008475.hg.1
LRRC8C	11.7	10.45	-2.38	TC0100018246.hg.1
CSNK1G3	9.02	7.77	-2.38	TC0500008494.hg.1
WBSCR22	9.8	8.55	-2.38	TC0700007986.hg.1
NME6	7.07	5.82	-2.38	TC0300011016.hg.1
FBN1	12.04	10.79	-2.37	TC1500009348.hg.1
LAPTM4B	10	8.75	-2.37	TC0800008321.hg.1
RNF130	11.95	10.71	-2.37	TC0500013429.hg.1
KRTCAP2	12.38	11.14	-2.37	TC0100018498.hg.1
TRIM47	7.08	5.84	-2.37	TC1700011774.hg.1
PUF60	8.87	7.63	-2.37	TC0800012167.hg.1
DGCR2; DGCR11	8.95	7.7	-2.37	TC2200007963.hg.1
TPRG1L	12.05	10.8	-2.37	TC0100006619.hg.1

COPS4	8.38	7.15	-2.36	TC0400007991.hg.1
ITGA6	13.03	11.79	-2.36	TC0200009973.hg.1
CNKSR3	6.67	5.43	-2.36	TC0600014361.hg.1
MAPK1IP1L	11.99	10.75	-2.36	TC1400007222.hg.1
ERAL1	8.61	7.38	-2.36	TC1700007399.hg.1
ECI2	10.62	9.38	-2.36	TC0600010647.hg.1
ZC3H14	11.2	9.96	-2.36	TC1400007906.hg.1
MRS2	6.91	5.67	-2.36	TC0600007196.hg.1
FTL	16.39	15.15	-2.36	TC1900008507.hg.1
UBE2J1	12.64	11.4	-2.36	TC0600012542.hg.1
HMGCL	8.14	6.9	-2.36	TC0100013303.hg.1
TLR3	7.73	6.5	-2.35	TC0400009543.hg.1
CLK4	9.52	8.29	-2.35	TC0500013020.hg.1
PIAS2	9.57	8.33	-2.35	TC1800009277.hg.1
SYNPO	13.87	12.64	-2.35	TC0500009097.hg.1
ETNK2	5.63	4.39	-2.35	TC0100017018.hg.1
H3F3A; H3F3AP4	13.42	12.19	-2.34	TC0100011777.hg.1
COA3	9.08	7.86	-2.34	TC1700010747.hg.1
HSPB8	7.92	6.69	-2.34	TC1200012714.hg.1
DNTTIP1	8.45	7.22	-2.34	TC2000007502.hg.1
ACOT8	7.16	5.94	-2.34	TC2000009245.hg.1
GNAI2	14.97	13.75	-2.33	TC0300007410.hg.1
SLC25A11	10.93	9.71	-2.33	TC1700009538.hg.1
TCEAL4	9.6	8.39	-2.32	TC0X00008009.hg.1
CACUL1	11.21	10	-2.32	TC1000011975.hg.1
NDUFA2	8.36	7.15	-2.31	TC0500012248.hg.1
CYB5RL	6.97	5.75	-2.31	TC0100018442.hg.1
BLMH	10.64	9.43	-2.31	TC1700010274.hg.1
STAT3	11.5	10.29	-2.31	TC1700010721.hg.1
SLAIN2	11.06	9.85	-2.3	TC0400007447.hg.1
RPLP1	14.41	13.21	-2.3	TC1500007700.hg.1
PRPF6	8.58	7.38	-2.3	TC2000008104.hg.1
PPIC	11.05	9.85	-2.3	TC0500011875.hg.1
NUDT9	8.49	7.29	-2.3	TC0400008074.hg.1
RPRD1B	8.35	7.14	-2.3	TC2000007300.hg.1
TEK	13.91	12.72	-2.29	TC0900006886.hg.1
TANC1	11.75	10.56	-2.29	TC0200009774.hg.1
AIMP2	7.2	6.01	-2.29	TC0700006634.hg.1
L3MBTL4	4.56	3.36	-2.29	TC1800006556.hg.1
ABLIM1	13.82	12.62	-2.29	TC1000011904.hg.1
ARRB1	13.54	12.35	-2.28	TC1100011643.hg.1
TPP2	10.6	9.41	-2.28	TC1300007884.hg.1

XAB2	5.73	4.55	-2.28	TC1900009487.hg.1
ARRDC4	7.75	6.57	-2.27	TC1500008470.hg.1
AAED1	8.24	7.05	-2.27	TC0900010920.hg.1
DNM3	5.52	4.34	-2.27	TC0100010609.hg.1
SLX4IP	7.55	6.37	-2.27	TC2000006694.hg.1
HIPK3	9.5	8.31	-2.27	TC1100007227.hg.1
CRBN	9.96	8.77	-2.27	TC0300010123.hg.1
RBX1	9.44	8.26	-2.27	TC2200009278.hg.1
NT5E	15.45	14.27	-2.26	TC0600008697.hg.1
FLI1	13.42	12.24	-2.26	TC1100009485.hg.1
GSN	12.38	11.21	-2.26	TC0900012167.hg.1
FBL	10.21	9.03	-2.26	TSUnmapped00000776.hg.1
HN1	12.17	10.99	-2.26	TC1700012468.hg.1
INTS1	7.08	5.91	-2.26	TC0700010015.hg.1
ARL14EP	9.18	8	-2.26	TC1100007168.hg.1
IL1R1	8.64	7.47	-2.25	TC0200008666.hg.1
CLU; MIR6843	15.25	14.07	-2.25	TC0800009961.hg.1
C2CD2	8.69	7.51	-2.25	TC2100008229.hg.1
NDUFAF3	13.5	12.33	-2.25	TC0300007359.hg.1
ZNF532	10.32	9.15	-2.25	TC1800007440.hg.1
ARFGAP3	9.94	8.77	-2.24	TC2200009356.hg.1
SFR1	9.3	8.13	-2.24	TC1000008798.hg.1
HIST1H2BG	8.61	7.44	-2.24	TC0600011136.hg.1
RTF1	11.38	10.22	-2.24	TC1500007004.hg.1
SLC27A3	5.98	4.82	-2.24	TC0100018299.hg.1
PTGIS	8.42	7.27	-2.23	TC2000009388.hg.1
DHRS13	7.69	6.53	-2.23	TC1700010221.hg.1
OAZ1	14.64	13.48	-2.23	TC1900011641.hg.1
BAG4	8.04	6.88	-2.23	TC0800007328.hg.1
LRRC28	9.05	7.89	-2.23	TC1500008511.hg.1
INPP5K	9.13	7.98	-2.22	TC1700009377.hg.1
FUNDC2	9.94	8.79	-2.22	TC0X00008862.hg.1
APOA1BP	11.35	10.2	-2.22	TC0100010185.hg.1
ZYG11B	9.71	8.56	-2.22	TC0100008332.hg.1
NFRKB	7.86	6.71	-2.22	TC1100012811.hg.1
SLC25A6	15.72	14.57	-2.22	TC0X00008908.hg.1
PSMF1	13.38	12.23	-2.22	TC2000009874.hg.1
ABCA8	10.9	9.75	-2.21	TC1700011574.hg.1
NSUN4	9.18	8.04	-2.21	TC0100008156.hg.1
GPR137B	9.14	8	-2.21	TC0100012089.hg.1
MAP2K5	7.19	6.05	-2.21	TC1500007645.hg.1
ELMO1	11.38	10.24	-2.21	TC0700010760.hg.1

SASS6	7.29	6.15	-2.21	TC0100015058.hg.1
PEF1	5.82	4.68	-2.21	TC0100013574.hg.1
RPL11	15	13.86	-2.2	TC0100007326.hg.1
S100A16	13.49	12.35	-2.2	TC0100015871.hg.1
MRPL32	9.24	8.11	-2.19	TC0700007334.hg.1
SAMD12	6.67	5.54	-2.19	TC0800011601.hg.1
FILIP1L	12.41	11.28	-2.19	TC0300011834.hg.1
DENND3	9.92	8.79	-2.19	TC0800009094.hg.1
DTX3L	8.03	6.9	-2.19	TC0300008558.hg.1
CISD2	7.11	5.98	-2.19	TC0400008287.hg.1
SMARCB1	9.87	8.74	-2.18	TC2200006862.hg.1
FAM78A	4.52	3.39	-2.18	TC0900011769.hg.1
SHE	10.34	9.22	-2.18	TC0100018495.hg.1
SET	14.17	13.05	-2.18	TC0900008879.hg.1
FOXO3	8.51	7.39	-2.18	TC0600009059.hg.1
DDX23	11.1	9.98	-2.18	TC1200010597.hg.1
NDUFB5	11.79	10.67	-2.18	TC0300009610.hg.1
BIVM	8.6	7.48	-2.17	TC1300009993.hg.1
IFITM1	14.84	13.73	-2.17	TC1100012949.hg.1
PCGF5	8.33	7.21	-2.17	TC1000008431.hg.1
PLD2	8.71	7.59	-2.17	TC1700006645.hg.1
TMEM14C	10.71	9.59	-2.17	TC0600014068.hg.1
WWTR1	12.34	11.23	-2.17	TC0300012781.hg.1
FGFR1	8.31	7.19	-2.17	TC0800010163.hg.1
ACKR3	14.78	13.66	-2.16	TC0200011219.hg.1
FAM120AOS	10.2	9.09	-2.16	TC0900010837.hg.1
ADAMTS18	13.11	12	-2.16	TC1600010914.hg.1
SYF2	9.53	8.42	-2.16	TC0100013348.hg.1
RCHY1	7.46	6.35	-2.16	TC0400011040.hg.1
BZW2	9.29	8.19	-2.15	TC0700006781.hg.1
FAM195B	7.56	6.45	-2.15	TC1700012070.hg.1
TAPBPL	8.04	6.94	-2.15	TC1200012584.hg.1
DYNLL1	13.16	12.05	-2.15	TC1200009131.hg.1
SLC7A7	6.79	5.69	-2.15	TC1400008677.hg.1
PHC2; MIR3605	7.09	5.99	-2.15	TC0100013651.hg.1
EIF2AK1	9.32	8.22	-2.15	TC0700010185.hg.1
PILRB; STAG3L5P; PVRIG2P; MIR6840; STAG3L5P- PVRIG2P- PILRB	10.2	9.09	-2.15	TC0700013428.hg.1
MIF4GD	7.57	6.47	-2.15	TC1700011744.hg.1
MUT	7.85	6.74	-2.15	TC0600011996.hg.1

HAUS1	7.3	6.2	-2.15	TC1800007215.hg.1
OCRL	5.97	4.87	-2.15	TC0X00008383.hg.1
KLHL9	6.86	5.76	-2.15	TC0900012218.hg.1
GMPR2	9.97	8.87	-2.15	TC1400006732.hg.1
SESN3	4.77	3.68	-2.14	TC1100012020.hg.1
TGM2	16.75	15.66	-2.14	TC2000009058.hg.1
FAM69B	12.62	11.53	-2.14	TC0900009231.hg.1
COPS3	11.3	10.2	-2.14	TC1700009928.hg.1
PHACTR2	12.22	11.12	-2.14	TC0600014188.hg.1
RABGEF1	7.94	6.85	-2.14	TC0700013383.hg.1
NNT	10.11	9.01	-2.14	TC0500007303.hg.1
FAM103A1	8.01	6.92	-2.13	TC0600013898.hg.1
ANKRD46	8.64	7.55	-2.13	TC0800011259.hg.1
CHCHD2	11.52	10.43	-2.13	TC0700011166.hg.1
DLL1	7.79	6.7	-2.13	TC0600014031.hg.1
TBC1D1	8.47	7.38	-2.13	TC0400007245.hg.1
SUMO2	14.61	13.53	-2.12	TC1700012469.hg.1
OXA1L	13.57	12.48	-2.12	TC1400006656.hg.1
KEAP1	8.49	7.41	-2.12	TC1900009630.hg.1
NCOA7	10.6	9.52	-2.12	TC0600009364.hg.1
SHB	9.47	8.39	-2.12	TC0900012231.hg.1
POLR2L	10.16	9.08	-2.12	TC1100009707.hg.1
IVD	7.78	6.7	-2.12	TC1500010720.hg.1
LRIG3	10.87	9.78	-2.12	TC1200011002.hg.1
LRP5	10.32	9.23	-2.12	TC1100008181.hg.1
HIST1H2BJ	5.88	4.79	-2.12	TC0600011184.hg.1
SLC25A29	7.34	6.27	-2.11	TC1400010791.hg.1
ULK1	7.84	6.76	-2.11	TC1200009457.hg.1
DEXI	9.15	8.07	-2.11	TC1600009381.hg.1
SERPINB1	8.32	7.25	-2.11	TC0600014217.hg.1
HOXA10; HOXA9; MIR196B	9.9	8.83	-2.11	TC0700010564.hg.1
NQO1	12.99	11.91	-2.11	TC1600010732.hg.1
SPG21	9.86	8.79	-2.11	TC1500009772.hg.1
VEZF1	10.93	9.86	-2.11	TC1700011237.hg.1
ARRDC2	7.5	6.42	-2.11	TC1900007358.hg.1
KCNN3	7.54	6.46	-2.11	TC0100015925.hg.1
TGFB1I1	12.56	11.49	-2.1	TC1600007537.hg.1
HIST1H2BK	12.15	11.08	-2.1	TC0600011185.hg.1
PNRC1	14.37	13.29	-2.1	TC0600008757.hg.1
RHOBTB2	6.84	5.77	-2.1	TC0800007004.hg.1
DPP7	9.05	7.98	-2.1	TC0900012033.hg.1
ADD1	13.89	12.82	-2.09	TC0400006579.hg.1

CDK2AP1	12.21	11.14	-2.09	TC1200012265.hg.1
API5	8.68	7.62	-2.09	TC1100007363.hg.1
GNAI3	11.92	10.85	-2.09	TC0100018257.hg.1
NDUFV1	10.23	9.17	-2.09	TC1100008147.hg.1
TUBA4A	10.25	9.19	-2.09	TC0200015771.hg.1
TAF9B	9.79	8.73	-2.09	TC0X00010136.hg.1
FAM20B	8.12	7.07	-2.08	TC0100010761.hg.1
POLR2J4	6.92	5.86	-2.08	TC0700010899.hg.1
KANSL1L	7.13	6.07	-2.08	TC0200015601.hg.1
SRR	10.26	9.2	-2.08	TC1700006546.hg.1
PCIF1	8.31	7.26	-2.07	TC2000007512.hg.1
RPL13; SNORD68	13.59	12.54	-2.07	TC1600008888.hg.1
TMCC3; MIR7844	8.89	7.85	-2.07	TC1200011567.hg.1
PSMB6	10.82	9.77	-2.07	TC1700006644.hg.1
AGFG2	8.65	7.6	-2.07	TC0700008552.hg.1
ZCCHC2	9.73	8.68	-2.07	TC1800007518.hg.1
CCDC25	10.95	9.9	-2.06	TC0800009968.hg.1
CLN6	8.63	7.58	-2.06	TC1500010887.hg.1
SCAF11	8.17	7.13	-2.06	TC1200007430.hg.1
VPS28	10.54	9.5	-2.06	TC0800012213.hg.1
SAP130	10.09	9.05	-2.06	TC0200014192.hg.1
ESYT2	10.6	9.56	-2.06	TC0700013291.hg.1
CADPS2	9.3	8.26	-2.06	TC0700012444.hg.1
PPP1R21	7.73	6.69	-2.06	TC0200007535.hg.1
MRPS17	8.79	7.74	-2.06	TC0700013362.hg.1
MAGED4; MAGED4B; SNORA11D; SNORA11E	8.52	7.48	-2.05	TC0X00009707.hg.1
OXCT1	9.21	8.18	-2.05	TC0500010599.hg.1
DNAJB5	8.02	6.98	-2.05	TC0900007064.hg.1
AIM1	8.06	7.02	-2.05	TC0600008981.hg.1
FUCA1	7.84	6.81	-2.04	TC0100013305.hg.1
WRAP73	6.75	5.72	-2.04	TC0100012593.hg.1
KCTD10	10.42	9.39	-2.04	TC1200011870.hg.1
ZC3H12A; MIR6732	6.62	5.59	-2.04	TC0100007832.hg.1
ZNF805	6.28	5.25	-2.04	TC1900008988.hg.1
UBE2A	10.79	9.76	-2.04	TC0X00008253.hg.1
USP11	9.97	8.94	-2.04	TC0X00007134.hg.1
GOLPH3	8.67	7.65	-2.03	TC0500010418.hg.1
THOC7	10.42	9.4	-2.03	TC0300011378.hg.1
RNF4	11.57	10.55	-2.03	TC0400012757.hg.1
BTBD7	10.18	9.15	-2.03	TC1400010022.hg.1
RBL2	10.32	9.3	-2.03	TC1600007887.hg.1

PALM	7.98	6.96	-2.03	TC1900006480.hg.1
IRF2BP2	8.58	7.56	-2.03	TC0100017793.hg.1
ATP6V0B	10.32	9.3	-2.02	TC0100008081.hg.1
CTR9	10.43	9.42	-2.02	TC1100006840.hg.1
HADHA	12.61	11.59	-2.02	TC0200012030.hg.1
ZNF22	7.95	6.93	-2.02	TC1000007462.hg.1
CDC37; MIR1181	12.99	11.97	-2.02	TC1900009628.hg.1
COLEC12	11.23	10.22	-2.02	TC1800007850.hg.1
SLC2A3	11.59	10.58	-2.01	TC1200009800.hg.1
CLEC14A	14.72	13.71	-2.01	TC1400008994.hg.1
GLUL	12.4	11.39	-2.01	TC0100016625.hg.1
SRSF8	9.05	8.05	-2.01	TC1100008827.hg.1
NRSN2	8.55	7.54	-2.01	TC2000006442.hg.1
MAGED4B; MAGED4; SNORA11D	8.66	7.66	-2.01	TC0X00007274.hg.1
CYP20A1	6.97	5.96	-2.01	TC0200010516.hg.1
PDAP1	8.09	7.09	-2.01	TC0700011938.hg.1
SNX24	8.75	7.74	-2.01	TC0500008483.hg.1
RICTOR	9.5	8.5	-2	TC0500010549.hg.1
PLIN2	10.3	9.3	-2	TC0900012212.hg.1
TCEAL1	10.01	9.01	-2	TC0X00011317.hg.1
B9D1	6.82	5.82	-2	TC1700010015.hg.1
AP4S1	6.47	5.47	-2	TC1400006833.hg.1
B4GALT6	7.77	6.77	-2	TC1800008399.hg.1
OXNAD1	8.14	7.14	-2	TC0300013795.hg.1
VPS29	11.29	10.29	-2	TC1200011909.hg.1
KIF1C	11.04	10.04	-2	TC1700006660.hg.1
BST1	7.97	6.97	-2	TC0400012769.hg.1
SLC25A3; SNORA53	13.74	12.75	-1.99	TC1200008573.hg.1
DMAPI	6.73	5.74	-1.99	TC0100008090.hg.1
MRPS18A	9.51	8.52	-1.99	TC0600011884.hg.1
SLAIN1	7.42	6.43	-1.99	TC1300007565.hg.1
PHC3	11.94	10.95	-1.99	TC0300013090.hg.1
MGEA5	8.09	7.1	-1.99	TC1000011659.hg.1
ZNF35	7.82	6.83	-1.99	TSUnmapped00000461.hg.1
BNIP3L	14.64	13.64	-1.99	TC0800007080.hg.1
PRKAA1	13.49	12.5	-1.98	TC0500010580.hg.1
ADCK2	5.49	4.51	-1.98	TC0700013467.hg.1
AP2A2	12.89	11.91	-1.98	TC1100006500.hg.1
NEK9	10.87	9.89	-1.98	TC1400009711.hg.1
PPP2R5C	11.95	10.97	-1.98	TC1400008333.hg.1
DOCK9	11.59	10.6	-1.98	TC1300009583.hg.1

SNX12	8.83	7.85	-1.98	TC0X00009977.hg.1
ADAM15	12.62	11.63	-1.98	TC0100018300.hg.1
C16orf72	5.78	4.79	-1.98	TC1600009331.hg.1
CHMP2A	11.13	10.15	-1.98	TC1900011635.hg.1
ADRM1	8.94	7.96	-1.98	TC2000008001.hg.1
VCAM1	7.07	6.08	-1.98	TC0100009221.hg.1
GBP3	10.71	9.72	-1.97	TC0100014849.hg.1
HINT1	11.61	10.63	-1.97	TC0500011984.hg.1
SAP30L	7.44	6.46	-1.97	TC0500009161.hg.1
PEL12	8.02	7.05	-1.97	TC1400007259.hg.1
RTKN	7.89	6.92	-1.97	TC0200013103.hg.1
WBP1	13.26	12.28	-1.97	TC0200016476.hg.1
UXT	10.22	9.25	-1.97	TC0X00009582.hg.1
LYRM2	8.92	7.95	-1.96	TC0600012550.hg.1
TMEM230	13.43	12.46	-1.96	TC2000009975.hg.1
ADIRF; AGAP11; BMS1P3	7.19	6.22	-1.96	TC1000012471.hg.1
GLTSCR2; SNORD23	7.56	6.59	-1.96	TC1900008433.hg.1
ATXN2	12.38	11.41	-1.96	TC1200011936.hg.1
PPIL4	8.46	7.49	-1.96	TC0600013523.hg.1
SUMF2	11.27	10.3	-1.96	TC0700007633.hg.1
AHCY	7.67	6.7	-1.96	TC2000008915.hg.1
MCM6	6.64	5.67	-1.96	TC0200014404.hg.1
EPS15	10.94	9.97	-1.96	TC0100014175.hg.1
TRIM2	7.41	6.44	-1.96	TC0400009033.hg.1
CD58	8.81	7.84	-1.96	TC0100015397.hg.1
CRNKL1	8.48	7.51	-1.95	TC2000008573.hg.1
DYNC1LI2	13.44	12.47	-1.95	TC1600010596.hg.1
NDUFB8	10	9.04	-1.95	TC1000012587.hg.1
DCUN1D3	9.29	8.33	-1.95	TC1600011500.hg.1
AK9	6.97	6	-1.95	TC0600012817.hg.1
ADAM17	10.92	9.96	-1.95	TC0200011688.hg.1
PPP2R5A	10.44	9.47	-1.95	TC0100011520.hg.1
SLC25A6	15.78	14.81	-1.95	TC0Y00006882.hg.1
NOVA1	8.65	7.69	-1.95	TC1400008780.hg.1
PLA1A	7.05	6.09	-1.94	TC0300008484.hg.1
SOX18	6.35	5.39	-1.94	TC2000010035.hg.1
TAS2R13	4.72	3.76	-1.94	TC1200009921.hg.1
RFTN2	8.15	7.2	-1.94	TC0200015350.hg.1
ST13	11.61	10.66	-1.94	TC2200008799.hg.1
RAB33B	9.54	8.58	-1.94	TC0400008803.hg.1
ZBTB7A	8.93	7.97	-1.94	TC1900009320.hg.1
LDOC1	11.42	10.47	-1.93	TC0X00010989.hg.1

PSMB8	9.27	8.31	-1.93	TC0600011507.hg.1
FAM167B	7.7	6.76	-1.93	TC0100007675.hg.1
PHLPP1	9.27	8.33	-1.93	TC1800007523.hg.1
YIPF3	13.07	12.12	-1.93	TC0600011876.hg.1
AASS	9.25	8.3	-1.93	TC0700012439.hg.1
RNF38	13.01	12.07	-1.93	TC0900012225.hg.1
AASDHPPT	9.32	8.37	-1.93	TC1100008955.hg.1
AMMECR1L	9.03	8.08	-1.92	TC0200014190.hg.1
RAB3GAP1	8.86	7.92	-1.92	TC0200009431.hg.1
SYNE3	6.43	5.49	-1.92	TC1400010784.hg.1
RPP40	8.26	7.31	-1.92	TC0600010681.hg.1
ZNF219	7.59	6.64	-1.92	TC1400008619.hg.1
VGLL4	8.96	8.02	-1.92	TC0300013938.hg.1
GUK1	12.64	11.7	-1.92	TC0100011855.hg.1
LRCH2	6.7	5.76	-1.92	TC0X00010559.hg.1
INPP5D	8.59	7.66	-1.91	TSUnmapped00000661.hg.1
PRMT2	11.1	10.17	-1.91	TC2100007474.hg.1
PLAG1	7.56	6.63	-1.91	TC0800010506.hg.1
NHEJ1	7.28	6.35	-1.91	TC0200016772.hg.1
RHNO1	10.01	9.07	-1.91	TC1200012573.hg.1
SCAP	10.11	9.18	-1.91	TC0300010982.hg.1
MRPL19	6.68	5.75	-1.91	TC0200008128.hg.1
RPL36AL	13.2	12.27	-1.91	TC1400009104.hg.1
MAPK1	11.76	10.83	-1.91	TC2200008105.hg.1
MAX	10.46	9.53	-1.91	TC1400009426.hg.1
PDK2	11.29	10.36	-1.91	TC1700008232.hg.1
RNFT1	7.21	6.29	-1.9	TC1700012440.hg.1
ELK3	12.89	11.97	-1.9	TC1200008535.hg.1
CLIC2	8.33	7.41	-1.9	TC0X00011238.hg.1
EIF2S3	12.99	12.07	-1.9	TC0X00006803.hg.1
MAN1C1	5.69	4.77	-1.9	TC0100007412.hg.1
SCRN1	10.7	9.78	-1.89	TC0700010619.hg.1
GSTK1	11.02	10.1	-1.89	TC0700009485.hg.1
OCLN	9.51	8.59	-1.89	TC0500007681.hg.1
FDX1L	8.3	7.38	-1.89	TC1900011863.hg.1
TRIM5	9.48	8.56	-1.89	TC1100009940.hg.1
MANSC1	12.32	11.4	-1.89	TSUnmapped00000243.hg.1
RFK	11.14	10.22	-1.89	TC0900010462.hg.1
ZNF2	5.78	4.87	-1.89	TC0200008458.hg.1
TMEM128	9.53	8.61	-1.89	TC0400009855.hg.1
AJUBA	8.34	7.42	-1.89	TC1400010715.hg.1
IL6	8.79	7.87	-1.89	TC0700006890.hg.1
POLR3GL	7.82	6.9	-1.89	TC0100018282.hg.1

MDK	10.88	9.96	-1.89	TC1100007453.hg.1
CRAT	8.79	7.87	-1.89	TC0900011673.hg.1
KPNB1	13	12.08	-1.89	TC1700008133.hg.1
UQCRB	12.18	11.27	-1.89	TC0800011171.hg.1
CYP1A1	9.14	8.22	-1.89	TC1500010042.hg.1
ELK4	15.09	14.18	-1.88	TC0100017072.hg.1
HSPB1	17.97	17.06	-1.88	TC0700008090.hg.1
CHAMP1	9.34	8.43	-1.88	TC1300008181.hg.1
COMMD9	6.7	5.79	-1.88	TC1100010546.hg.1
IFIT2	7.68	6.77	-1.88	TC1000008396.hg.1
ARHGAP26	8.98	8.07	-1.88	TC0500008941.hg.1
TAGLN2	13.11	12.2	-1.88	TC0100016112.hg.1
FAM58A	6.89	5.97	-1.88	TC0X00011163.hg.1
CYB5B	12.19	11.28	-1.88	TC1600008228.hg.1
PTRF	13.02	12.11	-1.88	TC1700010723.hg.1
WNK1	10.93	10.02	-1.88	TC1200006450.hg.1
KLHL15	7.57	6.67	-1.87	TC0X00009256.hg.1
CSF2RB	11.6	10.7	-1.87	TC2200007273.hg.1
MRPL18	8.01	7.11	-1.87	TC0600010060.hg.1
EHD4	12.4	11.5	-1.87	TC1500009173.hg.1
MTMR11	7.38	6.47	-1.87	TC0100015716.hg.1
SELP	7.78	6.88	-1.87	TC0100016357.hg.1
DUSP3	9.16	8.26	-1.87	TC1700010798.hg.1
GYG1	10.63	9.73	-1.87	TC0300009126.hg.1
PEX12	7.09	6.19	-1.87	TC1700010436.hg.1
ITGA3	11.59	10.69	-1.86	TC1700008228.hg.1
FBXO21	8.86	7.97	-1.86	TC1200012083.hg.1
SPRYD3	7	6.1	-1.86	TC1200010788.hg.1
COMMD4	8.86	7.97	-1.86	TC1500007883.hg.1
INPP5A	9.55	8.66	-1.86	TC1000009414.hg.1
ACTR1A	12.82	11.93	-1.86	TC1000011683.hg.1
NNMT	6.06	5.16	-1.85	TC1100009110.hg.1
GNB4	11.75	10.86	-1.85	TC0300013264.hg.1
RPA3	6.36	5.48	-1.85	TC0700010247.hg.1
GPI	11.29	10.4	-1.85	TC1900011707.hg.1
LGALS8	10.67	9.78	-1.85	TC0100012097.hg.1
PPP3CA	12.42	11.53	-1.85	TC0400011440.hg.1
HIST1H3I	10.18	9.29	-1.85	TC0600011233.hg.1
mar-02	9.63	8.75	-1.84	TC1900006895.hg.1
ATP5C1	13.25	12.37	-1.84	TC1000006703.hg.1
PLEKHJ1; MIR6789	7.7	6.82	-1.84	TC1900009217.hg.1
SYNJ2BP- COX16;	8.36	7.48	-1.84	TC1400009576.hg.1

COX16; SYNJ2BP				
NAF1	8.8	7.92	-1.84	TC0400012987.hg.1
EDEM3	9.3	8.42	-1.84	TC0100016676.hg.1
MRPL9	11.09	10.22	-1.84	TC0100015810.hg.1
MTSS1	10.68	9.79	-1.84	TC0800011713.hg.1
DNAJB12	9.65	8.78	-1.83	TC1000010990.hg.1
LPCAT3	9.16	8.29	-1.83	TC1200009768.hg.1
PUS3	7.76	6.89	-1.83	TC1100012717.hg.1
CORO1B	9.78	8.9	-1.83	TC1100013194.hg.1
UBE3D	6.72	5.85	-1.83	TC0600012428.hg.1
ABLIM3	9.42	8.55	-1.83	TC0500009055.hg.1
FAM127B	10.22	9.35	-1.83	TC0X00011399.hg.1
MARK1	6.04	5.18	-1.82	TC0100011661.hg.1
C21orf33	8.4	7.54	-1.82	TC2100008537.hg.1
ZNF404	5.36	4.5	-1.82	TC1900011972.hg.1
STRN4	8.69	7.83	-1.82	TC1900011001.hg.1
HIST1H2AB	6.89	6.03	-1.82	TC0600011125.hg.1
ADORA2A	10.45	9.59	-1.82	TC2200009233.hg.1
EXOSC5	5.86	4.99	-1.82	TC1900010746.hg.1
NTHL1	5.14	4.28	-1.82	TC1600009085.hg.1
RAP1GDS1	6.53	5.67	-1.81	TC0400008213.hg.1
PTMS	13.58	12.72	-1.81	TC1200006643.hg.1
SULT1B1	9.03	8.17	-1.81	TC0400010940.hg.1
LSP1P3	7.3	6.44	-1.81	TC0500007016.hg.1
PCBP2; PCBP2-OT1	16.71	15.85	-1.81	TC1200012636.hg.1
NKAIN2	7.87	7.01	-1.81	TC0600009343.hg.1
KLF4	5.8	4.94	-1.81	TC0900011120.hg.1
CFL2	10.52	9.66	-1.81	TC1400008919.hg.1
ASCC1	9.82	8.97	-1.81	TC1000010980.hg.1
ERMP1	9.23	8.38	-1.8	TC0900009470.hg.1
CRAMP1	7.48	6.63	-1.8	TC1600011325.hg.1
PINX1; MIR1322	9.26	8.42	-1.8	TC0800012386.hg.1
IFT52	10.17	9.32	-1.8	TC2000007435.hg.1
GTF2A2	8.1	7.25	-1.8	TC1500009621.hg.1
SEPW1	9.95	9.1	-1.8	TC1900008435.hg.1
C1orf54	9.42	8.57	-1.8	TC0100009899.hg.1
TCTA	9.44	8.59	-1.8	TC0300007380.hg.1
STPG1	9.1	8.25	-1.8	TC0100013323.hg.1
MEF2C	11.84	11	-1.8	TC0500011418.hg.1
SSSCA1	8.22	7.37	-1.8	TC1100013042.hg.1
HECTD2	6.37	5.52	-1.8	TC1000008435.hg.1
TMOD1	7.86	7.01	-1.8	TC0900008150.hg.1

PARP4	10.56	9.71	-1.8	TC1300008359.hg.1
EXOSC2	7.74	6.89	-1.8	TC0900008967.hg.1
TMEM205	8.91	8.07	-1.79	TC1900011867.hg.1
ZNF608	9.58	8.74	-1.79	TC0500011896.hg.1
PIP4K2A	11.43	10.59	-1.79	TC1000010022.hg.1
C19orf70	6.71	5.87	-1.79	TC1900009394.hg.1
BANF1	11.68	10.83	-1.79	TC1100008049.hg.1
MYOF	14.78	13.94	-1.79	TC1000011445.hg.1
COX8A	11.93	11.09	-1.79	TC1100013027.hg.1
FKBP1A; MIR6869	14.55	13.7	-1.79	TC2000009965.hg.1
ZSCAN31	7.6	6.76	-1.79	TC0600011252.hg.1
KAT7	9.23	8.39	-1.79	TC1700008216.hg.1
RPS29; RPL32P29	11.6	10.76	-1.79	TC1400010741.hg.1
CNRIP1	6.87	6.04	-1.78	TC0200012933.hg.1
TMEM129	7.37	6.54	-1.78	TC0400009747.hg.1
HMG20B	9.6	8.77	-1.78	TC1900006645.hg.1
TSHZ1	5.98	5.14	-1.78	TC1800007696.hg.1
EEF2KMT	7.18	6.34	-1.78	TC1600009260.hg.1
CRISPLD1	8.89	8.05	-1.78	TC0800007995.hg.1
RBM5	11.86	11.03	-1.78	TC0300013829.hg.1
GGA2	7.94	7.11	-1.78	TC1600009737.hg.1
MRPL3	9.54	8.71	-1.78	TC0300012445.hg.1
PLEKHA1	11.26	10.43	-1.78	TC1000009149.hg.1
CALHM2	9.97	9.14	-1.78	TC1000011718.hg.1
LRCH1	8.91	8.09	-1.78	TC1300007104.hg.1
PIGW	7.57	6.74	-1.78	TC1700007636.hg.1
CPT1A	11.13	10.3	-1.78	TC1100011395.hg.1
FBXL17	7.29	6.46	-1.78	TC0500011655.hg.1
CTNNB1	14.69	13.86	-1.78	TC0300007136.hg.1
TNFSF12	5.33	4.5	-1.78	TC1700012185.hg.1
GPX3	8.39	7.56	-1.77	TC0500009108.hg.1
SAMHD1	10.38	9.56	-1.77	TC2000009023.hg.1
CCDC159	6.99	6.16	-1.77	TC1900011664.hg.1
WDR47	8.72	7.9	-1.77	TC0100015180.hg.1
METTL18	6.55	5.73	-1.77	TC0100016363.hg.1
UBE2D4	8.65	7.82	-1.77	TC0700007361.hg.1
SPTLC2	13.53	12.71	-1.77	TC1400009787.hg.1
TMED5	11.37	10.54	-1.77	TC0100014947.hg.1
NDUFA10	9.06	8.24	-1.77	TC0200016787.hg.1
ID1	11.26	10.44	-1.77	TC2000007083.hg.1
UBR7	7.86	7.04	-1.77	TC1400010641.hg.1
DDT	9.13	8.31	-1.76	TC2200008203.hg.1

GOLGA7	11.19	10.37	-1.76	TC080007414.hg.1
EPS8	9.56	8.74	-1.76	TC1200010038.hg.1
HDAC7	8.12	7.31	-1.76	TC1200010556.hg.1
ELP5	8.81	8	-1.76	TC1700006733.hg.1
PSME1	10.42	9.6	-1.76	TC1400006718.hg.1
JADE3	8.31	7.5	-1.76	TC0X00007119.hg.1
ANGPTL2	9.26	8.45	-1.76	TC0900011565.hg.1
FGF2	9.55	8.73	-1.76	TC0400008618.hg.1
TYK2	9.6	8.79	-1.76	TC1900009627.hg.1
YBX1	15.86	15.05	-1.76	TC0100008025.hg.1
MECOM	13.97	13.16	-1.76	TC0300013068.hg.1
NOB1	10.41	9.6	-1.75	TC1600010734.hg.1
LAGE3	8.03	7.23	-1.75	TC0X00011204.hg.1
SRI	11.93	11.13	-1.75	TC0700011714.hg.1
ZNF568	7.59	6.78	-1.75	TC1900007957.hg.1
NAPRT	9.2	8.4	-1.75	TC0800012143.hg.1
PARP14	12.98	12.17	-1.75	TC0300008561.hg.1
VPS8	9.49	8.68	-1.75	TC0300009724.hg.1
TRMT1L	7.19	6.39	-1.75	TC0100016685.hg.1
ARHGEF6	8.25	7.44	-1.75	TC0X00010933.hg.1
MCCC1	9.16	8.36	-1.75	TC0300013334.hg.1
CTSF	8.38	7.58	-1.75	TC1100011294.hg.1
TSPYL4	7.05	6.24	-1.75	TC0600012958.hg.1
RPP21	6.18	5.37	-1.75	TC0600014095.hg.1
NDUFAF6	8.18	7.37	-1.75	TC0800012331.hg.1
GIMAP8	11.19	10.39	-1.74	TC0700009675.hg.1
ELP4	7.75	6.95	-1.74	TC1100007185.hg.1
PABPC3	10.16	9.36	-1.74	TC1300006633.hg.1
OTUD6B	8.12	7.32	-1.74	TC0800008197.hg.1
NOV	6.16	5.36	-1.74	TC0800008667.hg.1
PTPN13	6.73	5.93	-1.74	TC0400008041.hg.1
ELOVL4	6.56	5.76	-1.74	TC0600012379.hg.1
SLC48A1	10.06	9.26	-1.74	TC1200012622.hg.1
ACER3	8.48	7.68	-1.74	TC1100008518.hg.1
NDRG4	12.97	12.18	-1.73	TC1600008034.hg.1
GIMAP7	12.07	11.29	-1.73	TC0700009676.hg.1
STARD7	12.85	12.06	-1.73	TC0200013515.hg.1
RNASE1	17.49	16.69	-1.73	TC1400008606.hg.1
TMEM38B	6.24	5.45	-1.73	TC0900008318.hg.1
FLYWCH1	8.31	7.52	-1.73	TC1600006644.hg.1
TESK2	5.75	4.96	-1.73	TC0100014009.hg.1
PCMTD2	10.76	9.97	-1.73	TC2000009956.hg.1
MTMR2	11.61	10.82	-1.73	TC1100012033.hg.1

ARHGEF17	9.16	8.38	-1.72	TC1100008382.hg.1
TOMM22	9.83	9.04	-1.72	TC2200007361.hg.1
EXT2	11.06	10.28	-1.72	TC1100007390.hg.1
NAGLU	8.84	8.06	-1.72	TC1700012259.hg.1
STK24	6.76	5.97	-1.72	TC1300009570.hg.1
CNPY3	10.62	9.84	-1.72	TC0600008059.hg.1
ECH1	15.42	14.65	-1.72	TC1900011940.hg.1
DCP2	8.52	7.74	-1.71	TC0500008342.hg.1
MPC2	7.82	7.04	-1.71	TC0100016318.hg.1
ZC3HAV1L	7.8	7.03	-1.71	TC0700012760.hg.1
PGRMC1	11.94	11.16	-1.71	TC0X00008240.hg.1
CHCHD10	8.42	7.65	-1.71	TC2200008186.hg.1
CHMP2B	8.98	8.21	-1.71	TC0300008002.hg.1
ALDH9A1	9.22	8.45	-1.71	TC0100016260.hg.1
MYO9A	5.15	4.38	-1.71	TC1500007763.hg.1
TNFSF12	5.74	4.97	-1.71	TC1700012185.hg.1
C5orf30	6.98	6.2	-1.71	TC0500008233.hg.1
SMDT1	8.64	7.88	-1.7	TC2200009279.hg.1
PSMD11	11.49	10.73	-1.7	TC1700007519.hg.1
TST	9.06	8.29	-1.7	TC2200008630.hg.1
NDUFB2	8.16	7.39	-1.7	TC0700013468.hg.1
CAV1	16.15	15.38	-1.7	TC0700008873.hg.1
SLC16A4	6.97	6.2	-1.7	TC0100015234.hg.1
SHISA4	6.76	5.99	-1.7	TC0100011197.hg.1
IPO4	5.84	5.07	-1.7	TC1400010722.hg.1
HIST1H4K	5.79	5.03	-1.7	TC0600011227.hg.1
INPP5D	9.45	8.68	-1.7	TSUnmapped00000135.hg.1
ATP6V0D1	13.73	12.96	-1.7	TC1600010633.hg.1
HSD17B4	11.26	10.5	-1.69	TC0500013219.hg.1
MRPL44	9.19	8.44	-1.69	TC0200010927.hg.1
C10orf10	11.68	10.92	-1.69	TC1000010482.hg.1
CYC1	10.61	9.85	-1.69	TC0800009239.hg.1
NME5	5.78	5.02	-1.69	TC0500012160.hg.1
MKL2; TVP23CP2	8.86	8.1	-1.69	TC1600006979.hg.1
PCBD2	7	6.25	-1.69	TC0500013230.hg.1
NUDT21	10.26	9.5	-1.69	TC1600010407.hg.1
JUNB	6.18	5.42	-1.69	TC1900007096.hg.1
C14orf1	12.09	11.34	-1.68	TC1400009732.hg.1
RPS28	16.41	15.66	-1.68	TC1100008612.hg.1
DGCR14	10.95	10.2	-1.68	TC2200007971.hg.1
GCNT1	7.61	6.87	-1.68	TC0900012141.hg.1
GNB2L1; SNORD95; SNORD96A	18.08	17.33	-1.68	TC0500013430.hg.1

CXCL16	6.16	5.42	-1.68	TC1700009528.hg.1
CYP26B1	4.72	3.97	-1.68	TC0200013042.hg.1
YPEL3	11.46	10.71	-1.68	TC1600009952.hg.1
EIF3K	15.05	14.3	-1.68	TC1900008019.hg.1
HSPA4	10.86	10.12	-1.68	TC0500008664.hg.1
SH3GLB2	9.32	8.57	-1.68	TC0900011669.hg.1
KLHL3	7.07	6.32	-1.68	TC0500012145.hg.1
H2AFZ	11.27	10.53	-1.67	TC0400011424.hg.1
BBS2	8.31	7.57	-1.67	TC1600010409.hg.1
H3F3B	12.05	11.31	-1.67	TC1700012470.hg.1
FCF1	7.76	7.03	-1.67	TC1400007688.hg.1
RPL29	12.74	12	-1.67	TC0300011151.hg.1
CLK1	8.22	7.48	-1.67	TC0200015397.hg.1
BLOC1S6	10.96	10.22	-1.67	TC1500010736.hg.1
ADARB1	10.45	9.72	-1.67	TC2100007402.hg.1
GSPT2	6.53	5.79	-1.67	TC0X00007266.hg.1
IGIP	5.9	5.17	-1.67	TC0500008846.hg.1
SRPK1	7.36	6.62	-1.67	TC0600011644.hg.1
VPS35	11.42	10.67	-1.67	TC1600010171.hg.1
STXBP2	6.27	5.53	-1.67	TC1900011656.hg.1
RNF144A	6.81	6.07	-1.66	TC0200006583.hg.1
MAP3K8	7.25	6.52	-1.66	TC1000007176.hg.1
ACAD11	7.06	6.33	-1.66	TC0300014049.hg.1
CLINT1	11.1	10.36	-1.66	TC0500012611.hg.1
ZNF827	7.93	7.2	-1.66	TC0400012048.hg.1
MSH5; MSH5- SAPCD1; SAPCD1	6.48	5.75	-1.66	TC0600007610.hg.1
MINK1	8.58	7.85	-1.66	TC1700006646.hg.1
HNRNPLL	8.5	7.76	-1.66	TC0200012288.hg.1
CWC27	10.36	9.64	-1.66	TC0500007591.hg.1
EIF3D	13.18	12.45	-1.66	TC2200008611.hg.1
DNAJB2	7.48	6.75	-1.66	TC0200010840.hg.1
LIMS2	7.86	7.12	-1.66	TC0200014181.hg.1
B4GALT5	11.69	10.97	-1.65	TC2000009392.hg.1
COPG2; TSGA13	8.31	7.59	-1.65	TC0700012605.hg.1
PDCL	11.18	10.46	-1.65	TC0900011445.hg.1
GPR107	9.93	9.2	-1.65	TC0900008945.hg.1
IKZF5	9.8	9.07	-1.65	TC1000012090.hg.1
GLS	12.47	11.74	-1.65	TC0200010275.hg.1
DYNLRB1	12.45	11.73	-1.65	TC2000007191.hg.1
TRAPPC4	8.15	7.43	-1.65	TSUnmapped00000459.hg.1
FBLN2	5.52	4.8	-1.65	TC0300006658.hg.1

TMEM19	8.13	7.41	-1.65	TC1200012666.hg.1
RRP9	6.13	5.41	-1.65	TC0300011146.hg.1
SMARCD1	11.48	10.76	-1.65	TC1200007595.hg.1
FAM219A	7.43	6.71	-1.65	TC0900009897.hg.1
UBR3	9.28	8.56	-1.65	TC0200009922.hg.1
DES12	10.66	9.95	-1.64	TC0100012222.hg.1
DCAF7	11.55	10.84	-1.64	TC1700008563.hg.1
FOXO1	11.76	11.05	-1.64	TC1300008688.hg.1
RNF5	10.49	9.77	-1.64	TC0600007636.hg.1
CWC22	9.52	8.81	-1.64	TC0200015099.hg.1
ZDHHC14	8.55	7.83	-1.64	TC0600009980.hg.1
BCLAF1	11.84	11.13	-1.64	TC0600013272.hg.1
SSBP2	8.2	7.49	-1.64	TC0500013336.hg.1
ALDH1A1	13.26	12.55	-1.64	TC0900012245.hg.1
HLA-L	11.84	11.12	-1.64	TC0600007518.hg.1
HSD17B12	12.45	11.73	-1.64	TC1100012992.hg.1
BTBD2	10.89	10.18	-1.64	TC1900009198.hg.1
PLEKHF2	7.48	6.77	-1.64	TC0800008279.hg.1
CYB5D1	7.07	6.36	-1.64	TC1700006774.hg.1
TFAM	10.33	9.62	-1.64	TC1000007701.hg.1
TMOD3	12.81	12.1	-1.63	TC1500007240.hg.1
HK1	8.89	8.19	-1.63	TC1000007891.hg.1
KLHDC3	10.37	9.67	-1.63	TC0600008066.hg.1
SEMA6C	9.77	9.07	-1.63	TC0100015771.hg.1
NRROS	5.06	4.36	-1.63	TC0300013920.hg.1
PLEKHH2	7.3	6.59	-1.63	TC0200007399.hg.1
PIK3R3	8.25	7.56	-1.62	TC0100014040.hg.1
TMEM147	10.54	9.84	-1.62	TC1900007864.hg.1
MGAT1	7.88	7.19	-1.62	TC0500013106.hg.1
PCSK5	6.52	5.83	-1.62	TC0900007618.hg.1
VASH1	9.36	8.66	-1.62	TC1400007732.hg.1
COPE	12.42	11.72	-1.62	TC1900011909.hg.1
MEX3D	5.91	5.21	-1.62	TC1900009172.hg.1
BAX	11.81	11.12	-1.62	TC1900008505.hg.1
SMYD3	7.65	6.96	-1.62	TC0100018045.hg.1
ATP6V1E1	10.87	10.18	-1.62	TC2200007904.hg.1
CELF2	11.14	10.44	-1.62	TC1000006754.hg.1
RPL41	11.65	10.95	-1.62	TC2200008578.hg.1
STRIP2	7.91	7.21	-1.62	TC0700009089.hg.1
MYLIP; MIR4639	9.63	8.93	-1.62	TC0600007060.hg.1
ELOF1	8.58	7.9	-1.61	TC1900009682.hg.1
PITPNC1	8.15	7.46	-1.61	TC1700008690.hg.1

TMEM186	5.06	4.37	-1.61	TC1600011478.hg.1
CSDE1	14.72	14.03	-1.61	TC0100015353.hg.1
NARS	10.7	10.02	-1.6	TC1800008779.hg.1
FIS1	8.46	7.78	-1.6	TC0700012044.hg.1
STX7	9.69	9.02	-1.6	TC0600013193.hg.1
DDHD2	9.35	8.68	-1.6	TC0800007330.hg.1
ASXL2	10.09	9.41	-1.6	TC0200016645.hg.1
FBXO9	9.24	8.56	-1.6	TC0600008272.hg.1
DMPK	7.14	6.47	-1.6	TC1900011984.hg.1
PHF20L1	6.82	6.15	-1.59	TC0800008943.hg.1
PATZ1	8.19	7.53	-1.59	TC2200008477.hg.1
MOCS1	6.29	5.62	-1.59	TC0600014287.hg.1
ZNRF3	6.17	5.5	-1.59	TC2200009246.hg.1
LRRCC1	6.01	5.33	-1.59	TC0800008120.hg.1
UQCR10	8.99	8.32	-1.59	TC2200007035.hg.1
DLL4	9.68	9.01	-1.59	TC1500006981.hg.1
SOCS6	7.88	7.22	-1.59	TC1800007620.hg.1
ATP5G2	14.65	13.98	-1.59	TC1200012798.hg.1
ALG2	10.14	9.47	-1.59	TC0900010995.hg.1
ITGA10	8.36	7.7	-1.58	TC0100015594.hg.1
HIST1H3D; HIST1H2AD	7.45	6.79	-1.58	TC0600011135.hg.1
ZNF345	5.99	5.34	-1.58	TC1900007955.hg.1
CCDC102A	7.11	6.45	-1.58	TC1600010453.hg.1
UBE4B	11.66	11	-1.58	TC0100006806.hg.1
CCNI	16.63	15.98	-1.58	TC0400011087.hg.1
GFOD1	8.02	7.36	-1.58	TC0600010853.hg.1
WDR92	7.17	6.5	-1.58	TC0200016681.hg.1
IFIH1	7.83	7.18	-1.57	TC0200014772.hg.1
CRIP2	12.18	11.54	-1.57	TC1400008486.hg.1
PIN1	9.27	8.62	-1.57	TC1900006956.hg.1
APOL2	10.06	9.41	-1.57	TC2200008592.hg.1
RASA4	6.81	6.16	-1.57	TC0700013603.hg.1
BMPER	7.99	7.33	-1.57	TC0700007149.hg.1
ZNF664	8.75	8.1	-1.57	TC1200012723.hg.1
CSRP1	13.54	12.89	-1.57	TC0100016917.hg.1
KIAA1462	8.85	8.19	-1.57	TC1000010192.hg.1
MED22	7.55	6.89	-1.57	TC0900011840.hg.1
SLC25A35	7.62	6.97	-1.57	TC1700009686.hg.1
ATP5B	15.42	14.77	-1.57	TC1200010927.hg.1
SMG7	9.65	9.01	-1.56	TC0100010872.hg.1
SCMH1	8.85	8.2	-1.56	TC0100013854.hg.1
GTF2B	9.36	8.71	-1.56	TC0100014846.hg.1

LITAF	10.92	10.28	-1.56	TC1600011483.hg.1
YAP1	8.79	8.15	-1.56	TC1100008904.hg.1
MIEN1	8.47	7.83	-1.56	TC1700010584.hg.1
HOXA11	6.19	5.56	-1.56	TC0700010565.hg.1
MZT2B	10.69	10.04	-1.56	TC0200009281.hg.1
TESK1; MIR4667	11.67	11.03	-1.56	TC0900007085.hg.1
ENY2	11.4	10.76	-1.56	TC0800008546.hg.1
PSMB7	12.47	11.83	-1.56	TC0900011496.hg.1
TSPAN4	10.49	9.85	-1.56	TC1100006495.hg.1
SLC23A2	7.82	7.19	-1.55	TC2000008268.hg.1
EMP3	14.99	14.36	-1.55	TC1900011774.hg.1
ARL2	11.96	11.33	-1.55	TC1100013037.hg.1
NUCB1	14.05	13.42	-1.55	TC1900008498.hg.1
IRS2	6.88	6.24	-1.55	TC1300009765.hg.1
LAMP3	7.65	7.02	-1.55	TC0300013336.hg.1
ZFP36	6.97	6.35	-1.54	TC1900008057.hg.1
CAPNS1	15.79	15.17	-1.54	TC1900007908.hg.1
HOXA2	6.9	6.28	-1.54	TC0700010558.hg.1
CCDC130	7.3	6.67	-1.54	TC1900011673.hg.1
RNF13	11.9	11.29	-1.53	TC0300009147.hg.1
MAPK9	8.88	8.27	-1.53	TC0500013088.hg.1
FERMT2	11.67	11.06	-1.53	TC1400009194.hg.1
PREB	8.26	7.64	-1.53	TC0200012062.hg.1
PKP4	8.86	8.24	-1.53	TC0200009756.hg.1
NFIX	10.36	9.74	-1.53	TC1900007115.hg.1
NDUFA10	10.29	9.68	-1.53	TSUnmapped00000379.hg.1
FLOT1	9.57	8.95	-1.53	TC0600011381.hg.1
CHP1	14.02	13.41	-1.52	TC1500006994.hg.1
ZNF623	7.56	6.95	-1.52	TC0800009208.hg.1
ARHGEF7	10.42	9.82	-1.52	TC1300008044.hg.1
ZNF704	5.06	4.45	-1.52	TC0800010918.hg.1
SEC14L2	8.04	7.44	-1.52	TC2200009252.hg.1
COPS8	10.87	10.27	-1.51	TC0200011237.hg.1
MICU2	8.14	7.54	-1.51	TC1300008292.hg.1
CD151	13.04	12.44	-1.51	TC1100006494.hg.1
RNF139	10.09	9.49	-1.51	TC0800008770.hg.1
LYNX1	9.59	8.99	-1.51	TC0800012087.hg.1
NOPI4	7.87	7.29	-1.5	TC0400009791.hg.1
PTPRA; VPS16	13.72	13.13	-1.5	TC2000009882.hg.1
UROS	10.1	9.51	-1.5	TC1000012162.hg.1
NECAP1	7.23	6.65	-1.5	TC1200006701.hg.1
ZNF326	9.33	8.74	-1.5	TC0100008996.hg.1

DOLK	7.26	6.67	-1.5	TC0900011665.hg.1
SMPD1	9.79	9.2	-1.5	TC1100006726.hg.1
NMNAT1	7.24	6.66	-1.5	TC0100006801.hg.1
PHYH	8.02	7.44	-1.5	TC1000009841.hg.1
POLR2I	7	6.42	-1.5	TC1900010511.hg.1
WDR45B	10.56	9.98	-1.5	TC1700012141.hg.1
KLF11	8.08	7.5	-1.5	TC0200006674.hg.1
PLRG1	10.85	10.26	-1.5	TC0400012179.hg.1
RRM1	11.65	11.08	-1.49	TC1100006644.hg.1
KIAA0196	11.31	10.73	-1.49	TC0800011731.hg.1
TMEM259	8.85	8.27	-1.49	TC1900009128.hg.1
MRPL55	6.91	6.34	-1.49	TC0100017587.hg.1
ERVK13-1	7.27	6.69	-1.49	TC1600011465.hg.1
DNM1	7.24	6.67	-1.49	TC0900008851.hg.1
SNORA17A; SNORA17B; SNHG7	11.12	10.56	-1.48	TC0900011998.hg.1
HSF2	7.76	7.2	-1.48	TC0600009322.hg.1
MED11	6.75	6.19	-1.48	TC1700006640.hg.1
EIF2B1	10.47	9.91	-1.48	TC1200012281.hg.1
TNFRSF1B; MIR4632; MIR7846	8.51	7.94	-1.48	TC0100006881.hg.1
NPC2; MIR4709	10.64	10.08	-1.48	TC1400009697.hg.1
PHAX	10.89	10.33	-1.48	TC0500008540.hg.1
NRF1	8.13	7.58	-1.47	TC0700009099.hg.1
DUSP5	9.41	8.85	-1.47	TC1000008891.hg.1
BLVRB	8.56	8	-1.47	TC1900010708.hg.1
TMUB1	7.4	6.84	-1.47	TC0700013060.hg.1
KCTD21	8.36	7.8	-1.47	TC1100011742.hg.1
KLHL5	11.31	10.76	-1.47	TC0400007276.hg.1
PRKD1	7.15	6.6	-1.47	TC1400008816.hg.1
ASB9	5.79	5.23	-1.47	TC0X00011353.hg.1
NCKAP1	12.89	12.33	-1.47	TC0200016757.hg.1
JUND	5.56	5	-1.47	TC1900010009.hg.1
MPV17	13.8	13.25	-1.46	TC0200012072.hg.1
SRP68	9.84	9.3	-1.46	TC1700011783.hg.1
TPGS2	13.66	13.11	-1.46	TC1800008482.hg.1
ACTN4	14.22	13.67	-1.46	TC1900008020.hg.1
MEPCE	9.54	8.99	-1.46	TC0700008542.hg.1
ARID5B	8.16	7.62	-1.45	TC1000007761.hg.1
MAD2L2	7.48	6.95	-1.45	TC0100012889.hg.1
LY6G5B; CSNK2B	12.57	12.04	-1.45	TC0600007605.hg.1
CAMK2G	8.41	7.87	-1.45	TC1000011040.hg.1
AGPAT3	6.53	6	-1.45	TC2100007331.hg.1

TCEB2	7.8	7.27	-1.45	TC1600009137.hg.1
USP9X	11.42	10.88	-1.45	TC0X00007026.hg.1
UTP23	8.75	8.21	-1.45	TC0800008626.hg.1
CEBPG	9.78	9.25	-1.45	TC1900007777.hg.1
CBY1	7.2	6.67	-1.45	TC2200007360.hg.1
TADA2B	7.29	6.76	-1.45	TC0400006712.hg.1
COX4I1	9.26	8.72	-1.45	TC1600008709.hg.1
VPS72	7.54	7.01	-1.44	TC0100018489.hg.1
IFITM3	17.95	17.42	-1.44	TC1100009657.hg.1
GPR180	6.62	6.09	-1.44	TC1300007731.hg.1
PTPMT1	8.11	7.58	-1.44	TC1100012995.hg.1
RAB4B; MIA- RAB4B; RAB4B- EGLN2	6.1	5.57	-1.44	TC1900011733.hg.1
SLC25A36	8.25	7.72	-1.44	TC0300008989.hg.1
IRAK4	9.4	8.88	-1.44	TC1200007406.hg.1
DGUOK	7.1	6.58	-1.44	TC0200008063.hg.1
BTN3A2	9.58	9.05	-1.44	TC0600007301.hg.1
SFXN3	11.46	10.95	-1.43	TC1000008668.hg.1
SNX7	9.52	9	-1.43	TC0100009176.hg.1
BPHL	5.55	5.03	-1.43	TC0600006659.hg.1
ZDHHC3	9.19	8.67	-1.43	TSUnmapped00000494.hg.1
STMN1; MIR3917	11.65	11.15	-1.42	TC0100013369.hg.1
HSPA2	7.77	7.26	-1.42	TC1400007443.hg.1
SHMT2	13.93	13.43	-1.42	TC1200007866.hg.1
WDR82	11.58	11.07	-1.42	TC0300011158.hg.1
TCF7L1	7.97	7.46	-1.42	TC0200008236.hg.1
ALDH4A1	6.99	6.48	-1.42	TC0100018417.hg.1
GLRX	8.82	8.32	-1.42	TC0500011497.hg.1
ENSA	10.27	9.77	-1.41	TC0100015743.hg.1
SRP72	12.73	12.23	-1.41	TC0400007593.hg.1
NOP10	13.21	12.71	-1.41	TC1500008984.hg.1
AP2M1	12.15	11.65	-1.41	TC0300009693.hg.1
BAP1	5.94	5.44	-1.41	TC0300011167.hg.1
SHISA5	15.67	15.19	-1.4	TC0300011023.hg.1
H3F3AP4; H3F3A; H3F3B	13.15	12.67	-1.4	TC0200010021.hg.1
AP4B1	7.34	6.85	-1.4	TC0100015337.hg.1
MYNN	8.39	7.92	-1.39	TC0300009451.hg.1
TKT	12.32	11.85	-1.39	TC0300011200.hg.1
SMC3	11.75	11.27	-1.39	TC1000008896.hg.1
RPL41	15.58	15.1	-1.39	TC0500007434.hg.1
IL18R1	6.04	5.56	-1.39	TC0200016502.hg.1

COL4A3BP	10.21	9.74	-1.38	TC0500011163.hg.1
PNPLA6	13.38	12.91	-1.38	TC1900011654.hg.1
NDRG3	11.2	10.74	-1.38	TC2000009014.hg.1
ANG; RNASE4	7.84	7.38	-1.38	TC1400006529.hg.1
TLL7	8.97	8.5	-1.38	TC0100014743.hg.1
SWI5	5.71	5.24	-1.38	TC0900008854.hg.1
C16orf70	9.46	9	-1.38	TC1600008144.hg.1
CLDN15	7.85	7.38	-1.38	TC0700012043.hg.1
ABI2	8.47	8	-1.38	TC0200010518.hg.1
SF3A1	10.37	9.9	-1.38	TC2200008434.hg.1
PARP1	8.64	8.19	-1.37	TC0100017528.hg.1
RNF145	10.64	10.18	-1.37	TC0500012642.hg.1
FPGT	6.85	6.4	-1.37	TC0100018233.hg.1
RPL31	13.85	13.39	-1.37	TC0200008632.hg.1
TGIF2	9.12	8.67	-1.37	TC2000009914.hg.1
CEP68	10.3	9.85	-1.37	TC0200007825.hg.1
ACO1	11.61	11.16	-1.36	TC0900006937.hg.1
BTG2	9.13	8.69	-1.36	TC0100011253.hg.1
ANAPC7	10.84	10.4	-1.36	TC1200012842.hg.1
DNAJC21	8.33	7.89	-1.36	TC0500007123.hg.1
REL	9.35	8.91	-1.36	TC0200016452.hg.1
ZNF358	7.62	7.19	-1.35	TC1900011652.hg.1
PLD1	11.64	11.21	-1.35	TC0300013123.hg.1
NEU1	9.44	9.01	-1.35	TC0600011463.hg.1
SRSF3	9.65	9.22	-1.35	TC0600007842.hg.1
WBP1L	12.17	11.74	-1.35	TC1000008750.hg.1
NBR1	10.09	9.65	-1.35	TC1700007942.hg.1
RELL2	5.92	5.49	-1.35	TC0500008902.hg.1
DCTN2	11.39	10.95	-1.35	TC1200010971.hg.1
MED30	6.7	6.28	-1.34	TC0800008641.hg.1
PHF14	8.88	8.45	-1.34	TC0700006715.hg.1
SPTBN1	15.01	14.59	-1.33	TC0200007609.hg.1
UCP2	6.59	6.19	-1.32	TC1100011602.hg.1
MIA3	9.56	9.16	-1.32	TC0100011692.hg.1
FUZ	9.64	9.23	-1.32	TC1900012001.hg.1
ZNF322	8.39	8.01	-1.31	TC0600011162.hg.1
APH1B	10.37	9.98	-1.31	TC1500007520.hg.1
RPL15	16.78	16.39	-1.31	TC0300006846.hg.1
MRPS7	9.71	9.32	-1.31	TC1700008897.hg.1
ARMC8	11.64	11.25	-1.31	TC0300008940.hg.1
CUTA	10.75	10.36	-1.31	TC0600011546.hg.1
PLCG2	8.81	8.43	-1.31	TC1600008607.hg.1

UBE3A	9	8.62	-1.3	TC1500008751.hg.1
RAD23B	12.72	12.34	-1.3	TC0900008345.hg.1
DEDD	11	10.63	-1.29	TC0100016159.hg.1
NOS3	6.02	5.66	-1.29	TC0700009689.hg.1
HNRNPH2	11.48	11.11	-1.29	TC0X00011309.hg.1
DNAJC30	6.98	6.61	-1.29	TC0700011499.hg.1
SLK	12.84	12.49	-1.28	TC1000008795.hg.1
C21orf2	6.61	6.26	-1.28	TC2100008357.hg.1
COTL1	11.92	11.56	-1.28	TC1600011060.hg.1
TAF7	9.68	9.33	-1.28	TC0500012271.hg.1
RPS7	15.16	14.8	-1.28	TC0200006536.hg.1
EIF3E	15.28	14.95	-1.27	TC0800012451.hg.1
LNPEP	11.39	11.06	-1.26	TC0500008157.hg.1
ANO10	11.53	11.2	-1.26	TC0300013962.hg.1
RPL41P5	14.17	13.84	-1.26	TC1200011527.hg.1
MPDZ	10.11	9.77	-1.26	TC0900009557.hg.1
PCYOX1L	6.9	6.58	-1.25	TC0500009061.hg.1
KLF8	6.72	6.4	-1.25	TC0X00007390.hg.1
COPS6	11.76	11.44	-1.25	TC0700008522.hg.1
FSD1	5.48	5.18	-1.23	TC1900006685.hg.1
NGFRAP1	12.29	12.02	-1.21	TC0X00008002.hg.1

Chapter 8. References

Abbas, T., and Dutta, A. (2009). p21 in cancer: intricate networks and multiple activities. *Nature Reviews Cancer* 9, 400-414.

Ahn, H.J., Hernandez, C.M., Levenson, J.M., Lubin, F.D., Liou, H.C., and Sweatt, J.D. (2008). c-Rel, an NF-kappa B family transcription factor, is required for hippocampal long-term synaptic plasticity and memory formation. *Learning & Memory* 15, 539-549.

Akimoto, S., Mitsumata, M., Sasaguri, T., and Yoshida, Y. (2000). Laminar shear stress inhibits vascular endothelial cell proliferation by inducing cyclin-dependent kinase inhibitor p21(Sdi1/Cip1/Waf1). *Circulation Research* 86, 185-190.

Alves, B.N., Tsui, R., Almaden, J., Shokhirev, M.N., Davis-Turak, J., Fujimoto, J., Birnbaum, H., Ponomarenko, J., and Hoffmann, A. (2014). I kappa B epsilon Is a Key Regulator of B Cell Expansion by Providing Negative Feedback on cRel and RelA in a Stimulus-Specific Manner. *Journal of Immunology* 192, 3121-3132.

Ammirati, E., Moroni, F., Magnoni, M., and Camici, P.G. (2015). The role of T and B cells in human atherosclerosis and atherothrombosis. *Clinical and Experimental Immunology* 179, 173-187.

Anderson, D.M., Maraskovsky, E., Billingsley, W.L., Dougall, W.C., Tometsko, M.E., Roux, E.R., Teepe, M.C., DuBose, R.F., Cosman, D., and Galibert, L. (1997). A homologue of the TNF receptor and its ligand enhance T-cell growth and dendritic-cell function. *Nature* 390, 175-179.

Artinger, S., Deiner, C., Loddenkemper, C., Schwimbeck, P.L., Schultheiss, H.P., and Pels, K. (2009). Complex porcine model of atherosclerosis: Induction of early coronary lesions after long-term hyperlipidemia without sustained hyperglycemia. *Canadian Journal of Cardiology* 25, E109-E114.

Atochina, E.N., Balyasnikova, I.V., Danilov, S.M., Granger, D.N., Fisher, A.B., and Muzykantov, V.R. (1998). Immunotargeting of catalase to ACE or ICAM-1 protects perfused rat lungs against oxidative stress. *American Journal of Physiology-Lung Cellular and Molecular Physiology* 275, L806-L817.

Bai, Y., Wang, X.L., Zhao, S., Ma, C.Y., Cui, J.W., and Zheng, Y. (2015). Sulforaphane Protects against Cardiovascular Disease via Nrf2 Activation. *Oxidative Medicine and Cellular Longevity*.

Baigent, C., Keech, A., Kearney, P.M., Blackwell, L., Buck, G., Pollicino, C., Kirby, A., Sourjina, T., Peto, R., Collins, R., *et al.* (2005). Efficacy and safety of cholesterol-lowering treatment: prospective meta-analysis of data from 90,056 participants in 14 randomised trials of statins. *Lancet* 366, 1267-1278.

Baiguera, C., Alghisi, M., Pinna, A., Bellucci, A., De Luca, M.A., Frau, L., Morelli, M., Ingrassia, R., Benarese, M., Porrini, V., *et al.* (2012). Late-onset Parkinsonism in NF kappa B/c-Rel-deficient mice. *Brain* 135, 2750-2765.

Baker, R.G., Hayden, M.S., and Ghosh, S. (2011). NF-kappa B, Inflammation, and Metabolic Disease. *Cell Metabolism* 13, 11-22.

Bando, M., Yamada, H., Kusunose, K., Fukuda, D., Amano, R., Tamai, R., Torii, Y., Hirata, Y., Nishio, S., Yamaguchi, K., *et al.* (2015). Comparison of carotid plaque tissue characteristics in patients with acute coronary syndrome or stable angina pectoris: assessment by iPlaque, transcutaneous carotid ultrasonography with integrated backscatter analysis. *Cardiovascular Ultrasound* 13.

Bao, X.P., Lu, C.Y., and Frangos, J.A. (1999). Temporal gradient in shear but not steady shear stress induces PDGF-A and MCP-1 expression in endothelial cells - Role of NO, NF kappa B, and egr-1. *Arteriosclerosis Thrombosis and Vascular Biology* 19, 996-1003.

Barth, T.F.E., Martin-Subero, J.I., Joos, S., Menz, C.K., Hasel, C., Mechttersheimer, G., Parwaresch, R.M., Lichter, P., Siebert, R., and Moller, P. (2003). Gains of 2p involving the REL locus correlate with nuclear c-Rel protein accumulation in neoplastic cells of classical Hodgkin lymphoma. *Blood* 101, 3681-3686.

Belguise, K., and Sonenshein, G.E. (2007). PKC theta promotes c-Rel-driven mammary tumorigenesis in mice and humans by repressing estrogen receptor alpha synthesis. *Journal of Clinical Investigation* 117, 4009-4021.

Benslimane-Ahmim, Z., Heymann, D., Dizier, B., Lokajczyk, A., Brion, R., Laurendeau, I., Bieche, I., Smadja, D.M., Galy-Fauroux, I., Collic-Jouault, S., *et al.* (2011). Osteoprotegerin, a new actor

in vasculogenesis, stimulates endothelial colony-forming cells properties. *Journal of Thrombosis and Haemostasis* *9*, 834-843.

Bentzon, J.F., Otsuka, F., Virmani, R., and Falk, E. (2014). Mechanisms of Plaque Formation and Rupture. *Circulation Research* *114*, 1852-1866.

Bernard, D., Quatannens, B., Begue, A., Vandenbunder, B., and Abbadie, C. (2001). Antiproliferative and antiapoptotic effects of cRel may occur within the same cells via the up-regulation of manganese superoxide dismutase. *Cancer Research* *61*, 2656-2664.

Bertrand, M.J.M., Milutinovic, S., Dickson, K.M., Ho, W.C., Boudreault, A., Durkin, J., Gillard, J.W., Jaquith, J.B., Morris, S.J., and Barker, P.A. (2008). cIAP1 and cIAP2 facilitate cancer cell survival by functioning as E3 ligases that promote RIP1 ubiquitination. *Molecular Cell* *30*, 689-700.

Boon, R.A., Leyen, T.A., Fontijn, R.D., Flederius, J.O., Baggen, J.M.C., Volger, O.L., Amerongen, G.P.V., and Horrevoets, A.J.G. (2010). KLF2-induced actin shear fibers control both alignment to flow and JNK signaling in vascular endothelium. *Blood* *115*, 2533-2542.

Bowden, N., Bryan, M.T., Duckles, H., Feng, S., Hsiao, S., Kim, H.R., Mahmoud, M., Moers, B., Serbanovic-Canic, J., Xanthis, I., *et al.* (2016). Experimental Approaches to Study Endothelial Responses to Shear Stress. *Antioxidants & Redox Signaling* *25*, 389-400.

Brand, K., Page, S., Rogler, G., Bartsch, A., Brandl, R., Knuechel, R., Page, M., Kaltschmidt, C., Baeuerle, P.A., and Neumeier, D. (1996). Activated transcription factor nuclear factor-kappa B is present in the atherosclerotic lesion. *Journal of Clinical Investigation* *97*, 1715-1722.

Brown, K., Park, S., Kanno, T., Franzoso, G., and Siebenlist, U. (1993). MUTUAL REGULATION OF THE TRANSCRIPTIONAL ACTIVATOR NF-KAPPA-B AND ITS INHIBITOR, I-KAPPA-B-ALPHA. *Clinical Research* *41*, A137-A137.

Bryan, M.T., Duckles, H., Feng, S., Hsiao, S.T., Kim, H.R., Serbanovic-Canic, J., and Evans, P.C. (2014). Mechanoresponsive Networks Controlling Vascular Inflammation. *Arteriosclerosis Thrombosis and Vascular Biology* *34*, 2199-2205.

Budde, L.M., Wu, C., Tilman, C., Douglas, I., and Ghosh, S. (2002). Regulation of I kappa B beta expression in testis. *Molecular Biology of the Cell* *13*, 4179-4194.

Bunting, K., Rao, S., Hardy, K., Woltring, D., Denyer, G.S., Wang, J., Gerondakis, S., and Shannon, M.F. (2007). Genome-wide analysis of gene expression in T cells to identify targets of the NF-kappa B transcription factor c-Rel. *Journal of Immunology* *178*, 7097-7109.

Burkitt, M.D., Hanedi, A.F., Duckworth, C.A., Williams, J.M., Tang, J.M., O'Reilly, L.A., Putoczki, T.L., Gerondakis, S., Dimaline, R., Caamano, J.H., *et al.* (2015). NF-B1, NF-B2 and c-Rel differentially regulate susceptibility to colitis-associated adenoma development in C57BL/6 mice. *Journal of Pathology* *236*, 326-336.

Burkitt, M.D., Williams, J.M., Duckworth, C.A., O'Hara, A., Hanedi, A., Varro, A., Caamano, J.H., and Pritchard, D.M. (2013). Signaling mediated by the NF-kappa B sub-units NF-kappa B1, NF-kappa B2 and c-Rel differentially regulate *Helicobacter felis*-induced gastric carcinogenesis in C57BL/6 mice. *Oncogene* *32*, 5563-5573.

Bustin, S.A. (2002). Quantification of mRNA using real-time reverse transcription PCR (RT-PCR): trends and problems. *Journal of Molecular Endocrinology* *29*.

Carayol, N., and Wang, C.Y. (2006). IKK alpha stabilizes cytosolic beta-catenin by inhibiting both canonical and non-canonical degradation pathways. *Cellular Signalling* *18*, 1941-1946.

Caro, C.G., Fitzgerald, J.M., and Schroter, R.C. (1969). Arterial wall shear and distribution of early atheroma in man. *Nature* *223*, 1159-1161.

Caspritz, G., Alpermann, H.G., and Schleyerbach, R. (1986). INFLUENCE OF THE NEW ANGIOTENSIN CONVERTING-ENZYME-INHIBITOR RAMIPRIL ON SEVERAL MODELS OF ACUTE-INFLAMMATION AND THE ADJUVANT ARTHRITIS IN THE RAT. *Arzneimittelforschung-Drug Research* *36-2*, 1605-1608.

Castelli, W.P., Garrison, R.J., Wilson, P.W.F., Abbott, R.D., Kalousdian, S., and Kannel, W.B. (1986). INCIDENCE OF CORONARY HEART-DISEASE AND LIPOPROTEIN CHOLESTEROL LEVELS - THE FRAMINGHAM-STUDY. *Jama-Journal of the American Medical Association* *256*, 2835-2838.

Celermajer, D.S. (1997). Endothelial dysfunction: Does it matter? Is it reversible? *Journal of the American College of Cardiology* 30, 325-333.

Chappell, D.C., Varner, S.E., Nerem, R.M., Medford, R.M., and Alexander, R.W. (1998). Oscillatory shear stress stimulates adhesion molecule expression in cultured human endothelium. *Circulation Research* 82, 532-539.

Chatzizisis, Y.S., Coskun, A.U., Jonas, M., Edelman, E.R., Feldman, C.L., and Stone, P.H. (2007). Role of endothelial shear stress in the natural history of coronary atherosclerosis and vascular remodeling - Molecular, cellular, and vascular behavior. *Journal of the American College of Cardiology* 49, 2379-2393.

Chaudhury, H., Zakkar, M., Boyle, J., Cuhlmann, S., van der Heiden, K., Luong, L.A., Davis, J., Platt, A., Mason, J.C., Krams, R., *et al.* (2010). c-Jun N-Terminal Kinase Primes Endothelial Cells at Atheroprone Sites for Apoptosis. *Arteriosclerosis Thrombosis and Vascular Biology* 30, 546-U393.

Chen, E., Hrdlickova, R., Nehyba, J., Longo, D.L., Bose, H.R., and Li, C.C.H. (1998). Degradation of proto-oncoprotein c-Rel by the ubiquitin-proteasome pathway. *Journal of Biological Chemistry* 273, 35201-35207.

Chen, G.B., Hardy, K., Bunting, K., Daley, S., Ma, L.N., and Shannon, M.F. (2010). Regulation of the IL-21 Gene by the NF-kappa B Transcription Factor c-Rel. *Journal of Immunology* 185, 2350-2359.

Chen, P.-Y., Qin, L., Li, G., Wang, Z., Dahlman, J.E., Malagon-Lopez, J., Guija, S., Cilfone, N.A., Kauffman, K.J., Sun, L., *et al.* (2019). Endothelial TGF- β signalling drives vascular inflammation and atherosclerosis (*Nature Metabolism*), pp. 912 –926.

Chen, P.Y., Qin, L.F., Baeyens, N., Li, G.X., Afolabi, T., Budatha, M., Tellides, G., Schwartz, M.A., and Simons, M. (2015). Endothelial-to-mesenchymal transition drives atherosclerosis progression. *Journal of Clinical Investigation* 125, 4514-4528.

Cheng, P.Y., Zlobin, A., Volgina, V., Gottipati, S., Osborne, B., Simel, E.J., Miele, L., and Gabrilovich, D.I. (2001). Notch-1 regulates NF-kappa B activity in hemopoietic progenitor cells. *Journal of Immunology* 167, 4458-4467.

Chiang, H.Y., Korshunov, V.A., Serour, A., Shi, F., and Sottile, J. (2009). Fibronectin Is an Important Regulator of Flow-Induced Vascular Remodeling. *Arteriosclerosis Thrombosis and Vascular Biology* 29, 1074-U1157.

Chuaqui, R.F., Bonner, R.F., Best, C.J.M., Gillespie, J.W., Flaig, M.J., Hewitt, S.M., Phillips, J.L., Krizman, D.B., Tangrea, M.A., Ahram, M., *et al.* (2002). Post-analysis follow-up and validation of microarray experiments. *Nature Genetics* 32, 509-514.

Clozel, M. (2003). Effects of bosentan on cellular processes involved in pulmonary arterial hypertension: do they explain the long-term benefit? *Annals of Medicine* 35, 605-613.

Cockerill, G.W., Rye, K.A., Gamble, J.R., Vadas, M.A., and Barter, P.J. (1995). HIGH-DENSITY-LIPOPROTEINS INHIBIT CYTOKINE-INDUCED EXPRESSION OF ENDOTHELIAL-CELL ADHESION MOLECULES. *Arteriosclerosis Thrombosis and Vascular Biology* 15, 1987-1994.

Coskun, A., Serteser, M., and Unsal, I. (2013). INHIBITION OF CHOLESTEROL BIOSYNTHESIS IN HYPERCHOLESTEROLEMIA - IS IT THE RIGHT CHOICE? *Journal of Medical Biochemistry* 32, 16-19.

Csordas, A., and Bernhard, D. (2013). The biology behind the atherothrombotic effects of cigarette smoke. *Nature Reviews Cardiology* 10, 219-230.

Cuhlmann, S., Van der Heiden, K., Saliba, D., Tremoleda, J.L., Khalil, M., Zakkar, M., Chaudhury, H., Luong, L.A., Mason, J.C., Udalova, I., *et al.* (2011). Disturbed Blood Flow Induces RelA Expression via c-Jun N-Terminal Kinase 1 A Novel Mode of NF-kappa B Regulation That Promotes Arterial Inflammation. *Circulation Research* 108, 950-959.

Cunningham, K.S., and Gotlieb, A.I. (2005). The role of shear stress in the pathogenesis of atherosclerosis. *Laboratory Investigation* 85, 9-23.

Daniel, J.M., Penzkofer, D., Teske, R., Dutzmann, J., Koch, A., Bielenberg, W., Bonauer, A., Boon, R.A., Fischer, A., Bauersachs, J., *et al.* (2014). Inhibition of miR-92a improves re-

endothelialization and prevents neointima formation following vascular injury. *Cardiovascular Research* 103, 564-572.

Dardik, A., Chen, L.L., Frattini, J., Asada, H., Aziz, F., Kudo, F.A., and Sumpio, B.E. (2005). Differential effects of orbital and laminar shear stress on endothelial cells. *Journal of Vascular Surgery* 41, 869-880.

Davenport, P., and Tipping, P.G. (2003). The role of interleukin-4 and interleukin-12 in the progression of atherosclerosis in apolipoprotein E-deficient mice. *American Journal of Pathology* 163, 1117-1125.

Davies, P.F. (1995). FLOW-MEDIATED ENDOTHELIAL MECHANOTRANSDUCTION. *Physiological Reviews* 75, 519-560.

Davies, P.F. (2007). Endothelial mechanisms of flow-mediated athero-protection and susceptibility. *Circulation Research* 101, 10-12.

Davies, P.F., Remuzzi, A., Gordon, E.J., Dewey, C.F., and Gimbrone, M.A. (1986). TURBULENT FLUID SHEAR-STRESS INDUCES VASCULAR ENDOTHELIAL-CELL TURNOVER INVITRO. *Proceedings of the National Academy of Sciences of the United States of America* 83, 2114-2117.

Davignon, J., and Ganz, P. (2004). Role of endothelial dysfunction in atherosclerosis. *Circulation* 109, 27-32.

Davis, M.E., Cai, H., Drummond, G.R., and Harrison, D.G. (2001). Shear stress regulates endothelial nitric oxide synthase expression through c-Src by divergent signaling pathways. *Circulation Research* 89, 1073-1080.

De Donatis, G.M., Le Pape, E., Pierron, A., Cheli, Y., Hofman, V., Hofman, P., Allegra, M., Zahaf, K., Bahadoran, P., Rocchi, S., *et al.* (2016). NF- κ B induces senescence bypass in melanoma via a direct transcriptional activation of EZH2. *Oncogene* 35, 2735-2745.

De Silva, N.S., Anderson, M.M., Carette, A., Silva, K., Heise, N., Bhagat, G., and Klein, U. (2016). Transcription factors of the alternative NF- κ B pathway are required for germinal center B-cell development.

de Winther, M.P.J., Kanters, E., Kraal, G., and Hofker, M.H. (2005). Nuclear factor kappa B signaling in atherogenesis. *Arteriosclerosis Thrombosis and Vascular Biology* 25, 904-914.

Dejardin, E., Droin, N.M., Delhase, M., Haas, E., Cao, Y.X., Makris, C., Li, Z.W., Karin, M., Ware, C.F., and Green, D.R. (2002). The lymphotoxin-beta receptor induces different patterns of gene expression via two NF-kappa B pathways. *Immunity* 17, 525-535.

Demartin, R., Vanhove, B., Cheng, Q., Hofer, E., Cszimadia, V., Winkler, H., and Bach, F.H. (1993). CYTOKINE-INDUCIBLE EXPRESSION IN ENDOTHELIAL-CELLS OF AN I-KAPPA-B-ALPHA-LIKE GENE IS REGULATED BY NF-KAPPA-B. *Embo Journal* 12, 2773-2779.

DeVerse, J.S., Sandhu, A.S., Mendoza, N., Edwards, C.M., Sun, C.X., Simon, S.I., and Passerini, A.G. (2013). Shear stress modulates VCAM-1 expression in response to TNF-alpha and dietary lipids via interferon regulatory factor-1 in cultured endothelium. *American Journal of Physiology-Heart and Circulatory Physiology* 305, H1149-H1157.

Dimmeler, S., Assmus, B., Hermann, C., Haendeler, J., and Zeiher, A.M. (1998). Fluid shear stress stimulates phosphorylation of Akt in human endothelial cells - Involvement in suppression of apoptosis. *Circulation Research* 83, 334-341.

Dimmeler, S., Hermann, C., Galle, J., and Zeiher, A.M. (1999). Upregulation of superoxide dismutase and nitric oxide synthase mediates the apoptosis-suppressive effects of shear stress on endothelial cells. *Arteriosclerosis Thrombosis and Vascular Biology* 19, 656-664.

Divanovic, S., Trompette, A., Atabani, S.F., Madan, R., Golenbock, D.T., Visintin, A., Finberg, R.W., Tarakhovskiy, A., Vogel, S.N., Belkaid, Y., *et al.* (2005). Negative regulation of Toll-like receptor 4 signaling by the Toll-like receptor homolog RP105. *Nature Immunology* 6, 571-578.

Djuric, Z., Kashif, M., Fleming, T., Muhammad, S., Piel, D., von Bauer, R., Bea, F., Herzig, S., Zeier, M., Pizzi, M., *et al.* (2012). Targeting Activation of Specific NF-kappa B Subunits Prevents Stress-Dependent Atherothrombotic Gene Expression. *Molecular Medicine* 18, 1375-1386.

Du, F., Yu, F., Wang, Y.Z., Hui, Y., Carnevale, K., Fu, M.G., Lu, H., and Fan, D.P. (2014). MicroRNA-155 Deficiency Results in Decreased Macrophage Inflammation and Attenuated Atherogenesis

in Apolipoprotein E-Deficient Mice. *Arteriosclerosis Thrombosis and Vascular Biology* 34, 759-767.

Ea, C.K., Deng, L., Xia, Z.P., Pineda, G., and Chen, Z.J.J. (2006). Activation of IKK by TNF alpha requires site-specific ubiquitination of RIP1 and polyubiquitin binding by NEMO. *Molecular Cell* 22, 245-257.

Edfeldt, K.K., Swedenborg, K.J., Hansson, K.G., and Yan, K.Z.-Q. (2002). Expression of Toll-Like Receptors in Human Atherosclerotic Lesions: A Possible Pathway for Plaque Activation. *Circulation: Journal of the American Heart Association* 105, 1158-1161.

Enesa, K., Zakkar, M., Chaudhury, H., Luong, L.A., Rawlinson, L., Mason, J.C., Haskard, D.O., Dean, J.L.E., and Evans, P.C. (2008). NF-kappa B suppression by the deubiquitinating enzyme Cezanne - A novel negative feedback loop in pro-inflammatory signaling. *Journal of Biological Chemistry* 283, 7036-7045.

Erbel, C., Dengler, T.J., Wangler, S., Lasitschka, F., Bea, F., Wambsganss, N., Hakimi, M., Bockler, D., Katus, H.A., and Gleissner, C.A. (2011). Expression of IL-17A in human atherosclerotic lesions is associated with increased inflammation and plaque vulnerability. *Basic Research in Cardiology* 106, 125-134.

Evans, P.C. (2011). The influence of sulforaphane on vascular health and its relevance to nutritional approaches to prevent cardiovascular disease. *EPMA J* 2, 9-14.

Everett, B.M., Pradhan, A.D., Solomon, D.H., Paynter, N., MacFadyen, J., Zaharris, E., Gupta, M., Clearfield, M., Libby, P., Hasan, A.A.K., *et al.* (2013). Rationale and design of the Cardiovascular Inflammation Reduction Trial: A test of the inflammatory hypothesis of atherothrombosis. *American Heart Journal* 166, 199-+.

Falk, E., Nakano, M., Bentzon, J.F., Finn, A.V., and Virmani, R. (2013). Update on acute coronary syndromes: the pathologists' view. *European Heart Journal* 34, 719-728.

Fang, Y., Shi, C.Z., Manduchi, E., Civelek, M., and Davies, P.F. (2010). MicroRNA-10a regulation of proinflammatory phenotype in athero-susceptible endothelium in vivo and in vitro. *Proceedings of the National Academy of Sciences of the United States of America* 107, 13450-13455.

Fata, J.E., Kong, Y.Y., Li, J., Sasaki, T., Irie-Sasaki, J., Moorehead, R.A., Elliott, R., Scully, S., Voura, E.B., Lacey, D.L., *et al.* (2000). The osteoclast differentiation factor osteoprotegerin-ligand is essential for mammary gland development. *Cell* 103, 41-50.

Feintuch, A., Ruengsakulrach, P., Lin, A., Zhang, J., Zhou, Y.Q., Bishop, J., Davidson, L., Courtman, D., Foster, F.S., Steinman, D.A., *et al.* (2007). Hemodynamics in the mouse aortic arch as assessed by MRI, ultrasound, and numerical modeling. *American Journal of Physiology-Heart and Circulatory Physiology* 292, H884-H892.

Feng, B., Cheng, S.H., Hsia, C.Y., King, L.B., Monroe, J.G., and Liou, H.C. (2004). NF-kappa B inducible genes BCL-X and cyclin E promote immature B-cell proliferation and survival. *Cellular Immunology* 232, 9-20.

Feng, S., Bowden, N., Fragiadaki, M., Souilhol, C., Hsiao, S., Mahmoud, M., Allen, S., Pirri, D., Ayllon, B.T., Akhtar, S., *et al.* (2017). Mechanical Activation of Hypoxia-Inducible Factor 1 alpha Drives Endothelial Dysfunction at Atheroprone Sites. *Arteriosclerosis Thrombosis and Vascular Biology* 37, 2087-+.

Fledderus, J.O., Boon, R.A., Volger, O.L., Hurttala, H., Yla-Herttuala, S., Pannekoek, H., Levonen, A.L., and Horrevoets, A.J.G. (2008). KLF2 primes the antioxidant transcription factor Nrf2 for activation in endothelial cells. *Arteriosclerosis Thrombosis and Vascular Biology* 28, 1339-1346.

Fledderus, J.O., van Thienen, J.V., Boon, R.A., Dekker, R.J., Rohlena, J., Volger, O.L., Bijmens, A.-P.J.J., Daemen, M.J.A.P., Kuiper, J., van Berkel, T.J.C., *et al.* (2007). Prolonged shear stress and KLF2 suppress constitutive proinflammatory transcription through inhibition of ATF2. *Blood* 109, 4249-4257.

Foteinos, G., Hu, Y.H., Xiao, Q.Z., Metzler, B., and Xu, Q.B. (2008). Rapid endothelial turnover in atherosclerosis-prone areas coincides with stem cell repair in apolipoprotein E-deficient mice. *Circulation* 117, 1856-1863.

Franck, S.G., Mawson, K.T., Sausen, K.G., Salinas, J.M., Masson, J.G., Cole, J.A., Beltrami-Moreira, J.M., Chatzizisis, J.Y., Quillard, J.T., Tesmenitsky, J.Y., *et al.* (2017). Flow Perturbation Mediates Neutrophil Recruitment and Potentiates Endothelial Injury via TLR2 in Mice: Implications for Superficial Erosion. *Circulation Research* *121*, 31-42.

Freeman, W.M., Walker, S.J., and Vrana, K.E. (1999). Quantitative RT-PCR: Pitfalls and potential. *Biotechniques* *26*, 112-+.

Fullard, N., Moles, A., O'Reilly, S., van Laar, J.M., Faini, D., Diboll, J., Reynolds, N.J., Mann, D.A., Reichelt, J., and Oakley, F. (2013). The c-Rel Subunit of NF-kappa B Regulates Epidermal Homeostasis and Promotes Skin Fibrosis in Mice. *American Journal of Pathology* *182*, 2109-2120.

Fullard, N., Wilson, C.L., and Oakley, F. (2012). Roles of c-Rel signalling in inflammation and disease. *International Journal of Biochemistry & Cell Biology* *44*, 851-860.

Fusco, A.J., Huang, D.B., Miller, D., Wang, V.Y.F., Vu, D., and Ghosh, G. (2009). NF-kappa B p52:RelB heterodimer recognizes two classes of kappa B sites with two distinct modes. *Embo Reports* *10*, 152-159.

Galis, Z.S., and Khatry, J.J. (2002). Matrix metalloproteinases in vascular remodeling and atherogenesis - The good, the bad, and the ugly. *Circulation Research* *90*, 251-262.

Galis, Z.S., Sukhova, G.K., and Libby, P. (1995). MICROSCOPIC LOCALIZATION OF ACTIVE PROTEASES BY IN-SITU ZYMOGRAPHY - DETECTION OF MATRIX METALLOPROTEINASE ACTIVITY IN VASCULAR TISSUE. *Faseb Journal* *9*, 974-980.

Gareus, R., Kotsaki, E., Xanthoulea, S., van der Made, I., Gijbels, M.J.J., Kardakaris, R., Polykratis, A., Kollias, G., de Winther, M.P.J., and Pasparakis, M. (2008). Endothelial Cell-Specific NF-kappa B Inhibition Protects Mice from Atherosclerosis. *Cell Metabolism* *8*, 372-383.

Garin, G., Abe, J.-I., Mohan, A., Lu, W., Yan, C., Newby, A.C., Rhaman, A., and Berk, B.C. (2007). Flow antagonizes TNF-alpha signaling in endothelial cells by inhibiting caspase-dependent PKC zeta processing. *Circulation Research* *101*, 97-105.

Gaspar-Pereira, S., Fullard, N., Townsend, P.A., Banks, P.S., Ellis, E.L., Fox, C., Maxwell, A.G., Murphy, L.B., Kirk, A., Bauer, R., *et al.* (2012). The NF-kappa B Subunit c-Rel Stimulates Cardiac Hypertrophy and Fibrosis. *American Journal of Pathology* *180*, 929-939.

Gielsing, R.G., Elsharkawy, A.M., Caamano, J.H., Cowie, D.E., Wright, M.C., Ebrahimkhani, M.R., Burt, A.D., Mann, J., Raychaudhuri, P., Liou, H.C., *et al.* (2010). The c-Rel Subunit of Nuclear Factor-kappa B Regulates Murine Liver Inflammation, Wound-Healing, and Hepatocyte Proliferation. *Hepatology* *51*, 922-931.

Gilmore, T.D., Cormier, C., Jean-Jacques, J., and Gapuzan, M.E. (2001). Malignant transformation of primary chicken spleen cells by human transcription factor c-Rel. *Oncogene* *20*, 7098-7103.

Gilmore, T.D., and Gerondakis, S. (2011). The c- Rel Transcription Factor in Development and Disease. *Genes and Cancer* *2*, 695-711.

Goldstein, J.L., and Brown, M.S. (2015). A Century of Cholesterol and Coronaries: From Plaques to Genes to Statins. *Cell* *161*, 161-172.

Gomez, I., Ward, B., Souilhol, C., Recarti, C., Ariaans, M., Johnston, J., Burnett, A., Mahmoud, M., Luong, L., West, L., *et al.* (2020). Neutrophil microvesicles drive atherosclerosis by delivering miR-155 to atheroprone endothelium. *Nature Communications* *11*.

Gonzalez-Suarez, E., Branstetter, D., Armstrong, A., Dinh, H., Blumberg, H., and Dougall, W.C. (2007). RANK overexpression in transgenic mice with mouse mammary tumor virus promoter-controlled RANK increases proliferation and impairs alveolar differentiation in the mammary epithelia and disrupts lumen formation in cultured epithelial acini. *Molecular and Cellular Biology* *27*, 1442-1454.

Gordon, J.D., Probstfield, L.J., Garrison, J.R., Neaton, D.J., Castelli, P.W., Knoke, D.J., Jacobs, R.D., Bangdiwala, A.S., and Tyroler, A.H. (1989). High-Density Lipoprotein Cholesterol and Cardiovascular Disease: Four Prospective American Studies. *Circulation* *79*, 8-15.

Gordon, T., Castelli, W.P., Hjortland, M.C., Kannel, W.B., and Dawber, T.R. (1977). High density lipoprotein as a protective factor against coronary heart disease. The Framingham study :

Gordon T, Castelli WP, Hjortland MC, Kannel WB, Dawber TR: *Am J Med* 62: 707–714, 1977. *The American Journal of Medicine* 62, A77-A77.

Gray, C.M., Remouchamps, C., McCorkell, K.A., Solt, L.A., Dejardin, E., Orange, J.S., and May, M.J. (2014). Noncanonical NF-kappa B Signaling Is Limited by Classical NF-kappa B Activity. *Science Signaling* 7.

Grinberg-Bleyer, Y., Caron, R., Seeley, J.J., De Silva, N.S., Schindler, C.W., Hayden, M.S., Klein, U., and Ghosh, S. (2018). The Alternative NF- κ B Pathway in Regulatory T Cell Homeostasis and Suppressive Function.

Grinberg-Bleyer, Y., Oh, H., Desrichard, A., Bhatt, D.M., Caron, R., Chan, T.A., Schmid, R.M., Klein, U., Hayden, M.S., and Ghosh, S. (2017). NF- κ B c-Rel Is Crucial for the Regulatory T Cell Immune Checkpoint in Cancer.

Grumont, R.J., and Gerondakis, S. (2000). Rel induces interferon regulatory factor 4 (IRF-4) expression in lymphocytes: Modulation of interferon-regulated gene expression by Rel/nuclear factor kappa B. *Journal of Experimental Medicine* 191, 1281-1291.

Grumont, R.J., Rourke, I.J., and Gerondakis, S. (1999a). Rel-dependent induction of A1 transcription is required to protect B cells from antigen receptor ligation-induced apoptosis. *Genes & Development* 13, 400-411.

Grumont, R.J., Rourke, I.J., and Gerondakis, S. (1999b). Rel-dependent induction of A1 transcription is required to protect B cells from antigen receptor ligation-induced apoptosis. *Genes & Development* 13, 400-411.

Grumont, R.J., Rourke, I.J., O'Reilly, L.A., Strasser, A., Miyake, K., Sha, W., and Gerondakis, S. (1998). B lymphocytes differentially use the Rel and nuclear factor kappa B1 (NF-kappa B1) transcription factors to regulate cell cycle progression and apoptosis in quiescent and mitogen-activated cells. *Journal of Experimental Medicine* 187, 663-674.

Grumont, R.J., Strasser, A., and Gerondakis, S. (2002). B cell growth is controlled by phosphatidylinositol 3-kinase-dependent Rel/NF-kappa B regulated induction of c-myc transcription. *Molecular Cell* 10, 1283-1294.

Hahn, C., and Schwartz, M.A. (2009). Mechanotransduction in vascular physiology and atherogenesis. *Nature Reviews Molecular Cell Biology* 10, 53-62.

Hajra, L., Evans, A.I., Chen, M., Hyduk, S.J., Collins, T., and Cybulsky, M.I. (2000). The NF-kappa B signal transduction pathway in aortic endothelial cells is primed for activation in regions predisposed to atherosclerotic lesion formation. *Proceedings of the National Academy of Sciences of the United States of America* 97, 9052-9057.

Hamik, A., Lin, Z.Y., Kumar, A., Balcells, M., Sinha, S., Katz, J., Feinberg, M.W., Gerzsten, R.E., Edelman, E.R., and Jain, M.K. (2007). Kruppel-like factor 4 regulates endothelial inflammation. *Journal of Biological Chemistry* 282, 13769-13779.

Han, H.C., Liu, Q., and Jiang, Z.L. (2016). Mechanical behavior and wall remodeling of blood vessels under axial twist. *Yi Yong Sheng Wu Li Xue* 31, 319-326.

Hassing, H.C., Surendran, R.P., Mooij, H.L., Stroes, E.S., Nieuwdorp, M., and Dallinga-Thie, G.M. (2012). Pathophysiology of hypertriglyceridemia. *Biochimica Et Biophysica Acta-Molecular and Cell Biology of Lipids* 1821, 826-832.

Hausenloy, D.J., and Yellon, D.M. (2008). Targeting residual cardiovascular risk: raising high-density lipoprotein cholesterol levels. *Heart* 94, 706-714.

Hayden, M.S., and Ghosh, S. (2004). Signaling to NF-kappa B. *Genes & Development* 18, 2195-2224.

Hayden, M.S., and Ghosh, S. (2008). Shared principles in NF-kappa B signaling. *Cell* 132, 344-362.

Hayden, M.S., and Ghosh, S. (2011). NF-kappa B in immunobiology. *Cell Research* 21, 223-244.

Heise, N., De Silva, N., Silva, K., Carette, A., Simonetti, G., Pasparakis, M., and Klein, U. (2014). Germinal center B cell maintenance and differentiation are controlled by distinct NF- Kappa B transcription factor subunits. *Journal of Experimental Medicine* 211, 2103-2118.

Heitzer, T., Schlinzig, T., Krohn, K., Meinertz, T., and Munzel, T. (2001). Endothelial dysfunction, oxidative stress, and risk of cardiovascular events in patients with coronary artery disease. *Circulation* *104*, 2673-2678.

Heo, K.-S., Lee, H., Nigro, P., Thomas, T., Le, N.-T., Chang, E., McClain, C., Reinhart-King, C.A., King, M.R., Berk, B.C., *et al.* (2011a). PKC zeta mediates disturbed flow-induced endothelial apoptosis via p53 SUMOylation. *Journal of Cell Biology* *193*, 867-884.

Heo, S.H., Cho, C.H., Kim, H.O., Jo, Y.H., Yoon, K.S., Lee, J.H., Park, J.C., Park, K.C., Ahn, T.B., Chung, K.C., *et al.* (2011b). Plaque Rupture is a Determinant of Vascular Events in Carotid Artery Atherosclerotic Disease: Involvement of Matrix Metalloproteinases 2 and 9. *Journal of Clinical Neurology* *7*, 69-76.

Herrmann, R.A., Malinauskas, R.A., and Truskey, G.A. (1994). Characterization of sites with elevated LDL permeability at intercostal, celiac and iliac branches of the normal rabbit aorta. *Arteriosclerosis and Thrombosis* *14*, 313-323.

Hood, E., Simone, E., Wattamwar, P., Dziubla, T., and Muzykantov, V. (2011). Nanocarriers for vascular delivery of antioxidants. *Nanomedicine* *6*, 1257-1272.

Hsiai, T.K., Cho, S.K., Wong, P.K., Ing, M., Salazar, A., Sevastian, A., Navab, M., Demer, L.L., and Ho, C.M. (2003). Monocyte recruitment to endothelial cells in response to oscillatory shear stress. *Faseb Journal* *17*, 1648-1657.

Hsu, H.L., Huang, J.N., Shu, H.B., Baichwal, V., and Goeddel, D.V. (1996). TNF-Dependent recruitment of the protein kinase RIP to the TNF receptor-1 signaling complex. *Immunity* *4*, 387-396.

Hsu, H.L., Xiong, J., and Goeddel, D.V. (1995). THE TNF RECEPTOR 1-ASSOCIATED PROTEIN TRADD SIGNALS CELL-DEATH AND NF-KAPPA-B ACTIVATION. *Cell* *81*, 495-504.

Hubacek, J.A. (2016). Apolipoprotein A5 fifteen years anniversary: Lessons from genetic epidemiology. *Gene* *592*, 193-199.

Ingrassia, R., Lanzillotta, A., Sarnico, I., Benarese, M., Blasi, F., Borgese, L., Bilo, F., Depero, L., Chiarugi, A., Spano, P.F., *et al.* (2012). 1B/(-)IRE DMT1 Expression during Brain Ischemia Contributes to Cell Death Mediated by NF-kappa B/RelA Acetylation at Lys310. *Plos One* *7*.

Jia, H., Abtahian, F., Aguirre, A.D., Lee, S., Chia, S., Lowe, H., Kato, K., Yonetsu, T., Vergallo, R., Hu, S., *et al.* (2013). In Vivo Diagnosis of Plaque Erosion and Calcified Nodule in Patients With Acute Coronary Syndrome by Intravascular Optical Coherence Tomography. *Journal of the American College of Cardiology* *62*, 1748-1758.

Jo, H., Dull, R.O., Hollis, T.M., and Tarbell, J.M. (1991). Endothelial albumin permeability is shear dependent, time-dependent, and reversible. *American Journal of Physiology* *260*, H1992-H1996.

Jufri, N.F., Mohamedali, A., Avolio, A., and Baker, M.S. (2015). Mechanical stretch: physiological and pathological implications for human vascular endothelial cells. *Vascular Cell* *7*.

Jurikova, M., Danihel, L., Polak, S., and Varga, I. (2016). Ki67, PCNA, and MCM proteins: Markers of proliferation in the diagnosis of breast cancer. *Acta Histochemica* *118*, 544-552.

Karin, M. (2006). Nuclear factor-kappa B in cancer development and progression. *Nature* *441*, 431-436.

Kheirrolomoom, A., Kim, C.W., Seo, J.W., Kumar, S., Son, D.J., Gagnon, M.K.J., Ingham, E.S., Ferrara, K.W., and Jo, H. (2015). Multifunctional Nanoparticles Facilitate Molecular Targeting and miRNA Delivery to Inhibit Atherosclerosis in ApoE(-/-) Mice. *Acs Nano* *9*, 8885-8897.

Kim, Y.M., Lee, Y.M., Kim, H.S., Kim, J.D., Choi, Y., Kim, K.W., Lee, S.Y., and Kwon, Y.G. (2002). TNF-related activation-induced cytokine (TRANCE) induces angiogenesis through the activation of Src and phospholipase C (PLC) in human endothelial cells. *Journal of Biological Chemistry* *277*, 6799-6805.

Kirsch, J., Schneider, H., Pagel, J.I., Rehberg, M., Singer, M., Hellfritsch, J., Chillo, O., Schubert, K.M., Qiu, J.H., Pogoda, K., *et al.* (2016). Endothelial Dysfunction, and A Prothrombotic, Proinflammatory Phenotype Is Caused by Loss of Mitochondrial Thioredoxin Reductase in Endothelium. *Arteriosclerosis Thrombosis and Vascular Biology* *36*, 1891-1899.

- Kolodgie, D.F., Burke, P.A., Farb, K.A., Weber, N.D., Kutys, N.R., Wight, N.T., and Virmani, N.R. (2002). Differential Accumulation of Proteoglycans and Hyaluronan in Culprit Lesions: Insights Into Plaque Erosion. *Arteriosclerosis, Thrombosis, and Vascular Biology: Journal of the American Heart Association* 22, 1642-1648.
- Kontgen, F., Grumont, R.J., Strasser, A., Metcalf, D., Li, R.L., Tarlinton, D., and Gerondakis, S. (1995a). Mice lacking the C-Rel protooncogene exhibit defects in lymphocyte-proliferation, humoral immunity and interleukin-2 expression. *Genes & Development* 9, 1965-1977.
- Kontgen, F., Grumont, R.J., Strasser, A., Metcalf, D., Li, R.L., Tarlinton, D., and Gerondakis, S. (1995b). Mice lacking the C-Rel protooncogene exhibit defects in lymphocyte-proliferation, humoral immunity and interleukin-2 expression. *Genes & Development* 9, 1965-1977.
- Krikos, A., Laherty, C.D., and Dixit, V.M. (1992). Transcriptional activation of the tumor-necrosis-factor alpha-inducible zinc finger protein, A20, is mediated by kappa-B elements. *Journal of Biological Chemistry* 267, 17971-17976.
- Kuhlmann, M.T., Cuhlmann, S., Hoppe, I., Krams, R., Evans, P.C., Strijkers, G.J., Nicolay, K., Hermann, S., and Schafers, M. (2012). Implantation of a Carotid Cuff for Triggering Shear-stress Induced Atherosclerosis in Mice. *Jove-Journal of Visualized Experiments*.
- Kukita, A., and Kukita, T. (2013). Multifunctional properties of RANKL/RANK in cell differentiation, proliferation and metastasis. *Future Oncology* 9, 1609-1622.
- Kumar, A., Takada, Y., Boriek, A.M., and Aggarwal, B.B. (2004). Nuclear factor-kappa B: its role in health and disease. *Journal of Molecular Medicine-Jmm* 82, 434-448.
- Kwak, B.R., Baeck, M., Bochaton-Piallat, M.-L., Caligiuri, G., Daemens, M.J.A.P., Davies, P.F., Hoefler, I.E., Holvoet, P., Jo, H., Krams, R., *et al.* (2014). Biomechanical factors in atherosclerosis: mechanisms and clinical implications. *European Heart Journal* 35, 3013-3020.
- LaMack, J.A., Himburg, H.A., Zhang, J., and Friedman, M.H. (2010). Endothelial Gene Expression in Regions of Defined Shear Exposure in the Porcine Iliac Arteries. *Annals of Biomedical Engineering* 38, 2252-2262.
- Lantz, J., Gardhagen, R., and Karlsson, M. (2012). Quantifying turbulent wall shear stress in a subject specific human aorta using large eddy simulation. *Medical Engineering & Physics* 34, 1139-1148.
- Laufs, U., La Fata, V., Plutzky, J., and Liao, J.K. (1998). Upregulation of endothelial nitric oxide synthase by HMG CoA reductase inhibitors. *Circulation* 97, 1129-1135.
- Lawrence, T., Bebien, M., Liu, G.Y., Nizet, V., and Karin, M. (2005). IKK alpha limits macrophage NF-kappa B activation and contributes to the resolution of inflammation. *Nature* 434, 1138-1143.
- Lee, T.S., Yen, H.C., Pan, C.C., and Chau, L.Y. (1999). The role of interleukin 12 in the development of atherosclerosis in ApoE-deficient mice. *Arteriosclerosis Thrombosis and Vascular Biology* 19, 734-742.
- Leroyer, A.S., Rautou, P.E., Silvestre, J.S., Castier, Y., Lesèche, G., Devue, C., Duriez, M., Brandes, R.P., Lutgens, E., Tedgui, A., *et al.* (2008). CD40 ligand+ microparticles from human atherosclerotic plaques stimulate endothelial proliferation and angiogenesis a potential mechanism for intraplaque neovascularization. *J Am Coll Cardiol* 52, 1302-1311.
- Levenson, J.M., Choi, S., Lee, S.Y., Cao, Y.A., Ahn, H.J., Worley, K.C., Pizzi, M., Liou, H.C., and Sweatt, J.D. (2004). A bioinformatics analysis of memory consolidation reveals involvement of the transcription factor c-Rel. *Journal of Neuroscience* 24, 3933-3943.
- Li, J., Hou, B., Tumova, S., Muraki, K., Bruns, A., Ludlow, M.J., Sedo, A., Hyman, A.J., McKeown, L., Young, R.S., *et al.* (2014). Piezol integration of vascular architecture with physiological force. *Nature* 515, 279-U308.
- Li, J.M., Fan, L.M., George, V.T., and Brooks, G. (2007). Nox2 regulates endothelial cell cycle arrest and apoptosis via p21 (cip1) and p53. *Free Radical Biology and Medicine* 43, 976-986.
- Li, L., Xu-Monette, Z.Y., Ok, C.Y., Tzankov, A., Manyam, G.C., Sun, R.F., Visco, C., Zhang, M.Z., Montes-Moreno, S., Dybkaer, K., *et al.* (2015). Prognostic impact of c-Rel nuclear expression and

REL amplification and crosstalk between c-Rel and the p53 pathway in diffuse large B-cell lymphoma. *Oncotarget* 6, 23157-23180.

Libby, P. (2002). Inflammation in atherosclerosis. *Nature* 420, 868-874.

Libby, P., Buring, J.E., Badimon, L., Hansson, C.K., Deanfield, J., Bittencourt, M.S., Tokgozoglu, L., and Lewis, E.F. (2019a). Atherosclerosis. *Nature Reviews Disease Primers* 5.

Libby, P., Pasterkamp, G., Crea, F., and Jang, I.-K. (2019b). Reassessing the Mechanisms of Acute Coronary Syndromes: The “Vulnerable Plaque” and Superficial Erosion. *Circulation Research* 124, 150-160.

Lin, K., Hsu, P.P., Chen, B.P., Yuan, S., Usami, S., Shyy, J.Y.J., Li, Y.S., and Chien, S. (2000). Molecular mechanism of endothelial growth arrest by laminar shear stress. *Proceedings of the National Academy of Sciences of the United States of America* 97, 9385-9389.

Liu, W.H., Kang, S.G., Huang, Z., Wu, C.J., Jin, H.Y., Maine, C.J., Liu, Y., Shepherd, J., Sabouri-Ghomi, M., Gonzalez-Martin, A., *et al.* (2016). A miR-155-Peli1-c-Rel pathway controls the generation and function of T follicular helper cells. *Journal of Experimental Medicine* 213, 1901-1919.

Lomaga, M.A., Yeh, W.C., Sarosi, I., Duncan, G.S., Furlonger, C., Ho, A., Morony, S., Capparelli, C., Van, G., Kaufman, S., *et al.* (1999). TRAF6 deficiency results in osteopetrosis and defective interleukin-1, CD40, and LPS signaling. *Genes & Development* 13, 1015-1024.

Loyer, X., Potteaux, S., Vion, A.C., Guerin, C.L., Boulkroun, S., Rautou, P.E., Ramkhelawon, B., Esposito, B., Dalloz, M., Paul, J.L., *et al.* (2015). INHIBITION OF MICRORNA-92A PREVENTS ENDOTHELIAL DYSFUNCTION AND ATHEROSCLEROSIS IN MICE. *Journal of Vascular Research* 52, 4-5.

Lu, H., Yang, X.P., Duggal, P., Allen, C.T., Yan, B., Cohen, J., Nottingham, L., Romano, R.A., Sinha, S., King, K.E., *et al.* (2011). TNF-alpha Promotes c-REL/Delta Np63 alpha Interaction and TAp73 Dissociation from Key Genes That Mediate Growth Arrest and Apoptosis in Head and Neck Cancer. *Cancer Research* 71, 6867-6877.

Lu, J., and Holmgren, A. (2014). The thioredoxin antioxidant system. *Free Radical Biology and Medicine* 66, 75-87.

Mack, J.J., Mosqueiro, T.S., Archer, B.J., Jones, W.M., Sunshine, H., Faas, G.C., Briot, A., Aragon, R.L., Su, T., Romay, M.C., *et al.* (2017). NOTCH1 is a mechanosensor in adult arteries. *Nature Communications* 8.

Magid, R., and Davies, P.F. (2005). Endothelial protein kinase C isoform identity and differential activity of PKC xi in an athero-susceptible region of porcine aorta. *Circulation Research* 97, 443-449.

Mahmoud, M.M., Kim, H.R., Xing, R.Y., Hsiao, S., Mammoto, A., Chen, J., Serbanovic-Canic, J., Feng, S., Bowden, N.P., Maguire, R., *et al.* (2016). TWIST1 Integrates Endothelial Responses to Flow in Vascular Dysfunction and Atherosclerosis. *Circulation Research* 119, 450-462.

Mahmoud, M.M., Serbanovic-Canic, J., Feng, S., Souilhol, C., Xing, R.Y., Hsiao, S., Mammoto, A., Chen, J., Ariaans, M., Francis, S.E., *et al.* (2017). Shear stress induces endothelial-to-mesenchymal transition via the transcription factor Snail. *Scientific Reports* 7.

Maja, M., Nicole, H., Nilushi, S.D.S., Michael, M.A., Kathryn, S., Amanda, C., Fabiano, O., Govind, B., and Ulf, K. (2016). Differential requirements for the canonical NF-κB transcription factors c-REL and RELA during the generation and activation of mature B-cells. *Immunology and Cell Biology* 95.

Malek, A.M., Alper, S.L., and Izumo, S. (1999). Hemodynamic shear stress and its role in atherosclerosis. *Jama-Journal of the American Medical Association* 282, 2035-2042.

Maltese, W.A., and Aprille, J.R. (1985). RELATION OF MEVALONATE SYNTHESIS TO MITOCHONDRIAL UBIQUINONE CONTENT AND RESPIRATORY-FUNCTION IN CULTURED NEUROBLASTOMA CELLS. *Journal of Biological Chemistry* 260, 1524-1529.

Martin, A.G., and Fresno, M. (2000). Tumor necrosis factor-alpha activation of NF-kappa B requires the phosphorylation of Ser-471 in the transactivation domain of c-Rel. *Journal of Biological Chemistry* 275, 24383-24391.

Martins e Silva, J. (2008). Leonardo da Vinci and the first hemodynamic observations. *Rev Port Cardiol* 27, 243-272.

Mendoza, F.A., Artlett, C.M., Sandorfi, N., Latinis, K., Piera-Velazquez, S., and Jimenez, S.A. (2006). Description of 12 cases of nephrogenic fibrosing dermopathy and review of the literature. *Seminars in Arthritis and Rheumatism* 35, 238-249.

Min, J.K., Cho, Y.L., Choi, J.H., Kim, Y., Kim, J.H., Yu, Y.S., Rho, J., Mochizuki, N., Kim, Y.M., Oh, G.T., *et al.* (2007). Receptor activator of nuclear factor (NF)-kappa B ligand (RANKL) increases vascular permeability: impaired permeability and angiogenesis in eNOS-deficient mice. *Blood* 109, 1495-1502.

Mohan, S., Mohan, N., and Sprague, E.A. (1997). Differential activation of NF-kappa B in human aortic endothelial cells conditioned to specific flow environments. *American Journal of Physiology-Cell Physiology* 273, C572-C578.

Mokhtari, D., Barbu, A., Mehmeti, I., Vercamer, C., and Welsh, N. (2009). Overexpression of the nuclear factor-kappa B subunit c-Rel protects against human islet cell death in vitro. *American Journal of Physiology-Endocrinology and Metabolism* 297, E1067-E1077.

Monaco, C., Andreakos, E., Kiriakidis, S., Mauri, C., Bicknell, C., Foxwell, B., Cheshire, N., Paleolog, E., and Feldmann, M. (2004). Canonical pathway of nuclear factor kappa B activation selectively regulates proinflammatory and prothrombotic responses in human atherosclerosis. *Proceedings of the National Academy of Sciences of the United States of America* 101, 5634-5639.

Montgomery, D.H., Ververis, J.J., McGorisk, G., Frohwein, S., Martin, R.P., and Taylor, W.R. (1996). Natural history of severe atheromatous disease of the thoracic aorta: A transesophageal echocardiographic study. *Journal of the American College of Cardiology* 27, 95-101.

Monvoisin, A., Alva, J.A., Hofmann, J.J., Zovein, A.C., Lane, T.F., and Iruela-Arispe, M.L. (2006). VE-cadherin-CreERT2 transgenic mouse: a model for inducible recombination in the endothelium. *Developmental dynamics : an official publication of the American Association of Anatomists* 235, 3413-3422.

Morey, J.S., Ryan, J.C., and Van Dolah, F.M. (2006). Microarray validation: factors influencing correlation between oligonucleotide microarrays and real-time PCR. *Biological Procedures Online* 8, 175-193.

Mosialos, G., Hamer, P., Capobianco, A.J., Laursen, R.A., and Gilmore, T.D. (1991). A protein kinase-A recognition sequence is structurally linked to transformation by P59V-Rel and cytoplasmic retention of P68C-Rel. *Molecular and Cellular Biology* 11, 5867-5877.

Mullick, A., Soldau, K., Kiosses, W., Bell, T., Tobias, P., and Curtiss, L. (2008). Increased endothelial expression of Toll-like receptor 2 at sites of disturbed blood flow exacerbates early atherogenic events. *Journal of Experimental Medicine* 205, 373-383.

Mullick, A., Tobias, P., and Curtiss, L. (2005). Modulation of atherosclerosis in mice by Toll-like receptor 2. *Journal of Clinical Investigation* 115, 3149-3156.

Nagel, T., Resnick, N., Atkinson, W.J., Dewey, C.F., and Gimbrone, M.A. (1994). Sheer stress selectively up-regulates intercellular-adhesion molecule-1 expression in cultured human vascular endothelial-cells. *Journal of Clinical Investigation* 94, 885-891.

Naito, A., Azuma, S., Tanaka, S., Miyazaki, T., Takaki, S., Takatsu, K., Nakao, K., Nakamura, K., Katsuki, M., Yamamoto, T., *et al.* (1999). Severe osteopetrosis, defective interleukin-1 signalling and lymph node organogenesis in TRAF6-deficient mice. *Genes to Cells* 4, 353-362.

Nam, D., Ni, C.W., Rezvan, A., Suo, J., Budzyn, K., Llanos, A., Harrison, D., Giddens, D., and Jo, H. (2009). Partial carotid ligation is a model of acutely induced disturbed flow, leading to rapid endothelial dysfunction and atherosclerosis. *American Journal of Physiology-Heart and Circulatory Physiology* 297, H1535-H1543.

Natoli, G., and Chiocca, S. (2008). Nuclear Ubiquitin Ligases, NF-kappa B Degradation, and the Control of Inflammation. *Science Signaling* 1.

Nelson, D.E., Ihekweba, A.E.C., Elliott, M., Johnson, J.R., Gibney, C.A., Foreman, B.E., Nelson, G., See, V., Horton, C.A., Spiller, D.G., *et al.* (2004). Oscillations in NF-kappa B signaling control the dynamics of gene expression. *Science* 306, 704-708.

Ni, C.W., Qiu, H.W., Rezvan, A., Kwon, K., Nam, D., Son, D.J., Visvader, J.E., and Jo, H. (2010). Discovery of novel mechanosensitive genes in vivo using mouse carotid artery endothelium exposed to disturbed flow. *Blood* *116*, E66-E73.

Nigro, P., Abe, J., Woo, C.H., Satoh, K., McClain, C., O'Dell, M.R., Lee, H., Lim, J.H., Li, J.D., Heo, K.S., *et al.* (2010). PKC zeta decreases eNOS protein stability via inhibitory phosphorylation of ERK5. *Blood* *116*, 1971-1979.

Ninomiya-Tsuji, J., Kishimoto, K., Hiyama, A., Inoue, J., Cao, Z.D., and Matsumoto, K. (1999). The kinase TAK1 can activate the NIK-I kappa B as well as the MAP kinase cascade in the IL-1 signalling pathway. *Nature* *398*, 252-256.

Niu, X.Y., He, D.Y., Zhang, X., Yue, T., Li, N.L., Zhang, J.W.Z., Dong, C., and Chen, G.J. (2010). IL-21 regulates Th17 cells in rheumatoid arthritis. *Human Immunology* *71*, 334-341.

Nofer, J.R., Levkau, B., Wolinska, I., Junker, R., Fobker, M., von Eckardstein, A., Seedorf, U., and Assmann, G. (2001). Suppression of endothelial cell apoptosis by high density lipoproteins (HDL) and HDL-associated lysophingolipids. *Journal of Biological Chemistry* *276*, 34480-34485.

Novack, D.V., Yin, L., Hagen-Stapleton, A., Schreiber, R.D., Goeddel, D.V., Ross, F.P., and Teitelbaum, S.L. (2003). The I kappa B function of NF-kappa B2 p100 controls stimulated osteoclastogenesis. *Journal of Experimental Medicine* *198*, 771-781.

Obikane, H., Abiko, Y., Ueno, H., Kusumi, Y., Esumi, M., and Mitsumata, M. (2010). Effect of endothelial cell proliferation on atherogenesis: A role of p21(Sdi/Cip/Waf1) in monocyte adhesion to endothelial cells. *Atherosclerosis* *212*, 116-122.

Oeckinghaus, A., and Ghosh, S. (2009). The NF-kappa B Family of Transcription Factors and Its Regulation. *Cold Spring Harbor Perspectives in Biology* *1*.

Oeckinghaus, A., Hayden, M.S., and Ghosh, S. (2011). Crosstalk in NF-kappa B signaling pathways. *Nature Immunology* *12*, 695-708.

Oh, H., Grinberg-Bleyer, Y., Liao, W., Maloney, D., Wang, P., Wu, Z., Wang, J., Bhatt, D.M., Heise, N., Schmid, R.M., *et al.* (2017). An NF- κ B Transcription-Factor-Dependent Lineage-Specific Transcriptional Program Promotes Regulatory T Cell Identity and Function.

Orr, A.W., Sanders, J.M., Bevard, M., Coleman, E., Sarembock, I.J., and Schwartz, M.A. (2005). The subendothelial extracellular matrix modulates NF-kappa B activation by flow: a potential role in atherosclerosis. *Journal of Cell Biology* *169*, 191-202.

Osipo, C., Golde, T.E., Osborne, B.A., and Miele, L.A. (2008). Off the beaten pathway: the complex cross talk between Notch and NF-kappa B. *Laboratory Investigation* *88*, 11-17.

Owyang, A.M., Tumang, J.R., Schram, B.R., Hsia, C.Y., Behrens, T.W., Rothstein, T.L., and Liou, H.C. (2001). c-Rel is required for the protection of B cells from antigen receptor-mediated, but not Fas-mediated, apoptosis. *Journal of Immunology* *167*, 4948-4956.

Panza, J.A., Quyyumi, A.A., Brush, J.E., and Epstein, S.E. (1990). Abnormal endothelium-dependent vascular relaxation in patients with essential-hypertension. *New England Journal of Medicine* *323*, 22-27.

Papadaki, M., and Eskin, S.G. (1997). Effects of fluid shear stress on gene regulation of vascular cells. *Biotechnology Progress* *13*, 209-221.

Partridge, J., Carlsen, H., Enesa, K., Chaudhury, H., Zakkar, M., Luong, L., Kinderlerer, A., Johns, M., Blomhoff, R., Mason, J.C., *et al.* (2007). Laminar shear stress acts as a switch to regulate divergent functions of NF-kappa B in endothelial cells. *Faseb Journal* *21*, 3553-3561.

Passerini, A.G., Polacek, D.C., Shi, C.Z., Francesco, N.M., Manduchi, E., Grant, G.R., Pritchard, W.F., Powell, S., Chang, G.Y., Stoeckert, C.J., *et al.* (2004). Coexisting proinflammatory and antioxidative endothelial transcription profiles in a disturbed flow region of the adult porcine aorta. *Proceedings of the National Academy of Sciences of the United States of America* *101*, 2482-2487.

Perkins, N.D. (2007). Integrating cell-signalling pathways with NF-kappa B and IKK function. *Nature Reviews Molecular Cell Biology* *8*, 49-62.

Petzold, T., Orr, A.W., Hahn, C., Jhaveri, K.A., Parsons, J.T., and Schwartz, M.A. (2009). Focal adhesion kinase modulates activation of NF-kappa B by flow in endothelial cells. *American Journal of Physiology-Cell Physiology* 297, C814-C822.

Piera-Velazquez, S., Louneva, N., Fertala, J., Wermuth, P.J., Del Galdo, F., and Jimenez, S.A. (2010). Persistent activation of dermal fibroblasts from patients with gadolinium-associated nephrogenic systemic fibrosis. *Annals of the Rheumatic Diseases* 69, 2017-2023.

Pikuleva, I.A. (2008). Cholesterol-metabolizing cytochromes P450: implications for cholesterol lowering. *Expert Opinion on Drug Metabolism & Toxicology* 4, 1403-1414.

Quillard, T., Araújo, H.A., Franck, G., Shvartz, E., Sukhova, G., and Libby, P. (2015). TLR2 and neutrophils potentiate endothelial stress, apoptosis and detachment: implications for superficial erosion. *European Heart Journal* 36, 1394-1404.

Rajagopalan, S., Meng, X.P., Ramasamy, S., Harrison, D.G., and Galis, Z.S. (1996). Reactive oxygen species produced by macrophage-derived foam cells regulate the activity of vascular matrix metalloproteinases in vitro - Implications for atherosclerotic plaque stability. *Journal of Clinical Investigation* 98, 2572-2579.

Ramachandiran, S., Adon, A., Guo, X.X., Wang, Y., Wang, H.C., Chen, Z.J., Kowalski, J., Sunay, U.R., Young, A.N., Brown, T., *et al.* (2015). Chromosome instability in diffuse large B cell lymphomas is suppressed by activation of the noncanonical NF-kappa B pathway. *International Journal of Cancer* 136, 2341-2351.

Rao, S., Gerondakis, S., Woltring, D., and Shannon, M.F. (2003). c-Rel is required for chromatin remodeling across the IL-2 gene promoter. *Journal of Immunology* 170, 3724-3731.

Repa, J.J., and Mangelsdorf, D.J. (2000). The role of orphan nuclear receptors in the regulation of cholesterol homeostasis. *Annual Review of Cell and Developmental Biology* 16, 459-481.

Ricci, R., Sumara, G., Sumara, I., Rozenberg, I., Kurrer, M., Akhmedov, A., Hersberger, M., Eriksson, U., Eberli, F.R., Becher, B., *et al.* (2004). Requirement of JNK2 for scavenger receptor A-mediated foam cell formation in atherogenesis. *Science* 306, 1558-1561.

Rice, N.R., Copeland, T.D., Simek, S., Oroszlan, S., and Gilden, R.V. (1986). Detection and characterization of the protein encoded by the V-Rel oncogene. *Virology* 149, 217-229.

Ridker, P.M., Everett, B.M., Thuren, T., MacFadyen, J.G., Chang, W.H., Ballantyne, C., Fonseca, F., Nicolau, J., Koenig, W., Anker, S.D., *et al.* (2017). Antiinflammatory Therapy with Canakinumab for Atherosclerotic Disease. *New England Journal of Medicine* 377, 1119-1131.

Ridker, P.M., Libby, P., MacFadyen, J.G., Thuren, T., Bauantyne, C., Fonseca, F., Koenig, W., Shimokawa, H., Everett, B.M., Glynn, R.J., *et al.* (2018). Modulation of the interleukin-6 signalling pathway and incidence rates of atherosclerotic events and all-cause mortality: analyses from the Canakinumab Anti-Inflammatory Thrombosis Outcomes Study (CANTOS). *European Heart Journal* 39, 3499-3507.

Ridker, P.M., Thuren, T., Zalewski, A., Libby, P., and Grp, C.S. (2011). Interleukin-1 beta inhibition and the prevention of recurrent cardiovascular events: Rationale and Design of the Canakinumab Anti-inflammatory Thrombosis Outcomes Study (CANTOS). *American Heart Journal* 162, 597-605.

Rokitansky, K. (1952). *A Manual of Pathological Anatomy*.

Ruan, Q.G., Kameswaran, V., Zhang, Y., Zheng, S.J., Sun, J., Wang, J.M., DeVirgiliis, J., Liou, H.C., Beg, A.A., and Chen, Y.H. (2011a). The Th17 immune response is controlled by the Rel-ROR gamma-ROR gamma T transcriptional axis. *Journal of Experimental Medicine* 208, 2321-2333.

Ruan, Q.G., Wang, T., Kameswaran, V., Wei, Q., Johnson, D.S., Matschinsky, F., Shi, W.Y., and Chen, Y.H.H. (2011b). The microRNA-21-PDCD4 axis prevents type 1 diabetes by blocking pancreatic beta cell death. *Proceedings of the National Academy of Sciences of the United States of America* 108, 12030-12035.

Saitoh, M., Nishitoh, H., Fujii, M., Takeda, K., Tobiume, K., Sawada, Y., Kawabata, M., Miyazono, K., and Ichijo, H. (1998). Mammalian thioredoxin is a direct inhibitor of apoptosis signal-regulating kinase (ASK) 1. *Embo Journal* 17, 2596-2606.

Sanchez-Valdepenas, C., Martin, A.G., Ramakrishnan, P., Wallach, D., and Fresno, M. (2006). NF-kappa B-inducing kinase is involved in the activation of the CD28 responsive element through phosphorylation of c-Rel and regulation of its transactivating activity. *Journal of Immunology* *176*, 4666-4674.

Sanchez-Valdepenas, C., Punzon, C., San-Antonio, B., Martin, A.G., and Fresno, M. (2007). Differential regulation of p65 and c-Rel NF-kappa B transactivating activity by Cot, protein kinase C zeta and NIK protein kinases in CD3/CD28 activated T cells. *Cellular Signalling* *19*, 528-537.

Sanchez-Valdepeñas, C., Casanova, L., Colmenero, I., Arriero, M., Gonzalez, A., Lozano, N., Gonzalez-Vicent, M., Diaz, M.A., Madero, L., Fresno, M., *et al.* (2010). Nuclear factor-kappa B inducing kinase is required for graft-versus-host disease. *Haematologica-the Hematology Journal* *95*, 2111-2118.

Sarnico, I., Lanzillotta, A., Boroni, F., Benarese, M., Alghisi, M., Schwaninger, M., Inta, I., Battistin, L., Spano, P., and Pizzi, M. (2009). NF-kappa B p50/RelA and c-Rel-containing dimers: opposite regulators of neuron vulnerability to ischaemia. *Journal of Neurochemistry* *108*, 475-485.

Scheibner, K.A., Lutz, M.A., Boodoo, S., Fenton, M.J., Powell, J.D., and Horton, M.R. (2006). Hyaluronan fragments act as an endogenous danger signal by engaging TLR2. *Journal of immunology (Baltimore, Md : 1950)* *177*, 1272-1281.

Schober, A., Nazari-Jahantigh, M., Wei, Y.Y., Bidzhekov, K., Gremse, F., Grommes, J., Megens, R.T.A., Heyll, K., Noels, H., Hristov, M., *et al.* (2014). MicroRNA-126-5p promotes endothelial proliferation and limits atherosclerosis by suppressing Dlk1. *Nature Medicine* *20*, 368-+.

Schumm, K., Rocha, S., Caamano, J., and Perkins, N.D. (2006). Regulation of p53 tumour suppressor target gene expression by the p52 NF-kappa B subunit. *Embo Journal* *25*, 4820-4832.

Scott, M.L., Fujita, T., Liou, H.C., Nolan, G.P., and Baltimore, D. (1993). THE P65-SUBUNIT OF NF-KAPPA-B REGULATES I-KAPPA-B BY 2 DISTINCT MECHANISMS. *Genes & Development* *7*, 1266-1276.

SenBanerjee, S., Lin, Z.Y., Atkins, G.B., Greif, D.M., Rao, R.M., Kumar, A., Feinberg, M.W., Chen, Z.P., Simon, D.I., Luscinskas, F.W., *et al.* (2004). KLF2 is a novel transcriptional regulator of endothelial proinflammatory activation. *Journal of Experimental Medicine* *199*, 1305-1315.

Senftleben, U., Cao, Y.X., Xiao, G.T., Greten, F.R., Krahn, G., Bonizzi, G., Chen, Y., Hu, Y.L., Fong, A., Sun, S.C., *et al.* (2001). Activation by IKK alpha of a second, evolutionary conserved, NF-kappa B signaling pathway. *Science* *293*, 1495-1499.

Serbanovic-Canic, J., de Luca, A., Warboys, C., Ferreira, P.F., Luong, L.A., Hsiao, S., Gauci, I., Mahmoud, M., Feng, S., Souilhol, C., *et al.* (2017). Zebrafish Model for Functional Screening of Flow-Responsive Genes. *Arteriosclerosis Thrombosis and Vascular Biology* *37*, 130-+.

Shapiro, M.D., and Fazio, S. (2017). PCSK9 and Atherosclerosis - Lipids and Beyond. *Journal of Atherosclerosis and Thrombosis* *24*, 462-472.

Shepherd, J. (2001). The role of the exogenous pathway in hypercholesterolaemia. *European Heart Journal Supplements* *3*, E2-E5.

Shih, V.F.S., Tsui, R., Caldwell, A., and Hoffmann, A. (2011). A single NF kappa B system for both canonical and non-canonical signaling. *Cell Research* *21*, 86-102.

Shin, H.M., Minter, L.M., Cho, O.H., Gottipati, S., Fauq, A.H., Golde, T.E., Sonenshein, G.E., and Osborne, B.A. (2006). Notch1 augments NF-kappa B activity by facilitating its nuclear retention. *Embo Journal* *25*, 129-138.

Shono, Y., Tuckett, A.Z., Liou, H.C., Doubrovina, E., Derenzini, E., Ouk, S., Tsai, J.J., Smith, O.M., Levy, E.R., Kreines, F.M., *et al.* (2016). Characterization of a c-Rel Inhibitor That Mediates Anticancer Properties in Hematologic Malignancies by Blocking NF-kappa B-Controlled Oxidative Stress Responses. *Cancer Research* *76*, 377-389.

Shono, Y., Tuckett, A.Z., Ouk, S., Liou, H.C., Altan-Bonnet, G., Tsai, J.J., Oyler, J.E., Smith, O.M., West, M.L., Singer, N.V., *et al.* (2014). A Small-Molecule c-Rel Inhibitor Reduces Alloactivation of T Cells without Compromising Antitumor Activity. *Cancer Discovery* *4*, 578-591.

Shuvaev, V.V., Tliba, S., Nakada, M., Albelda, S.M., and Muzykantov, V.R. (2007). Platelet-endothelial cell adhesion molecule-1-directed endothelial targeting of superoxide dismutase

alleviates oxidative stress caused by either extracellular or intracellular superoxide. *Journal of Pharmacology and Experimental Therapeutics* 323, 450-457.

Silvola, J.M., Saraste, A., Forsback, S., Laine, V.J., Saukko, P., Heinonen, S.E., Ylä-Herttuala, S., Roivainen, A., and Knuuti, J. (2011). Detection of hypoxia by [18F]EF5 in atherosclerotic plaques in mice. *Arterioscler Thromb Vasc Biol* 31, 1011-1015.

Skaug, B., Jiang, X.M., and Chen, Z.J. (2009). The Role of Ubiquitin in NF-kappa B Regulatory Pathways. *Annual Review of Biochemistry* 78, 769-796.

Soehnlein, O., Schmeisser, A., Cicha, I., Reiss, C., Ulbrich, H., Lindbom, L., Daniel, W.G., and Garlichs, C.D. (2005). ACE inhibition lowers angiotensin-II-induced monocyte adhesion to HUVEC by reduction of p65 translocation and AT1 expression. *Journal of Vascular Research* 42, 399-407.

Son, J.S., Sahoo, A., Chae, C.S., Hwang, J.S., Park, Z.Y., and Im, S.H. (2011). JunB and c-Rel cooperatively enhance Foxp3 expression during induced regulatory T cell differentiation. *Biochemical and Biophysical Research Communications* 407, 141-147.

Song, L.L., Peng, Y., Yun, J., Rizzo, P., Chaturvedi, V., Weijzen, S., Kast, W.M., Stone, P.J.B., Santos, L., Loreda, A., *et al.* (2008). Notch-1 associates with IKK alpha and regulates IKK activity in cervical cancer cells. *Oncogene* 27, 5833-5844.

Sorensen, I., Adams, R.H., and Gossler, A. (2009). DLL1-mediated Notch activation regulates endothelial identity in mouse fetal arteries. *Blood* 113, 5680-5688.

Staughton, T.J., Lever, M.J., and Weinberg, P.D. (2001). Effect of altered flow on the pattern of permeability around rabbit aortic branches. *American Journal of Physiology-Heart and Circulatory Physiology* 281, H53-H59.

Stoneman, V.E.A., and Bennett, M.R. (2004). Role of apoptosis in atherosclerosis and its therapeutic implications. *Clinical Science* 107, 343-354.

Sun, S.C. (2011). Non-canonical NF-kappa B signaling pathway. *Cell Research* 21, 71-85.

Sun, S.C., Ganchi, P.A., Ballard, D.W., and Greene, W.C. (1993). NF-KAPPA-B CONTROLS EXPRESSION OF INHIBITOR I-KAPPA-B-ALPHA - EVIDENCE FOR AN INDUCIBLE AUTOREGULATORY PATHWAY. *Science* 259, 1912-1915.

Sun, S.C., and Ley, S.C. (2008). New insights into NF-kappa B regulation and function. *Trends in Immunology* 29, 469-478.

Sun, X.H., He, S.L., Wara, A.K.M., Icli, B., Shvartz, E., Tesmenitsky, Y., Belkin, N., Li, D.Z., Blackwell, T.S., Sukhova, G.K., *et al.* (2014). Systemic Delivery of MicroRNA-181b Inhibits Nuclear Factor-kappa B Activation, Vascular Inflammation, and Atherosclerosis in Apolipoprotein E-Deficient Mice. *Circulation Research* 114, 32-40.

Sweitzer, T.D., Thomas, A.P., Wiewrodt, R., Nakada, M.T., Branco, F., and Muzykantov, V.R. (2003). PECAM-directed immunotargeting of catalase: Specific, rapid and transient protection against hydrogen peroxide. *Free Radical Biology and Medicine* 34, 1035-1046.

Swindle, M.M., Makin, A., Herron, A.J., Clubb, F.J., and Frazier, K.S. (2012). Swine as Models in Biomedical Research and Toxicology Testing. *Veterinary Pathology* 49, 344-356.

Tada, K., Okazaki, T., Sakon, S., Kobarai, T., Kurosawa, K., Yamaoka, S., Hashimoto, H., Mak, T.W., Yagita, H., Okumura, K., *et al.* (2001). Critical roles of TRAF2 and TRAF5 in tumor necrosis factor-induced NF-kappa B activation and protection from cell death. *Journal of Biological Chemistry* 276, 36530-36534.

Takagi, Y., Gon, Y., Todaka, T., Nozaki, K., Nishiyama, A., Sono, H., Hashimoto, N., Kikuchi, H., and Yodoi, J. (1998). Expression of thioredoxin is enhanced in atherosclerotic plaques and during neointima formation in rat arteries. *Laboratory Investigation* 78, 957-966.

Tarbell, J.M. (2003). Mass transport in arteries and the localization of atherosclerosis. *Annual Review of Biomedical Engineering* 5, 79-118.

Tedgui, A., and Mallat, Z. (2006). Cytokines in atherosclerosis: Pathogenic and regulatory pathways. *Physiological Reviews* 86, 515-581.

Theill, L.E., Boyle, W.J., and Penninger, J.M. (2002). RANK-L AND RANK: T cells, bone loss, and mammalian evolution. *Annual Review of Immunology* 20, 795-823.

Thelen, A.M., and Zoncu, R. (2017). Emerging Roles for the Lysosome in Lipid Metabolism. *Trends in Cell Biology* 27, 843-860.

Thompson, R.C., Allam, A.H., Lombardi, G.P., Wann, L.S., Sutherland, M.L., Sutherland, J.D., Soliman, M.A., Frohlich, B., Mininberg, D.T., Monge, J.M., *et al.* (2013). Atherosclerosis across 4000 years of human history: the Horus study of four ancient populations. *Lancet* 381, 1211-1222.

Thorin, E., and Clozel, M. (2010). The Cardiovascular Physiology and Pharmacology of Endothelin-1. *Cardiovascular Pharmacology: Endothelial Control* 60, 1-26.

Totzke, G., Essmann, F., Pohlmann, S., Lindenblatt, C., Janicke, R.U., and Schulze-Osthoff, K. (2006). A novel member of the I kappa B family, human I kappa B-zeta, inhibits transactivation of p65 and its DNA binding. *Journal of Biological Chemistry* 281, 12645-12654.

Trigueros-Motos, L., Gonzalez-Granado, J.M., Cheung, C., Fernandez, P., Sanchez-Cabo, F., Dopazo, A., Sinha, S., and Andres, V. (2013). Embryological-Origin-Dependent Differences in Homeobox Expression in Adult Aorta Role in Regional Phenotypic Variability and Regulation of NF-kappa B Activity. *Arteriosclerosis Thrombosis and Vascular Biology* 33, 1248-+.

Trinchieri, G. (2003). Interleukin-12 and the regulation of innate resistance and adaptive immunity. *Nature Reviews Immunology* 3, 133-146.

Tseng, H., Peterson, T.E., and Berk, B.C. (1995). Fluid shear-stress stimulates mitogen-activated protein-kinase in endothelial cells. *Circulation Research* 77, 869-878.

Tzima, E., Irani-Tehrani, M., Kiosses, W.B., Dejana, E., Schultz, D.A., Engelhardt, B., Cao, G.Y., DeLisser, H., and Schwartz, M.A. (2005). A mechanosensory complex that mediates the endothelial cell response to fluid shear stress. *Nature* 437, 426-431.

Vallabhapurapu, S., Matsuzawa, A., Zhang, W.Z., Tseng, P.H., Keats, J.J., Wang, H.P., Vignali, D.A.A., Bergsagel, P.L., and Karin, M. (2008). Nonredundant and complementary functions of TRAF2 and TRAF3 in a ubiquitination cascade that activates NIK-dependent alternative NF-kappa B signaling. *Nature Immunology* 9, 1364-1370.

van Thienen, J.V., Fledderus, J.O., Dekker, R.J., Rohlena, J., van Ijzendoorn, G.A., Kootstra, N.A., Pannekoek, H., and Horrevoets, A.J.G. (2006). Shear stress sustains atheroprotective endothelial KLF2 expression more potently than statins through mRNA stabilization. *Cardiovascular Research* 72, 231-240.

VanderLaan, P.A., Reardon, C.A., and Getz, G.S. (2004). Site specificity of atherosclerosis - Site-selective responses to atherosclerotic modulators. *Arteriosclerosis Thrombosis and Vascular Biology* 24, 12-22.

Vince, J.E., Pantaki, D., Feltham, R., Mace, P.D., Cordier, S.M., Schmukle, A.C., Davidson, A.J., Callus, B.A., Wong, W.W.L., Gentle, I.E., *et al.* (2009). TRAF2 Must Bind to Cellular Inhibitors of Apoptosis for Tumor Necrosis Factor (TNF) to Efficiently Activate NF-kappa B and to Prevent TNF-induced Apoptosis. *Journal of Biological Chemistry* 284, 35906-35915.

Vion, A.C., Ramkhalawon, B., Loyer, X., Chironi, G., Devue, C., Loirand, G., Tedgui, A., Lehoux, S., and Boulanger, C.M. (2013). Shear Stress Regulates Endothelial Microparticle Release. *Circulation Research* 112, 1323-+.

Virchow, R. (1860). Cellular Pathology as Based Upon Physiological and Pathological Histology.

Virmani, D.R., Kolodgie, P.F., Burke, M.A., Farb, M.A., and Schwartz, M.S. (2000). Lessons From Sudden Coronary Death: A Comprehensive Morphological Classification Scheme for Atherosclerotic Lesions. *Arteriosclerosis, Thrombosis, and Vascular Biology: Journal of the American Heart Association* 20, 1262-1275.

Virmani, R., Burke, A.P., and Farb, A. (1999). Plaque rupture and plaque erosion. *Thrombosis and haemostasis* 82 suppl 1, 1-3.

Vita, J.A., Treasure, C.B., Nabel, E.G., McLenachan, J.M., Fish, R.D., Yeung, A.C., Vekshtein, V.I., Selwyn, A.P., and Ganz, P. (1990). Coronary vasomotor response to acetylcholine relates to risk-factors for coronary-artery disease. *Circulation* 81, 491-497.

Wajant, H., Henkler, F., and Scheurich, P. (2001). The TNF-receptor-associated factor family - Scaffold molecules for cytokine receptors, kinases and their regulators. *Cellular Signalling* *13*, 389-400.

Walpola, P.L., Gotlieb, A.I., Cybulsky, M.I., and Langille, B.L. (1995). EXPRESSION OF ICAM-1 AND VCAM-1 AND MONOCYTE ADHERENCE IN ARTERIES EXPOSED TO ALTERED SHEAR-STRESS. *Arteriosclerosis Thrombosis and Vascular Biology* *15*, 2-10.

Wang, C., Deng, L., Hong, M., Akkaraju, G.R., Inoue, J., and Chen, Z.J.J. (2001). TAK1 is a ubiquitin-dependent kinase of MKK and IKK. *Nature* *412*, 346-351.

Wang, N.P., Miao, H., Li, Y.S., Zhang, P., Haga, J.H., Hu, Y.L., Young, A., Yuan, S.L., Nguyen, P., Wu, C.C., *et al.* (2006). Shear stress regulation of Kruppel-like factor 2 expression is flow pattern-specific. *Biochemical and Biophysical Research Communications* *341*, 1244-1251.

Wang, X.Q., Nigro, P., World, C., Fujiwara, K., Yan, C., and Berk, B.C. (2012). Thioredoxin Interacting Protein Promotes Endothelial Cell Inflammation in Response to Disturbed Flow by Increasing Leukocyte Adhesion and Repressing Kruppel-Like Factor 2. *Circulation Research* *110*, 560-U141.

Wang, Y., Rickman, B.H., Poutahidis, T., Schlieper, K., Jackson, E.A., Erdman, S.E., Fox, J.G., and Horwitz, B.H. (2008). c-Rel is essential for the development of innate and T cell-induced colitis. *Journal of Immunology* *180*, 8118-8125.

Warboys, C.M., Amini, N., de Luca, A., and Evans, P.C. (2011). The role of blood flow in determining the sites of atherosclerotic plaques. *F1000 medicine reports* *3*, 5-5.

Warboys, C.M., Berson, R.E., Mann, G.E., Pearson, J.D., and Weinberg, P.D. (2010). Acute and chronic exposure to shear stress have opposite effects on endothelial permeability to macromolecules. *American Journal of Physiology-Heart and Circulatory Physiology* *298*, H1850-H1856.

Warboys, C.M., de Luca, A., Amini, N., Luong, L., Duckles, H., Hsiao, S., White, A., Biswas, S., Khamis, R., Chong, C.K., *et al.* (2014). Disturbed Flow Promotes Endothelial Senescence via a p53-Dependent Pathway. *Arteriosclerosis Thrombosis and Vascular Biology* *34*, 985-995.

Warnholtz, A., Nickenig, G., Schulz, E., Macharzina, R., Brasen, J.H., Skatchkov, M., Heitzer, T., Stasch, J.P., Griendling, K.K., Harrison, D.G., *et al.* (1999). Increased NADH-oxidase-mediated superoxide production in the early stages of atherosclerosis - Evidence for involvement of the renin-angiotensin system. *Circulation* *99*, 2027-2033.

Wassmann, S., Stumpf, M., Strehlow, K., Schmid, A., Schieffer, B., Bohm, M., and Nickenig, G. (2004). Interleukin-6 induces oxidative stress and endothelial dysfunction by overexpression of the angiotensin II type 1 receptor. *Circulation Research* *94*, 534-541.

Weber, C., and Noels, H. (2011). Atherosclerosis: current pathogenesis and therapeutic options. *Nature Medicine* *17*, 1410-1422.

Weniger, M.A., Gesk, S., Ehrlich, S., Martin-Subero, J.I., Dyer, M.J.S., Siebert, R., Moller, P., and Barth, T.F.E. (2007). Gains of REL in primary mediastinal B-cell lymphoma coincide with nuclear accumulation of REL protein. *Genes Chromosomes & Cancer* *46*, 406-415.

Wertz, I.E., O'Rourke, K.M., Zhou, H.L., Eby, M., Aravind, L., Seshagiri, S., Wu, P., Wiesmann, C., Baker, R., Boone, D.L., *et al.* (2004). De-ubiquitination and ubiquitin ligase domains of A20 downregulate NF-kappa B signalling. *Nature* *430*, 694-699.

Whitman, S.C., Ravisankar, P., Elam, H., and Daugherty, A. (2000). Exogenous interferon-gamma enhances atherosclerosis in apolipoprotein E-/- mice. *American Journal of Pathology* *157*, 1819-1824.

Wild, S., and Byrne, C.D. (2008). Time to rethink high-density lipoprotein? *Heart* *94*, 692.

Witztum, J.L. (1994). The oxidation hypothesis of atherosclerosis. *Lancet* *344*, 793-795.

Wolfrum, S., Teupser, D., Tan, M., Chen, K.Y., and Breslow, J.L. (2007). The protective effect of A20 on atherosclerosis in apolipoprotein E-deficient mice is associated with reduced expression of NF-kappa B target genes. *Proceedings of the National Academy of Sciences of the United States of America* *104*, 18601-18606.

Wung, B.S., Hsu, M.C., Wu, C.C., and Hsieh, C.W. (2005). Resveratrol suppresses IL-6-induced ICAM-1 gene expression in endothelial cells: Effects on the inhibition of STAT3 phosphorylation. *Life Sciences* 78, 389-397.

Xia, N., Daiber, A., Forstermann, U., and Li, H.G. (2017). Antioxidant effects of resveratrol in the cardiovascular system. *British Journal of Pharmacology* 174, 1633-1646.

Xiao, G.T., Harhaj, E.W., and Sun, S.C. (2001). NF-kappa B-inducing kinase regulates the processing of NF-kappa B2 p100. *Molecular Cell* 7, 401-409.

Yamawaki, H., Pan, S., Lee, R.T., and Berk, B.C. (2005). Fluid shear stress inhibits vascular inflammation by decreasing thioredoxin-interacting protein in endothelial cells. *Journal of Clinical Investigation* 115, 733-738.

Yurdagul, A., Finney, A.C., Woolard, M.D., and Orr, A.W. (2016). The arterial microenvironment: the where and why of atherosclerosis. *Biochemical Journal* 473, 1281-1295.

Zakkar, M., Chaudhury, H., Sandvik, G., Enesa, K., Luong, L.A., Cuhlmann, S., Mason, J.C., Krams, R., Clark, A.R., Haskard, D.O., *et al.* (2008). Increased endothelial mitogen-activated protein kinase phosphatase-1 expression suppresses proinflammatory activation at sites that are resistant to atherosclerosis. *Circulation Research* 103, 726-732.

Zakkar, M., Van der Heiden, K., Luong, L.A., Chaudhury, H., Cuhlmann, S., Hamdulay, S.S., Krams, R., Edirisinghe, I., Rahman, I., Carlsen, H., *et al.* (2009). Activation of Nrf2 in Endothelial Cells Protects Arteries From Exhibiting a Proinflammatory State. *Arteriosclerosis Thrombosis and Vascular Biology* 29, 1851-U1353.

Zarnegar, B.J., Wang, Y.Y., Mahoney, D.J., Dempsey, P.W., Cheung, H.H., He, J., Shiba, T., Yang, X.L., Yeh, W.C., Mak, T.W., *et al.* (2008). Noncanonical NF-kappa B activation requires coordinated assembly of a regulatory complex of the adaptors cIAP1, cIAP2, TRAF2 and TRAF3 and the kinase NIK. *Nature Immunology* 9, 1371-1378.

Zeng, L., Zampetaki, A., Margariti, A., Pepe, A.E., Alam, S., Martin, D., Xiao, Q., Wang, W., Jin, Z.-G., Cockerill, G., *et al.* (2009). Sustained activation of XBP1 splicing leads to endothelial apoptosis and atherosclerosis development in response to disturbed flow. *Proceedings of the National Academy of Sciences of the United States of America* 106, 8326-8331.

Zerjatke, T., Gak, I.A., Kirova, D., Fuhrmann, M., Daniel, K., Gonciarz, M., Muller, D., Glauche, I., and Mansfeld, J. (2017). Quantitative Cell Cycle Analysis Based on an Endogenous All-in-One Reporter for Cell Tracking and Classification. *Cell Reports* 19, 1953-1966.

Zhang, H.L., Bi, J.C., Yi, H.Q., Fan, T.T., Ruan, Q.G., Cai, L.T., Chen, Y.H., and Wan, X.C. (2017). Silencing c-Rel in macrophages dampens Th1 and Th17 immune responses and alleviates experimental autoimmune encephalomyelitis in mice. *Immunology and Cell Biology* 95, 593-600.

Zhang, J., Olson, W., Ewert, D., Bargmann, W., and Bose, H.R. (1991). The v-rel oncogene of avian reticuloendotheliosis virus transforms immature and mature lymphoid cells of the B cell lineage in vitro. *Virology* 183, 457-466.

Zhao, Y.Y., Gao, X.P., Zhao, Y.D.D., Mirza, M.K., Frey, R.S., Kalinichenko, V.V., Wang, I.C., Costa, R.H., and Malik, A.B. (2006). Endothelial cell-restricted disruption of FoxM1 impairs endothelial repair following LPS-induced vascular injury. *Journal of Clinical Investigation* 116, 2333-2343.

Zimmerman, M.R. (1993). The paleopathology of the cardiovascular-system. *Texas Heart Institute Journal* 20, 252-257.